

IL NUOVO CIMENTO

ORGANO DELLA SOCIETÀ ITALIANA DI FISICA

SOTTO GLI AUSPICI DEL CONSIGLIO NAZIONALE DELLE RICERCHE

VOL. IV, N. 2

Serie decima

1° Agosto 1956

On the Study of the Bremsstrahlung by Bloch and Nordsieck's Method.

R. ASCOLI and G. BUSSETTI

Istituto di Fisica dell'Università - Torino

Istituto Nazionale di Fisica Nucleare - Sezione di Torino

(ricevuto il 5 Aprile 1956)

Summary. — The single bremsstrahlung is studied here with Bloch and Nordsieck's approximation. The resulting formula is compared with that obtained by the perturbation method. The agreement of the two formulae for low energy photons is verified. Then we study the polarization of the emitted radiation, using our approximate formula. In particular we show in a simple way that, for emission angles lying in a certain range of values, the emitted radiation is mostly polarized with its electric vector perpendicular to the emission plane, in agreement with Wick's results. Moreover it appears that, for a certain angle of emission, the low energy photons are entirely polarized with the electric vector perpendicular to the emission plane.

Lately some authors ⁽¹⁻³⁾ have applied Bloch and Nordsieck's approximation to the study of electromagnetic phenomena for which the perturbation calculation should have been too complicated, such as multiple bremsstrahlung and multiple production of photons in electron positron annihilation. The

⁽¹⁾ E. CORINALDESI: *Nuovo Cimento*, **12**, 571 (1954).

⁽²⁾ R. ASCOLI: *Nuovo Cimento*, **2**, 1 (1955).

⁽³⁾ R. ARNOWITT and S. DESER: *Nuovo Cimento*, **2**, 707 (1955).

purpose of this paper is to apply the Bloch and Nordsieck's treatment ⁽⁴⁾ (in its covariant formulation by Thirring and Touschek ⁽⁵⁾) to the study of single bremsstrahlung. So, a comparison with the result of the perturbation theory is possible, and we verify the agreement of the two methods for low energy photons.

As a result of our approximate treatment, we show that the emitted radiation is mostly polarized with its electric vector perpendicular to the emission plane for an emission angle lying in a certain range of values; moreover an emission angle exists, for which the radiation is entirely polarized perpendicularly to the emission plane. These results agree for low energy photons with those of WICK ⁽⁶⁾, MAY and WICK ⁽⁷⁾, GLUCKSTERN, HULL and BREIT ^(8,9); moreover they are deduced in a very simple manner and they hold either taking into account the screening or not. Since, as we shall see, Bloch and Nordsieck's treatment of the bremsstrahlung leads to the same formula both in classical theory and in quantum theory, this confirms that Wick's result concerning the bremsstrahlung polarization has its source in the classical theory.

1. - Derivation of the Bremsstrahlung Formula in Bloch and Nordsieck's Approximation.

We call $d\sigma$ the cross section for the single bremsstrahlung process in which an electron of initial momentum \mathbf{p}_0 takes a final momentum \mathbf{p} contained in the solid angle $d\Omega_p$, whereas a photon is emitted with momentum \mathbf{k} in the solid angle $d\Omega_k$, with an energy between k and $k + dk$ ⁽¹⁰⁾ and a polarization vector ϵ (ϵ gives the direction of the electric field of the emitted photon). Besides, E_0 and E are the initial and final total energy of the electron, and α is the angle between \mathbf{p}_0 and \mathbf{p} .

To apply Bloch and Nordsieck's method to the single bremsstrahlung we must study the emission of one photon in the elastic scattering of an electron by a nucleus, neglecting the reaction of the photon on the electron.

If we call $I(\alpha)d\Omega_p$ the cross section for the scattering of the electron within the solid angle $d\Omega_p$, then the cross section $d\sigma$ is obtained multiplying

⁽⁴⁾ F. BLOCH and A. NORDSIECK: *Phys. Rev.*, **52**, 54 (1937).

⁽⁵⁾ W. THIRRING and B. TOUSCHEK: *Phil. Mag.*, **42**, 245 (1951).

⁽⁶⁾ G. C. WICK: *Phys. Rev.*, **81**, 467 (1951).

⁽⁷⁾ M. MAY and G. C. WICK: *Phys. Rev.*, **81**, 628 (1951).

⁽⁸⁾ R. L. GLUCKSTERN, M. H. HULL jr. and G. BREIT: *Phys. Rev.*, **90**, 1026 (1953).

⁽⁹⁾ R. L. GLUCKSTERN and M. H. HULL jr.: *Phys. Rev.*, **90**, 1030 (1953).

⁽¹⁰⁾ We use natural units, $\hbar = 1$, $c = 1$.

$I(\alpha)d\Omega_p$ by the probability $w_1 d\Omega_k dk$ for the emission of a photon having a momentum contained in the solid angle $d\Omega_k$, an energy comprised in the range between k and $k + dk$ and a polarization vector ϵ .

The photons are emitted independently from each other, so the probability w_N for the emission of N photons, is given by Poisson's formula:

$$(1) \quad w_N = \frac{\bar{N}^N}{N!} \exp[-\bar{N}],$$

where \bar{N} is the mean number of the emitted photons.

In our case is $\bar{N} \ll 1$, ($\bar{N} \cong 10^{-2}$)⁽²⁾, $\exp[-\bar{N}] \cong 1$, and, for $N = 1$,

$$(2) \quad w_1 = \bar{N} \exp[-\bar{N}] \cong \bar{N}.$$

Therefore we may put $w_1 d\Omega_k dk = \bar{n} d\Omega_k dk$ where \bar{n} is the mean number of the photons emitted per unit solid angle and per unit energy range with polarization vector ϵ . So we obtain:

$$(3) \quad d\sigma = I(\alpha) d\Omega_p \bar{n} d\Omega_k dk.$$

The elastic scattering cross section for an electron of velocity $v_0 = \beta_0$ in the Coulomb field of a nucleus of charge Ze , is⁽¹¹⁾:

$$(4) \quad I(\alpha) d\Omega_p = \frac{Z^2 e^4}{(2mv_0^2)^2} (1 - v_0^2) \left(1 - v_0^2 \sin^2 \frac{\alpha}{2}\right) \frac{d\Omega_p}{\sin^4 \alpha/2}.$$

Calling $\mathbf{q} = \mathbf{p}_0 - \mathbf{p}$ the momentum transferred to the nucleus, it is $q^2 = 4p_0^2 \sin^2 \alpha/2$; therefore a simple calculation gives:

$$(5) \quad I(\alpha) d\Omega_p = Z^2 e^4 \frac{4E_0^2 - q^2}{q^4} d\Omega_p.$$

On the other hand, Bloch and Nordsieck's method, in the generalized form of Thirring and Touschek^(5,2,12), gives the following formula

⁽¹¹⁾ N. F. MOTT and H. S. W. MASSEY: *Theory of Atomic Collisions* (Oxford, 1933), p. 58.

⁽¹²⁾ See also J. M. JAUCH and F. ROHRlich: *Helv. Phys. Acta*, **27**, 613 (1954).

for \bar{n} ⁽¹³⁾:

$$(6) \quad \bar{n} = \frac{e^2}{2\pi^2} \cdot \frac{|\mathbf{k}|}{2} \cdot \left| \frac{\mathbf{p}_0 \cdot \boldsymbol{\epsilon}}{p_{0\mu} k_\mu} - \frac{\mathbf{p} \cdot \boldsymbol{\epsilon}}{p_\mu k_\mu} \right|^2 \quad (14).$$

Calling ϑ_0 and ϑ the angles of \mathbf{p}_0 and \mathbf{p} with respect to \mathbf{k} and putting $\mathbf{p}_0 \cdot \boldsymbol{\epsilon} = p_{0l}$, $\mathbf{p} \cdot \boldsymbol{\epsilon} = p_l$ we obtain ⁽¹⁵⁾:

$$(7) \quad \bar{n} d\Omega_k dk = \frac{e^2}{4\pi^2} d\Omega_k \frac{dk}{k} \left| \frac{p_{0l}}{E_0 - p_0 \cos \vartheta_0} - \frac{p_l}{E - p \cos \vartheta} \right|^2.$$

In our case we must apply this formula to the elastic scattering of the electrons by the nuclei; so $p_0 = p$, $E_0 = E$ and we have:

$$(8) \quad \bar{n} d\Omega_k dk = \frac{e^2}{4\pi^2} d\Omega_k \frac{dk}{k} \left| \frac{p_{0l}}{E_0 - p_0 \cos \vartheta_0} - \frac{p_l}{E_0 - p_0 \cos \vartheta} \right|^2.$$

At last, substituting (8) and (5) in (3), we obtain:

$$(9) \quad d\sigma = \frac{Z^2 e^6}{4\pi^2} d\Omega_p d\Omega_k \frac{dk}{k} \frac{4E_0^2 - q^2}{q^4} \left| \frac{p_{0l}}{E_0 - p_0 \cos \vartheta_0} - \frac{p_l}{E_0 - p_0 \cos \vartheta} \right|^2.$$

We may now compare these results with those obtained from the perturbation theory.

This latter gives ^(8,16):

$$(10) \quad d\sigma = \frac{Z^2 e^6}{4\pi^2} \frac{p}{p_0} \frac{dk}{k q^4} d\Omega_p d\Omega_k \cdot$$

$$\cdot \left[(4E_0^2 - q^2) \left(\frac{p_l}{E - p \cos \vartheta} \right)^2 + (4E^2 - q^2) \left(\frac{p_{0l}}{E_0 - p_0 \cos \vartheta_0} \right)^2 - \right.$$

$$- 2(4EE_0 - q^2) \frac{p_l p_{0l}}{(E - p \cos \vartheta)(E_0 - p_0 \cos \vartheta_0)} -$$

$$\left. - k^2 \left(\frac{E - p \cos \vartheta}{E_0 - p_0 \cos \vartheta_0} + \frac{E_0 - p_0 \cos \vartheta_0}{E - p \cos \vartheta} - 2 - \frac{q^2}{(E - p \cos \vartheta)(E_0 - p_0 \cos \vartheta_0)} \right) \right],$$

where here $\mathbf{q} = \mathbf{p}_0 - \mathbf{p} = \mathbf{k}$.

⁽¹³⁾ The formula for \bar{n} has been derived by THIRRING and TOUSCHEK for a classical electron. Arguments for the validity of the formula for a quantized electron have been given by JAUCH and ROHRlich. A proof of the formula for a quantized electron has been deduced by one of us (R. ASCOLI) and will appear in a following paper.

⁽¹⁴⁾ In this paper we use non rationalized units for the charge. $p_{0\mu}$, p_μ , k_μ are four-dimensional vectors; $p_{0\mu} k_\mu$ and $p_\mu k_\mu$ denote four-dimensional scalar products.

⁽¹⁵⁾ We put here $p_0 = |\mathbf{p}_0|$, $p = |\mathbf{p}|$.

⁽¹⁶⁾ M. MAY: *Phys. Rev.*, **84**, 265 (1951).

As the photon energy k tends to zero, the last term in the brackets tends to zero owing to k^2 . Moreover, $p = p_0$, $E = E_0$ and $\mathbf{q} = \mathbf{p}_0 - \mathbf{p}$; therefore the remaining terms in the brackets give

$$(4E_0^2 - q^2) \left(\frac{p_{0l}}{E_0 - p_0 \cos \vartheta_0} - \frac{p_l}{E_0 - p_0 \cos \vartheta} \right)^2.$$

So, whichever the electron energy is, formula (10) gets into formula (9), which had been obtained with Bloch and Nordsieck's approximation. If we compare (9) and (10) for $k \neq 0$, we see that the disagreement between the two formulae is mostly due to the difference in the value of the $1/q^4$ factor, which is very sensitive to the value of k . Therefore a better approximation than Bloch and Nordsieck's may be obtained in a very simple way taking into account the reaction of the fields on the electron only through the conservation of momenta⁽¹⁷⁾. This corresponds to put into (3), for $I(\alpha)$ the expression (5) in which it is $\mathbf{q} = \mathbf{p}_0 - \mathbf{p} - \mathbf{k}$ instead of $\mathbf{q} = \mathbf{p}_0 - \mathbf{p}$.

2. - Polarization of the Emitted Radiation.

We start here from formula (9) derived above by Bloch and Nordsieck's approximation, and we deduce some properties of the polarization of the emitted radiation.

We call φ the angle between the planes of \mathbf{p}_0 , \mathbf{k} and of \mathbf{p} , \mathbf{k} and ψ the angle which the direction of the photon electric vector $\boldsymbol{\epsilon}$ forms with the plane of \mathbf{p}_0 , \mathbf{k} (Fig. 1). Then, if p_{0l} and p_l are expressed as the projections of p_0 and p on the direction of $\boldsymbol{\epsilon}$, formula (9) becomes

$$(12) \quad d\sigma = \frac{Z^2 e^6}{4\pi^2} d\Omega_p d\Omega_k \frac{dk}{k} \frac{4E_0^2 - q^2}{q^4} \cdot \left[\frac{p_0 \cos \psi \sin \vartheta_0}{E_0 - p_0 \cos \vartheta_0} - \frac{p_0 \cos(\varphi - \psi) \sin \vartheta}{E_0 - p_0 \cos \vartheta} \right]^2.$$

First of all, we see from this formula that the radiation is, in our approximation, entirely polarized in some plane for a given direction of the scattered

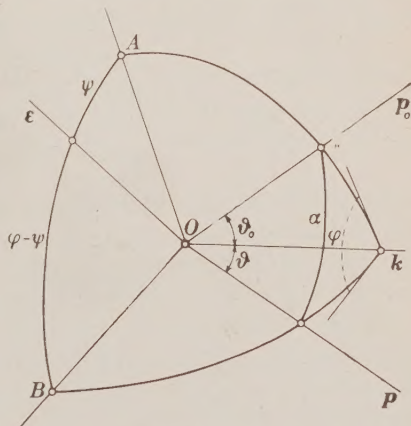


Fig. 1. - The directions of \mathbf{p}_0 , \mathbf{p} , \mathbf{k} and $\boldsymbol{\epsilon}$ are represented starting from the center O of a sphere. The plane AOB is perpendicular to \mathbf{k} . OA lies in the plane of \mathbf{p}_0 and \mathbf{k} . OB lies in the plane of \mathbf{p} and \mathbf{k} .

⁽¹⁷⁾ On this subject see also E. L. LOMON: *Nuclear Physics*, **1**, 101 (1956).

electron. In fact, the cross section $d\sigma$ depends on ψ only through the expression in the brackets. This is a sinusoidal function of ψ , so a direction of ϵ exists for which $d\sigma = 0$. The radiation is then entirely polarized perpendicularly to this direction.

To study the polarization direction, we call $d\sigma_{\parallel}$ the cross section for the emission of the photons, the polarization vector of which lies in the emission plane \mathbf{p}_0, \mathbf{k} ($\psi = 0$), and we call $d\sigma_{\perp}$ the cross section for the photons, the polarization vector of which is perpendicular to the emission plane ($\psi = \pi/2$).

We have from (12)

$$d\sigma_{\parallel} = \frac{Z^2 e^6}{4\pi^2} d\Omega_p d\Omega_k \frac{dk}{k} \frac{4E_0^2 - q^2}{q^4} \left[\frac{p_0 \sin \vartheta_0}{E_0 - p_0 \cos \vartheta_0} - \frac{p_0 \cos \varphi \sin \vartheta}{E_0 - p_0 \cos \vartheta} \right]^2,$$

and

$$d\sigma_{\perp} = \frac{Z^2 e^6}{4\pi^2} d\Omega_p d\Omega_k \frac{dk}{k} \frac{4E_0^2 - q^2}{q^4} \left(\frac{p_0 \sin \varphi \sin \vartheta}{E_0 - p_0 \cos \vartheta} \right)^2.$$

Therefore:

$$(13) \quad \frac{d\sigma_{\parallel}}{d\sigma_{\perp}} = \left(\frac{\sin \vartheta_0}{E_0 - p_0 \cos \vartheta_0} - \frac{\sin \vartheta \cos \varphi}{E_0 - p_0 \cos \vartheta} \right)^2 \left(\frac{E_0 - p_0 \cos \vartheta}{\sin \vartheta \sin \varphi} \right)^2.$$



Fig. 2. - Spheric triangle of sides $\vartheta_0, \vartheta, \alpha$. p_0, p and k denote the intersections of the vectors $\mathbf{p}_0, \mathbf{p}, \mathbf{k}$ with the sphere of Fig. 1.

Suppose we integrate (12) over the direction of the scattered electron. We call γ the angle between the planes of \mathbf{p}_0, \mathbf{p} and of \mathbf{p}_0, \mathbf{k} . Then for each value of γ the most important contribution to the integration comes from the neighbourhood of $q = 0$ (or $\alpha = 0$), owing to the $1/q^4$ factor. Therefore if we make the experiment without observing the direction of the scattered electron, some conclusion about the photon polarization may be driven by considering the behaviour of (13) for small values of α , keeping constant ϑ_0 and γ ⁽¹⁸⁾.

From the spheric triangle of sides ϑ_0, ϑ and α (Fig. 2) we have

$$\cos \alpha = \cos \vartheta_0 \cos \vartheta + \sin \vartheta_0 \sin \vartheta \cos \varphi,$$

$$\cos \vartheta = \cos \vartheta_0 \cos \alpha + \sin \vartheta_0 \sin \alpha \cos \gamma,$$

⁽¹⁸⁾ This reasoning leads to an exact result at the limit when the photon energy tends to zero, and it leads to an approximate result otherwise.

and

$$\sin \vartheta \sin \varphi = \sin \gamma \sin \alpha.$$

Using these relations and $p_0/E_0 = \beta_0$ formula (13) may be transformed into:

$$(14) \quad \frac{d\sigma_{\parallel}}{d\sigma_{\perp}} = \left[\frac{1}{\sin \gamma (1 - \beta_0 \cos \vartheta_0)} \left(\frac{\cos \alpha - 1}{\sin \alpha} \sin \vartheta_0 - (\cos \vartheta_0 - \beta_0) \cos \gamma \right) \right]^2,$$

which contains only ϑ_0 , γ and α .

For sufficiently small values of α , the expression $(\cos \alpha - 1)/\sin \alpha$ is very small and may be neglected.

Then the right hand side of (14) becomes:

$$(15) \quad \left[\frac{\beta_0 - \cos \vartheta_0}{1 - \beta_0 \cos \vartheta_0} \cotg \gamma \right]^2.$$

This expression vanishes as $\cos \vartheta_0 = \beta_0$. So a particular emission angle exists, for which the radiation is entirely polarized with its electric vector perpendicular to the emission plane.

Moreover for emission angles in the neighbourhood of this value the expression (15) is small and the radiation is mostly polarized with its electric vector perpendicular to the emission plane.

These conclusions agree exactly with those that Gluckstern, Hull and Breit have derived from the perturbation theory in the limit of vanishing photon energy and they agree approximately with the conclusions which hold for photons of unvanishing energy ^(6,7,16,8,9).

It is interesting to observe that both quantities $I(\alpha)$ and \bar{n} which enter in the expression (3) of $d\sigma$, are the same in classical theory and in quantum theory. Therefore our results hold in both theories. This shows that the prevalent polarization of the bremsstrahlung with the electric vector of the photons perpendicular to the emission plane has its source in the classical theory.

If we want to take into account the screening, we must only substitute in (3) the scattering cross section $I(\alpha)d\Omega_p$ for the electrons in a Coulomb field with that for the electrons in a screened Coulomb field, whereas the factor \bar{n} remains unchanged. Now the polarization direction of the photons appears only in the factor \bar{n} , therefore the conclusions concerning the polarization are the same even taking into account the screening.

RIASSUNTO

Si studia la bremsstrahlung semplice con l'approssimazione di Bloch e Nordsieck. Si confronta la formula ottenuta con quella data dal metodo perturbativo, e si verifica la concordanza delle due formole per fotoni di bassa energia. Usando il nostro risultato approssimativo si studia inoltre la polarizzazione della radiazione emessa. Si mostra in particolare in modo semplice che, per angoli di emissione compresi entro certi limiti, la radiazione emessa è prevalentemente polarizzata col vettore elettrico perpendicolare al piano di emissione in accordo coi risultati di Wick. Si mostra inoltre che per un certo angolo di emissione i fotoni di bassa energia sono totalmente polarizzati col vettore elettrico perpendicolare al piano di emissione.

Angular Correlation Methods for Determining the Spins of the Hyperons.

R. GATTO

Istituto di Fisica e Scuola di Perfezionamento dell'Università - Roma
Istituto Nazionale di Fisica Nucleare - Sezione di Roma

(ricevuto il 16 Aprile 1956)

Summary. — The intrinsic specification of the configuration of a cascade of two body decays — such as $\Xi^- \rightarrow \Lambda^0 + \pi^-$, $\Lambda^0 \rightarrow p + \pi^-$, or $\Sigma^0 \rightarrow \Lambda^0 + \gamma$. $\Lambda^0 \rightarrow p + \pi^-$ — requires a parameter, the distribution of which will reflect the dynamical features of the process. A detailed discussion is given of these distributions and it is shown that when a sufficient number of Ξ^- cascade decays, and, similarly, of Σ^0 cascade decays, will have been collected, the comparison with the theory will furnish information on the spins and parities of the hyperons involved.

1. — Introduction.

It was firstly pointed out by DALITZ ⁽¹⁾ that the angular and energy distribution of the three pions emitted in the τ^+ -decay could give information on the spin and parity of the τ^+ . In fact in the decay of a τ^+ at rest into three pions two parameters are required to specify the decay apart from the spatial orientation. The distribution of these parameters will reflect the dynamical features of the decay. On the other hand no intrinsic parameters are needed to specify, apart from the spatial orientation, the configuration of a two-body decay of a particle at rest, averaged over the final polarizations. However, a particularly favorable situation occurs in the case of cascade two-body decays. To specify, apart from the spatial orientation, the configuration of the cascade — which includes two successive two-body decays — an intrinsic parameter is required. A convenient choice for such parameter

⁽¹⁾ R. H. DALITZ: *Phil. Mag.*, **44**, 1068 (1953).

is the angle between the line of flight of the particle emitted in the first decay which subsequently disintegrates and the direction of emission of its decay products in the center of mass system. The distribution of this parameter will reflect the dynamical features of the transition.

The present statistics of the $K_{S\pi}^+$ events are consistent, excluding high spins, only with the spin-parity assignments 0^- or 2^- to the τ^+ -meson ⁽²⁾. However, if the τ -meson were 2^- one would expect the $\tau^+ \rightarrow \pi^+ + \gamma$ decay mode (monochromatic π^+ of ~ 127 MeV kinetic energy) to occur rather frequently but no evidence has been reported so far of such decay — forbidden for 0^- - τ -meson. RUDERMANN and KARPLUS ⁽³⁾, developing an argument similar to that proposed ⁽⁴⁾ to discard the suggested high spin explanation of the long lifetimes, conclude that the spin of the Λ^0 is $\frac{1}{2}$ or $\frac{3}{2}$ and its parity the same as that of the proton if the spin is $\frac{3}{2}$. The angular correlation discussed here will give information on the spins and parities of the different hyperons. A preliminary report of the present investigation has already been given ⁽⁵⁾. A feature of these methods is that no knowledge at all is required of the state of polarization of the parent particle of the cascade, the Ξ^- or the Σ^0 . Therefore the statistics may include Ξ^- and respectively Σ^0 of any origin — any cascade Ξ^- -decay, and similarly any cascade Σ^0 -decay, gives a new point in the statistics. The situation is here similar to the case of the determination of the spin of the τ^+ — no knowledge at all of the possible polarization of τ^+ is required. On the other hand, the angular correlations in reactions such as, for instance, the sequence $\pi^- + p \rightarrow Y + K$, $Y \rightarrow N + \pi$, essentially depend on the polarization of the produced Y — to be specified by a certain number of parameters, which however are expected to depend on the energy and on the angle of emission of the Y . In the case of cascade decays a similar situation would occur for the correlation between the first and the second decay plane — not considered here. In all such cases the collection of data relative to widely different experimental conditions will strongly reduce the correlation effects.

2. — The Cascade Decay of the Ξ^- .

2'1. — Consider the decay of the Ξ^- in its rest system (see Fig. 1). We choose as quantization axis for the angular momenta the direction of emission of the Λ^0 . The vector \mathbf{l}_1 of the relative angular momentum between the emitted Λ^0 and π^- will precess around the quantization axis, always orthogonal to it.

(2) Results obtained at Berkeley, MIT, Columbia, Bristol and Padua.

(3) M. RUDERMANN and R. KARPLUS: *Phys. Rev.* (in the press).

(4) R. GATTO: *Nuovo Cimento*, **1**, 372 (1955).

If the Ξ^- is in a state with component m_s of its spin S , the Λ^0 will be emitted in a state with component $m_s = m_s$ of its spin s . In the following we shall use the notation $[SPsp]$ to indicate the case referring to a Ξ^- with spin S and parity P (relative to the nucleon) and to a Λ^0 with spin s and parity p (relative to the nucleon). We assume that the Λ^0 does not suffer any appreciable change in polarization until it decays. Consider the decay of the Λ^0 in its rest system (Fig. 2). Let us denote with

$$(1) \quad \langle \mathbf{n}, \tfrac{1}{2}m_{\frac{1}{2}} | T_2 | sm_s \rangle,$$

the element of the transition matrix for the decay of the Λ^0 from the state with component m_s of the spin into a proton and into a pion, the latter being emitted in the direction of the unit vector \mathbf{n} . We call θ the angle formed by \mathbf{n} with the quantization axis — which coincides with the line of flight of the Λ^0 assuming that the Λ^0 has not suffered appreciable deviations. The distributions for the angle θ will be given by

$$(2) \quad \sum_{m_{\frac{1}{2}}} |\langle \mathbf{n}, \tfrac{1}{2}m_{\frac{1}{2}} | T_2 | sm_s \rangle|^2.$$

Only one value for the relative angular momentum l_2 between the final proton and pion is allowed by conservation of total angular momentum and of total parity: $l_2 = s - \frac{1}{2}$ if the parity of the Λ^0 relative to the proton is $(-)^{s+\frac{1}{2}}$, $l_2 = s + \frac{1}{2}$ if the parity is $(-)^{s-\frac{1}{2}}$. As a consequence the angular distribution (2) is completely determined from geometrical considerations. We can give an explicit form to (2) using the Racah technique. The matrix element (1) is first written as

$$\langle \mathbf{n}, \tfrac{1}{2}m_{\frac{1}{2}} | T_2 | sm_s \rangle = (l_2 \tfrac{1}{2}m, m_{\frac{1}{2}} | sm_s) Y_{l_2}^{m_{\frac{1}{2}}}(\mathbf{n}) \langle \tfrac{1}{2} || l_2 || s \rangle,$$

where $\langle \tfrac{1}{2} || l_2 || s \rangle$ is a reduced matrix element. To evaluate (2) we first use the addition theorem for spherical harmonics and then we carry out the summations over the magnetic quantum numbers — following Racah's method, after a suitable reshuffling of the arguments of the Clebsch-Gordon coefficients ⁽⁵⁾.

⁽⁵⁾ The general formalism can be found for instance in F. COESTER and J. M. JAUCH: *Helv. Phys. Acta*, **26**, 3, (1953).

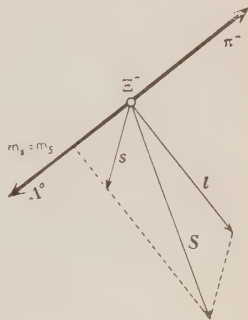


Fig. 1.

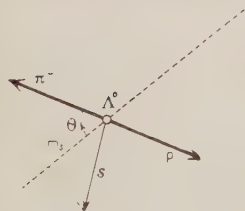


Fig. 2.

The final result is

$$(3) \quad (2) = \text{constant} \times \sum_l (l_2 l_2 00 | l 0) (s l m_s 0 | s m_s) W(ss l_2 l_2 \frac{1}{2} l) Y_l^0(\mathbf{n}).$$

Note that $(l_2 l_2 00 | l 0)$ limits the summation to even values of l (conservation of parity) from 0 to $2l_2$. However, when $l_2 = s + \frac{1}{2}$ the triangular condition for the other coefficient cannot be satisfied for $l = 2l_2$ and so the summation is in any case interrupted at $l = 2s - 1$ irrespective of the parity of the Λ^0 . Thus, for the particular case $s = \frac{1}{2}$ one always gets an isotropic distribution (independent of the polarization) — a well-known result ⁽⁶⁾. If we start from an unpolarized sample of Ξ^- the distribution for the angle θ will be given by

$$(4) \quad W(\cos \theta) = \sum_{m_s} \sum_{m_s} |\langle \mathbf{n}_0, s m_s | T_1 | S m_s \rangle|^2 \sum_{m_{\frac{1}{2}}} |\langle \mathbf{n}, \frac{1}{2} m_{\frac{1}{2}} | T_2 | s m_s \rangle|^2,$$

where

$$(5) \quad \langle \mathbf{n}_0 s m_s | T_1 | S m_s \rangle,$$

is the element of the transition matrix for the decay $\Xi^- \rightarrow \Lambda^0 + \pi^-$. The summation over m_s has been done incoherently: in fact our particular choice of the quantization axis destroys the interference terms — starting from the state m_s only the state with $m_s = m_s$ is reached. The matrix element (5) can be written as

$$(6) \quad \langle \mathbf{n}_0 s m_s | T_1 | S m_s \rangle = \sum_{l_1} (l_1 s 0 m_s | S m_s) T_1(l_1),$$

where $T_1(l_1)$ is proportional to the reduced matrix element. The values allowed for l_1 by conservation of total angular momentum and of total parity are reported in Table I for spin values up to $\frac{5}{2}$.

The values of $[SP]$ are indicated in the first column, the values of $[sp]$ referring to each column are given in the first row. After inserting (3) and (6) into (4) we again reshuffle the arguments of the Clebsch-Gordon coefficients and then use Racah's method to carry out the summations over the magnetic quantum numbers. Expressing in terms of Legendre polynomials the final result is

$$(7) \quad W(\cos \theta) = \\ = \text{constant} \times \sum_{\nu l_1 l'_1} T(l_1) T(l'_1) (l_1 l'_1 00 | \nu 0) (l_2 l_2 00 | \nu 0) W(ss l_1 l'_1 \nu S) W(ss l_2 l_2 \nu \frac{1}{2}) P_\nu(\cos \theta).$$

⁽⁶⁾ For a general proof on elementary arguments see R. GATTO: *Nuovo Cimento*, **2**, 841 (1955).

TABLE I. — Possible values of l_1 for $\Xi^- \rightarrow \Lambda^0 + \pi^-$.

$\Xi P \backslash s p$	$\frac{3}{2} + (l_2 = 1)$	$\frac{3}{2} - (l_2 = 2)$	$\frac{5}{2} + (l_2 = 3)$	$\frac{5}{2} - (l_2 = 2)$
$\frac{1}{2} +$	1	2	3	2
$\frac{1}{2} -$	2	1	2	3
$\frac{3}{2} +$	1, 3	0, 2	1, 3	2, 4
$\frac{3}{2} -$	0, 2	1, 3	2, 4	1, 3
$\frac{5}{2} +$	1, 3	2, 4	1, 3, 5	0, 2, 4
$\frac{5}{2} -$	2, 4	1, 3	0, 2, 4	1, 3, 5

2'2. — To illustrate the nature of the correlation it may be instructive to give an elementary derivation for the cases [$\frac{1}{2}P\frac{3}{2}p$]. It can be seen from (7) that in the cases [$\frac{1}{2}P\frac{3}{2}p$] the correlation has always the form

$$(8) \quad W(\cos \theta) = 1 + 3 \cos^2 \theta,$$

so that no conclusion on the relative parity of the Ξ^- and of the Λ^0 can be obtained from the measurement in these cases. The form (8) of the correlation comes out in the following way. We start from an unpolarized sample of Ξ^- . Due to our choice of the quantization axis the only transition which may occur are those which lead from the magnetic sublevel $+\frac{1}{2}$ for the Ξ^- 's spin to the magnetic sublevel $+\frac{1}{2}$ for the Λ^0 spin, and from the sublevel $-\frac{1}{2}$ for the Ξ^- to the sublevel $-\frac{1}{2}$ for the Λ^0 . The two sublevels $\mp\frac{1}{2}$ for the Λ^0 spin will therefore result equally populated — for symmetry reasons — while the two other sublevels $\mp\frac{3}{2}$ will result completely unpopulated. It will be sufficient to consider the subsequent decays from the sublevel $+\frac{1}{2}$. The two possibilities are: (i) final proton in the sublevel $+\frac{1}{2}$, and, accordingly, the component of the orbital angular momentum between the final pion and proton is zero; (ii) final proton in the sublevel $-\frac{1}{2}$ and component of the orbital angular momentum $+1$. The corresponding relative intensities — squared Clebsch-Gordon coefficients — are 2 and 1 respectively for case (i) and (ii), if $l_2 = 1$ ($p = +1$), and 2 and 3 respectively if $l_2 = 2$ ($p = -1$). In both cases we obtain

$$p = +1, l_2 = 1 \quad W(\cos \theta) = 2 |Y_1^0|^2 + |Y_1^1|^2 = 2 \cos^2 \theta + \frac{1}{2}(1 - \cos^2 \theta) \sim 1 + 3 \cos^2 \theta,$$

$$p = -1, l_2 = 2 \quad W(\cos \theta) = 2 |Y_2^0|^2 + 3 |Y_1^1|^2 = \frac{1}{2}(3 \cos^2 \theta - 1)^2 + \frac{3}{2} \cos^2 \theta (1 - \cos^2 \theta) \sim 1 + 3 \cos^2 \theta.$$

2'3. — Coming back to the general expression (7) we note that only even values of ν may contribute to the sum. Therefore the correlation has the form

$$(9) \quad W(\cos \theta) = \sum_{\nu=0,2,\dots,2S-1} a_{\nu}(\cos \theta)^{\nu},$$

as indeed follows from the more general theorems. Moreover the correlation only depends on the relative parity of the Ξ^- and of the Λ^0 . From Table I we see that in the cases $[\frac{3}{2} + \frac{3}{2} -]$ and $[\frac{3}{2} - \frac{3}{2} +]$, $[\frac{5}{2} + \frac{5}{2} -]$ and $[\frac{5}{2} - \frac{5}{2} +]$ the lowest l_1 is zero and therefore, if — as expected — the contribution of the higher values of l_1 is negligible, the correlation is nearly isotopic in these cases, and in the similar ones for higher spin values. In Table II we report the angular correlations which are found for the cases considered in Table I. For the cases where more values of l_1 are admitted we have introduced the parameter ξ to account for the possible admixture of the nearest possible l_1 — ξ is the ratio of the reduced matrix element of the next higher l_1 to that of the lowest l_1 , and it can only take real values. It is impossible to predict the value of ξ in the absence of a detailed theory. However, as a first approximation, one would assume $\xi = 0$. This assumption is sufficiently accurate

TABLE II. — *The angular correlation for the cascade $\Xi^- \rightarrow \Lambda^0 + \pi^-$, $\Lambda^0 \rightarrow p + \pi^-$.*

$\left. \begin{array}{l} [\frac{1}{2} + \frac{3}{2} +][\frac{1}{2} - \frac{3}{2} -] \\ [\frac{1}{2} + \frac{3}{2} -][\frac{1}{2} - \frac{3}{2} +] \end{array} \right\}$	$W(\cos \theta) = 0.500 + 1.500 \cos^2 \theta$
$\left. \begin{array}{l} [\frac{3}{2} + \frac{3}{2} +][\frac{3}{2} - \frac{3}{2} -] \end{array} \right\}$	$W(\cos \theta) = 1.400 - 1.200 \cos^2 \theta + \xi(0.600 - 1.800 \cos^2 \theta) + \xi^2(0.600 + 1.200 \cos^2 \theta)$
$[\frac{3}{2} + \frac{3}{2} -][\frac{3}{2} - \frac{3}{2} +]$	$W(\cos \theta) = 1.000 + \xi(0.448 - 1.340 \cos^2 \theta) + \xi^2 0.200$
$\left. \begin{array}{l} [\frac{5}{2} + \frac{5}{2} +][\frac{5}{2} - \frac{5}{2} -] \end{array} \right\}$	$W(\cos \theta) = 0.900 + 0.300 \cos^2 \theta + \xi(0.980 - 2.939 \cos^2 \theta) + \xi^2(1.100 - 0.300 \cos^2 \theta)$
$\left. \begin{array}{l} [\frac{5}{2} - \frac{3}{2} +][\frac{5}{2} + \frac{3}{2} -] \end{array} \right\}$	$W(\cos \theta) = 1.357 - 1.071 \cos^2 \theta + \xi(0.700 - 2.100 \cos^2 \theta) + \xi^2(0.643 + 1.071 \cos^2 \theta)$
$\left. \begin{array}{l} [\frac{1}{2} + \frac{5}{2} +][\frac{1}{2} - \frac{5}{2} -] \\ [\frac{1}{2} + \frac{5}{2} -][\frac{1}{2} - \frac{5}{2} +] \end{array} \right\}$	$W(\cos \theta) = 0.750 - 1.500 \cos^2 \theta + 3.750 \cos^4 \theta$
$\left. \begin{array}{l} [\frac{3}{2} + \frac{5}{2} +][\frac{3}{2} - \frac{5}{2} -] \end{array} \right\}$	$W(\cos \theta) = 0.600 + 1.198 \cos^2 \theta + \xi(-0.367 + 6.616 \cos^2 \theta - 9.186 \cos^4 \theta) + \xi^2(0.525 + 2.548 \cos^2 \theta - 1.875 \cos^4 \theta)$
$[\frac{3}{2} + \frac{5}{2} -][\frac{3}{2} - \frac{5}{2} +]$	$W(\cos \theta) = 0.429 + 4.286 \cos^2 \theta - 4.286 \cos^4 \theta + \xi(-0.249 + 4.724 \cos^2 \theta - 6.561 \cos^4 \theta) + \xi^2(-0.696 - 0.536 \cos^2 \theta + 2.411 \cos^4 \theta)$
$[\frac{5}{2} + \frac{5}{2} +][\frac{5}{2} - \frac{5}{2} -]$	$W(\cos \theta) = 1.457 - 1.371 \cos^2 \theta + \xi(1.231 - 7.056 \cos^2 \theta + 5.345 \cos^4 \theta) + \xi^2(0.858 + 1.550 \cos^2 \theta - 1.875 \cos^4 \theta)$
$[\frac{5}{2} + \frac{5}{2} -][\frac{5}{2} - \frac{5}{2} +]$	$W(\cos \theta) = 1 + \xi(0.478 - 1.434 \cos^2 \theta) + \xi^2(0.282 - 0.536 \cos^2 \theta + 0.482 \cos^4 \theta)$

unless the «size» of the Ξ^- is exceedingly large, comparable, say, to the nucleon Compton wavelength, and/or very strong interaction exists between the emitted Λ_0 and π^- — these last effects could however be evaluated by a procedure suggested by BRUECKNER and WATSON ⁽⁷⁾.

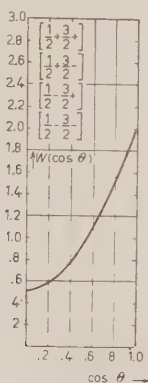


Fig. 3.

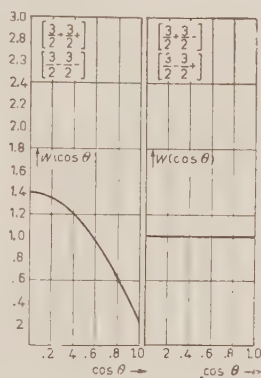


Fig. 4.

As a consequence of parity conservation the correlation can only depend on $\cos^2 \theta$. Therefore we can take for θ the acute angle between the direction of emission of the Λ^0 secondaries in the Λ^0 center of mass system and the line of flight of the Λ^0 , and reduce the comparison only to the values $0^\circ \leq \theta \leq 90^\circ$ — we assume *a priori* that parity conservation holds and are not interested in its verification. The angular correlation $W(\cos \theta)$ is the probability per unit

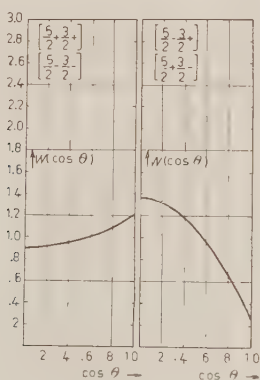


Fig. 5.

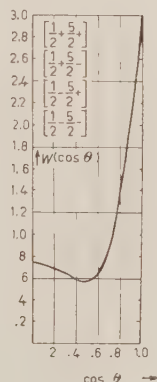


Fig. 6.

⁽⁷⁾ K. BRUECKNER and K. M. WATSON: *Phys. Rev.*, **87**, 621 (1952).

solid angle. In Table II the expressions are normalized such that the integral from 0 to $\pi/2$ of $W(\cos \theta) d(\cos \theta)$ is equal to 1 if all terms proportional to ξ and ξ^2 are neglected. In Fig. 3-8 we report the graphs of $W(\cos \theta)$ for the different cases of Table II, assuming that all terms proportional to ξ and ξ^2 are negligible.

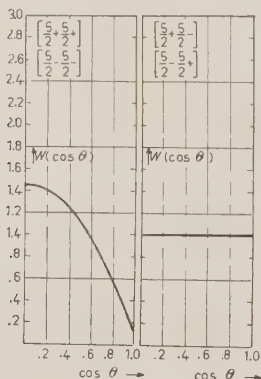


Fig. 7.

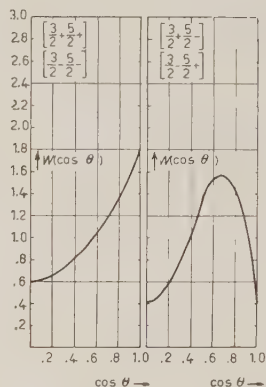


Fig. 8.

The recent analysis of RUDERMANN and KARPLUS⁽³⁾ of the mesonic non-mesonic ratio in the decay of hyperfragments predicts spin $\frac{1}{2}$ or $\frac{3}{2}$ for the Λ^0 ,

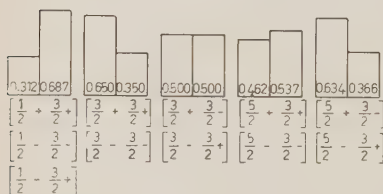


Fig. 9.

and, if the spin is $\frac{3}{2}$, parity $+1$ relative to the proton. If the Λ^0 has spin $\frac{1}{2}$ it must always decay isotropically, however polarized. Therefore a constant isotropy of the decay distributions under different conditions would indicate spin $\frac{1}{2}$. Recent results⁽³⁾ for associated production indicate a tendency for strong anisotropies — although the statistics are insufficient to draw any conclusion. For the cases corresponding to the Λ^0 spin $\frac{3}{2}$ the correlation is reported in histogram form in Fig. 9. We have divided in two equal regions the total interval $0 \leq \cos \theta \leq 1$ and reported for each region the expected frequency. This procedure is perhaps the most convenient one for comparison with experiment when a small number of data is available — the random fluctuations are reduced and the classification of the events according to the region in which they fall is less subject to experimental errors. An event lies in the first region, $0 \leq \cos \theta < 0.5$, if the acute angle between the direction of emission of

(3) See, for instance, W. D. WALKER and W. D. SHEPARD: *Phys. Rev.* (in the press).

the decay products of the Λ^0 (in the Λ^0 center of mass system) and the line of flight of the Λ^0 is between 60° and 90° ; the event lies in the second region $0.5 \leq \cos \theta \leq 1$ if the angle is between 0° and 60° . It can be seen from Fig. 9 that a choice between the cases, (i) Ξ^- with spin $\frac{1}{2}$, (ii) Ξ^- with spin $\frac{3}{2}$ and same parity as the Λ^0 , (iii) Ξ^- with spin $\frac{3}{2}$ and opposite parity to that of Λ^0 , should in any case be possible. However a distinction between the case (iii) and the case (iv), Ξ^- with spin $\frac{5}{2}$ and same parity as the Λ^0 , and between (ii) and (v), Ξ^- with spin $\frac{5}{2}$ and opposite parity to the Λ^0 , would require a better statistics. Up to now it has been possible to the author to collect the data from only four cascade decay events: two of them fall in the first region and the other two in the second region.

2'4. — As already remarked the distribution of the dihedral angle ψ ($0^\circ \leq \psi \leq 90^\circ$) between the first decay plane, that of $\Xi^- \rightarrow \Lambda^0 + \pi^-$, and the second decay plane, that of $\Lambda^0 \rightarrow p + \pi^-$, may give information on the spins, but its theoretical discussion requires a much better knowledge of the dynamics of the whole process. In any case from such distribution one can obtain lower limits for the spin of the Λ^0 — following a method due to TREIMAN and WYLD⁽⁹⁾. If the distribution is not isotropic the Λ^0 spin is $\geq \frac{3}{2}$. However, if the fraction of events with $\psi \leq \psi'$ is larger than

$$\frac{1}{\pi} (2\psi' + 0.577 \sin 2\psi')$$

(which is 0.174 for $\psi' = 10^\circ$, etc) then the Λ^0 spin is $\geq \frac{5}{2}$.

3. — The Cascade Decay of the Σ^0 .

3'1. — The correlation in the cascade $\Sigma^0 \rightarrow \Lambda^0 + \gamma$, $\Lambda^0 \rightarrow p + \pi^-$ can be written in the form

$$(10) \quad W(\cos \theta) = \\ = \text{const} \times \sum_{\nu l_1 l'_1} T(l_1) T(l'_1) (l_1 l'_1 1 -1 | \nu 0) (l_2 l_2 0 0 | \nu 0) W(ss l_1 l'_1 \nu S) W(ss l_2 l_2 \nu \frac{1}{2}) P_\nu(\cos \theta),$$

in a notation similar to that of (7) — the coefficients $(l_1 l'_1 0 0 | \nu 0)$ are substituted here by $(l_1 l'_1 1 -1 | \nu 0)$ corresponding to the vector and transverse nature of the emitted light quantum. In (10) S is the spin of the Σ^0 ; l_1 and l'_1 can take all values permitted for the relative orbital angular momentum between the emitted Λ^0 and γ . We shall use the notation $\{\mathcal{SQSp}\}$ to indicate the case re-

⁽⁹⁾ S. B. TREIMAN and H. W. WYLD: *Phys. Rev.*, **100**, 879 (1955).

ferring to Σ^0 with the spin \mathcal{S} and parity (relative to the proton) \mathcal{P} and to a Λ^0 with spin s and parity p (relative to the proton). The possible multipole orders for the emitted γ -ray in the Σ^0 decay are reported in Table III for spin values up to $\frac{3}{2}$. Electric transitions are denoted by (e) and magnetic transitions by (m) . The favored cases are denoted by (F) , the unfavored by (U) .

TABLE III. - *Multipole orders for $\Sigma^0 \rightarrow \Lambda^0 + \gamma$.*

$\begin{smallmatrix} \text{sp} \\ \mathcal{S}\mathcal{P} \end{smallmatrix}$	$\frac{3}{2} + \quad (l_2 = 1)$	$\frac{3}{2} - \quad (l_2 = 2)$	$\frac{5}{2} + \quad (l_2 = 3)$	$\frac{5}{2} - \quad (l_2 = 2)$
$\frac{1}{2} +$	1, 2 (m)(e) (U)	1, 2 (e)(m) (F)	2, 3 (e)(m) (F)	2, 3 (m)(e) (U)
$\frac{1}{2} -$	1, 2 (e)(m) (F)	1, 2 (m)(e) (U)	2, 3 (m)(e) (U)	2, 3 (e)(m) (F)
$\frac{3}{2} +$	1, 2, 3 (m)(e)(m) (U)	1, 2, 3 (e)(m)(e) (F)	1, 2, 3, 4 (m)(e)(m)(e) (U)	1, 2, 3, 4 (e)(m)(e)(m) (F)
$\frac{3}{2} -$	1, 2, 3 (e)(m)(e) (F)	1, 2, 3 (m)(e)(m) (U)	1, 2, 3, 4 (e)(m)(e)(m) (F)	1, 2, 3, 4 (m)(e)(m)(e) (U)
$\frac{5}{2} +$	1, 2, 3, 4 (m)(e)(m)(e) (U)	1, 2, 3, 4 (e)(m)(e)(m) (F)	1, 2, 3, 4, 5 (m)(e)(m)(e)(m) (U)	1, 2, 3, 4, 5 (e)(m)(e)(m)(e) (F)
$\frac{5}{2} -$	1, 2, 3, 4 (e)(m)(e)(m) (F)	1, 2, 3, 4 (m)(e)(m)(e) (U)	1, 2, 3, 4, 5 (e)(m)(e)(m)(e) (F)	1, 2, 3, 4, 5 (m)(e)(m)(e)(m) (U)

The values of $\{\mathcal{S}\mathcal{P}\}$ are in the first column, the values of $\{sp\}$ in the first row. The correlation (10) has still the form (9) according to the general theorem. In the favored cases one may assume that only the lowest multipole contributes. A rigorous justification of this assumption cannot be given at present. The emitted γ -ray in the Σ^0 decay has a wavelength $\approx 0.3 \cdot 10^{-12}$ cm — therefore it seems that, unless the involved « size » of the Σ^0 is unreasonable large, the assumption that only the lowest multipole intervenes in the favored cases should be generally valid. In the unfavored cases a similar assumption would require a better justification. In Table IV we report the explicit form of the angular correlations calculated for the cases considered in Table III, supposing that only the lowest multipoles contribute. The parameter ξ is the ratio of the reduced matrix element of the next higher l_1 to that of the lowest l_1 and it can only take real values — for the favored cases one may assume $\xi = 0$.

Since we are not interested in the verification of parity conservation we may *a priori* assume that the correlation will only depend on even powers of $\cos^2 \theta$. Therefore we take θ to be the acute angle between the direction of

TABLE IV. — *The angular correlation for the cascade $\Sigma^0 \rightarrow \Lambda^0 + \tau$, $\Lambda^0 \rightarrow p + \pi^-$.*

$[\frac{1}{2}\mathcal{D}\frac{3}{2}p]$	$W(\cos \theta) = 1.250 - 0.750 \cos^2 \theta + \xi(-0.866 + 2.598 \cos^2 \theta) +$ $+ \xi^2(0.750 + 0.750 \cos^2 \theta)$
$[\frac{3}{2}\mathcal{D}\frac{3}{2}p]$	$W(\cos \theta) = 0.800 + 0.600 \cos^2 \theta + \xi(-0.775 + 2.324 \cos^2 \theta) + \xi^2$
$[\frac{5}{2}\mathcal{D}\frac{3}{2}p]$	$W(\cos \theta) = 1.050 - 0.150 \cos^2 \theta + \xi(0.592 - 1.775 \cos^2 \theta) +$ $+ \xi^2(1.179 - 0.536 \cos^2 \theta)$
$[\frac{1}{2}\mathcal{D}\frac{5}{2}p]$	$W(\cos \theta) = 0.500 + 3.000 \cos^2 \theta - 2.500 \cos^4 \theta +$ $+ \xi(0.354 - 6.364 \cos^2 \theta + 8.839 \cos^4 \theta) +$ $+ \xi^2(-0.375 + 0.750 \cos^2 \theta + 0.625 \cos^4 \theta)$
$[\frac{3}{2}\mathcal{D}p\frac{5}{2}]$	$W(\cos \theta) = 1.200 - 0.600 \cos^2 \theta + \xi(-1.014 + 3.043 \cos^2 \theta) +$ $+ \xi^2(1.143 - 2.143 \cos^2 \theta + 2.857 \cos^4 \theta)$
$[\frac{5}{2}\mathcal{D}\frac{5}{2}p]$	$W(\cos \theta) = 0.771 + 0.686 \cos^2 \theta + \xi(-0.542 + 1.626 \cos^2 \theta) +$ $+ \xi^2(-0.964 + 1.071 \cos^2 \theta - 1.607 \cos^4 \theta)$

emission of the Λ^0 secondaries in the Λ^0 center of mass system and the line of flight of the Λ^0 , and reduce the comparison to values $0^\circ \leq \theta < 90^\circ$. In Table II the normalization is chosen such that if $\xi = 0$, the integral of $W(\cos \theta) d(\cos \theta)$

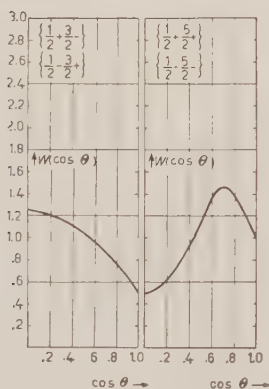


Fig. 10.

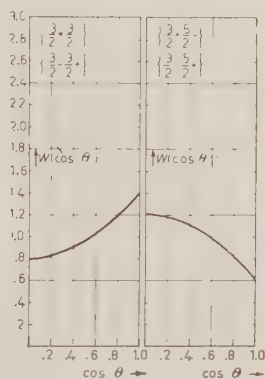


Fig. 11.

from 0 to $\pi/2$ is equal to 1. The corresponding graphs of $W(\cos \theta)$, for the favored cases — for which the assumption $\xi = 0$ should be valid — are reported in Figs. 10-12. If the Λ^0 spin is $\frac{1}{2}$ its decay distributions are always isotropic. If the Λ^0 has spin $\frac{3}{2}$ and if the Σ^0 has opposite parity to that of the Λ^0 it should be possible to distinguish between (i) Σ^0 with spin $\frac{1}{2}$, (ii) with spin $\frac{3}{2}$, (iii) with spin $\frac{5}{2}$, as the histograms of Fig. 13 illustrate. In the histograms of 13 we have divided the total interval in two regions, $60^\circ \leq \theta < 90^\circ$ and $0^\circ \leq \theta < 60^\circ$, and reported for each region the predicted frequency.

In general, reactions which lead to the production of Σ^0 are also expected — unless particular rules intervene different from strangeness conservation — to lead also to the direct production of Λ^0 (in place of Σ^0). Therefore, for the measurement of the correlation proposed here one must be able to find kinematical criteria for distinguishing between the Λ^0 which are produced directly and those which are produced by the successive decay of the Σ^0 . The distinction can be done easily in the case of the simplest production processes such as $\pi^- + p \rightarrow \Sigma^0(\Lambda^0) + K^0$, $K^- + p \rightarrow \Sigma^0(\Lambda^0) + \pi^0$, however it could be difficult in the case of complicated production processes. On the other hand one could hope to measure the emitted light

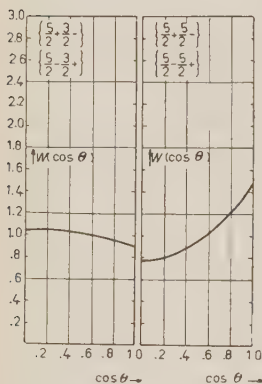


Fig. 12.

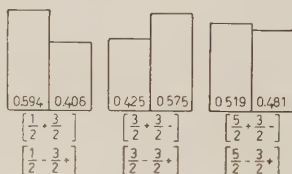


Fig. 13.

quantum in $\Sigma^0 \rightarrow \Lambda^0 + \gamma$, which in itself would be an important experimental result — and one would also have the possibility of triple correlation experiments. To show in simplest cases the possibility of distinguishing between

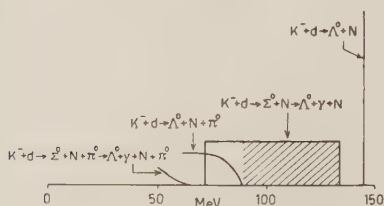


Fig. 14.

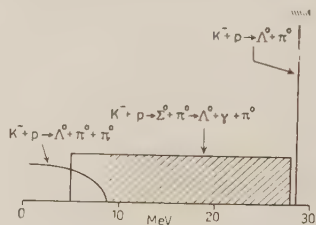


Fig. 15.

the Λ^0 produced directly and those produced through the intermediary Σ^0 — which only must be used for the statistics — we report in Fig. 14 the Λ^0 energy spectrum from K^- absorption at rest in hydrogen, and in Fig. 15 the Λ^0 energy spectrum from K^- -absorption at rest in deuterium⁽¹⁰⁾. The shadowed parts of the spectrum correspond to Λ^0 which are necessarily produced through intermediate Σ^0 .

(10) M. K. CASE, R. KARPLUS and C. N. YANG: *Phys. Rev.*, **101**, 358 (1956).

* * *

The author wishes to thank all those experimentalists who have contributed with several helpful comments and who have kindly supplied information on cascade decay events, in particular Prof. W. B. FRETTER, Prof. L. LEPRINCE-RINGUET and Prof. G. T. REYNOLDS.

RIASSUNTO

La specificazione intrinseca della configurazione di una cascata di decadimenti di due corpi — come $\Xi^- \rightarrow \Lambda^0 + \pi^-$, $\Lambda^0 \rightarrow p + \pi^-$, o $\Sigma^0 \rightarrow \Lambda^0 + \gamma$, $\Lambda^0 \rightarrow p + \pi^-$ — richiede un parametro, la cui distribuzione rifletterà gli aspetti dinamici del processo. Viene data una discussione dettagliata di queste distribuzioni, e viene mostrato, come, quando un sufficiente numero di decadimenti a cascata di Ξ^- , e, similmente, di decadimenti a cascata di Σ^0 , sarà stato riportato, il confronto con la teoria darà informazioni sugli spin e sulle parità degli iperoni.

On Some Solutions of Gürsey's Conformal-Invariant Spinor Wave Equation.

F. KORTEI

Institute for Theoretical Physics, University of Istanbul

(ricevuto il 23 Aprile 1956)

Summary. — Some classical solutions of Gürsey's conformal-invariant spinor wave equation are given.

Introduction.

Recently the conformal-invariant spinor wave equation

$$(1) \quad \gamma_\mu \frac{\partial \psi}{\partial x_\mu} + (\bar{\psi} \psi)^{\frac{1}{3}} \psi = 0$$

has been proposed by GÜRSEY ⁽¹⁾ as a possible basis for a unitary description of elementary particles. The present paper deals with several solutions of (1) some of which are also common to the more general equation

$$(2) \quad \gamma_\mu \frac{\partial \psi}{\partial x_\mu} + l^{3n-1} (\bar{\psi} \psi)^n \psi = 0,$$

where $l > 0$ has the dimension of a length and n is a real number. We begin by a study of (2) and then pass over to two solutions which are characteristic of the case $n = \frac{1}{3}$.

As already pointed out by GÜRSEY ⁽¹⁾, (2) has plane wave solutions from which one can obtain others by conformal transformations if $n = \frac{1}{3}$. Those solutions will not be considered here.

⁽¹⁾ F. GÜRSEY: *Nuovo Cimento*, **3**, 988 (1956).

Following HEISENBERG ⁽²⁾ we seek solutions of (2) of the form

$$(3) \quad \psi = (x_\mu \gamma_\mu \chi(s) + \varphi(s))a$$

with a an arbitrary constant spinor and $\chi(s)$ and $\varphi(s)$ real functions of the interval

$$s = -x_\mu^2 = t^2 - r^2. \quad (c = 1).$$

1. - Differential Equations for $\chi(s)$ and $\varphi(s)$.

Inserting (3) into (2) and equating the coefficients of a and $x_\mu \gamma_\mu a$ to zero, we obtain for $\chi(s)$ and $\varphi(s)$ the system of two ordinary non-linear differential equations

$$(4.1) \quad 2s\chi' + 4\chi + \alpha\varphi(s\chi^2 + \varphi^2)^n = 0,$$

$$(4.2) \quad -2\varphi' + \alpha\chi(s\chi^2 + \varphi^2)^n = 0,$$

where

$$(5) \quad \alpha = l^{3n-1}(\bar{a}a)^n.$$

In order that $\chi(s)$ and $\varphi(s)$ may be real, a must be such that α is real as well.

It is often more convenient to use a second set of variables defined by

$$(6) \quad \begin{cases} \chi = A|s|^{-\sigma}f(z), & \varphi = B|s|^{-\tau}g(z), & z = \ln|s|, \\ \tau = \frac{1}{4n}, & \sigma = \tau + \frac{1}{2}, & A = |\alpha|^{-1/2n}, & B = A \operatorname{sgn} \alpha. \end{cases}$$

In these new variables first introduced by HEISENBERG ⁽²⁾ the equations (4.1) and (4.2) read

$$(7.1) \quad 2f' + \left(3 - \frac{1}{2n}\right)f + g(f^2 + g^2)^n = 0,$$

$$(7.2) \quad -2g' + \frac{1}{2n}g + f(f^2 + g^2)^n = 0$$

⁽²⁾ W. HEISENBERG: *Zeits. f. Naturf.*, **9a**, 292 (1954).

for $s > 0$ and

$$(8.1) \quad 2f' + \left(3 - \frac{1}{2n}\right)f + g(g^2 - f^2)^n = 0,$$

$$(8.2) \quad 2g' - \frac{1}{2n}g + f(g^2 - f^2)^n = 0,$$

for $s < 0$.

2. — The Simplest Solution of (2).

Choose the constant spinor a so that $\bar{a}a = 0$. Then (4.1) and (4.2) are equivalent to

$$(9.1) \quad s\chi' + 2\chi = 0,$$

$$(9.2) \quad \varphi' = 0,$$

which are readily solved to give

$$(10) \quad \varphi = C, \quad \chi = D/s^2,$$

with C and D two arbitrary real constants. Absorbing D into a and putting $C/D = \kappa$ we have

$$(11) \quad \psi = \left(\frac{x_\mu \gamma_\mu}{s^2} + \kappa \right) a, \quad \bar{a}a = 0.$$

3. — $\chi(s)$ and $\varphi(s)$ as Powers of s .

We obtain a second solution of (2) valid for $s \geq 0$ and $n > \frac{1}{6}$, assuming $f(z)$ and $g(z)$ as constants, f_n and g_n say, to be determined from (7.1) and (7.2). We find for $\chi(s)$ and $\varphi(s)$

$$(12) \quad \begin{aligned} \chi &= Af_n s^{-(\frac{1}{2} + 1/4n)}, & \varphi &= Ag_n s g n \alpha s^{-1/4n}, & (s > 0), \\ \chi &= \varphi = 0, & & & (s < 0), \end{aligned}$$

where

$$f_n = \pm (6n)^{-\frac{1}{2}} (6n - 1)^{1/4n} (2n)^{-1/2n}, \quad g_n = \mp (6n - 1)^{\frac{1}{2}} f_n.$$

In particular, we have for $n = \frac{1}{3}$

$$(13) \quad \psi = s^{-1}(x_\mu \gamma_\mu s^{-\frac{1}{2}} + \kappa)a,$$

absorbing $Af_{\frac{1}{3}}$ into a and setting $g_{\frac{1}{3}}/f_{\frac{1}{3}} \cdot \operatorname{sgn} \kappa = \kappa$.

4. - Two Solutions of Gürsey's Equation (1).

The two solutions (11) and (12) given so far are common to (1) and (2). In this paragraph we present two further solutions which are valid for $n = \frac{1}{3}$ only.

4.1. - Let us try to find a solution of (2) assuming a linear relation

$$(14) \quad \varphi = \kappa \chi$$

between χ and φ with κ a real constant. Inserting (14) into (4.1) and (4.2) we easily find that in fact

$$\chi = \frac{K}{(s + \kappa^2)^2}, \quad \varphi = \frac{\kappa K}{(s + \kappa^2)^2}$$

will lead to a solution of (2) if $n = \frac{1}{3}$ and if the real numbers K , α , κ satisfy the condition

$$(15) \quad 4\kappa + \alpha K^{\frac{2}{3}} = 0.$$

Thus we get a solution

$$(16) \quad \psi = \frac{(x_\mu \gamma_\mu + \kappa)a}{(s + \kappa^2)^2}$$

of Gürsey's equation (1), absorbing K into the constant spinor a . It is interesting to observe that this solution has no singularity for $s > -\kappa^2$.

4.2. - Finally, we give the general solution of (1) which contains (16) as a special case. Writing (7.1) and (7.2) in the form

$$(17) \quad d\left[\frac{g}{2n} + f(f^2 + g^2)^n\right] + dg\left[\left(3 - \frac{1}{2n}\right)f + g(f^2 + g^2)^n\right] = 0,$$

we see that it is integrable if $n = \frac{1}{3}$. Similarly, it is seen that (8.1) and (8.2) form an integrable system if $n = \frac{1}{3}$. Denoting by C and D two constants of

integration, we have therefore

$$(18) \quad 4fg + (f^2 + g^2)^{\frac{4}{3}} = C, \quad (s > 0),$$

and

$$(19) \quad 4fg + (g^2 - f^2)^{\frac{4}{3}} = D, \quad (s < 0),$$

respectively. Let us first consider the domain $s > 0$.

Eliminating $(f^2 + g^2)^n$ between (7.1) and (7.2) we have for $n = \frac{1}{3}$

$$(20) \quad (f^2 + g^2)' + \frac{3}{2}(f^2 - g^2) = 0.$$

Clearly, (18) and (20) are satisfied by any solution of (7.1) and (7.2), provided that $n = \frac{1}{3}$. It can easily be shown that, inversely, any non-constant solution of (18) and (20) also solves (7.1) and (7.2) for $n = \frac{1}{3}$. Therefore it is sufficient to solve the system (18), (20) in order to obtain the general solution of (7.1) and (7.2) for $n = \frac{1}{3}$. This can be done by introducing the variables

$$(21) \quad \xi = f^2 + g^2, \quad \eta = f^2 - g^2,$$

in terms of which the system (18), (20) reads

$$(22.1) \quad \pm 2\sqrt{\xi^2 - \eta^2} + \xi^{\frac{4}{3}} = C,$$

$$(22.2) \quad \xi' + \frac{3}{2}\eta = 0.$$

Solving (22.1) for η we get

$$(23) \quad \eta = \pm \left(\xi^2 - \frac{(C - \xi^{\frac{4}{3}})^2}{4} \right)^{\frac{1}{2}},$$

and inserting this into (22.2) we find

$$(24) \quad \xi' \pm \frac{3}{2} \left(\xi^2 - \frac{(C - \xi^{\frac{4}{3}})^2}{4} \right)^{\frac{1}{2}} = 0.$$

A final substitution

$$\xi^{\frac{4}{3}} = u^2$$

and subsequent integration result in

$$(25) \quad z - z_0 = \ln \frac{s}{s_0} = \mp \int \frac{du}{\sqrt{u^2 - \frac{(C - u^2)^2}{4u}}}.$$

Similar considerations apply to the domain $s < 0$. Here $f(z)$ and $g(z)$ are determined from (19) and

$$(26) \quad (f^2 - g^2)' + \frac{3}{2}(f^2 + g^2) = 0,$$

which is obtained from (8.1) and (8.2) for $n = \frac{1}{3}$ by eliminating $(g^2 - f^2)^{\frac{1}{2}}$. Introducing again ξ and η as defined by (21) we get

$$(27.1) \quad \pm 2\sqrt{\xi^2 - \eta^2} + \eta^{\frac{1}{2}} = D,$$

$$(27.2) \quad \eta' + \frac{3}{2}\xi = 0,$$

from which we deduce

$$(28) \quad z - z'_0 = \ln \left| \frac{s}{s'_0} \right| = \mp \int \frac{dv}{\sqrt{v^2 + \frac{(D - v^2)^2}{4v}}}$$

by putting $\eta^{\frac{1}{2}} = v^2$.

Transforming back to s , $\chi(s)$, $\varphi(s)$ we see that for $s > 0$, $\chi(s)$ and $\varphi(s)$ are somewhat complicated functions of s and an Abelian function of $\ln s/s_0$, s_0 being an integration constant introduced in (25). The same applies of course to the domain $s < 0$. It should be noted that we have so far introduced four integration constants C , D , s_0 , s'_0 . They cannot be all independent; C and D are connected with each other by the condition of continuity at $s = 0$, and for the same reason s_0 and s'_0 depend on each other. On the other hand, if continuity at $s = 0$ is not required, C , D , s_0 , s'_0 are all independent.

The integrations in (25) and (29) can be carried out in an elementary way if $C = D = 0$; however, nothing new is obtained but another derivation of (16).

Some physical implications of the solutions described above will be treated in a sequel to this paper.

RIASSUNTO (*)

Si danno alcune soluzioni classiche dell'equazione d'onda spinoriale ad invarianza conforme di Gürsey.

(*) Traduzione à cura della Redazione.

General Dispersion Relations.

J. C. POLKINGHORNE (*)

California Institute of Technology - Pasadena, California, U.S.A.

(ricevuto il 28 Aprile 1956)

Summary. — A formalism is developed whereby dispersion relations may be obtained for all meson-nucleon scattering processes, including those in which mesons are created or destroyed. A suitable kinematical description of the processes is first given and a new amplitude is defined in terms of it. This amplitude has two important properties. Firstly it coincides with the Feynman amplitude for positive energies of the incoming and outgoing particles. Secondly it satisfies a certain causality condition. These enable one to obtain dispersion relations. The significance of these results in affording a new way of formulating quantum field theory is discussed.

1. — Introduction.

Recently there have been several investigations ^(1,2) of the results of applying the causality condition to the elastic scattering of a single meson by a nucleon. It is found possible to derive a dispersion relation for this process. In this paper the causality condition will be used to investigate the general process in which n_1 mesons interact with a nucleon to produce n_2 outgoing mesons. This includes, of course, the case of inelastic processes in which $n_1 \neq n_2$. The interest in doing this is twofold. Firstly we are enabled to write down exact relations for these processes. Secondly it has been suggested ⁽²⁾

(*) Commonwealth Fund Fellow; on leave of absence from Trinity College, Cambridge, England.

⁽¹⁾ M. GELL-MANN, M. L. GOLDBERGER and W. THIRRING: *Phys. Rev.*, **95**, 1612 (1954); M. L. GOLDBERGER: *Phys. Rev.*, **97**, 508 (1955); R. KARPLUS and M. A. RUDERMAN: *Phys. Rev.*, **98**, 771 (1955); M. L. GOLDBERGER: *Phys. Rev.*, **99**, 979 (1955); A. SALAM: *Nuovo Cimento*, **3**, 424 (1956).

⁽²⁾ M. GELL-MANN: unpublished.

that dispersion theory may provide a new way of formulating quantum field theory closely in accord with the original S matrix ideas of HEISENBERG⁽³⁾. In order for this to be true it is essential to be able to obtain a general dispersion theory for these processes.

For simplicity the case of neutral pseudoscalar mesons interacting with nucleons will be considered. It is very easy to introduce isotopic spin into the formalism if required. Consider the process in which mesons of momenta $p_1 \dots p_{n_1}$ are scattered by a nucleon into a state with outgoing mesons of momenta k_1, \dots, k_{n_2} . All these mesons are real, i.e. $p^2 = -\mu^2$, $k^2 = -\mu^2$. The process is described by the amplitude

$$(1) \quad F(k_i; p_j) = i \int_{-\infty}^{\infty} dx_i dy_j \exp[-i \sum k_i x_i + \sum p_j y_j] \cdot \\ \cdot \langle f | T[j(x_1) \dots j(x_{n_2}) j(y_1) \dots j(y_{n_1})] | i \rangle,$$

where $j(x)$ is the Heisenberg current density of the nucleon field and the state vectors refer to the initial and final states of the nucleon. The causality condition states that

$$(2) \quad [j(x), j(x')] = 0,$$

when x and x' are spatially separated.

The case that has been previously discussed^(1,2) is that of $F(k; p)$, representing the elastic scattering of a single meson. There the argument proceeds by constructing an amplitude $M(k; p)$ which coincides with $F(k; p)$ when k and p are positive timelike vectors and which also satisfies a causality condition leading to a dispersion relation. This amplitude is in fact given by"

$$(3) \quad M(k; p) = \int_{-\infty}^{\infty} dx dy \exp[-ikx + ipy] \eta(x-y) \langle f | [j(x), j(y)] | i \rangle.$$

The main task of this paper is to define the generalized amplitude $M(k_i; p_j)$ which must:

(i) coincide with $F(k_i; p_j)$ when all the k_i and p_j are positive timelike (the comparison theorem);

(ii) satisfy a certain causality condition, to be specified exactly later, which will ensure that it satisfies a dispersion relation.

(3) W. HEISENBERG: *Zeits. f. Phys.*, **120**, 513, 673 (1943).

In Sect. 2 the kinematics of the process is discussed. It is important to find the appropriate mode of description. For example in the single meson case ⁽²⁾ the momentum transfer must be fixed, not the scattering angle. In Sect. 3 the amplitude is defined and in Sect. 4 it is shown to satisfy the comparison theorem. In Sect. 5 the causality condition is defined and in the appendix it is shown that the amplitude satisfies it. This proof, though simple in technique, is somewhat prolix in statement since it proceeds by enumeration of the different cases. In Sect. 6 it is shown how this leads to a dispersion relation. In the concluding section the significance of these results is discussed.

2. — Kinematics.

The translational invariance of the theory implies that energy and momentum are conserved and so

$$(4) \quad \sum k_i - \sum p_j = \Delta,$$

where Δ is the change in the four-momentum of the nucleon. This is a space-like vector and it is convenient to use a frame of reference in which it has zero fourth component. Three-vectors in this frame will be denoted by bold face type. Thus Δ becomes $\mathbf{\Delta}$. We write

$$(5) \quad \begin{cases} k_{i0} = \omega v_i, & i = 1, \dots, n_2; \\ p_{j0} = -\omega v_{j+n_2}, & j = 1, \dots, n_1. \end{cases}$$

Thus for positive timelike k_i and p_j , v_1, \dots, v_{n_2} are positive and $v_{n_2+1}, \dots, v_{n_1+n_2}$ are negative, if ω is positive. In the chosen frame of reference we must have

$$(6) \quad \sum_{i=1}^n v_i = 0,$$

where $n = n_1 + n_2$. As part of the specification of the kinematics the v 's will be given fixed values. (In fact it is only their ratios together with their intrinsic signs that matter. Multiplication of each by a positive constant only has the effect of trivially redefining ω .) The spatial part of each vector is now determined in magnitude in terms of ω as being $\sqrt{\omega^2 v_i^2 - \mu^2}$ but the mutual orientations of these vectors have still to be specified.

From a four dimensional point of view the process is specified uniquely when the values of the invariants $k_i k_j$, $p_i p_j$, and $k_i p_j$ are all known. These may be specified in the following way:

For the given ν 's it is possible to construct other vectors in addition to Δ that have zero fourth component. (In particular a number of these vectors arise from the different correlations discussed in Sect. 5 when the causality condition is formulated). The spatial parts of a set of these vectors are given by

$$(7) \quad \delta^\alpha = \sum \lambda_i^\alpha \mathbf{k}_i + \sum \lambda_j^\alpha \mathbf{p}_j,$$

where λ 's are determined by the ν 's alone. Including Δ there are $n-1$ linearly independent δ^α corresponding to the $n-1$ linearly independent solutions of the equation

$$(8) \quad \sum \lambda_i^\alpha \nu_i = 0.$$

However to fix the magnitude of $\mathbf{k}_i \cdot \mathbf{k}_j$, $\mathbf{p}_i \cdot \mathbf{p}_j$, $\mathbf{k}_i \cdot \mathbf{p}_j$, it is necessary to fix the magnitudes of $n(n-1)/2$ of the δ^α . (The magnitudes assigned must satisfy certain consistency conditions, in the form of inequalities, that need not concern us in detail here). It is easy to see that it is possible to choose a set of δ^α , including Δ , so that this determination is unique. Any other δ^α not belonging to that set must *a fortiori* be linearly dependent on members of the set. Thus, since

$$(9) \quad |\sum \mu_\alpha \delta^\alpha| \leq \sum \mu_\alpha |\delta^\alpha|,$$

it follows that the magnitude of every δ^α is bounded as ω varies. This fact proves of the greatest importance in the derivation of dispersion relations.

In terms of this kinematical description we may write

$$(10) \quad F(k_i; p_j) = F(\omega; \nu_i; |\Delta|, |\delta^\alpha|),$$

and ω will be the only variable to be considered explicitly. For this reason we shall often write just $F(\omega)$.

3. — Definition of the Amplitude.

The amplitude is defined by

$$(11) \quad M(\omega; \nu_i; |\Delta|, |\delta^\alpha|) = M(k_i; p_j) = \int_{-\infty}^{\infty} dx_i dy_j \exp[-i \sum k_i x_i + i \sum p_j y_j] \cdot \langle f | A(x_1, \nu_1; \dots; x_{n_2}, \nu_{n_2}; y_1, \nu_{n_2+1}; \dots, y_{n_1}, \nu_n) | i \rangle,$$

where the operator A is defined by

$$(12) \quad A(z_1, \nu_1; \dots; z_n, \nu_n) = \sum j(z_{i_1}) \dots j(z_{i_n}) E(z_{i_1}, \nu_{i_1}; \dots; z_{i_n}, \nu_{i_n}).$$

The sum is taken over all permutations i_1, \dots, i_n of $1, \dots, n$ and the function E is defined by

$$(13) \quad E(z_1, v_1; \dots; z_n, v_n) = [\eta(z_1 - z_2)\eta'(v_1) - \eta(z_2 - z_1)\eta'(-v_1)] \cdot \\ \cdot [\eta(z_2 - z_3)\eta'(v_1 + v_2) - \eta(z_3 - z_2)\eta'(-v_1 - v_2)] \cdot \\ \cdot \dots \cdot \\ \cdot [\eta(z_{n-1} - z_n)\eta'(v_1 + \dots + v_{n-1}) - \eta(z_n - z_{n-1})\eta'(-v_1 - \dots - v_{n-1})].$$

Here

$$(14) \quad \left\{ \begin{array}{ll} \eta(z) = 1 & \text{if } z_0 > 0, \\ = 0 & \text{if } z_0 < 0; \end{array} \right.$$

$$(15) \quad \left\{ \begin{array}{ll} \eta'(v) = 1 & \text{if } v > 0, \\ = 0 & \text{if } v < 0. \end{array} \right.$$

This definition reduces to that given by eq. (3) in the single meson case.

If \widetilde{M} denotes the Hermitian conjugate of M with respect to the nucleon variables it follows that (*)

$$(16) \quad M(-\omega; v_i; |\Delta|, |\mathbf{s}^\alpha|) = \widetilde{M}(\omega; v_i; |\Delta|, |\mathbf{s}^\alpha|).$$

4. - The Comparison Theorem.

The case in which k_i and p_j are all positive timelike vectors is obtained by taking $\omega > 0$. Introducing sums over complete sets of intermediate states the amplitude may be written as

$$(17) \quad M(\omega) = \int_{-\infty}^{\infty} d\mathbf{x}_i d\mathbf{y}_j \exp[-i \sum \mathbf{k}_i \cdot \mathbf{x}_i + i \sum \mathbf{p}_j \cdot \mathbf{y}_j] \cdot \\ \cdot \sum_{\alpha_1, \dots, \alpha_{n-1}} \frac{\langle f | j(\mathbf{z}_{i_1}) | \alpha_1 \rangle \langle \alpha_1 | j(\mathbf{z}_{i_2}) | \alpha_2 \rangle \dots \langle \alpha_{n-1} | j(\mathbf{z}_{i_n}) | i \rangle}{(E_i - E_{\alpha_1} - \omega(v_n + \dots + v_2) \pm i\epsilon) \dots (E_i - E_{\alpha_{n-1}} - \omega v_n \pm i\epsilon)}.$$

Here E_i is the energy of the initial nucleon state and E_α is the energy of the state α . Only those states that contain one nucleon contribute to the sum and for them

$$(18) \quad E_\alpha \geq E_i.$$

(*) This is the Gell-Mann-Goldberger crossing theorem for this theory.

The term $+i\varepsilon$ occurs in a denominator if that denominator arises from $\eta(z)$ and the term $-i\varepsilon$ occurs if the denominator arises from $-\eta(-z)$. In the corresponding expression for $F(\omega)$ the term $\pm i\varepsilon$ occurs everywhere. The sign of this term only matters if the rest of the denominator vanishes for some term in the sum over states. Eqs. (6) and (13) together show that terms with $-i\varepsilon$ only occur for $\omega(\nu_n + \dots + \nu_j) > 0$ (if $\omega > 0$) and eq. (8) shows that in this case the denominator never vanishes. Hence

$$(19) \quad M(\omega; \nu_s; |\Delta|, |\delta^\alpha|) = F(\omega; \nu_i; |\Delta|, |\delta^\alpha|),$$

provided $\omega > 0$.

5. — The Causality Condition.

In the general case now being considered the definition of the causality condition satisfied by the amplitude is a matter of some complexity, though the physical notions underlying it are clear and simple. It takes the following form:

The amplitude M is divided into a number of terms each of which corresponds to a certain correlation of the points appearing in A . This correlation has the following form. Each point corresponding to the creation of an outgoing meson (i.e. an x in eq. (11)) is correlated with one or more points representing the annihilation of an incoming meson (i.e. a y in eq. (11)). The correlations are made in such a way that it is energetically possible for a given incoming meson to play a part in creating all the outgoing mesons with which it is correlated. Those outgoing mesons for which it is the only correlate must be created by it alone. An outgoing meson with several incoming correlates must be created by a process involving all its correlates. The possible sets of correlations depend on the ratios of the ν 's and are independent of ω .

This relationship will be made more easily understandable by the use of an example. Suppose mesons are annihilated at y_1 and y_2 with $\nu = -4$, $\nu = -5$, respectively, and mesons are created at x_1 , x_2 , x_3 , with $\nu = 6$, $\nu = 2$, $\nu = 1$. Denoting correlation by \sim , possible correlations are:

- (i) $x_1 \sim y_1, y_2; \quad x_2 \sim y_1; \quad x_3 \sim y_2.$
- (ii) $x_1 \sim y_1, y_2; \quad x_2 \sim y_2; \quad x_3 \sim y_1.$
- (iii) $x_1 \sim y_1, y_2; \quad x_2 \sim y_1; \quad x_3 \sim y_1.$
- (iv) $x_1 \sim y_1, y_2; \quad x_2 \sim y_2; \quad x_3 \sim y_2.$

The causality condition requires that each term in A vanishes unless every outgoing meson point is timelike advanced with respect to each of its incoming correlates. The fact that the amplitude defined in Sect. 3 possesses this property is proved in the Appendix. In the following Section it is shown how this leads to a dispersion relation.

6. — Dispersion Relations.

For simplicity we shall consider the case of two incoming mesons only. In particular consider the term corresponding to i_1, \dots, i_s correlated with α and i_s, \dots, i_n correlated with β . It is possible to write

$$(20) \quad \nu_s = \nu'_s + \nu''_s,$$

where

$$(21) \quad \begin{cases} \nu_1 + \dots + \nu_{s-1} + \nu'_s + \nu_\alpha = 0, \\ \nu_{s+1} + \dots + \nu_n + \nu''_s + \nu_\beta = 0. \end{cases}$$

The contribution of this term to $M(\omega)$ depends on ω through an exponential with exponent

$$(22) \quad \omega \{ \nu_1(x_{i_1 0} - x_{\alpha 0}) + \dots + \nu'_s(x_{i_s 0} - x_{\alpha 0}) + \nu''_s(x_{i_s 0} - x_{\beta 0}) + \dots + \nu_n(x_{i_n 0} - x_{\beta 0}) \} - \\ - \sqrt{\omega^2 \nu_1^2 - \mu^2 \mathbf{n}_1 \cdot \mathbf{x}_1} - \dots - \sqrt{\omega^2 \nu_n^2 - \mu^2 \mathbf{n}_n \cdot \mathbf{x}_n} + \\ + \sqrt{\omega^2 \nu_\alpha^2 - \mu^2 \mathbf{n}_\alpha \cdot \mathbf{x}_\alpha} + \sqrt{\omega^2 \nu_\beta^2 - \mu^2 \mathbf{n}_\beta \cdot \mathbf{x}_\beta}.$$

Here \mathbf{n}_i is the unit vector along the direction of the special momentum of the i -th meson. As $\omega \rightarrow \infty$ this becomes asymptotically equal to

$$(23) \quad \omega \{ \nu_1[(x_{i_1 0} - x_{\alpha 0}) - \mathbf{n}_1 \cdot (\mathbf{x}_{i_1} - \mathbf{x}_\alpha)] + \dots + \nu'_s[(x_{i_s 0} - x_{\alpha 0}) - \mathbf{n}_s \cdot (\mathbf{x}_{i_s} - \mathbf{x}_\alpha)] + \\ + \nu''_s[(x_{i_s 0} - x_{\beta 0}) - \mathbf{n}_s \cdot (\mathbf{x}_{i_s} - \mathbf{x}_\beta)] + \dots \} - \delta_\alpha \cdot \mathbf{x}_\alpha - \delta_\beta \cdot \mathbf{x}_\beta.$$

Here

$$(24) \quad \begin{cases} \delta_\alpha = \mathbf{p}_1 + \dots + \mathbf{p}_{s-1} + \nu'_s / \nu_s \mathbf{p}_s - \mathbf{p}_\alpha, \\ \delta_\beta = \mathbf{p}_{s+1} + \dots + \mathbf{p}_n + \nu''_s / \nu_s \mathbf{p}_s - \mathbf{p}_\beta. \end{cases}$$

Now δ_α and δ_β are each the spatial part of a four-vector of zero fourth component. According to the argument of Sect. 2 $|\delta_\alpha|$ and $|\delta_\beta|$ are bounded as $\omega \rightarrow \infty$. Thus (23) together with the causality condition implies that the exponent is asymptotically equal to $A\omega$, where $A > 0$, as $\omega \rightarrow \infty$.

Consider now $M'(\tau)$ the Fourier transform of $M(\omega)$. It is given by

$$(25) \quad M'(\tau) = \frac{1}{2\pi} \int d\omega M(\omega) \exp[-i\omega\tau],$$

Substitute for $M(\omega)$ the expression of eq. (11) and suppose that the orders of integration may be changed so that the integration over ω may be performed before the configuration space integrals (*). Then for $\tau' < 0$ we may complete the contour by the semi-circle at infinity in the upper half plane to show that the integral vanishes.

Thus $M(\omega)$ has a Fourier transform $M'(\tau)$ that vanishes for $\tau' < 0$. This is precisely what is required for a dispersion relation^(1,2). Therefore

$$(26) \quad M(\omega) = \frac{i}{\pi} P \int \frac{M(\omega')}{\omega' - \omega} d\omega',$$

provided the integral is convergent. If it is not convergent subtraction terms are required in the manner familiar from previous single-meson dispersion theory.

7. — Discussion.

The expansion given in eq. (7) enables us to understand why the definitions of eqs. (11)–(13) are necessary in order to give an amplitude that satisfies a dispersion relation. The infinitesimal terms in ϵ appearing in the denominators have the effect of displacing above or below the real axis those poles corresponding to real intermediate states. The Feynman amplitude prescribes a term $\pm i\epsilon$ everywhere and this has the effect of displacing the poles for positive ω below the real axis and the poles for negative ω above the real axis. The causal amplitude defined in this paper differs by prescribing $-i\epsilon$ for all poles for negative ω . This has the effect of displacing these poles below the real axis also. This is necessary because if a function is to satisfy a dispersion relation it must have no poles above the real axis.

The dispersion relation essentially connects the hermitian and anti-hermitian (with respect to the nucleon variables) parts of the scattering amplitude. In order to determine them both it is necessary to find another relation between them. This is provided by the unitarity condition on the S matrix. Furthermore eq. (26) requires a knowledge of $M(\omega)$ for all values of ω and not all

(*) This interchange of the order of integration in fact requires careful discussion. A similar problem arises in the single-meson case.

these values correspond to physical reality. $M(\omega)$ for $\omega < 0$ may be related to $M(\omega)$ for $\omega > 0$ by using eq. (16). There still remain unphysical ranges for ω . These occur in the neighbourhood of $\omega = \mu$ for the anti-hermitian part of the amplitude and correspond to angles between the spatial momentum vectors with cosines less than -1 . A similar difficulty arises in the single-meson case and the continuation arguments used in that case ⁽²⁾ need to be extended to the general situation. This will not be discussed further in this paper.

The resulting set of equations could be used to provide an alternative formulation of quantum field theory. They are close to the original notions of HEISENBERG ⁽³⁾ in that only particles with $p^2 = -\mu^2$ appear and energy is conserved. They are, however, of immense complexity, in the general case. There is also the problem of the uniqueness of their solutions ⁽⁴⁾.

* * *

I am deeply indebted to Professor GELL-MANN for many stimulating discussions on these and related topics. I wish to thank the Commonwealth Fund of New York for the award of a fellowship.

APPENDIX

In this appendix it will be shown that the amplitude A satisfies the causality condition. The argument is intolerably prolix for the general case but it will be sufficiently illustrated by consideration of the case of two incoming mesons, specified by v_α and v_β , and n outgoing mesons, specified by v_1, \dots, v_n . Of course

$$(A.1) \quad v_\alpha + v_\beta + v_1 + \dots + v_n = 0.$$

Consider the product

$$(A.2) \quad i_1 \dots i_r \alpha \dots i_s \dots i_l \beta \dots i_n,$$

occurring in A . i stands for $j(x_i)$. i_s is called the divider and is defined by

$$(A.3) \quad \begin{cases} v_{i_1} + \dots + v_{i_{s-1}} + v_\alpha < 0, \\ v_{i_1} + \dots + v_{i_s} + v_\alpha > 0. \end{cases}$$

⁽⁴⁾ L. CASTILLEJO, R. H. DALITZ and F. J. DYSON: *Phys. Rev.*, **101**, 453 (1956).

We shall suppose that a divider exists and consider the case of non-existence later. The form of E given by eq. (13) requires that

$$(A.4) \quad \left\{ \begin{array}{l} i_1 > i_2 > \dots > i_r > \alpha, \\ i_s > i_{s-1} > \dots > i_{r+1} > \alpha, \\ i_s > i_{s+1} > \dots > i_t > \beta, \\ i_n > i_{n-1} > \dots > i_{t+1} > \beta. \end{array} \right.$$

$i > j$ denotes $(x_i - x_j) > 0$. The inequalities (23) imply that the product is ordered forward in time both ways from α and from β , and backwards in time both ways from i_s .

A natural way of forming the correlations discussed in Sect. 5 would be to correlate i_1, \dots, i_s with α and i_s, \dots, i_n with β . The inequalities (A.3) ensure that this correlation would be energetically correct. If the ordering of inequalities (A.4), which refers to the chosen time axis, could be shown to be an invariant ordering then the causality condition would be satisfied also. This idea will be used as a guide and the set of correlations generated in this way will be called T (the tentative correlation). Actually T will have to be modified in some cases. The various correlations will correspond to the various possible choices of a divider and each term in A corresponding to a correlation in T will consist of sets of products having a given point as divider. For example one term will consist of all the products obtained by all permutations of i_1, \dots, i_{s-1} amongst themselves and i_{s+1}, \dots, i_n amongst themselves applied to (A.2).

The arguments employed in what follows are mainly based on the following simple lemma: if $i > j > \alpha$, i is spacelike with respect to α , and j is timelike with respect to α , then i and j are spacelike.

Each point will be considered in turn and the consequences of assuming it to be spacelike with respect to one of the incoming meson points will be examined. It will be assumed that all earlier outgoing points correlated with the incoming point are timelike with respect to it. This does not result in any loss of generality since it will be clear that it is only the earliest spacelike point that is of consequence when there are several such points. This assumption will not be restated for every case considered but it is always made in what follows. Together with the lemma and the causality condition eq. (2) it enables us to commute $j(i)$ from one side of the incoming meson operator to its correct time-order position on the other side of the operator if i is spacelike with respect to the incoming meson point. In each case considered the method used will be to associate with each product another product occurring in A but with opposite sign. For the case of spacelike separation considered the two products will be equal and so their sum will vanish.

We now proceed to a particular consideration of the various cases that arise:

(i) Suppose i_m ($r < m < s$) is spacelike with respect to α . Then (A.2) equals

$$(A.5) \quad i_1 \dots i_m \dots \alpha \dots i_s \dots \beta \dots i_n,$$

where i_m occupies its correct time-ordered position to the left of α . However the form of E shows that (A.5) occurs in A , but with opposite sign.

(ii) A similar argument applies for i_m ($m \leq r$) if $i_m < i_s$. If $i_m > i_s$ two possibilities occur. If

$$(A.6) \quad \nu_i + \dots + \nu_{i_{m-1}} + \nu_{i_{m+1}} + \dots + \nu_{i_s} + \nu_\alpha < 0,$$

then (A.2) equals

$$(A.7) \quad i_1 \dots \alpha \dots i_s i_m \dots \beta \dots i_n,$$

and this product occurs in A also, though with opposite sign, and i_m is now the divider. If (A.6) is not satisfied (A.2) and (A.7) are, of course, still equal but (A.7) does not occur in A for the given ν 's and time-orderings of the i 's and α and β . However in this case it is energetically possible to correlate i_m with either α or β , keeping the other correlations unchanged. Also if i_m is spacelike with respect to both α and β then (A.2) equals

$$(A.8) \quad i_1 \dots \alpha \dots i_s \dots \beta \dots i_m \dots i_n,$$

and this does occur in A with opposite sign. This implies that it is only necessary to consider the case in which i_m is spacelike with respect to one only of α and β . In this case T is modified, if necessary, so as to correlate i_m with the other incoming meson point.

(iii) Similar arguments to those presented in (i) and (ii) may be used to consider the case of i_m ($m > s$) spacelike with respect to β .

(iv) Suppose i_s is spacelike with respect to α . Four possibilities must be distinguished:

(a) $i_{s-1} > i_{s+1}$ and

$$(A.9) \quad \nu_1 + \dots + \nu_{s-2} + \nu_s + \nu_\alpha < 0.$$

Then (A.2) is equal to

$$(A.10) \quad i_1 \dots i_s \dots \alpha \dots i_{s-1} i_{s+1} \dots \beta \dots i_n,$$

and this product occurs in A with opposite sign, having i_{s-1} as divider.

(b) $i_{s-1} > i_{s+1}$ and

$$(A.11) \quad \nu_1 + \dots + \nu_{s-2} + \nu_s + \nu_\alpha > 0.$$

Then (A.2) is equal to

$$(A.12) \quad i_1 \dots \alpha \dots i_s i_{s-1} i_{s+1} \dots \beta \dots i_n,$$

and this product occurs in A with opposite sign, having i_s as divider.

(c) $i_{s-1} < i_{s+1}$ and i_{s+1} is timelike with respect to α . Then i_s and i_{s+1} must be spacelike. (A.2) is equal to

$$(A.13) \quad i_1 \dots \alpha \dots i_{s-1} i_{s-1} i_s \dots \beta \dots i_n,$$

and this occurs in A with opposite sign provided

$$(A.14) \quad v_1 + \dots + v_{s-1} + v_{s+1} + v_\alpha < 0.$$

If (A.14) is not satisfied then it is energetically possible to modify T so as to correlate i_{s+1} with α and β and i_s with β . For i_s spacelike with respect to β see (v) below.

(d) $i_{s-1} < i_{s+1}$ and i_{s+1} is spacelike with respect to α . Then i_{s+1} and i_{s-1} are spacelike.

Suppose first that $i_{s-1} > i_{s+2}$. If

$$(A.15) \quad v_1 + \dots + v_{s-2} + v_s + v_\alpha > 0,$$

then (A.2) is equal to

$$(A.16) \quad i_1 \dots \alpha \dots i_s i_{s-1} i_{s-1} \dots \beta \dots i_n,$$

and this occurs in A with opposite sign and i_s as divider. If (A.16) does not hold but

$$(A.17) \quad v_1 + \dots + v_{s-2} + v_s + v_{s+1} + v_\alpha > 0,$$

then (A.2) is also equal to

$$(A.18) \quad i_1 \dots i_s \dots \alpha \dots i_{s+1} i_{s-1} \dots \beta \dots i_n,$$

and this occurs in A with opposite sign and i_{s+1} as divider. If (A.18) does not hold then (A.2) also equals

$$(A.19) \quad i_1 \dots i_s \dots i_{s+1} \dots \alpha \dots i_{s-1} \dots \beta \dots i_n,$$

and this occurs in A with opposite sign and i_{s-1} as divider.

Suppose now that $i_{s+2} > i_{s-1} > i_{s+3}$. If i_{s+2} is timelike with respect to α and so spacelike with respect to i_s and i_{s+1} then (A.2) equals

$$(A.20) \quad i_1 \dots \alpha \dots i_{s-1} i_{s+2} i_s i_{s+1} \dots \beta \dots i_n,$$

and this occurs in A with opposite sign provided

$$(A.21) \quad v_1 + \dots + v_{s-1} + v_{s+2} + v_\alpha < 0.$$

If (A.21) does not hold it is energetically possible to correlate i_{s+2} with α

and β and i_s with β . The case of i_{s+2} spacelike with respect to α may be dealt with using arguments similar to those employed above. The extension of the argument to the further cases $i_{s+3} > i_{s+2} > i_{s+4}$, etc., will also be clear.

(v) Suppose i_s is spacelike with respect to β . Similar arguments to those employed in (iv) may be used. It is important to note that the cases requiring special arguments in (iv) (i.e. $i_{-1} < i_{-1}$) are just those that are straightforward now, and *vice versa*.

The only case remaining to be considered is that in which there is no divider. Consider first

$$(A.22) \quad i_1 \dots i_r \alpha \dots i_t \beta \dots i_u \dots i_n,$$

where

$$(A.23) \quad v_i + \dots + v_{i_r} + v_\alpha > 0.$$

The point i_u is defined by $\alpha > i_u$, $\alpha < i_{u+1}$. The form of E ensures that

$$(A.24) \quad \begin{cases} i_1 > \dots > i_r > \alpha > i_{r+1} > \dots > i_t > \beta, \\ i_n > \dots > i_{t+1} > \beta, \end{cases}$$

that is the product is ordered forward in time both ways from β .

The case of α and β mutually timelike will be considered first. This presents a considerable simplification in that any i_m ($m \leq r$) which is timelike with respect to α is timelike with respect to β also. It is easy to prove using the techniques employed above that every i_m ($m \leq n$) must be timelike with respect to β . If there is a set $i_{\alpha_1}, \dots, i_{\alpha_j}$ ($\alpha_1 \leq r, \dots, \alpha_j \leq r$) such that they are all timelike with respect to α and also

$$(A.25) \quad v_{\alpha_1} + \dots + v_{\alpha_j} + v_\alpha > 0,$$

then an energetically correct causal correlation can be formed. If this is not true it is possible to choose a set $i_{\beta_1}, \dots, i_{\beta_k}$ ($\beta_1 \leq r, \dots, \beta_k \leq r$) such that:

- (i) all i_α are spacelike with respect to α ,
- (ii) $i_{\beta_l} > i_{\beta_{l+1}}$ ($1 \leq l < k$),
- (iii) $v_1 + \dots + v_r + v_\alpha - v_{\beta_1} - \dots - v_{\beta_k} < 0$,
- (iv) $v_1 + \dots + v_r + v_\alpha - v_{\beta_2} - \dots - v_{\beta_k} > 0$,

and the i_β are the set closest in time to α having these properties. Then (A.22) is equal to

$$(A.26) \quad i_1 \dots \alpha i_{\beta_1} \dots i_{\beta_k} i_{r+1} \dots \beta \dots i_n,$$

and this occurs in A with opposite sign and i_{β_1} as divider.

Consider now the case of α and β mutually spacelike. It is easy to show

that i_{r+1}, \dots, i_u must be timelike with respect to β . Then (A.22) is equal to

$$(A.27) \quad i_1 \dots i_r i_{r+1} \dots \beta \dots i_u i_{u+1} \dots i_n,$$

and this occurs in A with opposite sign provided

$$(A.28) \quad v_{i_1} + \dots + v_{i_u} + v_\beta < 0.$$

If (A.28) does not hold the argument proceeds as follows. Conventional methods show that every i_m ($m \leq n$) must be timelike with respect to either α or β . Moreover the argument given above to show there must be a set i_α ($\alpha \leq r$) timelike with respect to α and satisfying (A.25) still holds good. An energetically correct causal correlation can be formed, therefore, if it can be shown that there is also a set $i_{\gamma_1}, \dots, i_{\gamma_c}$ ($\gamma_1 \leq u, \dots, \gamma_c \leq u$) all timelike with respect to β and satisfying

$$(A.29) \quad v_{\gamma_1} + \dots + v_{\gamma_c} + v_\beta > 0.$$

If this is not so a set $i_{\delta_1}, \dots, i_{\delta_d}$ ($\delta_1 \leq r, \dots, \delta_d \leq r$) may be chosen such that:

- (i) all i_δ are spacelike with respect to β ,
- (ii) $i_{\delta_l} > i_{\delta_{l+1}}$ ($1 \leq l < d$),
- (iii) $v_1 + \dots + v_u - v_{\delta_1} - \dots - v_{\delta_d} + v_\beta < 0$,
- (iv) $v_1 + \dots + v_u - v_{\delta_2} - \dots - v_{\delta_d} + v_\beta > 0$,

and the i_δ are the set closest in time to β having these properties. Then (A.22) is equal to

$$(A.30) \quad i_1 \dots \beta \dots i_u i_{\delta_1} \dots i_{\delta_d} \alpha \dots i_n,$$

and this occurs in A with opposite sign and i_{δ_1} as divider.

The remaining case to be considered is that of

$$(A.31) \quad i_1 \dots i_r \alpha \dots i_t \beta \dots i_n,$$

where

$$(A.32) \quad v_1 + \dots + v_i + v_\alpha < 0.$$

The form of E requires that

$$(A.33) \quad \begin{cases} i_1 > \dots > i_r > \alpha, \\ i_n > \dots > \beta > i_t > \dots > \alpha. \end{cases}$$

This case may be dealt with using similar arguments to those used for (11).

This concludes the proof of the causality condition for A when there are two incident mesons. The general case may be dealt with using arguments that are simple extensions of those given above.

RIASSUNTO (*)

Si sviluppa un meccanismo che permette di ottenere le relazioni di dispersione per tutti i processi di scattering mesone-nucleone, compresi quelli in cui si creano o distruggono mesoni. Prima si dà un'opportuna descrizione cinematica dei processi e in base alla stessa si definisce una nuova ampiezza. Questa ampiezza ha due importanti proprietà. In primo luogo coincide con l'ampiezza di Feynman per le energie positive delle particelle entranti ed uscenti. In secondo luogo essa soddisfa a determinate condizioni di causalità. Ciò permette di ottenere le relazioni di dispersione. Si discute il significato di questi risultati in quanto permettono di formulare una nuova teoria quantistica dei campi.

(*) Traduzione a cura della Redazione.

On Sums over Trajectories for Systems with Fermi Statistics.

D. J. CANDLIN

Institute for Advanced Study - Princeton, N. J.

(ricevuto il 29 Aprile 1956)

Summary. — A recent derivation of the Feynman action principle from the canonical formulation is extended to systems with Fermi statistics.

1. — Introduction.

The action principle introduced by FEYNMAN⁽¹⁾ for particle mechanics, and extended by him⁽²⁾, MATTHEWS and SALAM⁽³⁾ and others to describe quantized fields may be interpreted in two ways, until we can give an explicit meaning for the integral over all trajectories. We may either postulate^(4,5) that such integrals exist and possess certain reasonable properties, or we may assume that the expression is the limit of a multiple integral over the position (or field) variable at a number of infinitesimally separated points of time (or space-time). The second interpretation is the original one of FEYNMAN, and has been shown to follow from the first for particle mechanics by DAVISON⁽⁶⁾. Recently, TOBOCMAN⁽⁷⁾ has shown that it may also be derived from the canonical formulation for systems with a finite number of canonical co-ordinates and momenta, if these satisfy the usual commutation relations.

A similar derivation for anticommuting co-ordinates and momenta is given here. This is of particular interest, because the properties to be ascribed to

⁽¹⁾ R. P. FEYNMAN: *Rev. Mod. Phys.*, **20**, 367 (1948).

⁽²⁾ R. P. FEYNMAN: *Phys. Rev.*, **80**, 440 (1950); **84**, 108 (1951).

⁽³⁾ P. T. MATTHEWS and A. SALAM: *Nuovo Cimento*, **2**, 120 (1955).

⁽⁴⁾ J. C. POLKINGHORNE: *Proc. Roy. Soc., A* **230**, 272 (1955).

⁽⁵⁾ K. SYMANZIK: *Zeits. f. Naturfor.*, **9a**, 809 (1954).

⁽⁶⁾ B. DAVISON: *Proc. Roy. Soc., A* **225**, 252 (1954).

⁽⁷⁾ W. TOBOCMAN: *Nuovo Cimento*, **3**, 1213 (1956).

integrals over anticommuting functions in the first interpretation are not at all clear. In Sect. 2 the method is given for the simplest case, a single uncoupled Fermi oscillator; in the following section it is generalized to describe a number of coupled oscillators, and a slight change in the formalism gives the theory the symmetry between particle and antiparticle characteristic of the Dirac field. The idea of integration over anticommuting quantities and the interpretation of sets of values of the variables of integration as trajectories are discussed in Sections 4 and 5.

2. — A Single Fermi Oscillator.

First we consider the simple case of a system with Hamiltonian

$$(1) \quad H = m\eta^\dagger\eta,$$

where

$$(2) \quad \eta\eta^\dagger + \eta^\dagger\eta = 1.$$

There is only one essentially distinct matrix representation of these operators, and we adopt the usual form

$$(3) \quad \eta = \begin{pmatrix} 0 & 0 \\ 1 & 0 \end{pmatrix} \quad \text{and} \quad \eta^\dagger = \begin{pmatrix} 0 & 1 \\ 0 & 0 \end{pmatrix}.$$

To set up the action principle in the Bose case, TOBOCMAN (?) introduced resolutions of the identity belonging to the canonical conjugates x and p ; here, we shall need resolutions belonging to η and η^\dagger . Since these operators cannot be diagonalized, they can have no true eigenstates. However, it will be enough to construct «eigenstates with anticommuting eigenvalues»; that is, to find solutions of

$$(4) \quad \begin{cases} \eta|a\rangle = a|a\rangle, & \langle a|\eta = \langle a|a, \\ \eta^\dagger|a^*\rangle = a^*|a^*\rangle & \text{and} \quad \langle a^*|\eta^\dagger = \langle a^*|a^*, \end{cases}$$

where the quantities a and a^* are generalized numbers which all anticommute with each other and have zero squares. We shall call such quantities *a-numbers*. Since the vectors in (4) contain *a-numbers* as parameters, they do not have any direct physical significance, and we do not require any particular relation between the four vectors. «Eigenvalues» and other quantities will be distinguished by asterisks if they are associated with η^\dagger , but this does not imply

that they are complex conjugates of the quantities associated with η .

An immediate solution of (4) in the representation (3) is

$$(5) \quad \left\{ \begin{array}{l} |a\rangle = A^{-\frac{1}{2}} \begin{pmatrix} a \\ 1 \end{pmatrix}, \quad \langle a| = A^{-\frac{1}{2}}(1, a), \\ |a^*\rangle = A^{*\frac{1}{2}} \begin{pmatrix} 1 \\ a^* \end{pmatrix} \quad \text{and} \quad \langle a^*| = A^{*\frac{1}{2}}(a^*, 1). \end{array} \right.$$

A and A^* are ordinary numbers, and there is a solution for any a or a^* of the specified type. We should like to choose A and the set S of « eigenvalues » a such that

$$(6) \quad \sum_{a \in S} |a\rangle \langle a| \equiv \sum_{a \in S} A^{-1} \begin{pmatrix} a & 0 \\ 1 & a \end{pmatrix}$$

is the unit operator. This is impossible, but we can arrange in many ways that it should be the unit operator multiplied by any given a -number ϱ ; for instance, one could take $a = \pm \frac{1}{2}\varrho$ with $A = \pm 1$ respectively. We shall eventually use ⁽⁸⁾ a different set S , with suitable A . Similarly, we may arrange that

$$\sum_{a^* \in S^*} |a^*\rangle \langle a^*| = \varrho^*.$$

Suppose that we have a system with Hamiltonian $H(t)$ and that we require the transition amplitude between a state Ψ specified at time 0 and a state Φ specified at time T . Then, in the Schrödinger frame,

$$(7) \quad \begin{aligned} \langle \Phi | \Psi \rangle &= \langle \Phi(T) | \Psi(T) \rangle = \\ &= \langle \Phi(T) | \prod_{n=0}^{N-1} (1 - i\varepsilon H(t)) | \Psi(0) \rangle + O(\varepsilon) \end{aligned}$$

as $N \rightarrow \infty$, where $\varepsilon = T/N$ and $t_n = n\varepsilon$. We have assumed that Φ and Ψ are normalizable states, and that they remain so under any number of operations of H . This will be true for all physical problems other than those of divergent field theories, provided that we use wave-packets for scattering problems. For the Fermi oscillator (1) we introduce the representation (3),

⁽⁸⁾ For the Bose case, TOBOCMAN ⁽⁷⁾ naturally used resolutions of the identity $\sum |x\rangle \langle x|$ and $\sum |p\rangle \langle p|$ which involve linearly independent vectors. This is not essential to the method, and we may set up different forms for the transition amplitude by using different resolutions. These forms will not necessarily be Lagrangian, as Toboecman has shown.

and obtain

$$\begin{aligned}
 (8) \quad \varrho^* \varrho (1 - i\varepsilon H) &= \varrho^* \varrho (1 - i\varepsilon m \eta^\dagger \eta) = \\
 &= \sum (A^* A)^{-\frac{1}{2}} |a^*\rangle \langle a^*| 1 - i\varepsilon m \eta^\dagger \eta |a\rangle \langle a| = \\
 &= \sum (A^* A)^{-\frac{1}{2}} |a^*\rangle \{1 + (1 - i\varepsilon m) a^* a\} \langle a| = \\
 &= \sum (A^* A)^{-\frac{1}{2}} |a^*\rangle \exp[a^* a - i\varepsilon m a^* a] \langle a|,
 \end{aligned}$$

where the summation is over all values of a in S and of a^* in S^* . On substituting an expression of the type (8) for each factor in (7), and introducing an extra unit operator, we obtain

$$\begin{aligned}
 (9) \quad \varrho_N \varrho_{N-1}^* \varrho_{N-1} \cdots \varrho_0^* \varrho_0 \langle \Phi | \Psi \rangle &= \\
 &= \sum C^{-1} \langle \Phi | a_N \rangle \exp[iI(a_N, a_{N-1}^*, a_{N-1}, \dots, a_0^*, a_0)] \langle a_0 | \Psi \rangle,
 \end{aligned}$$

where

$$C = A_N^{\frac{1}{2}} A_{N-1}^* A_{N-1} \cdots A_0^* A_0^{\frac{1}{2}}$$

and

$$\begin{aligned}
 I &= -i(a_N a_{N-1}^* + a_{N-1}^* a_{N-1} + \cdots + a_0^* a_0) - \varepsilon m(a_{N-1}^* a_{N-1} + \cdots + a_0^* a_0) = \\
 &= \varepsilon \sum_{n=0}^{N-1} a_n^* \{i(a_{n+1} - a_n)/\varepsilon - m a_n\},
 \end{aligned}$$

which is the approximate form of the action

$$\int_0^T a^* (i\dot{a} - ma) dt$$

of the problem. If

$$|\Psi\rangle = \begin{pmatrix} \lambda \\ \mu \end{pmatrix}$$

then

$$\Psi(a) \equiv A^{\frac{1}{2}} \langle a | \Psi \rangle = \lambda + \mu a$$

is the « wave-function » of the state $|\Psi\rangle$.

We may eliminate the undesirable quantities ϱ and ϱ^* from the left hand side of (9) by comparing $\langle \Phi | \Psi \rangle$ with $\langle 0 | 0 \rangle = 1$, where $|0\rangle$ is the ground

state of the oscillator. This will also remove the normalization factors A and A^* , if they are independent of a and a^* , and has been the usual procedure in the formulation in terms of sums over trajectories ⁽³⁾.

Finally, we must show that arbitrarily many quantities q and q^* exist which anticommute, have zero squares and are such that the product of any number of them (all different) does not vanish. A matrix representation of them (in a space which of course has nothing to do with the state vector space) is given by the quantities $\hat{a}_n = \frac{1}{2}(\hat{\xi}_n + i\hat{\zeta}_n)$ introduced in a slightly different connexion by TOBOCHAN ⁽⁷⁾. We need an \hat{a}_n for each q and another one (not an \hat{a}_n^\dagger) for each q^* .

3. — The Dirac Oscillator.

By a Dirac oscillator we mean a system described in terms of four operators ψ_α and their adjoints, with the anticommutation relations

$$(10) \quad \{\psi_\alpha, \psi_\beta\} = 0 \quad \text{and} \quad \{\psi_\alpha, \psi_\beta^\dagger\} = \delta_{\alpha\beta}.$$

The Hamiltonian of the system is

$$(11) \quad H = \frac{1}{2}(\psi_\alpha^\dagger Q_{\alpha\beta} \psi_\beta - \psi_\beta Q_{\beta\alpha}^* \psi_\alpha^\dagger),$$

where Q is an Hermitian numerical matrix ⁽⁸⁾. For instance, Q is $\alpha \cdot \mathbf{k} + \beta \kappa$ for the uncoupled oscillator of momentum \mathbf{k} and mass κ . The method may be immediately generalized to describe a finite number of Dirac oscillators linearly coupled to a given external potential, or even interacting with each other through non-bilinear terms. We do not wish to discuss the Dirac field, since the transition to an infinity of degrees of freedom gives rise to difficulties which are not peculiar to Fermi quantization ⁽¹⁰⁾ and may presumably be more readily understood for a Bose field.

The 16 dimensional space \mathfrak{R} used for the well-known « number » representation of the operators defined by (10) is the product of four two-dimensional spaces $\mathfrak{R}^{(\alpha)}$, each corresponding to one degree of freedom. If $\psi^{(\alpha)}$ be the operator which is $\begin{pmatrix} 0 & 0 \\ 1 & 0 \end{pmatrix}$ in $\mathfrak{R}^{(\alpha)}$ and the unity elsewhere, then

⁽⁸⁾ From now on, we adopt the summation convention for the letters α and β only, which range from 1 to 4. Q^* is the complex conjugate of Q .

⁽¹⁰⁾ A. S. WIGHTMAN and S. S. SCHWEBER: *Phys. Rev.*, **98**, 812 (1955).

$$(12) \quad \begin{cases} \psi_\alpha = \psi^{(\alpha)} \prod_{\mu=1}^{\alpha-1} (\psi^{(\mu)\dagger} \psi^{(\mu)} - \psi^{(\mu)} \psi^{(\mu)\dagger}) \\ \psi_\alpha^\dagger = \psi^{(\alpha)\dagger} \prod_{\mu=1}^{\alpha-1} (\psi^{(\mu)\dagger} \psi^{(\mu)} - \psi^{(\mu)} \psi^{(\mu)\dagger}) \end{cases}$$

form the required representation. Corresponding to the vectors (5) introduced for one degree of freedom are the outer products

$$(13) \quad \begin{cases} |u\rangle \equiv |u_4 u_3 u_2 u_1\rangle = | - u_4 \rangle |u_3\rangle | - u_2 \rangle |u_1\rangle, \\ \langle u| \equiv \langle u_1 u_2 u_3 u_4| = \langle u_1| \langle u_2| \langle u_3| \langle u_4|, \\ |u^*\rangle \equiv |u_4^* u_3^* u_2^* u_1^*\rangle = |u_4^*\rangle |u_3^*\rangle |u_2^*\rangle |u_1^*\rangle \\ \langle u^*| \equiv \langle u_1^* u_2^* u_3^* u_4^*| = \langle u_1^*| \langle - u_2^*| \langle u_3^*| \langle - u_4^*|, \end{cases}$$

where the factors are given, in the appropriate $\mathfrak{H}^{(\alpha)}$, by (5). If a set of α -numbers ϱ_α and ϱ_α^* are introduced, and the summation is of the type described in Sect. 2, it can be seen at once that

$$(14) \quad \begin{cases} \sum_{u_1 u_2 u_3 u_4} |u\rangle \langle u| = \varrho_1 \varrho_2 \varrho_3 \varrho_4 \equiv \varrho, \quad \text{say}, \\ \sum_{u_1^* u_2^* u_3^* u_4^*} |u^*\rangle \langle u^*| = \varrho_4^* \varrho_3^* \varrho_2^* \varrho_1^* \equiv \varrho^*, \quad \text{say}, \end{cases}$$

which can again be associated in pairs in the representation of the transition amplitudes. Further, we see that

$$\begin{aligned} \langle u|u^*\rangle &= (A_1 A_1^* A_2 A_2^* A_3 A_3^* A_4 A_4^*)^{-\frac{1}{2}} \exp[u_\alpha u_\alpha^*], \\ \langle u|\psi_\alpha|u^*\rangle &= u_\alpha \langle u|u^*\rangle, \\ \langle u|\psi_\alpha^\dagger|u^*\rangle &= u_\alpha^* \langle u|u^*\rangle \end{aligned}$$

and

$$\langle u|\psi_\alpha \psi_\beta^\dagger|u^*\rangle = u_\alpha u_\beta^* \langle u|u^*\rangle,$$

together with similar equations in which u and u^* , ψ and ψ^\dagger are interchanged.

The transition amplitude is analogous to (9), except that to maintain the symmetry we introduce one more unit operator.

$$(15) \quad \varrho_N^* \varrho_N \varrho_{N-1}^* \varrho_{N-1} \cdots \varrho_0^* \varrho_0 \langle \Phi | \Psi \rangle = \sum_{u, u^*} O^{-1} \Phi(u_N^*, u_N) \exp[iI(u^*, u)] \Psi(u_0^*, u_0) + O(\varepsilon),$$

where

$$I = \varepsilon \sum_{n=0}^{N-1} L_n,$$

and

$$\begin{aligned} L_n = & -(i/2\varepsilon)(u_{\alpha,n+1}^* u_{\alpha,n+1} + 2u_{\alpha,n+1}^* u_{\alpha,n}^* + u_{\alpha,n}^* u_{\alpha,n}) + \frac{1}{2}(u_{\beta,n+1} Q_{\beta\alpha}^* u_{\alpha,n}^* - u_{\alpha,n}^* Q_{\alpha\beta} u_{\beta,n}) = \\ = & -(i/2)(u_{\alpha,n+1}^* - u_{\alpha,n}^*) u_{\alpha,n+1} / \varepsilon + (i/2) u_{\alpha,n}^* (u_{\alpha,n+1} - u_{\alpha,n}) / \varepsilon + \\ & + \frac{1}{2}(u_{\beta,n+1} Q_{\beta\alpha}^* u_{\alpha,n}^* - u_{\alpha,n}^* Q_{\alpha\beta} u_{\beta,n}), \end{aligned}$$

the properly symmetrized form of the approximate Lagrangian. To display the symmetry more explicitly, one might write $u_{\alpha,n+\frac{1}{2}}^*$ for $u_{\alpha,n}^*$, the suffix denoting the time in units of ε . The « wave function »

$$\Psi = \prod_{\mu=1}^4 A_{\mu,0}^{\frac{1}{2}} (1 + \frac{1}{2} u_{\mu,0}^* u_{\mu,0}) \langle u_0 | \Psi \rangle$$

in the symmetrized form involves both u_0 and u_0^* .

4. — The Continuous Realization.

We now give the alternative realization of (6) mentioned above, in which A is independent of u . It is only possible in the symmetrical form, when the sums over u and u^* may be associated in pairs. If u and u^* be such a pair, put

$$\begin{aligned} u &= (x - iy) \varrho \\ u^* &= (x + iy) \varrho^* \end{aligned}$$

and replace $\sum_{u \in S} \sum_{u^* \in S^*}$ by $\int_{-\lambda}^{\lambda} dx \int_{-\lambda}^{\lambda} dy$ (which we denote, according to custom, by $\int_j^{\lambda} du^* du$), with $A = A^* = (8/3)^{\frac{1}{2}} \lambda^2$. Then

$$\int_{-\lambda}^{\lambda} |u^* \rangle \langle u^*| F |u \rangle \langle u| du^* du = \varrho^* \varrho F + O(1/\lambda),$$

where F is any operator of the system. Thus (15) will remain true, provided we take λ of order ε^{-2} .

It is essentially this realization which MATTHEWS and SALAM⁽³⁾ use in the evaluation of their integrals over trajectories of the Dirac field. In general, however, there is no relation between the quantities u and u^* representing the operators ψ and ψ^\dagger , just as there is none between p_n and x_n in the Bose case⁽⁷⁾. They are not complex conjugates, so that they may anticommute without vanishing.

5. — The Sum Over Trajectories.

The presence of the a -numbers seems to make it impossible to interpret the expression for the transition amplitude as a sum over trajectories. In our picture, we cannot say that the field has such a strength at such an intermediate time in a given classical trajectory, for obviously no a -number can be the result of a measurement. Further, we know that ψ and ψ^\dagger , or even their real and imaginary parts, are not observable⁽¹¹⁾, and also that the problem has no classical trajectories.

However, one can show that our expression for the transition amplitude is a sum over trajectories in the only rigorous sense which this statement can have, in either Bose or Fermi quantization. The matrix element of any quantity observed at an intermediate time is obtained by inserting the appropriate function of the field variables into the multiple integral⁽¹²⁾. That is, the matrix element of *any* observable quantity is the average of that quantity weighted with the appropriate phase factor. This is the general expression of the idea of sums over trajectories. For particle mechanics, it is exactly equivalent to Feynman's original postulate⁽¹³⁾ if the observable is the projection operator into a given region \mathfrak{R} of space-time.

TOBOCMAN⁽⁷⁾ discusses the interpretation of momenta as generators of infinitesimal displacements in their conjugate coordinates. Although this probably has little physical meaning in the Fermi case, it may be verified. Considering for simplicity the single Fermi oscillator, we should have, for a variation δa in a ,

$$\delta|a\rangle = -iG_\eta|a\rangle = \eta^\dagger\delta a|a\rangle \quad (\text{in Schwinger's notation }^{(14)})$$

or

$$\delta \begin{pmatrix} a \\ 1 \end{pmatrix} = \begin{pmatrix} 0 & \delta a \\ 0 & 0 \end{pmatrix} \begin{pmatrix} a \\ 1 \end{pmatrix} = \begin{pmatrix} \delta a \\ 0 \end{pmatrix}.$$

⁽¹¹⁾ G. C. WICK, A. S. WIGHTMAN and E. P. WIGNER: *Phys. Rev.*, **88**, 101 (1952).

⁽¹²⁾ This may be proved for Fermi quantization by a simple extension of the method of Sect. 3.

⁽¹³⁾ Reference⁽¹⁾, equation (9).

⁽¹⁴⁾ J. SCHWINGER: *Phil. Mag.*, **44**, 1171 (1953).

* * *

I should like to thank Dr. W. TOBOCMAN for communicating his work to me before publication, Professor J. R. OPPENHEIMER for the hospitality of the Institute for Advanced Study, and the Commonwealth Fund for financial support.

RIASSUNTO (*)

Partendo dalla formulazione canonica, si estende a sistemi obbedienti a una statistica di Fermi una recente derivazione del principio di azione di Feynman.

(*) *Traduzione a cura della Redazione.*

Analysis of one Hundred Bevatron τ^+ Particles.

R. P. HADDOCK

Radiation Laboratory, University of California - Berkeley, California

(ricevuto il 30 Aprile 1956)

Summary. — One hundred τ^+ mesons, obtained from nuclear emulsion stacks exposed to the K^+ beam at the Bevatron, are analyzed for (a) Q -value of the τ -decay, (b) possible values of the spin-parity of the τ . A Q of $75.13 \pm .20$ MeV is obtained. The corresponding τ mass is $966.5 \pm .74 m_e$. The analyses by DALITZ and FABRI were used to assign possible spin-parity values to the τ . The case of 0^- gives the best agreement with the observed energy and angle distributions.

1. — Introduction.

One hundred τ^+ meson ($\tau^+ \rightarrow 2\pi^+ + \pi^- + Q$) found in the systematic scanning of three emulsion stacks have been analyzed (*).

The Q -values have been studied and an average Q obtained. The most important systematic errors were considered and their limits assigned to the Q -value.

The distribution of decay configurations has been compared with the analyses developed independently by DALITZ ^(1,2) and FABRI ⁽³⁾. All cases of spin and parity of the τ that are also possible for the $K_{\pi 2}$ were considered up to and including spin five.

(*) Twenty-four of these τ^+ 's were included in the data presented at the 1955 Conference on Elementary Particles held at Pisa, Italy.

(¹) R. H. DALITZ: *Proc. Phys. Soc.*, **64**, 710 (1953).

(²) R. H. DALITZ: *Phil. Mag.*, **44**, 1068 (1953).

(³) R. H. DALITZ: *Phys. Rev.*, **94**, 1046 (1954).

(⁴) E. FABRI: *Nuovo Cimento*, **11**, 479 (1954).

2. - Experimental Arrangement and Scanning Technique.

The strong-focusing spectrometer ⁽⁵⁾ at the Bevatron was used to select nearly monoenergetic positive K particles and focus them on three emulsion blocks.

The emulsion blocks were stacked (without tissue paper between the pellicles), backed with $\frac{1}{2}$ -inch bakelite, and held together with bolts passing through the bakelite and emulsion. The stack edges were then machined to close tolerances to permit accurate measurements (for volume and density determinations).

The scanning was done by the track-following method. Tracks in a grain count interval were selected at a region of the stacks where K particles would have several centimetres of residual range. These tracks were then followed to their ends and the particles were identified by their decay mode. This method is thus unbiased in regard to the τ -decay configuration.

3. - Measurements of the Q .

3.1. *Method.* - The densities and average plate thicknesses were determined from the dimensions and weight of the stacks.

The average plate thickness was used to compute the chord between points where there was either an integrated 10° change of direction in the plane of the emulsion or a visible change in the diving rate. The range of the pions was taken to be the sum of these chords when corrected for air gaps between pellicles. A full discussion of the range measurements is given in Section 3.2.

The range-energy relation given by BARKAS and YOUNG ⁽⁶⁾ was used. It is based on Vigneron's parameters; in particular, the mean ionization potential of 322 eV is used to extrapolate to high velocity. The relation is for C.2 emulsion of density 3.815 g/cm³ at a relative humidity of 55%.

3.2. *Errors.*

3.2.1. *Alignment.* - X-ray marks placed in the stacks before processing provide an accurate means of aligning the plates after development. Generally the position of neighboring plates is known to within 25 μ m, but there may be a systematic shift to the stack. To eliminate or reduce any systematic shift of this type the coordinates of the X-ray marks were measured with

⁽⁵⁾ L. T. KERTH and D. H. STORK: *Phys. Rev.*, **99**, 641 (A) (1955).

⁽⁶⁾ W. H. BARKAS and D. M. YOUNG: *Emulsion Tables. I. Heavy-Particle Functions*, in *University of California Radiation Laboratory Report No. UCRL-2549* (rev.), Setp. 1954.

a microscope stage and used when necessary. The error in alignment is then the error in estimating the center of the X-ray mark.

3'2.2. Distortion and Rub-off Errors. — The ranges were computed, not as the sum of path lengths in each plate, but as a chord between points where the track changes direction by 10° . Then the distortion and rub-off errors to first approximation enter only as errors in the position of the τ -decay and pion decay. An error in the position of an intermediate point such as to increase one chord length will reduce the following chord length by a like amount to the first order. The distortion and rub-off errors are then negligible.

3'2.3. Range Shortening. — The percent difference between the arc and chord lengths along a pion track was estimated to be 0.48% in range or 0.25% in energy. This estimate is good to 30%. The uncertainty of 30% is due mostly to an uncertainty in how closely the 10° criterion was followed. Then the average Q of the τ obtained by measuring chords should be increased by 0.19 MeV to account for the effect of range shortening.

3'2.4. Air Gaps. — The average densities of the emulsion stacks, obtained from their measured areal densities σ and the thickness of the stacks, were 0.7% to 1.1% less than 3.826 g/cm³. The latter is the density for Ilford G.5 emulsion when it is shipped from the factory. From measurements of individual pellicles of fresh emulsion it is evident that there is little water loss through the shipping wrappings. There also should be little change in the density during stacking of the emulsion or through the edges of the machined stack. The difference between the average density of the stacked emulsion and of individual pellicles is attributed to air gaps between pellicles. The air gaps (about 5 μ m thick on the average) increase the total stack thickness above its true value and so reduce the stack density.

Let t_m and q_m be the measured average plate thickness and density for the stack, and t_t and q_t the true average thickness and density of the emulsion. The ranges of the pions can then be computed as follows:

- (a) t_m is used to obtain the shrinkage factor. This gives the length of the track through both emulsion and air.
- (b) The true density q_t is assumed to be 3.826 g/cm³.
- (c) The average air gap thickness, t_a , is taken to be

$$t_a = t_m - t_t = \sigma \{1/q_m - 1/q_t\}.$$

(d) The range in emulsion alone, R_E , is then obtained from

$$(1) \quad R_E/R_i = Z_{E_i}/Z_i - Na_it_a/Z_i,$$

where R_{E_i} is the length of the i -th chord in emulsion,
 R_i is the length of the i -th chord in emulsion and air,
 Z_{E_i} is the vertical height between chord ends in emulsion,
 Z_i is the corresponding height through air and emulsion,
 Na_i is the number of air gaps traversed.

Then

$$R_E = \sum_i R_{E_i}.$$

Any uncertainty in q_e is due to an uncertainty in the equilibrium value of the relative humidity of the emulsion. Since the stopping power of emulsion per g cm² is a slowly varying function of its water content (relative humidity), an error in q_e leads to a relatively smaller error in Q . The effect of an error in q_e on the Q -values is given (see appendix) by

$$(2) \quad \Delta Q/Q = -0.046 \Delta q_e/q_e.$$

BARKAS and YOUNG (6) give the density of emulsion at 35% relative humidity as 3.90 g cm³. This is the upper limit of the emulsion density, and the measured stack density is the lower limit. Inspection of Eq. (2) shows that for 1% uncertainty in the emulsion density the uncertainty in the average Q will be 0.05% or $\Delta Q = 0.04$ MeV. The uncertainty in Q due to the uncertainty in emulsion density is therefore negligible.

3.3. Results. — An average Q of

$$\begin{aligned} &74.94 \text{ MeV} + .19 \text{ MeV (range shortening)} \\ &\quad + .04 \text{ MeV (uncertainty in water content of emulsion)} \\ &\quad - .07 \text{ MeV} \\ &\quad \pm .18 \text{ MeV (standard deviation of the average } Q) \\ &\quad \pm .07 \text{ MeV (uncertainty in the measurement of the} \\ &\quad \quad \text{stack density)} \end{aligned}$$

$$\text{or } 74.94 + .19 \pm .20 \text{ MeV}$$

was obtained for 67 τ 's. For these τ 's all three pions stopped in the stack and none of the pions made a large-angle scatter. Fig. 1 shows the distribution of Q -values. This distribution is quite consistent with a normal distribution (which is also plotted).

The corresponding mass of the τ (in electron mass, m_e) is

$$\begin{aligned}
 &966.1 m_e + .37 m_e \text{ (range shortening)} \\
 &\quad + .08 m_e \text{ (uncertainty in water content of emulsion)} \\
 &\quad \pm .36 m_e \text{ (standard deviation of the average } Q) \\
 &\quad \pm .62 m_e \text{ (standard deviation of the pion masses)} \\
 &\quad \pm .14 m_e \text{ (uncertainty in measurement of stack density)} \\
 &\text{or } 966.1 + .37 \pm .74 m_e.
 \end{aligned}$$

The pion masses found by BARKAS, BIRNBAUM, and SMITH ⁽⁷⁾ were used. These masses are

$$m_{\pi^+} = 273.3 \pm 0.3 m_e,$$

$$m_{\pi^-} = 272.8 \pm 0.4 m_e,$$

where the errors indicated are standard deviations.

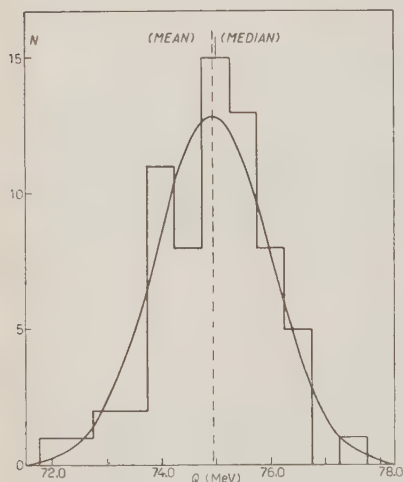


Fig. 1. — Plot of the distribution of Q -values for 67 τ 's which had all three pions staying in the stack and none of the pions making a large-angle scatter. The average Q is 74.94 MeV and the median is 75.0 MeV. The distribution is fitted with a normal curve and the agreement is observed to be quite good.

4. — Spin and Parity.

The dependence of the decay amplitude on the spin and parity of the τ has been independently investigated by DALITZ ^(1,3) and FABRI ⁽⁴⁾. AMALDI ⁽⁵⁾ has compared all available τ data with the analyses by DALITZ and FABRI, and concludes that the spin-parity of the τ may be 0^- , 2^- , 4^- , etc., and possible 3^- . I would like to review some of the analyses by DALITZ and FABRI in order to discuss the so-called ambiguous cases.

⁽⁷⁾ W. H. BARKAS, W. BIRNBAUM and F. M. SMITH: *The Mass Ratio Method Applied to the Measurement of L-Meson Masses and the Energy Balance in Pion Decay*, in *University of California Radiation Laboratory Report No. UCRL-3147*, Sept. 1955. Also to be published in *Phys. Rev.*, Jan. 15, 1956).

⁽⁸⁾ E. AMALDI: *Proceedings of the Conference on Elementary Particles at Pisa, Italy*, to be published as a *Supplemento* to the *Nuovo Cimento*.

4.1. Analysis by Dalitz and Fabri. — Relative co-ordinates are used to describe the decay configuration of the three final-state pions. The relative co-ordinate \mathbf{r} is proportional to the distance between like pions and \mathbf{r}' is proportional to the distance between the unlike pion and the center of mass of the like pion system. The momenta \mathbf{p} and \mathbf{p}' are the conjugate momenta and \mathbf{l} and \mathbf{l}' the corresponding angular momenta (\mathbf{l} is even by Bose-Einstein statistics).

If the orientation of the decay-plane normal and the rotations of the decay configuration about the decay-plane normal are neglected, then only two independent variables are necessary to determine the decay configuration. These are taken to be $|\mathbf{p}'|$ and $\cos \theta = \mathbf{p}\mathbf{p}'/pp'$. The conservation of angular momentum requires that the spin of the τ be the vector sum of \mathbf{l} and \mathbf{l}' , i.e. $\mathbf{J}_\tau = \mathbf{l} + \mathbf{l}'$. The conservation of parity requires that the parity of the τ be the product of the intrinsic parity of the three pions and their orbital parity, i.e., $P_\tau = (-1)^3(-1)^{l+l'} = (-1)^{l+l'+1}$.

If the Coulomb and pion-pion interactions are neglected, the final state of the τ can be thought of as three independent pions. The τ is coupled to three pion states having the same spin and parity. These three pion states are characterized by various values of l and l' . There are a variety of states of three pions having the same spin and parity, and therefore the final of the τ will be a linear combination of all these three pion states.

In order to estimate the relative probabilities for decay into different final states, DALITZ and FABRI assume that the probability amplitude of these states is proportional to the value of the corresponding wave function in the volume occupied by the τ . The radius of this volume is chosen to be τ Compton wave length, which is small compared with the wave length of the emitted pions. The free-pion wave functions near the origin are approximated by the lowest-order term, i.e., the spherical Bessel function of order l , $j_l \simeq (pr)^l (2l-1)!!$. Using these assumptions, one derives the magnitude of the relative decay amplitudes. TELEGI⁽⁹⁾ has pointed out that if final-state interactions are to be neglected then, on the basis of time reversibility, the ratios of the relative decay amplitudes are real. The sign, however, cannot be obtained without further assumptions about the details of the structure of the τ .

The decay amplitudes are shown to be small except for those states for which $l+l' = \min$. Then the distribution of the decay configurations is uniquely determined if only one state has $l+l' = \min$. If there are several states with the same $l+l' = \min$, the decay configurations also depend on the relative phases between these states. The latter are then the ambiguous cases.

A single state with $l+l' = \min$ exists for the cases of τ spin and parity

(⁹) V. L. TELEGI: Private communication.

$0-, 1+, 1-, 2+, 3-$. For all other cases (except $0+$, which is not a possible final state for three pions) there are two or more final states with $l+l' = \text{min.}$

4.2. Comparison of Angular and Odd-Pion Energy Distributions with the Analysis by Dalitz and Fabri.

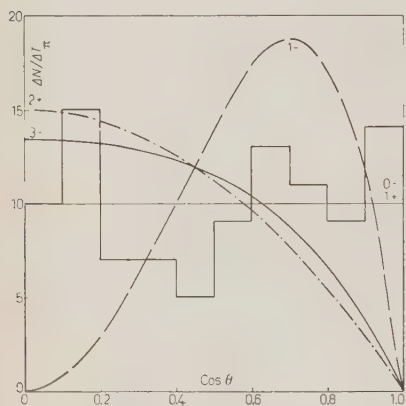


Fig. 2. — Plot of expected $\cos \theta$ distribution for τ spin-parity $0-, 1+, 1-, 2+, 3-$. Also shown is the experimental distribution.

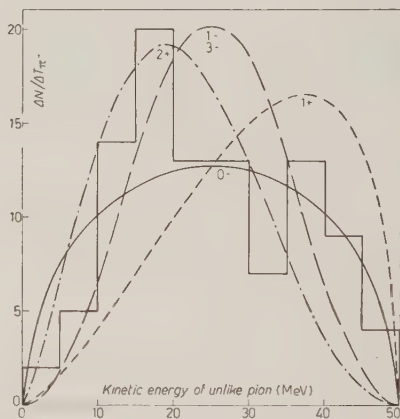


Fig. 3. — Plot of expected odd-pion energy distributions for τ spin-parity $0-, 1+, 1-, 2+, 3-$. Also shown is the experimental distribution.

4.2.1. Discussion. — One hundred τ^\pm mesons were found systematically by the track-following method described in Sect. 2. Where only two pions

stayed in the stack or where a pion made a large-angle scatter, the Q of these τ 's was assumed to be 74.9 MeV and the lost or scattered pion was assigned

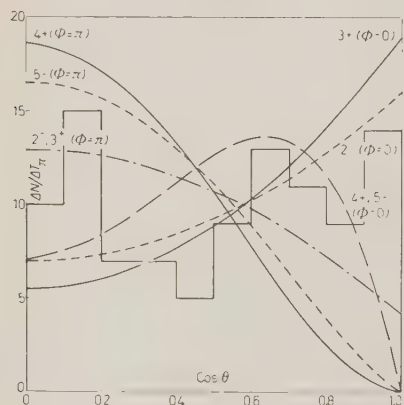


Fig. 4. — Plot of expected $\cos \theta$ distributions for τ spin-parity $2-, 3+, 4+, 5-$. Here φ is the relative phase between competing three-pion states. The cases of $2-$ and $3+$ for $\varphi = \pi$ are very similar and are drawn as a single curve. In like manner the cases of $4+, 5-$ for $\varphi = 0$ are very similar and are drawn as a single curve. Also shown is the experimental distribution.

an energy accordingly. (The conservation of momentum was also used to verify the assignment.)

All the theoretical distributions (*) were computed by use of the non-relativistic approximation. In this approximation the relative phase between three pion states appears only in the $\cos \theta$ distribution, and not in the unlike-pion-energy distribution. The relative phase is taken to be 0 or π for the non-unique cases.

Figs. 2 and 3 show the theoretical distributions for the unique cases, i.e., $0-$, $1+$, $1-$, $2+$, $3-$. Figs. 4 and 5 show the theoretical distributions for the non-unique cases, $2-$, $3+$, $4+$, and $5-$. In these only two three-pion states have the same $l+l' = \min$. Also shown in each figure is the corresponding observed distribution.

4.2.2 Statistics.—To determine the significance of the results of comparing two or more theoretical hypotheses with a sample of finite size, it is

necessary to consider the probability (a) that the sample comes from any one of the theoretical distributions, and (b) that a hypothesis will be rejected in favor of another, on the basis of (a) when in fact the hypothesis is false. If χ^2 (chi-square) is the statistic used for the comparison then the probability of (a) is the Pearson probability and the probability of (b) is called the power (¹⁰). The power depends only on the theoretical hypotheses, the sample size, and—of course—the confidence level of (a). Clearly for a pair of hypotheses I and II there are two powers, i.e., the probability of rejecting I in favor of II if in fact I is false, and vice versa.

Table I gives the Pearson probabilities for cases in which the τ spin-parity is $0-$, $1+$, $1-$, $2+$, $2-$, $3+$, $3-$, $4+$, and $5-$. Table II gives the power for the χ^2 test for comparing $0-$ with the remaining cases at the 5% confidence level of the Pearson probability. Five intervals were used for both the $\cos \theta$ and odd-pion energy distribution. As $\cos \theta$ and T_{π} have inde-

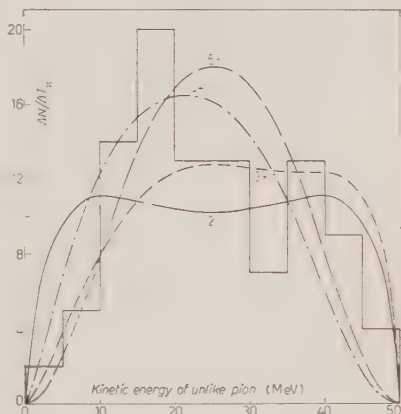


Fig. 5. — Plot of expected odd-pion energy distribution for τ spin-parity $2-$, $3+$, $4-$, $5-$. Also shown is the experimental distribution.

(*) All theoretical distributions were obtained from formulas (8) and (14) of FABRI's paper (⁴).

(¹⁰) See, for example, O. KEMPTHORNE: *Design and Analysis of Experiments* (New York, 1952), p. 219-223.

pendent χ^2 distributions, the χ^2 for each distribution may be added, and the corresponding Pearson probability and power are calculated for the sum of their degrees of freedom.

TABLE I. — *Pearson probabilities for various values of spin and parity. Here φ is the relative phase between competing three-pion states.*

Spin parity . . .	0 —	1 +	1 —	2 +	3 —
Probability . . .	$8 \cdot 10^{-2}$	$4 \cdot 10^{-8}$	10^{-26}	10^{-21}	$2 \cdot 10^{-10}$
Spin, parity . . .		2 —	3 +	4 +	5 —
Probability . . .	$\varphi = 0$	$2 \cdot 10^{-3}$	$5 \cdot 10^{-4}$	$2 \cdot 10^{-5}$	10^{-5}
	$\varphi = \pi$	$5 \cdot 10^{-5}$	$2 \cdot 10^{-4}$	10^{-50}	10^{-26}

TABLE II. — *Power for various values of spin and parity (there are two powers for each case).*

Spin, parity . . .	—	1 +	1 —	2 +	3 —
Powers	—	0.95	0.9997	0.9945	0.9900
		0.995	1.0000	1.0000	0.9959
Spin, parity . . .	—	2 —	3 +	4 +	5 —
Power	$\varphi = 0$	0.55	0.915	0.82	0.87
			0.930	0.945	0.91
	$\varphi = \pi$	0.55	0.65	0.9965	0.98
		0.65	0.86	1.0000	1.0000

4.3. *Conclusion.* — Assume a 5% confidence level for the Pearson probability and a 95% confidence level for the power as the criteria for rejecting or accepting a case of spin-parity. Inspection of Tables I and II shows that 0 — is the only case that is compatible with both requirements. The cases of 1 —, 2 +, and 3 — must be rejected. The case of 1 + is on the border line, but 2 —, 3 +, 4 +, and 5 — clearly cannot be rejected.

For the τ and $K_{\pi 2}$ to have compatible spin and parity the τ must have parity $P = (-1)^J$, i.e., either 1 —, 2 +, 3 —, 4 +, 5 —, etc. For these cases only 4 + and 5 — are significantly probable.

* * *

This paper is one aspect of a systematic investigation of positive K-particles by Dr. R. W. BIRGE, Dr. DONALD H. STORK, Dr. M. V. WHITEHEAD, Mr. L. T. KERTH, Mr. J. R. PETERSON, Mr. J. SANDWEISS and the author, using the strong-focusing spectrometer at the Bevatron, whose design and implementation is due to Mr. KERTH and Dr. STORK. I wish to thank Dr. BIRGE, Dr. STORK, and Dr. WHITEHEAD for their contributions and suggestions in

the course of this work; Dr. D. H. HOLLAND for assistance in writing the section on τ -decay theory; our scanners, Mrs. B. BALDRIDGE, Miss I. D'ARCHE, Mrs. E. GOODWIN, Mrs. M. HARBERT, and Miss K. PALMER; Mr. V. COOK, and Mr. G. PRESTON for their assistance with the measurements; and Dr. E. J. LOFGREN and the crew at the Bevatron.

This work was done under the auspices of the U. S. Atomic Energy Commission.

APPENDIX A

Error in Q Due to Moisture Content.

The error in Q due to an error in estimating the emulsion density to be $\varrho_E = 3.826 \text{ g/cm}^3$ arises strictly from the difference in water content between the assumed and true values of the emulsion density. To estimate the effect of this error:

1) $R_i, Z_i, R_{E_i}, Z_{E_i}$ are defined in Sect. 3.2.4. R_{t_i} is the chord length for the true emulsion density ϱ_t .

2) As in Sect. 3.2.4, we have

$$R_{E_i}/R_i = Z_{E_i}/Z_i, \quad R_{t_i}/R_i = Z_{t_i}/Z_i \quad \text{and} \quad \varrho t = \sigma = \varrho_E t_E = \varrho_t t_t.$$

Now we see

$$R_{E_i}/R_{t_i} = Z_{E_i}/Z_{t_i} \cong t_E/t_t = \varrho_t/\varrho_E$$

from which follows

$$\sum_i R_{E_i} \cong \varrho_t/\varrho_E \sum_i R_{t_i} \quad \text{or} \quad R_E \cong \varrho_t/\varrho_E R_t.$$

3) $dT/dx = \text{const} \cdot n \cdot f(v)$ where n is the number of electrons per unit volume of emulsion. To within the accuracy of measurement the water and dry emulsion volumes are additive. Therefore n depends linearly on the emulsion density, i.e., $n = b\varrho + d$. BARKAS and YOUNG⁽⁶⁾ give $n = (0.2522\varrho + 0.0830) \cdot 10^{24}/\text{cm}^3$ as the dependence of n on ϱ . Now the range is

$$R = \int_0^{T_0} \frac{dT}{dT/dx} = \frac{1}{\text{const } xn} \int_0^{T_0} \frac{dT}{f(v), \dots nR} = g(v).$$

Assume for convenience that $T = a(Rn)^k$, where $k = 1.171$. The range index k varies by about 14% over the region of interest; we have taken the mean value.

$$4) \quad T_i - T_E/T_E = \Delta T/T_E = (R_i n_i / R_E n_E)^k - 1 = (\varrho_E n_i / \varrho_i n_E)^k - 1.$$

5) Assume $\varrho_i = \varrho_E + A$ and make a Taylor's expansion of n_i/ϱ_i about n_E/ϱ_E . One obtains $n_i/\varrho_i = n_E/\varrho_E(1 - d\Delta p/n_E\varrho_E)$. Then $\Delta T/T_E = (1 - d\Delta\varrho/n_E\varrho_E)^k - 1 \cong \sim kd\Delta\varrho/n_E\varrho_E$. Putting in the values of k , d , and ϱ_E given above, one obtains $\Delta T/T = -0.046 \Delta\varrho/\varrho$. Then we have

$$\sum_{L=1}^3 \Delta T_i = \Delta Q = \sum_{L=1}^3 (-0.046) \frac{\Delta\varrho}{\varrho} T_i = Q(-0.046) \Delta\varrho/\varrho,$$

and

$$\Delta Q/Q = -0.046 \Delta\varrho/\varrho.$$

APPENDIX B

Original Data on the τ^+ Particles.

Energies of π Secondaries.

Particle	π^+	π^+	π^-	Q	$\cos \theta$
16-5P	46.0	11.4	17.3	74.7	.917
16-7P	32.7	12.4	29.8	74.9	.506
16-36P	47.8 (*)	17.6	9.5	74.9 (*)	1.007
16-40P	32.2	30.0	13.0	75.2	.066
16-51P	32.7	15.7	25.5	73.9	.427
16-85P	16.8	11.3	44.2	72.3	.300
16-86P	42.0	11.6	20.7	74.3	.774
16-103P	41.7 (*)	28.0	5.2	74.9 (*)	.603
16-123P	18.6	17.6	38.0	74.2	0.30
16-131P	46.0 (*)	20.0	8.9	74.9 (*)	.894
16-163P	39.3	20.7	15.0	75.0	.523
16-181P	14.6	13.4	49.5	77.5 (*)	.024
16-203P	39.5	17.5	18.2	75.2	.579
16-219P	30.0	9.0	35.8	74.8	.564
16-236P	21.7	14.2	39.1	75.0	.224
16-248P	42.2	21.6	11.6	75.4	.635
16-273P	31.2	23.4	21.3	75.9	.198
16-279P	42.2	6.4	25.7	74.3	.875
16-297P	30.2	12.3	31.3	73.8	.440

P: These tau's were included in the data presented at the Pisa Conference, 1955.

(*) One of the π 's left the stack or made a large-angle scatter.

Energies of π Secondaries (continued).

Particle	π^+	π^+	π^-	Q	$\cos \theta$
16-298P	28.5	2.7	43.7 (*)	74.9 (*)	.959
16-307P	35.3	21.4	17.6	74.3	.374
17-308P	39.0	17.2	18.7	74.9 (*)	.571
16-311P	31.5	22.0	30.5	74.0	.247
16-312	32.2	12.4	28.9	73.5	.501
16-315P	18.6	14.5	40.9	74.0	.139
16-328	17.2	11.5	44.3	73.0	.290
16-336	41.3	13.9	20.0	75.2	.700
16-338	20.7	13.9	39.6	74.2	.213
16-349	38.0	35.4	3.9	76.4	.175
16- τ A1	31.4	12.3	30.2	73.9	.485
16- τ A2	24.0	13.0	38.7	75.7	.316
16- τ A3	14.4	13.0	47.5 (*)	74.9 (*)	.149
16- τ A5	43.1	4.9	25.9	73.9	.934
16-N1	31.2	28.8	14.8	74.8	.068
16-N10	34.6	8.8	32.5	75.9	.641
16-N20	38.3	16.9	19.5	74.7	.555
16-N23	29.7	29.1	16.7	75.5	.016
16-N32	19.6	17.5	38.2	74.3	.060
16-N80	43.7	18.0	13.0	74.7	.759
16-N84	43.0	23.0	9.8	75.8	.659
16-N89	20.1	12.2	42.6 (*)	74.9 (*)	.285
16-N119	37.6	7.9	30.2	75.7	.724
16-N129	30.1	18.7	26.5	75.3	.282
16-N145	31.0	1.6	43.2	75.8	.986
16-N149	39.0	15.0	20.9 (*)	74.9 (*)	.610
16-N162	36.0	36.0	1.9	73.9	0
16-N194	32.6	25.3	17.7	75.6	.194
16-N197	28.6	23.3	25.5	77.4	.129
16-N210	35.0	28.9	12.7	76.6	.181
16-N214	39.3	5.4	30.7	75.4	.826
16-N225	44.9 (*)	3.4	26.6	74.9 (*)	.996
16-N241	47.2	7.8	20.0	75.0	.994
17-1	39.5	7.0	27.5	74.0	.800
17-7	37.9 (*)	25.9	11.1	74.9 (*)	.384
17-40	27.9 (*)	20.0	27.0	74.9 (*)	.197
17-42	32.2 (*)	27.0	15.7	74.9 (*)	.145
17-54	42.7	17.0	15.8	75.5	.703
17-90	45.4 (*)	9.5	20.0	74.9 (*)	.911
17-97	29.8 (*)	14.5	30.6	74.9 (*)	.385
17-115	46.0 (*)	7.1	21.8	74.9 (*)	.964

(*) One of the π 's left the stack or made a large-angle scatter.

Energies of π Secondaries (continued).

Particle	π^+	π^+	π^-	Q	$\cos \theta$
17-145	29.3	24.5	20.5	74.3	.125
17-152	46.3 (*)	8.4	20.2	74.9 (*)	.957
17-170	35.6	16.8	24.0	76.4	.462
17-187	40.5	16.5	18.5	75.5	.626
17-188	30.4 (*)	26.4	18.1	74.9 (*)	.107
17-193	43.2	9.0	23.6	75.8	.833
17-204	19.3	12.1	43.5 (*)	74.9 (*)	.280
17-215	41.7 (*)	2.20	11.2	74.9 (*)	.618
20-111	20.2	20.1	36.2	76.5	.003
20-126	35.0	1.0	39.5	75.5	.957
20-165	24.5	7.4	43.0 (*)	74.9 (*)	.613
20-200	30.5	2.9	41.6	75.0	.881
20-233	44.2	21.2	10.8	76.2	.725
20-268	35.0	33.0	7.0	75.0	.078
20-270	33.8	29.0	12.9	75.6	.143
20-274	46.1 (*)	18.0	10.8	74.9 (*)	.889
20-283	22.8	18.9	32.2	73.9	.102
20-297	39.0	9.0	26.0	74.0	.742
20-383	46.0	18.6	10.8	75.4	.865
20-393	39.4 (*)	21.1	14.4	74.9 (*)	.522
20-397	38.0	18.3	15.5	71.8	.560
20-408	37.2	1.3	37.0	75.5	.941
20-446	32.4	27.1	15.0	74.5	.151
20-480	20.7	19.7	34.5	74.9	.027
20-497	36.5	1.6	36.8 (*)	74.9 (*)	.925
20-506	34.9	23.2	17.8	75.9	.310
20-518	47.2 (*)	9.8	17.9	74.9 (*)	.976
20-534	31.9	5.2	37.7	74.8	.742
20-552	41.6	20.2	13.3	75.1	.626
20-644	39.7	8.8	28.2	76.7	.738
20-699	31.0	6.3	37.0	74.3	.685
20-703	34.1	5.9	36.0	76.0	.730
20-707	30.5 (*)	7.0	37.4	74.9 (*)	.650
20-734	24.8	6.4	42.0	73.2	.679
20-749	43.4 (*)	16.2	15.3	74.9 (*)	.755
20-759	45.8	31.2	17.5	76.5	.851
20-768	33.0	26.0	16.0	75.0	.193
20-794	38.2	26.6	10.5	75.3	.374
20-859	35.8	10.9	29.2	75.9	.607
20-966	35.0	17.0	21.7	73.6	.463

(*) One of the π 's left the stack or made a large-angle scatter.

RIASSUNTO (*)

Si analizzano in base (a) al valore Q del decadimento τ , (b) ai possibili valori della parità dello spin del τ , cento mesoni τ osservati in pacchi di emulsioni nucleari esposti al fascio di K^+ del bevatrone. Si ottiene un Q di 75.13 ± 20 MeV. La corrispondente massa del τ è $966.5 \pm .74 m_e$. Si sono usate le analisi di DALITZ e FABRI per assegnare ai τ possibili valori di parità e di spin. Il caso 0^- è quello che meglio si accorda con le distribuzioni di energia e angolari osservate.

(*) Traduzione a cura della Redazione.

Functional Integration in Quantum Field Theory.

W. K. BURTON and A. H. DE BORDE

Department of Natural Philosophy - University of Glasgow, Scotland

(ricevuto il 2 Maggio 1956)

Summary. — The problem of constructing explicit definitions for the vacuum expectation values of time ordered products of field operators as functional integrals is discussed with particular reference to systems in which the Fermi fields are involved bilinearly in the Lagrange function. Whereas a pure Bose system is comparatively easy to treat in this way, the presence of Fermi fields involves a complication due to the occurrence of non-commuting quantities in the classical action function. We give a definition involving only two non-commuting quantities, and work out some illustrative examples.

Up to the present time, the Feynman function integral ^(1,2) in field theory has been used mainly as a formal device ⁽³⁾; that is to say, it has not been precisely defined as a mathematical object. This is particularly true in the case of its applications to Fermi systems, where non-commuting quantities necessarily appear in the integral. For Bose systems, the situation is comparatively simple, in fact a reasonable definition of the transformation function $\langle x''t'' | x't' \rangle$ for particle mechanics as a functional integral has been given by DAVISON ⁽⁴⁾, and illustrations of its practical use have been given by the present authors ⁽⁵⁾. DAVISON's result is that

$$\langle x_a t_a | x_b t_b \rangle = \left(\frac{m}{2\pi i \hbar t_{ab}} \right)^{\frac{1}{2}} \lim_{n \rightarrow \infty} \int_{-\infty}^{\infty} da_1 \int_{-\infty}^{\infty} da_2 \dots \int_{-\infty}^{\infty} da_n \exp \left[\frac{i}{\hbar} \int_{t_b}^{t_a} L(x(t), \dot{x}(t)) dt \right],$$

⁽¹⁾ R. P. FEYNMAN: *Rev. Mod. Phys.*, **20**, 367 (1948).

⁽²⁾ R. P. FEYNMAN: *Phys. Rev.*, **80**, 440 (1950).

⁽³⁾ J. C. POLKINGHORNE: *Proc. Roy. Soc.*, A **230**, 272 (1955).

⁽⁴⁾ B. DAVISON: *Proc. Roy. Soc.*, A **225**, 252 (1954).

⁽⁵⁾ W. K. BURTON and A. H. DE BORDE: *Nuovo Cimento*, **2**, 197 (1955).

where

$$\dot{x}(t) = \left(\frac{2\pi i \hbar}{m t_{ab}} \right)^{\frac{1}{2}} \sum_{n=0}^{\infty} a_n \varphi_n \left(\frac{t - t_b}{t_{ab}} \right), \quad t_{ab} = t_a - t_b,$$

and $\varphi_n(Z)$ is a complete orthonormal set of functions on the interval $(0, 1)$ with $\varphi_0(Z) \equiv 1$, for example

$$\varphi_n(z) = \sqrt{2} \cos n\pi z \quad \text{for } n > 0, \varphi_0(z) \equiv 1$$

This is for a system with Lagrange function

$$L = \frac{1}{2} m \dot{x}^2 - V(x).$$

Thus DAVISON defines integration over a space of (integrable square) functions as the limit of a sequence of n -fold ordinary integrals over expansion coefficients. This notion has been developed further by SYMANZIK ⁽⁶⁾ and by MATTHEWS and SALAM ⁽⁷⁾ in connection with field theory. For these authors the aim is to express propagators by functional integrals of the type

$$\frac{(0|T[\varphi_1(x_1)\varphi_2(x_2)\dots\varphi_n(x_n)]|0)}{(0|0)} = \frac{(\int \varphi_1(x_1)\varphi_2(x_2)\dots\varphi_n(x_n) \exp[iS] d(\varphi))}{\int \exp[iS] d(\varphi)},$$

where S is the classical action for the fields under consideration. Again the attempt is to define the functional integral as the limit of a sequence of ordinary multiple integrals over suitable expansion coefficients, due regard being taken of the requisite vacuum boundary conditions. These authors appeal to the notion of anti-commuting functions $\varphi_i(x)$ when they treat Fermi fields in order to reproduce the desired symmetry properties in the expectation values of T -products (i.e. of T -ordered products of quantum operators). SYMANZIK ⁽⁶⁾ regards the functions over which the integrations are to be performed as anti-commuting, whereas MATTHEWS and SALAM ⁽⁷⁾ appeal to the existence of what they call "complete sets of anti-commuting functions $\varphi_i(x)$, normalized so that

$$\int \bar{\varphi}_i(x) \{ \gamma_\mu \gamma_\nu - m + g \gamma_\mu \gamma_\nu \} \varphi_j(x) dx = \delta_{ij} \delta_{\mu\nu}.$$

Here the φ_i are "real" and the φ are in the Majorana gauge. This "complete set" plays the role that DAVISON's ⁽⁵⁾ $\varphi_n(x)$ would play in the case $V(x) = 0$.

⁽⁶⁾ K. SYMANZIK: *Zeits. f. Naturfor.*, **9a**, 809 (1954).

⁽⁷⁾ P. T. MATTHEWS and A. SALAM: *Nuovo Cimento*, **2**, 120 (1955).

namely the functional integral becomes the limit of a multiple integral of an exponential of sums of squares, which is easy to evaluate. It is by no means clear, however, whether such a set can be found, or indeed what precisely is meant by the phrase « complete set of anti-commuting functions ». SYMANZIK's⁽⁶⁾ Fermi functional integral must be considered as purely formal until the actual process of summing is made more explicit.

In this paper we try to give a definition which covers both the Bose and Fermi cases, and which may be regarded as an extension of Davison's formula⁽⁴⁾.

1. — In view of their comparative simplicity, we confine our remarks at first to the case of Bose systems. Precise definitions have been given of the coordinate-to-coordinate transformation functions⁽⁴⁾ $\langle x| x' t' \rangle$ in particle mechanics and these may easily be extended to matrix elements of quantum mechanical operators in the coordinate representation. Analogous definitions are feasible in field theory, for matrix elements of functions of field operators in a representation in which a basic set of field variables is diagonal. However such matrix elements are not the most useful ones; in fact it would be desirable to express vacuum-to-vacuum matrix elements of T -ordered operators directly in terms of functional integrals. Such notions have already been employed, but in a somewhat imprecise sense.

In order to develop a suitable definition of vacuum matrix elements, we first examine how they may be derived from the corresponding coordinate matrix elements, in the case of particle mechanics. Consider for example, the following identity:

$$(1) \quad \langle x(t) | \mathbf{x}(t_1) \mathbf{x}(t_2) | x' t' \rangle = \int d\alpha_1 d\alpha_2 \langle x(t) | x_1 t_1 \rangle x_1(x_1 t_1) | x_2 t_2 \rangle x_2(x_2 t_2) | x' t' \rangle,$$

where $t > t_1 > t_2 > t'$, $\mathbf{x}(t_1)$ and $\mathbf{x}(t_2)$ are coordinate operators corresponding to the times t_1 and t_2 , and x_1 and x_2 are the eigenvalues of $\mathbf{x}(t_1)$ and $\mathbf{x}(t_2)$ respectively. Then if $\psi_n(x)$ represent a normalized complete set of energy eigenfunctions for the problem, we can write

$$(2) \quad \langle x(t) | \mathbf{x}(t_1) \mathbf{x}(t_2) | x' t' \rangle = \sum_{n, n'} \int \psi_n(x) \psi_n^*(x_1) x_1 dx_1 \psi_{n'}(x_1) \psi_{n'}^*(x_2) x_2 dx_2 \psi_{n'}(x_2) \psi_n^*(x') \cdot \\ \cdot \exp [-i[E_n(t-t_1) + E_{n'}(t_1-t_2) + E_{n'}(t_2-t')]].$$

By definition

$$(3) \quad \langle x(t_1) x(t_2) \rangle \equiv \frac{(\text{vac}, t | T \mathbf{x}(t_1) \mathbf{x}(t_2) | \text{vac}, t')}{(\text{vac}, t | \text{vac}, t')} = \\ = \sum_n \exp [-i(E_n - E_0)(t_1 - t_2)] \int dx_1 dx_2 \psi_0^*(x_1) x_1 \psi_n(x_1) \psi_n^*(x_2) x_2 \psi_0(x_2),$$

where the «vac» notation means that the matrix elements refer to states of minimum energy E_0 . If we set $x = x'$ in (2) and integrate over x , we find

$$(4) \quad \int dx \langle x(t) | \mathbf{x}(t_1) \mathbf{x}(t_2) | x'(t') \rangle = \sum_{n,n'} \exp [-i[E_n(t-t_1+t_2-t') + E_{n'}(t_1-t_2)]] \cdot \\ \cdot \int dx_1 dx_2 \psi_n^*(x_1) x_1 \psi_{n'}(x_1) \psi_{n'}^*(x_2) x_2 \psi_n(x_2).$$

If we can now pick out from the sum over n in (4) the term $n = 0$, division by $\langle \text{vac}, t | \text{vac}, t' \rangle$ will produce the expression $\langle x(t_1)x(t_2) \rangle$ of (3). Let us then divide both sides of (4) by $\langle \text{vac}, t | \text{vac}, t' \rangle$ and then replace E_n by $E_n(1 - i\varepsilon)$, where $\varepsilon > 0$; this produces an expression which has the following property: if we let $t \rightarrow \infty$, $t' \rightarrow -\infty$ and subsequently let $\varepsilon \rightarrow +0$, we are left with $x(t_1)x(t_2)$.

In Davison's (4) definition of (1), the integration is over a set of functions $x(t)$ taking the values x and x' at t and t' respectively. Since in obtaining $\langle x(t_1)x(t_2) \rangle$ from (1) we set $x = x'$ and integrated over all values of x , this suggests that we should define the functional integral for $x(t_1)x(t_2)$ as an integral over a set of functions satisfying periodic boundary conditions at t, t' , adding a term $i\varepsilon H$ to L , where H and L are the classical energy and Lagrange functions, and subsequently taking the limits $t \rightarrow \infty$, $t' \rightarrow -\infty$, $\varepsilon \rightarrow +0$ in this order.

We therefore adopt as the definition of the vacuum expectation value of T -products of quantum dynamical variables

$$(5) \quad \langle \varphi(x_1) \dots \varphi(x_n) \rangle \equiv \frac{(\text{vac} | T\boldsymbol{\varphi}(x_1) \dots \boldsymbol{\varphi}(x_n) | \text{vac})}{(\text{vac} | \text{vac})} = \\ = \lim \frac{\int \varphi(x_1) \dots \varphi(x_n) \exp [iS[\varphi]] d(\varphi)}{\exp [iS[\varphi]] d(\varphi)},$$

where x_1, \dots, x_n mean space-time points in a field theory and the times t_1, \dots, t_n in particle mechanics. The functional integral is to be performed in the following way. Write

$$(6) \quad \varphi(x) = \sum_{j=1}^k a_j \varphi_j(x),$$

where the $\varphi_j(x)$ form a complete orthogonal set satisfying periodic boundary conditions in a volume V in space-time. Then $S[\varphi]$ is to mean

$$(7) \quad S[\varphi] = \int dx (\mathcal{L} + i\varepsilon \mathcal{H}),$$

where

$$(8) \quad \mathcal{L} = \mathcal{L}(\varphi, \partial_\mu \varphi), \quad \mathcal{H} = \mathcal{H}(\varphi, \partial_\mu \varphi)$$

are the classical Lagrange density and energy density, respectively, for the problem. At this stage we shall have $S[\varphi] = S(a_1, \dots, a_k)$, and (5) represents a k -fold ordinary integral, the volume element being

$$(9) \quad d(\varphi) = \prod_{j=1}^k da_j.$$

Finally the expression $\langle \varphi(x_1) \dots \varphi(x_n) \rangle$ is obtained by letting $k \rightarrow \infty$, $V \rightarrow \infty$ and $\varepsilon \rightarrow +0$ in that order. This procedure will in future be indicated by the notation «lim» as in (5).

The systems of quantum mechanics may be divided into two classes, one in which S vanishes identically (perhaps after the addition of a total derivative to \mathcal{L}) when the $\varphi(x)$'s are interpreted as numerical functions: these are the Fermi systems; the other class of systems, the Bose systems, do not show this behaviour. We shall call the corresponding functional integrals Fermi integrals and Bose integrals respectively. Our definition so far applies only to Bose integrals. Before considering Fermi integrals we shall consider a simple first order Bose system by a method which may be easily extended to apply to a similar Fermi system.

2. — We take as our Lagrangian

$$(10) \quad L^B(x) = -x^{tr}(i\beta D + \omega)x, \quad D = d/dt$$

where x represents a real two-component vector and the matrix β is

$$(11) \quad \beta = \begin{pmatrix} 0 & i \\ -i & 0 \end{pmatrix}; \quad \beta^2 = \begin{pmatrix} 1 & 0 \\ 0 & 1 \end{pmatrix}.$$

This system is a harmonic oscillator, and has been discussed previously together with the analogous Fermi oscillator by BURTON and TOUSCHEK⁽⁸⁾. Since the classical energy is $\omega x^{tr}x$, ω being a scalar constant (the frequency), the effect of the term $i\varepsilon\mathcal{H}$ in (7) is taken care of by supposing that ω has a negative imaginary part. As pointed out by MATTHEWS and SALAM⁽⁷⁾, the

(8) W. K. BURTON and B. F. TOUSCHEK: *Phil. Mag.*, **44**, 161 (1953).

calculation can be considerably simplified by a special choice of the complete orthogonal set mentioned above. We consider the $x_n(t)$ which satisfy

$$(12) \quad (i\beta D + \omega)x_n = \lambda_n x_n,$$

or

$$(13) \quad (i\beta D + \Omega_n)x_n = 0, \quad \Omega_n = \omega - \lambda_n$$

where $x_n(t)$ satisfy periodic boundary conditions over a time T . It is easily verified that the general solution of (13) is

$$(14) \quad x_n = (\sigma_1 - i\sigma_2\beta)r_n$$

where

$$(15) \quad r_n = \begin{pmatrix} \cos \Omega_n t \\ \sin \Omega_n t \end{pmatrix},$$

$$(16) \quad \Omega_n = 2\pi n/T, \quad n \text{ integral,}$$

and σ_1, σ_2 are arbitrary (possibly operator) constants, independent of t . If we choose a particular σ_1 and σ_2 , then for a given n there is a second solution

$$(17) \quad x'_n = (\sigma_1 + i\sigma_2\beta)r_n,$$

which is linearly independent of x_n . If we choose

$$(18) \quad \sigma_1^2 = \sigma_2^2,$$

we find that x_m and x'_n are orthogonal in the sense that

$$(19) \quad \int_{\vec{x}} x_m^* (i\beta D + \omega) x'_n dt = 0,$$

and in fact the entire system of functions x_m, x'_n form an orthogonal set:

$$(20) \quad \int_{\vec{x}} x_m^* (i\beta D + \omega) x_n dt = \int_{\vec{x}} x_m^* (i\beta D + \omega) x'_n dt = \lambda_n T (\sigma_1^2 - \sigma_2^2) \delta_{mn}.$$

If σ_1, σ_2 are thought of as numbers the orthogonal set is complete. If not, the question of whether the set can be extended further is considered in the discussion of the not so trivial Fermi case below.

We now expand $x(t)$ in the form

$$(21) \quad x(t) = \sum \{a_n x_n(t) + b_n x'_n(t)\}.$$

Then

$$(22) \quad S = - \sum \lambda_n T (a_n^2 + b_n^2) (\sigma_1^2 + \sigma_2^2).$$

We define

$$(23) \quad x^\pm(t) = x^{(1)}(t) \pm ix^{(2)}(t),$$

where $x^{(1)}$ and $x^{(2)}$ are the components of the vector x . By (14), (17) and (20) we have

$$(24) \quad x^\pm(t) = \sum \{a_n(\sigma_1 \mp i\sigma_2) \exp[\pm i\Omega_n t] + b_n(\sigma_1 \pm i\sigma_2) \exp[\pm i\Omega_n t]\}.$$

We are now in a position to evaluate $\langle x^-(t_1)x^+(t_2) \rangle$. Omitting certain terms which vanish on integration by parts, we have, putting $\sigma_3 = \frac{1}{2}i[\sigma_1, \sigma_2]$

$$\begin{aligned} (25) \quad \langle x^-(t_1)x^+(t_2) \rangle &= \\ &= \lim \frac{\int d(a) d(b) \sum_n \{a_n^2(\sigma_1^2 + \sigma_2^2 - 2\sigma_3) + b_n^2(\sigma_1^2 + \sigma_2^2 + 2\sigma_3)\} e^{-i\Omega_n(t_1-t_2)} \exp[-iT(\sigma_1^2 + \sigma_2^2) \sum_m \lambda_m(a_m^2 + b_m^2)]}{\int d(a) d(b) \exp[-iT(\sigma_1^2 + \sigma_2^2) \sum_m \lambda_m(a_m^2 + b_m^2)]} \\ &= \lim \sum_n \frac{\exp[-i\Omega_n(t_1-t_2)]}{i\lambda_n T}. \end{aligned}$$

Here we have used an additional limiting process to ensure the convergence of the integrals. Taking the limit $T \rightarrow \infty$, (25) gives

$$\begin{aligned} (26) \quad \langle x^-(t_1)x^+(t_2) \rangle &= \lim_{\epsilon \rightarrow +0} - \frac{1}{2\pi i} \int_{-\infty}^{\infty} \frac{\exp[-i\Omega(t_1-t_2)]}{\Omega - \omega + i\epsilon} d\Omega = \\ &= \theta(t_1-t_2) \exp[-i\omega(t_1-t_2)] = \langle x^+(t_2)x^-(t_1) \rangle, \end{aligned}$$

where

$$(27) \quad \begin{aligned} \theta(t) &= 1 & \text{for } t > 0, \\ &= 0 & \text{for } t < 0. \end{aligned}$$

Similar calculations show that

$$(28) \quad \langle x^-(t_1)x^-(t_2) \rangle = \langle x^+(t_1)x^+(t_2) \rangle = 0.$$

Using these results, definition (23) yields $\langle x^{(\alpha)}(t_1)x^{(\beta)}(t_2) \rangle$ where $\alpha, \beta = 1, 2$.

3. — We now consider the Fermi system with Lagrangian

$$(29) \quad L^F(x) = -x^{tr}(iD + \omega\beta)x = -x^{tr}\beta(i\beta D + \omega)x.$$

If the components of x be conceived of as commuting quantities, the Lagrangian is merely a total time derivative. It is therefore necessary to attribute operator properties to the components of x in order to obtain non-trivial results. We shall do this by exploiting the operator solutions (14) and (17) of (12). In fact, using (14) we find

$$(30) \quad \int_T x_m^{tr}\beta(i\beta D + \omega)x_n dt = i\lambda_n T \delta_{mn}[\sigma_2, \sigma_1] = -2\lambda_n T \sigma_3 \delta_{mn},$$

so that the x_n are still orthogonal in the new scalar product (30). The second solution (17) also satisfies (30) apart from a change of sign ($\sigma_2 \rightarrow -\sigma_2$).

However

$$(31) \quad \int_T x_m^{tr}\beta(i\beta D + \omega)x'_n dt = i\lambda_n T \{\sigma_1, \sigma_2\} \delta_{mn}.$$

This will vanish for all m, n if and only if we choose

$$(32) \quad \{\sigma_1, \sigma_2\} = \sigma_1\sigma_2 + \sigma_2\sigma_1 = 0.$$

We have now found a set of functions orthogonal in the scalar product (30) analogous to the set found for the Bose case. The question now is: can this set be extended further? The answer is no if the operators concerned are to be non singular. For suppose $y = \sum_n (\sigma_3^{(n)} - i\sigma_4^{(n)}\beta)r_n$ were another function, orthogonal to all members of the set already found. Then we should have

$$\begin{aligned} \int_T y^{tr}\beta(i\beta D + \omega)x_n dt &= i\lambda_n T(\sigma_4^{(n)}\sigma_1 - \sigma_3^{(n)}\sigma_2) = 0, \\ \int_T y^{tr}\beta(i\beta D + \omega)x'_n dt &= i\lambda_n T(\sigma_4^{(n)}\sigma_1 + \sigma_3^{(n)}\sigma_1) = 0, \end{aligned}$$

so that

$$\sigma_4^{(n)}\sigma_1 = \sigma_3^{(n)}\sigma_2 = 0.$$

This is impossible if $\sigma_1, \sigma_2, \sigma_3^{(n)}, \sigma_4^{(n)}$ are all to be non-singular. If σ_1 and σ_2 are

non-singular, then $\sigma_3^{(n)}$ and $\sigma_4^{(n)}$ vanish for each n , and we conclude that $y = 0$. However the set (x_n, x'_n) is not complete in the usual sense. For example, the function $\sigma_2 r_m$ cannot be expanded as $\sum (a_n x_n + b_n x'_n)$ where the a_n, b_n are numerical coefficients. A corresponding result can also be proved for the Bose case. If there the σ 's are taken to be numerical quantities, the (x_n, x'_n) form a complete numerical set in the usual sense.

Defining $x^\pm(t)$ by (23) as before, again omitting terms which vanish on integration by parts

$$(33) \quad \langle x^-(t_1)x^+(t_2) \rangle = \frac{\int d(a)d(b) \sum_n \{ a_n^2(\sigma_1^2 + \sigma_2^2 - 2\sigma_3) + b_n^2(\sigma_1^2 + \sigma_2^2 + 2\sigma_3) \} \exp[-i\Omega_n(t_1 - t_2)] \exp[iS]}{\int d(a)d(b) \exp[iS]},$$

where

$$iS = 2iT\sigma_3 \sum \lambda_m(a_m^2 - b_m^2).$$

Hence

$$\langle x^-(t_1)x^+(t_2) \rangle = \lim \sum_n \frac{\exp[-i\Omega_n(t_1 - t_2)]}{i\lambda_n T},$$

which is the same result as we found in (26) for the Bose example.

Two important differences between the two cases are the following:

(i) If we evaluate $\langle x^+(t_2)x^-(t_1) \rangle$ we get $\langle x^-(t_1)x^+(t_2) \rangle$ in the Bose case and $-\langle x^-(t_1)x^+(t_2) \rangle$ in the Fermi case, thus showing that the correct T -product behaviour is reproduced.

(ii) If we evaluate T -products of four factors in the two cases the results will not be the same. For example

$$\langle x^-(t_1)x^-(t_2)x^+(t_3)x^+(t_4) \rangle$$

vanishes in the Fermi case if $t_1 > t_2 > t_3 > t_4$ but not in the Bose case. This is because the Fermi oscillator has only two energy levels and the $x^\pm(t)$ act as creation and annihilation operators. Corresponding results hold for six factors and so on.

The extension to the case of the Fermi system with Lagrangian

$$(34) \quad L(y) = -y^tr\beta(i\beta D + \omega + f(t))y$$

where $f(t)$ is any function of the time is made by making expansions in terms of the functions y_n satisfying,

$$(35) \quad (i\beta D + \omega + f)y_n = \lambda'_n y_n.$$

It is seen that if we take

$$(36) \quad y_n = \exp \left[i\beta \int_0^t (f - \bar{f}) dt' \right] \cdot x_n, \quad \bar{f} = \frac{1}{T} \int_0^T f(t) dt,$$

where x_n is of the form (14) or (17), satisfying (12), then y_n satisfies (35) with $\lambda'_n = \lambda_n = \bar{f}$, and takes the same boundary values as x_n : Expanding y in terms of the set y_n we find

$$(37) \quad y^\pm(t) = \exp \left[\pm i \int_0^t (f - \bar{f}) dt' \right] \cdot x^\pm(t),$$

which gives ultimately

$$(38) \quad \langle y^-(t_1) y^+(t_2) \rangle = \exp \left[-i \int_{t_2}^{t_1} f(t) dt \right] \cdot \langle x^-(t_1) x^+(t_2) \rangle,$$

where $\langle x^-(t_1) x^+(t_2) \rangle$ is given by (33).

4. — We shall now examine the corresponding field theoretical case. For the free Dirac field we have the Lagrange density

$$(39) \quad \mathcal{L} = \frac{1}{2} [\bar{\psi}, \mathcal{D}\psi] = i(\psi_a^{tr} \gamma_0 \mathcal{D}\psi_a + \psi_b^{tr} \gamma_0 \mathcal{D}\psi_b), \quad \bar{\psi} = i\psi^\dagger \gamma_0$$

where

$$(40) \quad \mathcal{D} = \gamma_\mu \hat{c}_\mu + m, \quad \psi = \psi_a + i\psi_b$$

and, following MATTHEWS and SALAM⁽⁷⁾, we have split the total field ψ into real parts ψ_a and ψ_b (Majorana gauge, real γ_μ , $\mu = 0, \dots, 3$). The elements of γ_0 are $\gamma_0^{14} = \gamma_0^{23} = -\gamma_0^{32} = -\gamma_0^{41} = 1$, all others zero. ψ^{tr} means the transpose of ψ and ψ^\dagger its Hermitian conjugate).

Following the lines suggested by our previous example, we contemplate expansions of the ψ_a and ψ_b in terms of real quantities $\varphi^{(ns)}(x)$ satisfying

$$(41) \quad (\gamma_\mu \hat{c}_\mu + \Omega)\varphi = 0, \quad \Omega = m - \lambda$$

with periodic boundary conditions over a space-time hypercube. A complete set of $\varphi^{(ns)}$ is given by

$$(42) \quad \varphi^{(ns)} = (\Omega_n - \gamma \hat{c}) \cos p^{(n)} x \cdot u^{(s)},$$

where the $u^{(s)}$ form a complete set of constant spinors, and

$$\Omega_n = \pm (-p^{(n)2})^{\frac{1}{2}}, \quad p_0 \geq 0.$$

The $p_\mu^{(n)}$ take on the discrete values implied by the boundary conditions.

As in the Fermi example previously considered, it is necessary to include non-numerical functions in our expansions. It is adequate to take for the spinors

$$(43) \quad \begin{cases} u^{(1)} = (\sigma_1, & 0, & 0, & \sigma_2) & u^{(3)} = (0, & \sigma_1, & \sigma_2, & 0) \\ u^{(2)} = (\sigma_1, & 0, & 0, & -\sigma_2) & u^{(4)} = (0, & \sigma_1, & -\sigma_2, & 0) \end{cases}$$

With this choice, we have

$$(44) \quad u^{(s)lr} \gamma_0 u^{(s')} = 2i(-1)^s \sigma_3 \delta_{ss'}$$

provided we take as before $\{\sigma_1, \sigma_2\} = 0$. Then a simple calculation shows that

$$(45) \quad \int_V \bar{\varphi}^{(ns)} (\gamma \partial + m) \varphi^{(n's')} dx = -2\Omega_n^2 (m - \Omega_n) V \sigma_3 (-1)^s \delta_{ss'} \delta_{nn'},$$

where V is the hypervolume of the periodicity hypercube. An argument similar to that used previously shows that if σ_1 and σ_2 are non-singular, any further function φ satisfying

$$\int_V \bar{\varphi}^{(ns)} \mathcal{D} \varphi dx = 0,$$

for all n and s , must vanish.

If we now expand ψ_a and ψ_b in the form

$$(46) \quad \psi_a = \sum_{ns} a_{ns} \varphi^{(ns)}, \quad \psi_b = \sum_{ns} b_{ns} \varphi^{(ns)},$$

we find

$$(47) \quad S = - \sum_{ns} 2\Omega_n^2 (m - \Omega_n) V \sigma_3 (-1)^s (a_{ns}^2 + b_{ns}^2).$$

Then the normalized expectation value of the T -product of $\psi_a(x)$ and $\psi_b(x')$ is given by

$$(48) \quad \begin{aligned} \langle \psi_{a\alpha}(x) \psi_{b\beta}(x') \rangle &= \\ &= \lim \frac{\int d(a) \sum_{ns} a_{ns}^2 \varphi_{\alpha}^{(ns)}(x) \varphi_{\beta}^{(ns)}(x') \exp[-\sum_{ns} 2i\sigma_3 V \Omega_n^2 (m - \Omega_n) a_{ns}^2 (-1)^s]}{\int d(a) \exp[-\sum_{ns} 2i\sigma_3 V \Omega_n^2 (m - \Omega_n) a_{ns}^2 (-1)^s]} = \\ &= \lim \sum_{ns} \frac{\varphi_{\alpha}^{(ns)}(x) \varphi_{\beta}^{(ns)}(x') (-1)^s}{4i\sigma_3 \Omega_n^2 (m - \Omega_n) V} = \\ &= \lim \sum_n \frac{[(\Omega_n - \gamma \hat{c})(\Omega_n + \gamma \hat{c}') \gamma_0]_{\alpha\beta} \cos p^{(n)} x \cdot \cos p^{(n)} x'}{2\Omega_n^2 (m - \Omega_n) V}. \end{aligned}$$

Consider

$$(49) \quad I(x, x') = \lim \sum_n \frac{(\Omega_n - \gamma\hat{c})(\Omega_n + \gamma\hat{c}')\gamma_0 \exp[ip^{(n)}(x - x')]}{2\Omega_n^2(m - \Omega_n)V}.$$

In the summation, for every term $-\Omega_n$ there is also a term $-\Omega_n$. Taking these together we find

$$(50) \quad I(x, x') = \lim \sum \exp[ip^{(n)}(x - x')].$$

$$\cdot \left\{ \frac{(\Omega_n - i\gamma p^{(n)})(\Omega_n - i\gamma p^{(n)})\gamma_0}{2\Omega_n^2(m - \Omega_n)V} + \frac{(\Omega_n + i\gamma p^{(n)})(\Omega_n + i\gamma p^{(n)})\gamma_0}{2\Omega_n^2(m + \Omega_n)V} \right\} =$$

$$= \lim \sum \exp[ip^{(n)}(x - x')] \cdot \frac{2(m - i\gamma p^{(n)})\gamma_0}{(p^{(n)2} + m^2)V},$$

using $p^{(n)2} + \Omega_n^2 = 0$, the latter relation also implying that $I(x, -x') = -I(-x, x') = 0$. In the limit $V \rightarrow \infty$, $(1/V) \sum$ becomes replaced by $(2\pi)^{-4} \int d\rho$, which gives

$$(51) \quad \langle \psi_a(x) \psi_a(x') \rangle = \frac{1}{2}(2\pi)^{-4}(m - \gamma\hat{c}) \int_{p_0 > 0} d\rho \frac{\exp[ip(x - x')] + \exp[-ip(x - x')]}{p^2 + m^2} \gamma_0 =$$

$$= \frac{1}{2}(2\pi)^{-4}(m - \gamma\hat{c}) \int d\rho \frac{\exp[ip(x - x')]}{p^2 + m^2} \gamma_0.$$

Since $\langle \psi_a(x) \psi_b(x') \rangle = 0$, we obtain finally the well-known result

$$(52) \quad \langle \psi(x) \bar{\psi}(x') \rangle = -i(2\pi)^{-4}(m - \gamma\hat{c}) \int d\rho \frac{\exp[ip(x - x')]}{p^2 + m^2},$$

where the integral over p_0 is performed with m having a negative imaginary part which is made to tend to zero after the integration.

5. - Having treated a number of specific examples of the evaluation of vacuum expectations of T -products for Fermi systems as functional integrals, we now come to the general case of functional integration over the Fermi fields for a system consisting of both Fermi and Bose fields in interaction, in which the Fermi field variables are involved bilinearly in the Lagrange function. If the Fermi integrations are performed first, the Bose fields may at this stage

be treated as external classical fields. Then the action may always be written

$$(53) \quad S = \int \psi L \psi \, dx,$$

where L is an imaginary antisymmetric operator. In the example in Sect. 4, ψ would comprise ψ_a and ψ_b , together forming an eight component spinor.

Let $\varphi_n(x)$ be a complete set of real numerical functions with the same number of components as ψ . Define

$$(54) \quad \int \varphi_m L \varphi_n \, dx = L_{mn}.$$

The matrix L_{mn} , being imaginary and antisymmetrical, and therefore Hermitian, can be diagonalized by means of a unitary transformation U :

$$(55) \quad \sum_{rs} U_{mr}^\dagger L_{rs} U_{sn} = \lambda_m \delta_{mn}, \quad \lambda_m = \lambda_m^*$$

the λ_m being real. Now define

$$(56) \quad \psi_n' = \sum_s U_{ns}^{tr} \varphi_s$$

$$(57) \quad \psi_n'^* = \sum_s U_{sn}^\dagger \varphi_s$$

where (57) is the complex conjugate equation to (56). Then

$$(58) \quad \int \psi_m'^* L \psi_n' \, dx = \sum_{rs} U_{mr}^\dagger \int \varphi_r L \varphi_s \, dx \cdot U_{ns}^{tr} = \sum_{rs} U_{mr}^\dagger L_{rs} U_{sn} = \lambda_m \delta_{mn},$$

and

$$(59) \quad \int \psi_m' L \psi_n'^* \, dx = -\lambda_m \delta_{mn},$$

which follows by taking the complex conjugate of (58).

Let us arrange the numbering of the rows and columns of U in such a way that, using (55)

$$(60) \quad \sum_s L_{rs} U_{st} = \lambda_t U_{rt},$$

with

$$(61) \quad \lambda_t > 0 \quad \text{when} \quad t > 0, \quad \lambda_t < 0 \quad \text{when} \quad t < 0.$$

Then

$$(62) \quad \int \psi'_m L \psi'_n dx = \sum_{r,s} U_{mr}^{rs} L_{rs} U_{sn} = \lambda_n \sum_r U_{mr}^{rr} U_{rn} = -\lambda_m \sum_s U_{ms}^{rr} U_{sn}.$$

which shows that

$$(63) \quad (\lambda_m + \lambda_n) \sum_r U_{mr}^{rr} U_{rn} = 0.$$

Hence, using (61)

$$(64) \quad \int \psi'_m L \psi'_n dx = \int \psi'^*_m L \psi'^*_n dx = 0, \quad \text{for } m, n > 0.$$

Define, for positive values of n

$$(65) \quad \begin{cases} \psi_{n1} = \sigma_1 \psi'_n - i\sigma_2 \psi'^*_n, \\ \psi_{n2} = \sigma_1 \psi'_n + i\sigma_2 \psi'^*_n. \end{cases}$$

Then (58), (59) and (64) show that

$$(66) \quad \int \psi_{mr} L \psi_{ns} dx = -2\lambda_n \sigma_3 (-1)^r \delta_{mn} \delta_{rs}, \quad (r, s = 1, 2; m > 0, n > 0),$$

provided that we take

$$(67) \quad \{\sigma_1, \sigma_2\} = 0, \quad \sigma_3 = \frac{1}{2}i[\sigma_1, \sigma_2] = i\sigma_1\sigma_2.$$

If we expand $\psi(x)$ as

$$(68) \quad \psi(x) = \sum_{n>0} \{a_n \psi_{n1}(x) + b_n \psi_{n2}(x)\},$$

we obtain

$$\begin{aligned} (69) \quad \langle \psi(x) \psi(x') \rangle &= \\ &= \lim_{n_1 > 0} \frac{\int d(a) d(b) \sum_{n_2 > 0} \{a_{n_2}^2 \psi_{n_2 1}(x) \psi_{n_2 1}(x') - b_{n_2}^2 \psi_{n_2 2}(x) \psi_{n_2 2}(x')\} \exp[2i\sigma_3 \sum_{n_1 > 0} \lambda_{n_1} (a_{n_1}^2 - b_{n_1}^2)]}{\int d(a) d(b) \exp[2i\sigma_3 \sum_{n_1 > 0} \lambda_{n_1} (a_{n_1}^2 - b_{n_1}^2)]} = \\ &= -\lim_{n_1 > 0} \sum (4i\lambda_{n_1} \sigma_3)^{-1} \{ \psi_{n_1 1}(x) \psi_{n_1 1}(x') - \psi_{n_1 2}(x) \psi_{n_1 2}(x') \} = \\ &= \lim_{n_1 > 0} \sum (2i\lambda_{n_1})^{-1} \{ \psi'_{n_1}(x) \psi'^*_n(x') - \psi'^*_n(x) \psi'_{n_1}(x') \}, \end{aligned}$$

where we have used (65) and (67). In view of (61), we can extend the sum-

mation over all values of n , which gives

$$\begin{aligned}
 (70) \quad \langle \psi(x)\psi(x') \rangle &= \sum_n (2i\lambda_n)^{-1} \psi'_n(x) \psi'^*_n(x') \\
 &= \sum_{nr_s} (2i)^{-1} \varphi_r(x) U_{rn} \lambda_n^{-1} U_{ns}^\dagger \varphi_s(x') \\
 &= (2i)^{-1} \sum_{rs} \varphi_r(x) (L^{-1})_{rs} \varphi_s(x').
 \end{aligned}$$

This presents $\langle \psi(x)\psi(x') \rangle$ as a Green's function, as can be seen in the following way. First

$$(71) \quad L\varphi_t(x) = \sum_s \int dx' \varphi_s(x') L\varphi_t(x') \varphi_s(x) = \sum_s L_{st} \varphi_s(x).$$

Then

$$\begin{aligned}
 (72) \quad L\langle \psi(x)\psi(x') \rangle &= (2i)^{-1} \sum_{rst} L_{tr} \varphi_t(x) (L^{-1})_{rs} \varphi_s(x') \\
 &= (2i)^{-1} \sum_s \varphi_s(x) \varphi_s(x') \\
 &= (2i)^{-1} \delta(x - x').
 \end{aligned}$$

The formulae (70) are to be understood in the sense that L_{rs} contains an imaginary part (as explained in Sect. 1) which is made to tend to zero at the end of the calculation. This prescription prevents L_{rs} having a zero eigenvalue, and results in the $\langle \psi(x)\psi(x') \rangle$ being the Green's function which satisfies the Feynman vacuum boundary conditions.

In this section we have made no assumptions of periodicity on the φ_n : all we have assumed is that the φ_n form a complete orthonormal set. We see, therefore, that the restriction to periodic boundary conditions imposed in the previous sections may be removed.

6. — It should be noted that the expansions suggested throughout this paper are by no means unique. For example in Sect. 3 we might replace the x'_n of (17) by

$$x'_n = (\sigma_2 - i\sigma_1\beta)v_n.$$

If we now choose $\sigma_1^2 = \sigma_2^2$ instead of $\{\sigma_1, \sigma_2\} = 0$, we find that in the Fermi case

$$\int x_m^{tr} \beta (i\beta D + \omega) x_n dt = i\lambda_n T (\sigma_1^2 - \sigma_2^2) = 0,$$

and $\langle x(t_1)x(t_2) \rangle$ may be evaluated to give the same result as before. Similar changes may be carried out in the other examples considered.

RIASSUNTO (*)

Si discute, con particolare riguardo ai sistemi in cui i campi fermionici compaiono linearmente nella funzione di Lagrange, il problema della costruzione di definizioni esplicite per i probabili valori del vuoto di prodotti di operatori di campo temporalmente ordinati. Mentre un sistema puramente bosonico è relativamente agevole da trattare in tal modo, la presenza di campi fermionici introduce complicazioni dovute al sorgere di grandezze non commutative nella funzione d'azione classica. Diamo una definizione comprendente solo due grandezze non commutative e sviluppiamo alcuni esempi illustrativi.

(*) *Traduzione a cura della Redazione.*

Renormalized Dirac Maxwell Equations.

P. SEN (*)

Dehra Dun - India

(ricevuto il 9 Maggio 1956)

Summary. — The Dirac Maxwell equations are reformulated by eliminating that part of the interaction term which contributes only to the mass and charge of the bare electron and then by replacing the bare mass and charge of the electron by its experimental mass and charge. Then it is shown that a renormalization scheme is contained within them. Two schemes for renormalization are described and it is shown that the first scheme, although not the same, follows the pattern of Dyson's renormalization program.

1. — Introduction.

In the quantum electrodynamics described by the Dirac Maxwell equations the existence of virtual particles gives additional mass and charge to the mass charge of a bare free electron, and when they are added together then only do we obtain the experimental mass and charge of the free electron. This renormalization program, which has been constructed by DYSON (¹), is not contained in the Dirac-Maxwell equations and is added to them as a necessary auxiliary condition on physical grounds. We should like to show that there exists a physically sensible reformulation of the Dirac-Maxwell equations in which a renormalization scheme is contained within them.

The reformulation of the Dirac and Maxwell equations is obtained by removing from them all the contribution of their interaction term and of its

(*) Now at the Istituto di Fisica dell'Università, Torino.

(¹) F. J. DYSON: *Phys. Rev.*, **75**, 486, 1736 (1949); A. SALAM: *Phys. Rev.*, **82**, 217 (1951).

derivative which correspond to the energy of a free electron or photon respectively, and then by replacing the bare electron mass and charge by its experimental mass and charge. This redistribution is made by means of a «principle energy value» operator. To obtain a consistent scheme of renormalization we have also to define suitably the region of the Feynman graph and the manner in which a particular principle energy value operator acts. Such a definition can be simply formulated in several ways specially since it is not necessary that the reformulated Dirac-Maxwell equations be equal to the original Dirac-Maxwell equations and result from only a redistribution of the terms within them.

Two such reformulations and the consequent subtraction schemes are described. While it seems possible to give a simpler statement for the second scheme, the first scheme follows the pattern but is not exactly the same as Dyson's renormalization program and differs from it specially for the contributions of the higher order irreducible vertex graphs. Both the subtraction schemes have been designed to give the usual contribution for the second order Feynman graphs and thus about the same physical magnitudes are obtained from them and from the Dyson's renormalization program.

2. - The Reformulated Dirac Equation.

To include a renormalization program within the Dirac-Maxwell equations let us consider, in the notation of an earlier paper ⁽²⁾, the Dirac equations

$$(1) \quad \{H(1) - i\lambda(a'(1) + a'_e(1))\}\psi'(1) = 0, \quad \bar{\psi}'(1)\{\bar{H}(1) + i\lambda(a'(1) + a'_e(1))\} = 0,$$

where the external potential has been written explicitly and so $A'_\mu(1)$ shall henceforth denote the internal electromagnetic potential only. Then we shall define the wavefunction of a free electron to be

$$(2) \quad \mathcal{E}(1)(\psi'(1)) = \frac{1}{(2\pi)^4} \int d^4p \, d^4p_0 \exp[-i1(p - p_0)] \mathcal{E}(p; p_0)(\psi'(p, p_0))$$

where p_μ and $p_{0\mu}$ are the initial energy momentum vectors of the electron and photon respectively, and where the «free energy operator» $\mathcal{E}(1)$, acting at the space time point $x_\mu(1)$ projects the free energy part of the Dirac wavefunction $\psi'(1)$. Since we wish to indicate two separate possible definitions of the operators introduced in this section their specific definitions are given later and only their general properties, which are true in either case, are de-

(2) P. SEN: *Nuovo Cimento*, **3**, 390 (1956). The notation of its Sect. 2 is followed here.

fined here. Now an alternate description of the free electron must be given by the wave equations

$$(3) \quad \begin{cases} H^*(1)\psi^*(1) = 0, & \bar{\psi}^*(1)\bar{H}^*(1) = 0, \\ H^*(1)K^*(12) = i\delta(12), & K^*(12)\bar{H}^*(2) = -i\delta(12), \\ H^*(x_\mu) = \gamma_\mu \frac{\partial}{\partial x_\mu} + \kappa^*, & \bar{H}^*(x_\mu) = \gamma_\mu \frac{\partial}{\partial x_\mu} - \kappa, \quad \kappa^* = \frac{m^*}{\hbar c}, \end{cases}$$

where the experimental magnitudes of an electron have been denoted by adding a suffix * to its corresponding bare magnitudes.

Let us now rewrite the Dirac equations in the form

$$(4) \quad \begin{cases} \{H^*(1) - i\lambda^*(\mathcal{P}(1)a'(1) + a'_e(1))\}\psi^*(1) = 0 \\ \bar{\psi}^*(1)\{\bar{H}^*(1) + i\lambda^*(\mathcal{P}(1)a'(1) + a'_e(1))\} = 0 \end{cases}$$

where $\lambda^* = e^*/\hbar c$. Here a « principle energy value » operator $\mathcal{P}(1)$ has been introduced and it acts at the point of the internal potential $A'_\mu(1)$. To obtain an insight about its physical significance let us write

$$(5) \quad \mathcal{P}(1) = 1 - \mathcal{E}(1).$$

Then according to the equations (2) and (3) the terms removed by the principle energy operator are exactly those which when added to the bare mass and charge of an electron give its experimental mass and charge, and thus the equations (4) are derived from the equations (1). But as we proceed further, particularly due to the necessity of defining the region of operation of the $\mathcal{P}(r)$'s and their ordering for the overlapping Feynman graphs, perhaps the relation between the operators $\mathcal{P}(1)$ and $\mathcal{E}(1)$, will not appear as obvious will not appear as obvious as the relation (5) and in that case we should like to emphasize that, since henceforth we shall use the equation (4) only, it can be considered to be the true Dirac wave equation and the validity of the relation (5) is not necessary for our considerations. Then in the absence of external electromagnetic field $\psi^*(1)$ will be equal to $\psi^*(1)$.

Let $K^{*'}(1, 2)$ denote the Feynman propagation operator corresponding to the wave function $\psi^*(1)$. Then we obtain the Feynman integral equation

$$(6) \quad K^{*'}(1, 2) = K^*(12) + \lambda^* \int K^*(13)(\mathcal{P}(3)a'(3) + a'_e(3))K^{*'}(3, 2) d3,$$

and

$$(7) \quad \psi^*(1) = \psi^*(1) + \lambda^* \int K^*(1, 3)(\mathcal{P}(3)a'(3) + a'_e(3))\psi^*(3) d3.$$

We also note that the general vertex operator is given by

$$(8) \quad \Lambda_{\mu}^{*'}(1, 2) = \bar{\psi}^{*'}(1) \gamma_{\mu} \psi^{*'}(2).$$

Henceforth the suffix * which occurs in all the terms shall be left out and κ and λ shall denote the experimental mass and charge quantities. To include the external potentials also in the illustration of the definition of $\mathcal{Q}(r)$ let us consider the vertex graph $\Lambda'_{\mu}(1, 2)$ in the first Born approximation in the external potential and let $p_{1\mu}$ and $p_{2\mu}$ be the initial and final energy momentum vectors of the electron. Then the external potential terms of the equation (7) can be neglected and, by the procedure of iteration, (8) becomes

$$(9) \quad \Lambda'_{\mu}(1, 2) = \bar{\psi}(1) \gamma_{\mu} \psi(2) - \lambda^2 \int \bar{\psi}(4) \mathcal{Q}(4) a(4) K(41) \gamma_{\mu} K(23) \cdot \\ \cdot \mathcal{Q}(3) a(3) \psi(3) d3 d4 \dots - \lambda^{2n} \int \dots \int \bar{\psi}(m) \mathcal{Q}(m) a(m) \dots \gamma_{\mu} \dots \mathcal{Q}(r) a(r) \psi(r) dm \dots dr \dots$$

The operators $\mathcal{Q}(r)$ and $\mathcal{Q}(t)$ which act at the two terminals of a photon line $L'_{\mu\nu}(r, t)$ are defined to operate on those electron lines which are contained within these terminals. The electron lines preceeding $a(r)$ and succeeding $a(t)$, which are also functions of $x_{\mu}(r)$ and $x_{\mu}(t)$, will also be used in the specific definition of $\mathcal{Q}(r)$ and $\mathcal{Q}(t)$ but in such a way that these electron lines are reproduced after the completion of the operation. Thus, corresponding to every photon line of a continuous electron line and hence to every virtual energy momentum variable, this combination $\mathcal{Q}(r, t)$, acting from the left and the right, can be used to eliminate the divergent terms of the integrand for this variable and every integral in a Feynman graph can be made convergent.

We must also, as in Dyson's procedure perform the calculations for the innermost graph first that is, defining the internal photon line $L_{\mu\nu}(k)$ in the momentum representation by

$$(10) \quad \dots A_{\mu}(k) \dots A_{\nu}(k) \dots$$

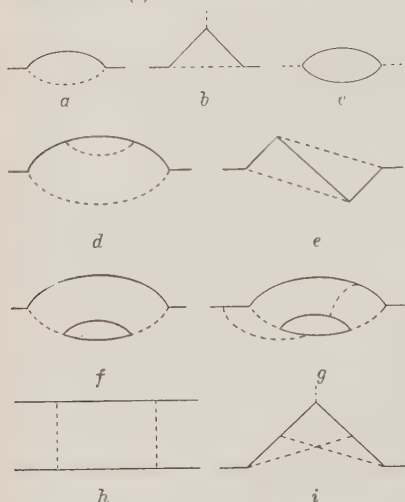
the operation $\dots \mathcal{Q}a(k) \dots \mathcal{Q}a(k) \dots$ which is contained in an operation of the form $\dots \mathcal{Q}a(k_1) \dots \mathcal{Q}a(k_1) \dots$ must be performed first. But for overlapping divergences it becomes necessary to define the operation of one \mathcal{Q} on another. This is done by increasing the range of the inner \mathcal{Q} till it covers the whole overlapping region and thus removing the overlap of the \mathcal{Q} 's.

We note that in the absence of an external electromagnetic field $\mathcal{Q}(1)a(1)\psi'(1)$ is zero and $\mathcal{E}(1)a(1)\psi'(1)$ contributes only to the mass and charge of the electron. In the presence of an external electromagnetic field let us as an example consider its contribution to the Lamb Retherford shift. There if the

calculations are performed according to the procedure of BETHE⁽³⁾ the contribution of $\mathcal{E}(1)a(1)\psi'(1)$ changes because $\psi'(1)$ now includes the effects of the external electromagnetic field and their difference gives the Lamb Retherford shift, but if the calculations are performed according to FEYNMAN⁽⁴⁾ $\psi'(1)$ remains unchanged and the Lamb shift is obtained from the term $\mathcal{D}(1)a(1)\psi'(1)$.

3. - The Reformulated Maxwell Equations.

The Maxwell equations can also be reformulated similarly in terms of the experimental mass and charge of the electron and in accordance with (4) we shall write (5)



$$(11) \quad \square^2(1)A'_\mu(1) = -\frac{ie\hbar}{2} (\bar{\psi}'(1)\mathcal{D}(1)\psi'(1) + \bar{\psi}'^c(1)\mathcal{D}(1)\psi'^c(1)) \\ = -\frac{ie\hbar}{2} \int \mathcal{D}(1) \Pi_{\mu\nu}(1, 2) A'_\nu(2) d2.$$

Fig. 1.

within a electron selfenergy graph, as in Fig. 1-f, shall vanish and we should use the operator \mathcal{D} after removing such terms. The integral equations corresponding to the Maxwell equations are

$$(12) \quad L'_{\mu\nu}(1, 2) = L_{\mu\nu}(12) + \lambda^2 \iint L_{\mu\alpha}(13) \mathcal{D}(3) \Pi_{\alpha\beta}(3, 4) L'_{\beta\nu}(4, 2) d3 d4,$$

(3) H. A. BETHE: *Phys. Rev.*, **72**, 339 (1947).

(4) R. P. FEYNMAN: *Phys. Rev.*, **76**, 749, 769 (1949).

(5) We should like to point out that in (2) the right hand side of (32) and the corresponding part of (9) should be multiplied by (-1); in the line below (35) the term $\Pi''_{\mu\alpha}(1,4)$ should be replaced by $2\Pi''_{\mu\alpha}(1,4)$; in (49) the factor $(u-)$ should be replaced by $(u-1)$; and in (44), $L_{\mu\nu}(12)$ should be replaced by $\frac{1}{2}L_{\mu\nu}(12)$.

and

$$(13) \quad A'_\mu(1) = A_\mu(1) + \lambda^2 \iint L'_{\mu x}(1, 3) \mathcal{P}(3) \Pi_{\alpha\beta}(3, 4) A_\beta(4) d3 d4 .$$

We note that equations (6) and (12) also lead to Feynman graphs of the type shown in Fig. 1-*g*. Here the photon line $L_{\mu\nu}(k)$ in

$$(14) \quad \dots \mathcal{P} A_\mu(k) \dots \text{Tr} \dots \mathcal{P} (\dots \mathcal{P} A_\nu(k) \dots)$$

does not enclose any electron lines and hence we can put the expression (14) equal to

$$(15) \quad \dots A_\mu(k) \dots \text{Tr} \dots \mathcal{P} (\dots A_\nu(k) \dots) ,$$

and no terms are subtracted from the corresponding integral. Thus we note that when two $A_\mu(k)$'s do not lie on the continuation of the same electron line, but are situated on separate continuous electron lines of a Feynman graph as in Fig. 1-*g* and 1-*h*, then the principle energy operator leaves the corresponding integral unaffected, and it is also not necessary to subtract terms from such integrals to obtain convergence.

Here we should like to summarize the rules for the region and the operation of \mathcal{P} 's that have been given in the last and in this section. A combination of \mathcal{P} 's acting at the two terminals of a photon line operates on the continuous electron line between these two terminals. The electron lines in the immediate neighbourhood of this region are also used in the definition of the operation of \mathcal{P} 's but they are reproduced after the operation has been performed. The \mathcal{P} combination for a photon line which connects two separate electron lines does not affect the Feynman graph. For closed electron loops in a photon line we have a single \mathcal{P} acting on the closed loop. If a combination of \mathcal{P} 's is contained within another combination of \mathcal{P} 's then the operation corresponding to the inner \mathcal{P} 's must be performed first. For overlapping graphs, in which a combination of \mathcal{P} 's contains single \mathcal{P} 's, the operation of the combination of \mathcal{P} 's is performed first and then the single \mathcal{P} 's are placed just outside the region of the combination of \mathcal{P} 's so that they cover the whole overlapping region.

4. - The First Subtraction Scheme.

We can now proceed to define the free and principle energy value operators and in this section a particular choice which makes the subtracted terms similar to those removed by Dyson's renormalization program is given. Let

us make the replacements

$$(16) \quad \begin{cases} \mathcal{E}(1) \rightarrow \mathcal{E}_F(1), \\ \mathcal{D}(1) \rightarrow \mathcal{D}_F(1), \end{cases}$$

and, in the momentum representation

$$(17) \quad \mathcal{E}_F(p)(X(p)) = \mathcal{E}'_F(p)(X(p)) + H(p)\mathcal{E}'_F(p)(K(p)\{X(p) - \mathcal{E}'_F(p)(X(p))\}),$$

where

$$(18) \quad \mathcal{E}'_F(p)(X(p)) = (X(p))_{i\gamma p + \kappa = 0, p^2 + \kappa^2 = 0}.$$

We shall use the Dyson integral equations for the propagation operators and therefore use (6) for the selfenergy graphs and replace the general vertex graph expression (8) by

$$(19) \quad \Lambda'_\mu(1, 3, 2) = K'(1, 3)\gamma_\mu K'(3, 2).$$

Then, the operation of the combination of $\mathcal{D}_F(r)$ and $\mathcal{D}_F(t)$ for the photon line $L_{\mu\nu}(r, t)$ is defined in the general term of the expansion of (19), in the momentum representation, by

$$(20) \quad \begin{aligned} & K\mathcal{D}_F(p_1)a(k_1)K(p_1, k_1) \dots K\mathcal{D}_F(p_1, k')a(k_r) \dots \gamma_\mu \dots \\ & \cdot a(k_s)K\mathcal{D}_F(p_2, k_1 \dots k_s) \dots a(k_t)K\mathcal{D}_F(p_2, k'') \dots a(k_{2n})K\mathcal{D}_F(p_2) = \\ & = \dots K(p_1, k')\mathcal{D}_F(p_1, k' | p_2, k'')(X_{\mu\xi}(p_1, p_2, k))A_\xi(k_s)K\mathcal{D}_F(p_2, k'') \dots = \\ & = \dots K(p_1, k')[X_{\mu\xi}(p_1, p_2, k) - \mathcal{E}_F(p_1, k' | p_2, k'')(X_{\mu\xi}(p_1, p_2, k))A_\xi(k_s)K\mathcal{D}_F(p_2, k'') \dots \\ & = \dots K(p_1, k')[X_{\mu\xi}(p_1, p_2, k) - \mathcal{E}'_F(p_1, k')\mathcal{E}'_F(p_2, k'')(X_{\mu\xi}(p_1, p_2, k)) - \\ & \quad \mathcal{E}'_F(p_1, k')(H(p_1, k')\mathcal{E}'_F(p_2, k'')(K(p_1, k')\{X_{\mu\xi}(p_1, p_2, k) - \mathcal{E}'_F(p_1, k')\mathcal{E}'_F(p_2, k'') \\ & \quad \cdot (X_{\mu\xi}(p_1, p_2, k))\})K(p_2, k''))H(p_2, k'')]A_\xi(k_s)K\mathcal{D}_F(p_2, k'') \dots \end{aligned}$$

where

$$(21) \quad X_{\mu\xi}(p_1, p_2, k) = L_{\alpha\beta}(k_r)\gamma_\alpha K(p_1, k_1, \dots, k_r) \dots \gamma_\mu \dots \gamma_\xi \dots K(p_2, k_1, \dots, k_{t-1})\gamma_\beta.$$

Here we have used the abbreviations (p_1, k') , (p_2, k'') and (p_1, p_2, k) for $(p_1, k_1, \dots, k_{r-1})$, (p_2, k_1, \dots, k_t) and $(p_1, p_2, k_1, \dots, k_{t-1})$ respectively. The principle energy operator $\mathcal{D}_F(r)$ is a function of the coordinates $x_\mu(r)$ and it has been so defined in (20) that the principle energy value is taken with respect to the energy of the electron propagation function immediately preceding

it at the initial point of the photon line and with respect to the energy of the electron propagation function immediately succeeding it at the final point of the photon line.

When in $\mathcal{D}_j(p, t)$ the principle energy value operations corresponding to $\mathcal{D}_r(r)$ and $\mathcal{D}_j(t)$ are taken with respect to different energies then the last term in the square bracket of equation (20) is found to vanish and the square bracket becomes

$$(22) \quad X_{\mu_2^+}(p_1, p_2, k) = \mathcal{E}_r'(p_1, k') \mathcal{E}_r'(p_2, k') (X_{\mu_2^+}(p_1, p_2, k)) .$$

But when $\mathcal{D}_r(r)$ and $\mathcal{D}_j(t)$ lie on the same side of γ_μ and when

$$(23) \quad (p_1, k') = (p_2, k')$$

so that the definitions of $\mathcal{D}_r, \dots, \mathcal{D}_j(t)$ for electron self-energy graphs is obtained then the square bracket of becomes

$$(24) \quad X_{\mu_2^+}(p_1, p_2, k) = \mathcal{E}_r(p_1, k') (X_{\mu_2^+}(p_1, p_2, k)) .$$

Then, in this particular case, to show the equivalence to (1) and (4) by the use of (2) we shall put $p_{1,\mu} = p_{2,\mu} = p_\mu$ and then note that the relation (24) can be derived from the definition

$$(25) \quad \mathcal{D}_r(p, k') (X_{\mu_2^+}(p, k)) = X_{\mu_2^+}(p, k) - \mathcal{E}_r(p, k') (X_{\mu_2^+}(p, k)) ,$$

since

$$(26) \quad \mathcal{D}_r(p, k') \mathcal{D}_r(p, k') (X_{\mu_2^+}(p, k)) = \mathcal{D}_r(p, k') (X_{\mu_2^+}(p, k)) .$$

We also note that the operation in (20) decomposes into the simple operations (22) and (24) and obtains its complex form from the composition of the operations (22) and (24) into a single operation.

Similarly, for an external electromagnetic field we can define the principle energy operator $\mathcal{D}_{F,0}(p)$ of the Maxwell equations by the relations

$$(27) \quad \mathcal{D}_{F,0}(p_0) (\Pi_{\mu\nu}(p_0, k)) = \Pi_{\mu\nu}(p_0, k) - \mathcal{E}_{F,0}(p_0) (\Pi_{\mu\nu}(p_0, k)) ,$$

$$(28) \quad \mathcal{E}_{F,0}(p_0) (\Pi_{\mu\nu}(p_0, k)) = \\ = \mathcal{E}_{F,0}(p_0) \{ (\Pi_{\mu\nu}(p_0, k)) - p_0 \mathcal{E}_{F,0}(p_0, p_0^{-1}) \Pi_{\mu\nu}(p_0, k) - \mathcal{E}_{F,0}(\Pi_{\mu\nu}(p_0, k)) \} ,$$

and

$$(29) \quad \mathcal{E}_{F,0}'(p_0) (\Pi_{\mu\nu}(p_0, k)) = (\Pi_{\mu\nu}(p_0, k))_{p_0^2=0} .$$

Here p_0 is the energy-momentum vector of the photon that produces the closed electron loop corresponding to the polarization term $\Pi_{\mu\nu}(p_0, k)$.

Using the equations (20) and (27) or the equations (22), (24) and (27) we note the usual contributions are obtained for the second order graphs and the contribution of the Feynman graph shown in Fig. 1-d is

$$\begin{aligned}
 (30) \quad \Sigma^{(1d)}(12) = & i \frac{\lambda^4 (\hbar c)^2}{(2\pi)^{12}} \iint \int d^4 p \, d^4 k_1 \, d^4 k_2 \exp[-ip(12)] [K\mathcal{D}_F(p)a(k_1) \cdot \\
 & \cdot K\mathcal{D}_F(p-k_1)a(k_2)K(p-k_1-k_2)a(k_2)K\mathcal{D}_F(p-k_1)a(k_1)K\mathcal{D}_F(p) = \\
 & \cdot i \frac{\lambda^4 (\hbar c)^2}{(2\pi)^{12}} \iint \int d^4 p \, d^4 k_1 \, d^4 k_2 \exp[-ip(12)] [K\mathcal{D}_F(p)a(k_1)K(p-k_1)\gamma_\alpha \cdot \\
 & \cdot \left[\frac{K(p-k_1-k_2)}{k_2^2} \epsilon_F(p-k_1) \left(\frac{K(p-k_1-k_2)}{k_2^2} \right) \right] \gamma_\alpha K(p-k_1)a(k_1)K\mathcal{D}_F(p) ,
 \end{aligned}$$

and after operating with the combination of $\mathcal{D}_F(p)$'s we obtain the same contribution as is obtained by the Dyson's renormalization program. Similarly we obtain for the electron selfenergy graph shown in Fig. 1e,

$$\begin{aligned}
 (31) \quad \Sigma^{(1e)}(12) = & i \frac{\lambda^4 (\hbar c)^2}{(2\pi)^{12}} \iint \int d^4 p \, d^4 k_1 \, d^4 k_2 \exp[-ip(12)] [K\mathcal{D}_F(p)a(k_1) \cdot \\
 & \cdot K\mathcal{D}_F(p-k_1)a(k_2)K(p-k_1-k_2)a(k_1)K\mathcal{D}_F(p-k_2)a(k_2)K\mathcal{D}_F(p) = \\
 & = i \frac{\lambda^4 (\hbar c)^2}{(2\pi)^{12}} \iint \int d^4 p \, d^4 k_1 \, d^4 k_2 \exp[-ip(12)] [K\mathcal{D}_F(p)\gamma_\alpha A_\alpha(k_1)K(p-k_1) \cdot \\
 & \cdot (X_\beta(p, k_1, k_2) - \epsilon'_F(p)\epsilon'_F(p-k_1)[X_\beta(p, k_1, k_2)]) A_\beta(k_1)K\mathcal{D}_F(p) = \\
 & = i \frac{\lambda^4 (\hbar c)^2}{(2\pi)^{12}} \iint \int d^4 p \, d^4 k_1 \, d^4 k_2 \exp[-ip(12)] K(p) \cdot \\
 & \cdot (Y(p, k_1, k_2) - \epsilon_F(p)[Y(p, k_1, k_2)]) K(p) ,
 \end{aligned}$$

where

$$X_\beta(p, k_1, k_2) = \gamma_\mu K(p-k_1-k_2)\gamma_\beta K(p-k_2)\gamma_\mu \cdot 1/k_2^2,$$

$$Y(p, k_1, k_2) = \gamma_\beta K(p-k_1)(X_\beta(p, k_1, k_2) - \epsilon'_F(p)\epsilon'_F(p-k_1)[X_\beta(p, k_1, k_2)]) \frac{\partial_{\alpha\beta}}{k_1^2},$$

and this is also similar to the expression obtained by DYSON.

The difference between this subtraction scheme and DYSON's renormalization program occurs in the treatment of the higher order irreducible vertex graphs. There while DYSON is able to remove the renormalization terms in one step we note by considering for example the Feynman graph in Fig. 1-i that in our case two subtractions occur. Thus our procedure does not distinguish between the reducible and the irreducible graphs. Another difference occurs due to the use of different principle energy value operations for closed electron loops which are produced by external or internal photon lines and it can be avoided by the use of the external photon principle energy operator

in both places. But we have been following the general procedure of DYSON which is to obtain a scheme which makes convergent the graphs of a given order and then to note that in the next order graphs we must first remove those terms which contain the divergent terms of the previous order graphs as factors and then remove the remaining divergences by the same procedure as for the lowest order graphs. But by presenting the statement in the inverse order DYSON's conclusions can be obtained in a very simple manner.

5. - The Second Subtraction Scheme.

We shall now give an alternate definition of the free and principle energy value operators and let this choice, which is called the second subtraction scheme, be denoted by the replacements

$$(32) \quad \begin{cases} \mathcal{E}(1) \rightarrow \mathcal{E}_s(1), \\ \mathcal{D}(1) \rightarrow \mathcal{D}_s(1). \end{cases}$$

Let us consider a function $X(p)$ which can be represented by

$$(33) \quad X(p) = \sum_{n=-\infty}^{\infty} \alpha_n H^n(p),$$

where $H(p) = \gamma p + \kappa$. Then $\mathcal{E}_s(1)$ in the momentum representation is defined by

$$(34) \quad \mathcal{E}_s(p)(X(p)) = \sum_{n=-\infty}^0 \alpha_n H^n(p),$$

and we note that the free energy operator projects the free energy part of the function $X(p)$, taking into account its singularities. Similarly if

$$(35) \quad X(p_1, p_2) = \sum_{m, n=-\infty}^{\infty} \alpha_{mn} H^m(p_1) H^n(p_2),$$

then we shall define the projection operator $\mathcal{E}_s(p_1|p_2)$ by

$$(36) \quad \mathcal{E}_s(p_1|p_2)(X(p_1, p_2)) = \sum_{\substack{m \text{ or } n = -i\nu\epsilon, \\ \text{or } m = n = 0 \\ m, n = -\infty}} \alpha_{mn} H^m(p_1) H^n(p_2),$$

and we note that when $p_{1\mu} = p_{2\mu} = p_\mu$,

$$(37) \quad \mathcal{E}_s(p_1|p_2) = \mathcal{E}_s(p).$$

Then corresponding to the equation (20) we define the principle energy value operation $\dots \mathcal{D}_s(r) \dots \mathcal{D}_s(t) \dots$ corresponding to the internal photon line, $L_{\mu\nu}(rt)$

in the general term of the integrand of (9), in the momentum representation, by the relation

$$\begin{aligned}
 (38) \quad & \bar{\psi} \mathcal{D}_s(p_1) a(k_1) K(p_1, k_1) \dots K \mathcal{D}_s(p_1, k') a(k_r) \dots \gamma_\mu \dots \\
 & \cdot a(k_s) K \mathcal{D}_s(p_2, k_1, \dots, k_s) \dots a(k_t) K \mathcal{D}(p_2, k'') \dots a(k_{2n}) \psi \mathcal{D}_s(p_2) = \\
 & = \dots \{K(p_1, k') K^{-1}(p_1, k')\} \mathcal{D}_s(p_1, k' | p_2, k'') (Y_{\mu\xi}(p_1, p_2, k)) \cdot \\
 & \cdot \{K^{-1}(p_2, k'') A_\xi(k_s) K \mathcal{D}_s(p_2, k'')\} \dots = \\
 & \dots \{K^{-1}(p_1, k') K^{-1}(p_1, k')\} [Y_{\mu\xi}(p_1, p_2, k) - \mathcal{E}_s(p_1, k' | p_2, k'') Y_{\mu\xi}(p_1, p_2, k)] \cdot \\
 & \cdot \{K^{-1}(p_2, k'') A_\xi(k_s) K \mathcal{D}_s(p_2, k'')\} \dots,
 \end{aligned}$$

where

$$\begin{aligned}
 (39) \quad & Y_{\mu\xi}(p_1, p_2, k) = \\
 & = L_{\alpha\beta}(k_t) K(p_1, k') \gamma_\alpha K(p_1, k_1, \dots, k_r) \dots \gamma_\mu \dots \gamma_\xi \dots K(p_2, k_1, \dots, k_{t-1}) \gamma_\beta K(p_2, k'').
 \end{aligned}$$

Here $k_t = k_r$ and we have taken the spacetime points $x_\mu(r)$ and $x_\mu(t)$ to lie on either side of γ_μ in order to indicate that then the free energy operation corresponding to $\dots a(k_r) \dots a(k_t) \dots$ has to be performed with respect to different energy momentum vectors by using $\mathcal{E}_s(p_1, k' | p_2, k'')$. If they lie on the same side of γ : and are equal then we should use

$$(40) \quad \mathcal{E}_s(p_1, k' | p_2, k'') = \mathcal{E}_s(p_1, k').$$

Now $K(p_1, k')$ or $K(p_2, k'')$ can always be extracted from $\mathcal{E}_s(p_1, k' | p_2, k'')$ $\cdot (Y_{\mu\xi}(p_1, p_2, k))$ after the free energy operation has been performed either because they represent the external lines of the Feynman graph or are not singular for $H(p_1) = 0$ or $H(p_2) = 0$ and so do not materially affect the operation of the free energy operator or otherwise they are of the form $K(p_1, k')$ or $K(p_2, k'')$ and can be reproduced by a multiplication by $H(p_1, k')$ or $H(p_2, k'')$ and the K^{-1} terms in the curly brackets just cancel them. Hence the curly brackets have been introduced to obtain the correct ordering for the overlapping divergences and may be neglected in the derivation of the energy relation between $\mathcal{E}_s(p)$ and $\mathcal{D}_s(p)$. Then using the same arguments by which the relation was derived, we obtain

$$(41) \quad \mathcal{D}_s(p, k')^\eta Y_{\mu\xi}(p, k) = Y_{\mu\xi}(p, k) - \mathcal{E}_s(p, k') (Y_{\mu\xi}(p, k)),$$

since

$$(42) \quad \mathcal{D}_s(p, k') \mathcal{D}_s(p, k') (Y_{\mu\xi}(p, k)) = \mathcal{D}_s(p, k') (Y_{\mu\xi}(p, k)).$$

Similarly for an external electromagnetic field we can replace the operator $\mathcal{D}(1)$ which occurs in the Maxwell equations by $\mathcal{D}_0(1)$ and define it for an expression

$$(43) \quad Y(p_0) = \sum_{n=-\infty}^{\infty} \alpha_n p_0^{2n}$$

by

$$(44) \quad P_{s,0}(p_0)(Y(p_0)) = Y(p_0) - \mathcal{E}_{s,0}(Y(p_0)),$$

where

$$(45) \quad \mathcal{E}_{s,0}(p_0)(Y(p_0)) = \sum_{n=-\infty}^0 \alpha_n p_0^{2n}.$$

Here p_{00} is the energy momentum vector of the photon. We note that in Fig. 1-f the photon principle energy value is taken with respect to the energy momentum of the photon which produces the closed electron loop.

The operation (38) can now be used in the expressions for the Feynman graphs obtained from the equations (7) and (8), where the external electron lines are explicitly denoted and the usual renormalization values are obtained for the second order graphs shown in the Figs. 1 a, b and c. For the higher order graphs the subtracted terms are different from those obtained by Dyson's renormalization program and we shall illustrate this as well as the application of (38) by considering the fourth order selfenergy Feynman graph shown in Fig. 1 d. Its contribution is found to be

$$\begin{aligned} (46) \quad \Sigma^{(4d)}(12) &= -i \frac{\lambda^4 (\hbar c)^2}{(2\pi)^{12}} \int \int \int d^4 p \, d^4 p_1 \, d^4 k_2 \exp[-ip(12)] K \mathcal{D}_s(p) a(k_1) \cdot \\ &\quad \cdot K \mathcal{D}_s(p - k_1) a(k_2) K(p - k_1 - k_2) a(k_1) K \mathcal{D}_s(p - k_1) a(k_2) \cdot \\ &= -i \frac{\lambda^4 (\hbar c)^2}{(2\pi)^{12}} \int \int \int d^4 p \, d^4 k_1 \, d^4 k_2 \exp[-ip(12)] K \mathcal{D}_s(p) a(k_1) K(p - k_1) \cdot \\ &\quad \cdot (X(p, k_1, k_2) - K^{-1}(p - k_1) \mathcal{E}_s(p - k_1) [K(p - k_1) X(p, k_1, k_2) K(p - k_1)] \cdot \\ &\quad \cdot K^{-1}(p - k_1)) K(p - k_1) a(k_1) \psi \mathcal{D}_s(p) = \\ &= -i \frac{\lambda^4 (\hbar c)^2}{(2\pi)^{12}} \int \int \int d^4 p \, d^4 k_1 \, d^4 k_2 \exp[-ip(12)] (Y(p, k_1, k_2) - \mathcal{E}_s(p) [Y(p, k_1, k_2)] \psi(p), \end{aligned}$$

where

$$X(p, k_1, k_2) = \gamma_\alpha K(p - h_1 - h_2) \gamma_\alpha \frac{1}{h_2^2},$$

$$\begin{aligned} Y(p, k_1, k_2) &= K(p) \gamma_\beta K(p - k_1) (X(p, k_1, k_2) - K^{-1}(p - k_1) \cdot \\ &\quad \cdot \mathcal{E}_s(p - k_1) [K(p - k_1) X(p, k_1, k_2) K(p - k_1)] K^{-1}(p - k_1)) K(p - k_1) \gamma_\beta \frac{1}{k_1^2}. \end{aligned}$$

6. - Conclusion.

We have shown that the reformulated Dirac and Maxwell equations (4) and (11) are renormalized and follow from the original Dirac-Maxwell equations in a physically sensible way, and since they give the same results as the usual procedure of renormalization for the second order Feynman graphs these results agree approximately with the observed values. Since we are not able to define the principle energy operator that occurs in them uniquely, two possible definitions (20) and (38) are given which lead to the first and second subtraction schemes, and the procedure for the ordering of these operators which is given in Sect. 2 and 3 should be considered to be a part of these definitions. While it seems possible to state the second more concisely the first scheme is more similar to Dyson's renormalization program and differs from it significantly for the higher order irreducible vertex graphs only. Perhaps the scheme that satisfies the relation (5) will be the most favoured.

Thus we obtain again but in a very simple manner the results of DYSON from the reformulated Dirac-Maxwell equations and furthermore since the renormalization scheme is contained within them when they are solved by some approximation other than the Born approximation the new approximate solutions will also be renormalized automatically. The presence of divergent terms which occur, although they cancel one another, can be avoided by following the procedure of ⁽²⁾, and by combining these two procedures we obtain a quantum electrodynamics that is free of divergences and of a renormalization program.

* * *

The author is very grateful to Professor G. WATAGHIN for kind hospitality at the Istituto di Fisica dell'Università di Turin and for many helpful discussions.

RIASSUNTO (*)

Si dà una nuova formulazione delle equazioni di Dirac-Maxwell eliminando quella parte del termine di interazione che dà contributo solo alla massa e alla carica dell'elettrone nudo e sostituendo poi alla massa e alla carica nude dell'elettrone la massa e carica sperimentali. Si dimostra poi che in tali espressioni è insito uno schema di rinormalizzazione. Si descrivono due schemi di rinormalizzazione e si dimostra che il primo di essi segue il modello del programma di rinormalizzazione di Dyson, pur non essendo uguale allo stesso.

(*) Traduzione a cura della Redazione.

A Diffusion Chamber Study of Very Slow Mesons.

IV. Absorption of Pions in Light Nuclei (*).

P. AMMIRAJU and L. M. LEDERMAN

*Nevis Cyclotron Laboratories, Columbia University, Physics Department
Irvington-on-Hudson, New York*

(ricevuto l'11 Maggio 1956)

Summary. — The absorption of slow negative pions has been studied in the light nuclei helium, carbon and nitrogen. The dominant reaction in each case has been observed to be: (1) $\pi^- + {}^4\text{He} \rightarrow \text{p} + 3\text{n}$; (2) $\pi^- + {}^{12}\text{C} \rightarrow 2\alpha + 1\text{p} + 3\text{n}$; (3) $\pi^- + {}^{14}\text{N} \rightarrow 3\alpha + 2\text{n}$. Prong distributions, proton and alpha spectra have been compiled and compared with the theory of Clark and Ruddelsten. The frequency of α -emission gives strong qualitative support to the α -particle model of nuclear structure. This is supported by the similarity of the proton spectra in reactions (1) and (2). The low average energy of protons in (1) and (2) and of α -particles in (3) supports the two nucleon recoil model in the primary absorption act. In this case (np) initial nucleon states 3S_1 are favored over (pp) states 1S_0 in agreement with the inverse reaction — production of mesons in nucleon-nucleon collisions.

1. — Introduction.

The problem of the absorption of slow negative pions in complex nuclei has attracted great attention in the early development of meson physics. Substantially all of the previous work (1-7) on this subject has been done using

(*) This research is supported in part by the joint program of the Office of Naval Research and the Atomic Energy Commission.

(1) For a detailed history of this subject, with references to earlier work see R. MARSHAK: *Meson Physics* (New York, 1952), Chapter 5.

(2) M. G. K. MENON, M. MUIRHEAD and O. ROCHAT: *Phil. Mag.*, **41**, 583 (1950).

(3) F. L. ADELMAN: *Phys. Rev.*, **85**, 249 (1952).

(4) S. ENOMOTO, S. FUJIMOTO, S. HORIE and Y. TSUZUKI: *Prog. Theor. Phys.*, **7**, 612 (1952).

(5) W. CHESTON and L. GOLDFARB: *Phys. Rev.*, **78**, 683 (1950).

(6) G. VANDERHAEGHE and M. DEMEUR (Private communication).

(7) G. PUPPI, V. DE SABBATA and V. MANARESI: *Nuovo Cimento*, **10**, 1704 (1953).

nuclear emulsions in which heavy elements, chiefly silver and bromine, are mixed with a group of lighter elements, mostly hydrogen, carbon, nitrogen, and oxygen.

Although the π interactions in heavy elements could be separated from those due to lighter elements using sandwiched emulsions and criteria based on the effect of potential barrier of the nuclei on the ejected charged particles, the emulsion technique is comparatively unsuited for the detailed investigation of the absorption process in any specific element.

The π^- meson disintegrations in heavy elements such as silver and bromine, have been extensively studied and the results have been interpreted⁽⁷⁻⁹⁾ with some success using the evaporation theory which is not applicable in the case of light elements.

It is desirable to study the disintegrations in light nuclei under conditions in which the complications due to the presence of heavy nuclei are eliminated. To this end, the Nevis diffusion cloud chamber was filled consecutively with helium, ethylene (carbon) and nitrogen, and absorption of slow negative pions in these light elements was investigated. The continuously sensitive, gas filled cloud chamber is particularly suited for the observation of complex reactions in pure elements. These advantages are offset by the unfortunate geometry and low density of the sensitive volume which introduces strong bias in many of the detailed measurements. Thus, such interesting aspects as the spectrum of α -particles and protons are subject to large geometrical corrections in this technique, and the unambiguous distinction between recoiling hydrogen isotopes and between helium isotopes is quite difficult to make.

When a negative pion of several MeV energy is brought to rest in matter, the Coulomb field of the nucleus acts to bind the meson in an atomic orbit. Auger and radiative transitions as well as inelastic collisions with neighbouring atoms lead to a rapid cascade down to the lowest lying states. In these states (1s, 2p), the meson is very close to the nucleus and the well-known strong Yukawa interaction ($\pi^- + p \rightarrow n$) manifests itself in various forms.

The capture of a π^- meson in hydrogen⁽¹⁰⁾ leads either to high energy γ -rays by radiative absorption or to lower energy γ -rays via neutral mesons by charge exchange reaction. In deuterium,⁽¹¹⁾ however, the γ -rays are observed in only 30 percent of the cases, while 70 percent of the absorptions lead to two neutrons. In nuclei heavier than deuterium, the γ -emission is very much reduced because of the requirements of the Pauli principle. Theo-

(8) K. J. LE COUTEUR: *Proc. Phys. Soc.*, A **63**, 259 (1950).

(9) Y. YAMAGUCHI: *Prog. Theor. Phys.*, **5**, 896 (1950).

(10) W. K. H. PANOFSKY, R. L. AAMODT and J. F. HADLEY: *Phys. Rev.*, **81**, 565 (1951).

(11) W. CHINOWSKY and J. STEINBERGER: *Phys. Rev.*, **95**, 1561 (1954).

retical estimates ⁽¹²⁾ show that in carbon the γ -emission is no higher than 0.5 percent.

The principal theoretical interest in the capture of slow π^- mesons by helium, carbon, and nitrogen stems from the possibility that it may throw some light on the mechanism of absorption of slow negative pions by these nuclei and incidentally thereby give new information as to the structure of nuclei. An interesting feature of meson absorption ($\pi^- + P \rightarrow N$) in a nucleus is that the conservation laws require at least two nucleons to share the energy released by conversion of the pion rest mass. This requirement ties the process in with an important aspect of nuclear structure: the so-called high momentum component or strong correlations of particles in a nucleus ⁽¹³⁾.

2. - Experimental Arrangement.

The experimental arrangement is similar to that employed by SARGENT *et al.* ⁽¹⁴⁾.

The chamber, in a magnetic field of 10 kilogauss, was filled consecutively with ethylene, nitrogen, and helium at gauge pressures of 24, 18, and 206 lbs sq inches respectively. Oxygen was found not to work in the diffusion chamber due to its paramagnetism which caused turbulence in the strong magnetic and density gradients.

Using the technique developed in earlier runs, negative pions are moderated in copper absorber and allowed to enter the chamber through the light portal, where about one meson per 4 photographs spirals to rest in the gas. The negative meson is trapped in Bohr orbits of the gas nucleus and is captured into the nucleus in a time short compared to that for decay. According to CAMAC *et al.* ⁽¹⁵⁾ most of the captures in carbon and nitrogen occur from the $2p$ level. In the case of helium ⁽¹⁶⁾ it is estimated that 80 percent of the captures take place from the S -state of the mesic helium atom. Experiments ⁽¹⁷⁾ in solid hydro-carbons indicate that no more than about 1 percent of the arrested negative pions are absorbed by the hydrogen. That this situation is approximately unchanged in gaseous media is indicated by the results discussed below.

⁽¹²⁾ K. A. BRUECKNER, R. SERBER and K. M. WATSON: *Phys. Rev.*, **81**, 575 (1951); *Phys. Rev.*, **84**, 258 (1951).

⁽¹³⁾ K. A. BRUECKNER, R. J. EDEN and R. C. FRANCIS: *Phys. Rev.*, **98**, 1445 (1955).

⁽¹⁴⁾ C. P. SARGENT, R. C. CORNELIUS, M. C. RINEHART, L. M. LEDERMAN and K. C. ROGERS, *Phys. Rev.*, **98**, 1349 (1955); **99**, 885 (1955), **100**, 883 (1955).

⁽¹⁵⁾ M. CAMAC, A. D. MCGUIRE, J. B. PLATT and H. J. SCHULTE: *Phys. Rev.*, **99**, 897 (1955).

⁽¹⁶⁾ A. G. PETSCHKE: *Phys. Rev.*, **90**, 959 (1953).

⁽¹⁷⁾ J. TINLOT and A. ROBERTS: *Phys. Rev.*, **95**, 137 (1954).

3. — Experimental Results.

3.1. *Frequency vs. Prong Number of Pion Stars in Carbon and Nitrogen.* — The meson beam entering the diffusion cloud chamber consists chiefly of negative pions contaminated with negative muons and electrons. Stopped negative muons can for the most part be recognized by their associated decay electrons. For a given magnetic field and velocity of the meson, the radius of curvature of the stopping pion or muon depends on its mass only. The thirty-two percent difference in the mass of the mesons would result in a change in the radius of curvature for a given residual range of the meson. In fact, for a residual range of 10 cm the momentum of a pion is 22 percent greater than that of a muon in ethylene at -40°C and 2.8 atmospheres pressure. This enables us to separate the muons from pions in the case of meson tracks of residual range greater than 10 cm. The small contribution due to muon stars thus obtained is subtracted from the total observed meson stars to give the corrected number of pion stars in carbon and nitrogen.

Any track of length greater than a millimeter and of definite direction is classified as a prong. Sometimes at the end of meson's range, a small visible blob of extension no larger than 0.5 mm is clearly seen and these have been attributed to recoil nuclei.

After subtracting the contribution due to muon stars as explained above, the frequency vs. prong distribution of negative pion stars for carbon and nitrogen is given in Table I. A total of 944 stars have been observed in carbon while the number of stars examined in nitrogen is 130. It is clear that in both cases, the three prong stars predominate.

TABLE I. *Prong Distribution of Pion Stars in Carbon and Nitrogen.*

No. of prongs per star		0	1	2	3	4	5
Light nucleus							
Carbon (944 stars)	percent	16.3	13.9	23.3	39.1	7.1	0.3
Nitrogen (430 stars)	percent	13.7	14.7	20.0	34.0	15.6	2.0

Since ethylene (C_2H_4) is the filling gas, in the case of carbon, the prong distribution has to be corrected for the effect of hydrogen. That this correction is unimportant is obvious from a comparison of zero prong stars without recoil in C_2H_4 and in N. This implies that hydrogen occurring in gaseous mixtures such as ethylene (C_2H_4) is relatively ineffective in capturing slow π^- me-

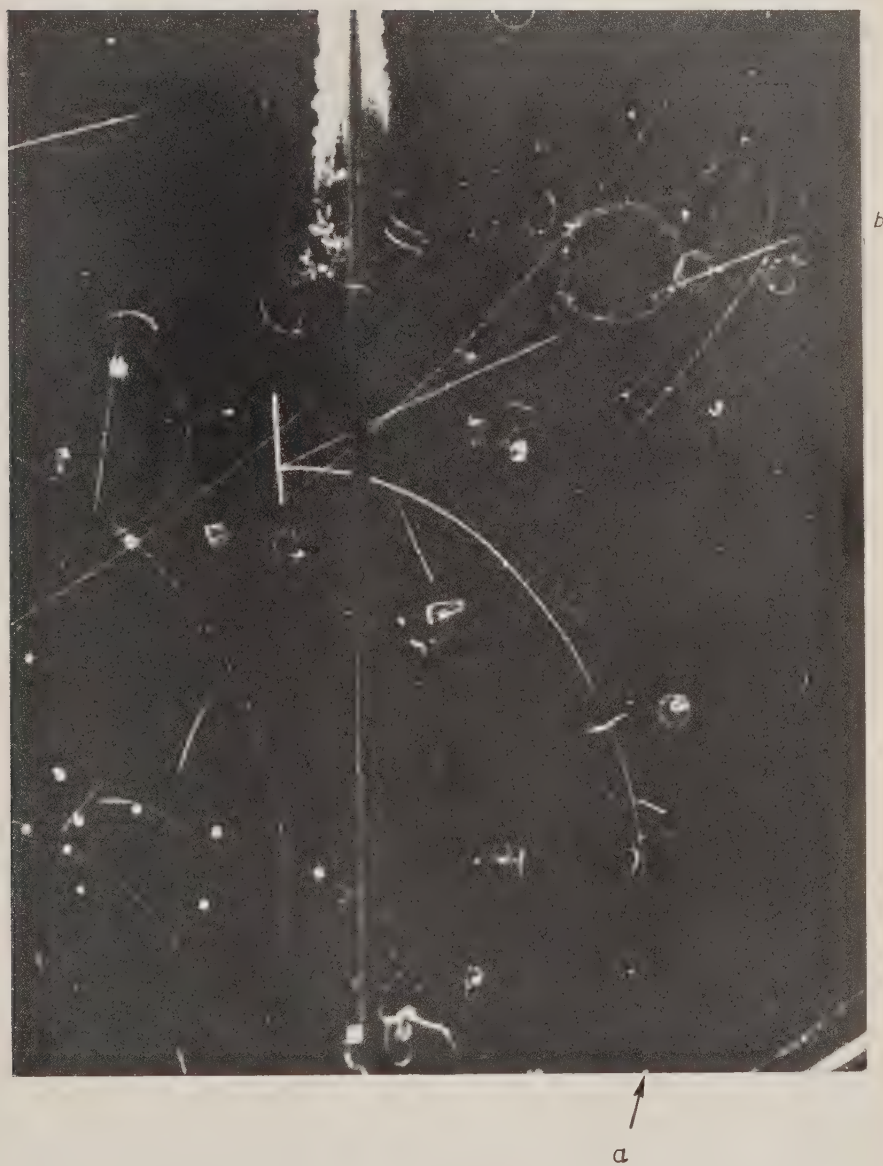


Fig. 1. - Three prong star in carbon: $\pi^- + C \rightarrow 2\alpha + 1p + 3n$. a is the incident slow meson, b is the proton and the two heavy tracks represent the α -particles

sons, in agreement with the earlier results (¹⁷). This is explained (¹⁰) as due to the high probability of the π meson being transferred from hydrogen to carbon atom before the mesic K-shell in hydrogen is reached.

In slow π^- meson absorption experiments using nuclear emulsions one finds a preponderance of three prong stars in the disintegration of light elements. These results are consistent with our results except for the proportion of zero prong stars. In the experiments using nuclear emulsions, 28 percent of the π^- meson captures lead to stars with no visible prongs except for occasional observable heavy recoils and these zero prong stars have been attributed exclusively to the heavy elements present in the emulsion. This number can at best represent an upper limit since it cannot be excluded that light elements do give rise to stars with zero prongs, even assuming that the zero prongs occur more frequently in heavy elements. Indeed, more recent experiments (¹⁸) using emulsions diluted with gelatin in varying proportions show that 10 percent of the captures in light elements lead to stars with no visible prongs. This is consistent with the present experimental results especially since the zero prong stars in nuclear emulsions are due to several competing nuclei. To appreciate the significance of zero prong stars, we present below the maximum energy of recoil fragments which would still not be observed because the range is of the order of track thickness.

recoil fragment	max. unobservable energy
proton	.25 MeV
α	1.0 MeV
${}^7\text{Li}$	1.5 MeV

3'2. Mesic Absorption Reactions.

3'2.1. Identification of Prongs. — The primary characteristic which serves to distinguish protons from α -particles is the ionization density. Over most of the energy region encountered, the ionization of an α -particle is of the order of sixteen times that of a proton of the same energy. In case of corresponding isotopes (${}^3\text{He}:$ ${}^3\text{H}$), the minimum ratios of ionizations in the same energy range is of the order of four. The various factors which relate ionizing power and track density serve to decrease this difference. The ionization produced by the doubly (or triply) charged ions is enormously greater than that produced by the electrons or protons and is too great in fact for the local vapor supply. Nevertheless, to establish the feasibility of separating hydrogen isotopes from α -particles the following procedure was adopted.

(¹⁸) M. G. K. MENON: Private communication.

In carbon, the three prong stars are often of the type shown in Fig. 1. Two of the tracks are heavy and often come to rest in the gas. The remaining prong is lighter and practically never comes to rest. This event can be represented with very small uncertainty as a $2\alpha 1p$ -event (the «p» includes the possibility of hydrogen isotopes). 63 percent of the three prong carbon stars fall in this category. 84 percent of the four prong stars in carbon are of the type $1\alpha 3p$ where one of the tracks is heavy and often comes to rest in the gas while the remaining three are relatively lighter and of the same ionizing power. For the estimation of the relative ionization of a track, the width of the re-projected track image is measured. The widths of tracks measured range from 0.3 mm to 1.5 mm and the width can be measured to an accuracy of 0.1 mm by a Bausch and Lomb magnifier. Since the stars are formed in regions where the degree of supersaturation is not always the same, it was necessary to normalize the width of each track relative to that of the incident meson, the meson track width being measured at 1 cm from the center of the star. Empirically it has been found that the square of the relative width of a track is a convenient measure of its ionization. The favourable cases in carbon are plotted in Fig. 2 where the ordinate represents the number of tracks and the abscissa the square of the relative width of the track multiplied by ten (for a convenient scale of representation). We can see a fairly clear separation into two main groups, corresponding to singly and doubly charged particles. Tracks having

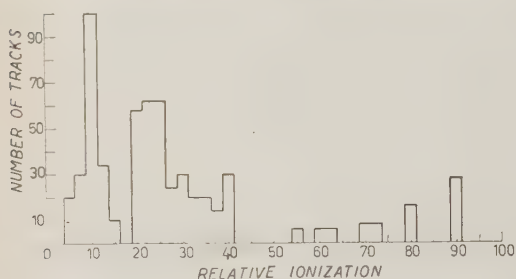


Fig. 2. — Relative ionization vs. number of tracks in ethylene.

relative ionization less than or equal to 15 are tentatively classified as protons, while tracks whose relative ionization is between 20 and 40 are classified as α -particles. The tracks that correspond to relative ionization larger than α -particles come from three prong stars where one of the prongs is heavy and short and the other two fall into the proton group. These heavy

tracks can be classified as triply charged ions, consistent with charge conservation in the overall reaction. This plot serves to make the intuitive classification more quantitative. Particles which are tentatively classified on the basis of the histogram are observed for additional criteria: range, curvature, and conservation of charge in the reaction. These criteria generally strengthen the above interpretation of Fig. 2. If the additional criteria are consistent with the classification, the prong identification is assumed correct. In cases for which the relative ioniz-



Fig. 3. — Four prong stars in nitrogen: $\pi^- + {}^{14}\text{Ni} \rightarrow 2\alpha + 2p + 4n$. a is the incident slow meson, b and c are the protons and the remaining tracks constitute the α -particles.

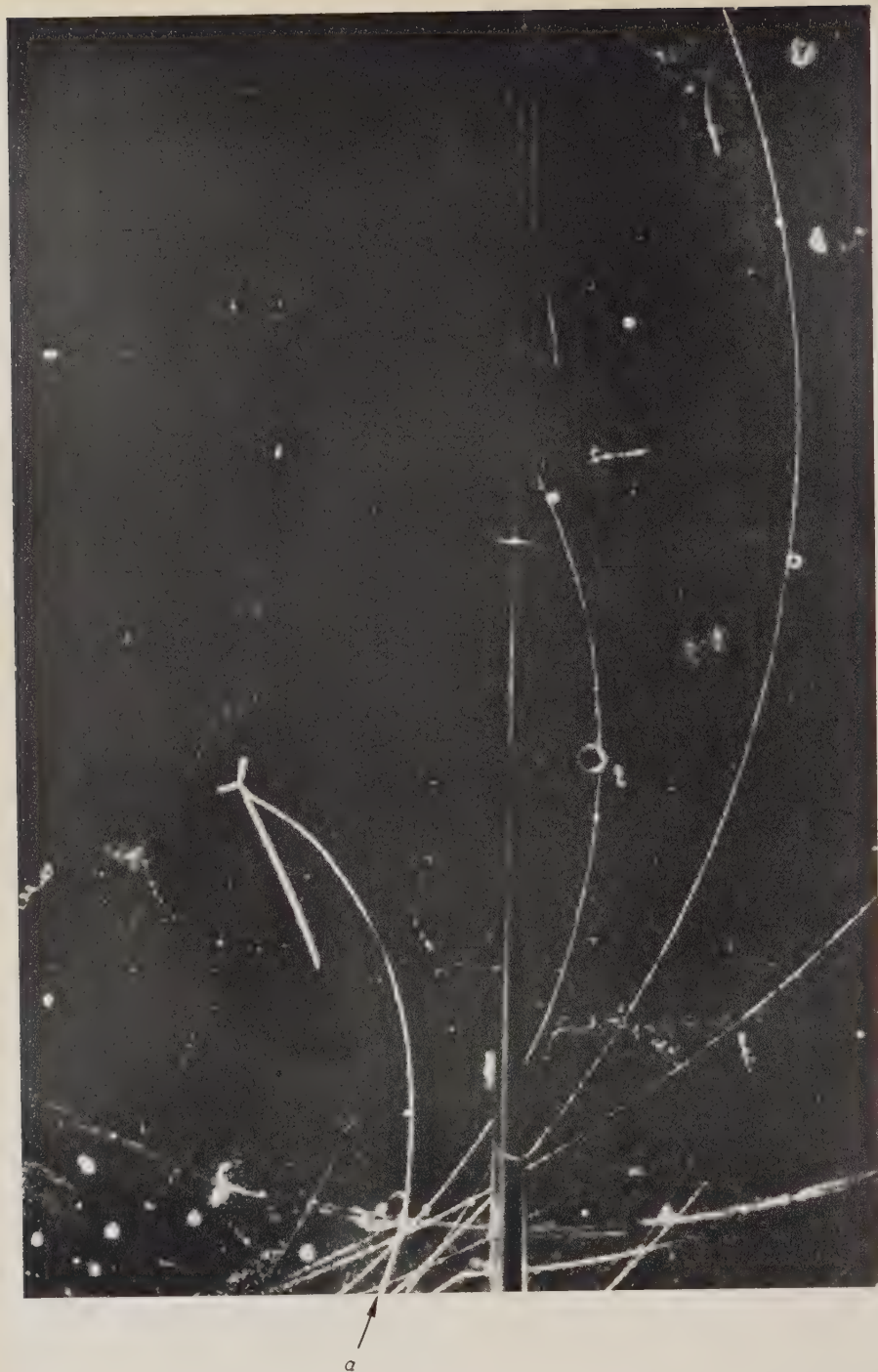


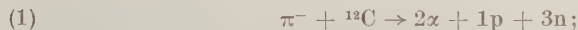
Fig. 4. - Three prong star in nitrogen: $\pi^- + {}^{14}\text{N} \rightarrow 3\alpha + 2n$. a is the incident meson.

ation is between 15 and 20, or where range, curvature, or charge conservation information is inconsistent, the prong is unclassified. These usually occur in particularly poor regions of the chamber. Using this procedure, for example, 75 percent of the three prong stars in carbon are classified.

Fig. 3 shows a typical four prong star in nitrogen where two of the tracks are heavy and come to rest in the gas. One of the remaining prongs is very light and is identified as a proton; the other has an ionization density intermediate between the two heavy tracks and the light one. Conservation of charge demands that it be a singly charged particle. This event is classified as a $2\alpha 2p$ -event (again «p» includes the possibility of hydrogen isotopes). Fig. 4 shows the example of a three prong star in nitrogen. All the tracks are heavy and exhibit the same relative ionization. These events which constitute more than 55 percent of the three prong stars in nitrogen are classified as 3α -type.

3.2.2. Carbon Reactions.

(a) Classification of reactions. — A total of 369 three prong stars is examined. On the basis of conservation of charge and estimates of relative ionization (Fig. 2), we find that 63 percent of these stars are identified as following the reaction



11 percent of the three prong stars are classified as consisting of two «protons» and one heavy fragment while the remainder constitute the unclassified events. In addition, the reaction



has been determined to be the dominant 4 prong reaction. Table II gives the frequency of the dominant modes of reaction in the case of carbon and nitrogen. Under the column «others» are included zero, one and two prong stars as well as three, four, and five prong stars in which the identification of the reaction could not be made. The qualitative predominance of reaction (1) is an important fact which will be discussed below.

(b) Indirect disintegration of ${}^{12}\text{C}$. — An attempt is made to determine whether in the disintegration of ${}^{12}\text{C}$ by slow negative pion according to the reaction: $\pi^- + {}^{12}\text{C} \rightarrow 2\alpha + 1p + 3n$, the two α -particles are emitted directly or via one of the levels of an excited ${}^8\text{Be}$ nucleus. In the sensitive region of the diffusion cloud chamber the two α -particles form a fork apparently originating from the point of disintegration, because the processes under consideration occur within a very short time interval. For instance, the ground

TABLE II. — *Classification of mesic absorption reactions in carbon and nitrogen.*

Light Nucleus \ Type of Star	Dominant type		Distribution among Others					
	2 α 1p	1 α 3p	Number of Prongs					
			0	1	2	3	4	5
Carbon (total 944)	25.0	5.9	16.3	13.9	23.3	14.1	1.2	0.3
Nitrogen (total 430)	3 α	2 α 2p						
	$\gtrsim 18.8$	14.2	13.7	14.7	20.0	$\lesssim 15.1$	1.4	2.1

state of ^8Be decays into two α -particles with half life of $< 5 \cdot 10^{-11}$ s⁽¹⁹⁾ while the well known level at 3.0 MeV has a half life of 10^{-21} s against disintegration into two α -particles.

The energy of excitation of the beryllium nucleus can be calculated from the energies of the two α -particles and the angle between their directions of emission. If φ is the space angle between the α -particles, E_1 and E_2 are their kinetic energies, then, from the laws of momentum and energy conservation, the excitation energy Q is given by

$$Q = \frac{E_1 + E_2}{2} - \sqrt{E_1 E_2} \cos \varphi.$$

For those pairs of α -particles that stop in the gas of the chamber, the energies of the α -particles are obtained from their measured ranges. The space angle between them is calculated from the measured projected angle and the dip angles of the two α -particles. Q has a significant value only when E_1 and E_2 refer to the particles of the reaction $\pi^- + ^{12}\text{C} \rightarrow (^8\text{Be})^* + 1\text{p} + 3\text{n}$; $(^8\text{Be})^* \rightarrow 2\alpha$ and is then equal to the excitation energy of the beryllium nucleus plus the energy released (0.096 MeV) when the ground state of beryllium nucleus disintegrates into two free α -particles. If any levels of excited beryllium nucleus are operative, a histogram of all Q -values would show peaks corresponding to the levels. A plot of such a histogram is given in Fig. 5. In plotting the frequency of events vs. the excitation energy, the energy interval selected is larger than the error involved in the calculated Q -values due to errors in the energy estimation of the α -particles. Only 20 percent of the stars are included in the plot. The paucity of the events and the non-resolution of the peaks renders difficult the identification of any particular level. Peaks are barely discernable at 0.1 MeV, 3 MeV, and 7 MeV, and these may correspond to

(19) F. AJZENBERG and T. LAURITSEN: *Rev. Mod. Phys.*, **27**, 77 (1955).

the known ^8Be levels at 0.1, 3.0, and 7.6 MeV ⁽¹⁹⁾. The fact that fewer than 20 percent of the stars are represented in this plot together with the detection bias in favor of ^8Be α -particles indicates that this indirect disintegration occurs in less than 20 percent of the $2\alpha 1p$ -events. This conclusion is strengthened by a study of the angular correlation between α -particles.

(c) Energy spectrum of α -particles. - Of the total of 369 three prong stars in carbon, 233 have been assigned to the reaction: $\pi^- + ^{12}\text{C} \rightarrow \rightarrow 2\alpha + 1p + 3n$. This corresponds to a total of 466 identified α -particles. Of these 329 stop in the gas and their energies have been measured from their ranges in the gas. The geometrical losses, as explained in Appendix II, account for an additional number of 95, thus giving a corrected number of α -particles of 424. In this way, we account for about 91 percent of the 466 identified α -particles.

We have compared our spectrum with the theory of CLARK and RUDELSDEN ⁽²⁰⁾ who calculated the disintegration of carbon into two α -particles and one singly charged particle by attributing an α -structure to the carbon nucleus. The incoming π^- meson is assumed to interact with a proton of one of the α -clusters in the initial state, and the transition to the final state is treated by the methods of first order perturbation theory. Gaussian wave functions are used for the α -clusters and plane waves for the emitted particles.

The α -spectrum thus obtained does not depend on the details of any specific mechanism of pion absorption in the disrupted α -particle. (For example, the inclusion of any meson-nucleon interaction or the participation of a correlated pair of nucleons in the absorption process would only affect the momenta of the nucleons constituting the disrupted α -particle.) The spectrum, on the other hand, depends on the partition of meson rest energy between the disrupted α -particle and the residual α -particles. The low average energy of

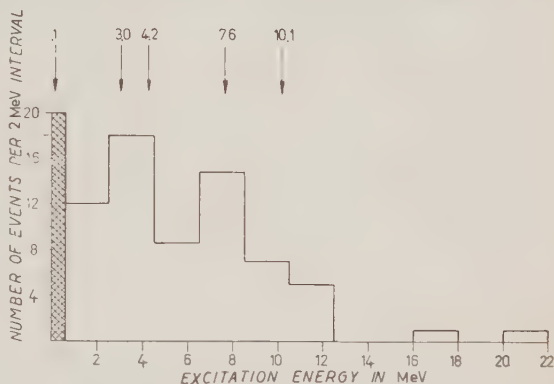


Fig. 5. - Distribution of excitation energy of ^8Be nucleus in the reaction: $\pi^- + ^{12}\text{C} \rightarrow (^8\text{Be})^* + p + 3n$; $(^8\text{Be})^* \rightarrow 2\alpha$. The arrows point to the known levels in ^8Be that decay into two α -particles.

⁽²⁰⁾ A. C. CLARK and S. N. RUDELSDEN: *Proc. Phys. Soc.*, A **64**, 1060 (1950).

the α -particles calculated from the fitted theoretical curve indicates that the residual α -particles receive a small fraction of the meson rest energy, the partitioning of which is expressed by a factor γ . γ is a function of the parameters in the initial Gaussian wave function assumed for the carbon nucleus and of the energy available in the reaction. The spectrum is obtained assuming a constant for the meson nucleon interaction and is called a « standard » energy spectrum. More specifically, the initial spatial wave-function is given by

$$\Psi = \psi_{\alpha}^1 \psi_{\alpha}^2 \psi_{\alpha}^3 \exp \left[-b \sum_i^3 R_{ij}^2 \right]$$

where R_{ij} is the distance between the centers of the i -th and j -th α -particles and B is a parameter which measures the extent of the distribution of α -clusters. The spatial part of ψ_{α}^i ($i = 1, 2, 3$) is of the form

$$\exp \left[-a \sum_i^3 r_{ij}^2 \right],$$

where r_{ij} is the inter-nucleon distance and a is a parameter measuring the extent of the α -cluster. Defining $c = 3b/16a$, we have

$$\gamma = \left(\frac{1}{c} \right) \left(\frac{ME}{4\hbar^2 a} \right),$$

where E is the energy available in the reaction. As c varies from 0 to 1, γ varies from ∞ to 0. The case $c = 1$ corresponds to no α -particle subdivision and the spatial part of the wavefunction reduces to

$$\exp \left[-\frac{a}{3} \sum_i^3 r_{ij}^2 \right].$$

On the other hand, $c = 0$ corresponds to three free α -particles. Our spectrum fits quite well with the theoretical curve for $\gamma = 12$, in agreement with previous results by MENON *et al.* We may use this value of γ to obtain a crude estimate of the extent of the α -particle cluster inside of the carbon nucleus. HOFSTADTER^(21,22) has determined the r.m.s. radius of carbon and helium by electron scattering experiments. He obtains $R_c = (2.40 \pm .25) \cdot 10^{-13}$ cm, $R_{He} = (1.40 \pm .2) \cdot 10^{-13}$ cm. R_c determines a relation between the parameters a and b in the Clark and Ruddelsden wave functions:

$$R^2 = \frac{3}{4} \cdot \frac{2 + 9c}{48ca}.$$

(21) J. H. FREGEAN and R. HOFSTADTER: *Phys. Rev.*, **99**, 1503 (1955).

(22) R. HOFSTADTER, R. McALLISTER and E. WIENER: *Phys. Rev.*, **96**, 854A (1954).

Eliminating c , we obtain for the α -cluster extent parameter $a^{-\frac{1}{2}} = 5.4 \cdot 10^{-13}$ cm. This is to be compared with $R_{He} = 1.4 \cdot 10^{-13}$ cm. This implies that the α -clusters in light nuclei are more loosely bound structures than free α -particles. It is recognized that the above argument is weakened by the approximations in the choice of wave functions and in the calculation of transition probabilities. One also assumes that the charge distribution and the «proton» distribution ($\pi^- + p \rightarrow n$) are identical.

The case $\gamma = 0$ corresponds to no special tendency to group into α -particle clusters. This case is called a «statistical spectrum». Our spectrum is in disagreement with such a statistical spectrum. (See Fig. 6.)

The standard spectrum is obtained on the assumption that the α -particles are emitted directly. To estimate the effect of the formation of excited beryllium nucleus on the energy spectrum of the α -particles, CLARK and RUDELSDEN calculated the α -particle energy spectrum for a specific choice of the wave-function of the intermediate state of beryllium nucleus excited to 3.0 MeV. Our experimental results are compared with the theoretical curves for various values of γ . The agreement is poor compared to that obtained in the case of direct disintegration as discussed above and this was examined by a χ^2 -test with the two α -particle energy spectra. We estimate from this that the contribution from the indirect disintegration is less than 20 percent.

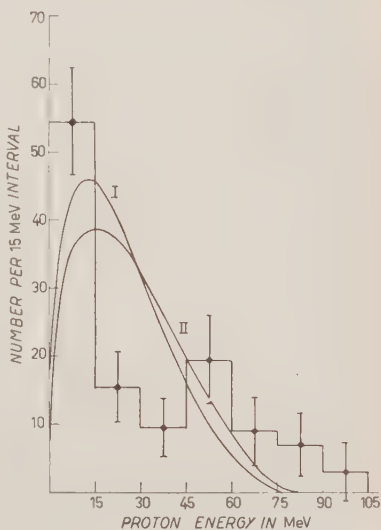


Fig. 6.—Experimental histogram of the energy spectrum of α -particles in the reaction: $\pi^- + {}^{12}\text{C} \rightarrow 2\alpha + 1p + 3n$. Curve I is the standard spectrum and Curve II is the statistical spectrum of the energy of the α -particles calculated by CLARK and RUDELSDEN. The errors attached to the experimental points are statistical but corrected for the geometrical inefficiency.

(d) Angular correlation of α -particles in the reaction $\pi^- + {}^{12}\text{C} \rightarrow 2\alpha + 1p + 3n$. — The projected angular distribution of α -particles to be expected from the direct and indirect (i.e. via beryllium) disintegration is compared with experiment. The theoretical space angle distributions are folded into a projected angular distribution by means of an efficiency factor

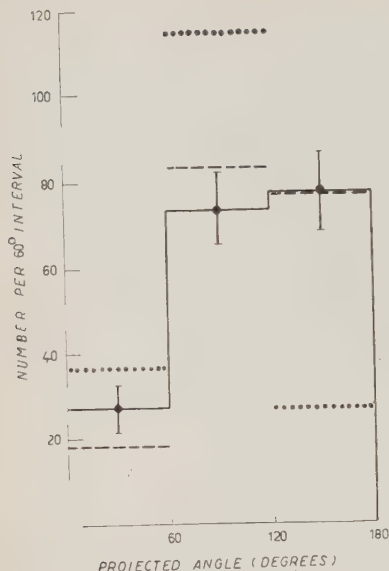


Fig. 7. — Angular correlation of α -particles in the reaction: $\pi^- + {}^{12}\text{C} \rightarrow 2\alpha + 1p + 3n$

ions. — A total of 430 stars is analyzed in nitrogen. In the case of three and four prong stars, the following reactions have been identified:



19 percent of the stars are classified as following (3) while 14 percent follow the reaction (4). The results are given in Table III.

(b) Energy spectrum of α -particles. — Out of a total of 146 three prong stars, 81 have been definitely assigned to the reaction (a). 179 out

Fig. 8. — Experimental histogram of the energy spectrum of the α -particles in the reaction: $\pi^- + {}^{14}\text{N} \rightarrow 3\alpha + 2n$. The errors attached to the experimental points are statistical but corrected for the geometrical inefficiency. No events are observed in the energy $15 \div 20$ MeV but the error is computed for two events.

given by

$$E(\theta) = \int_{\varphi_1}^{\varphi_2} \sin^{-1}(\text{tg } \varphi / \text{tg } \theta) d\varphi,$$

where φ is the projected angle and θ is the space angle.

The solid histogram (Fig. 7), representing the experimental results, agrees quite well with the theoretical distribution (dashed lines) to be expected from the direct disintegration of the α -particles, while it is in very poor agreement with the assumption of an indirect disintegration (dotted lines). This confirms the previous conclusion that the indirect disintegration contributes less than 20 percent to the $2\alpha 1p$ -reaction.

3.2.3. Nitrogen Reactions.

(a) Classification of react-

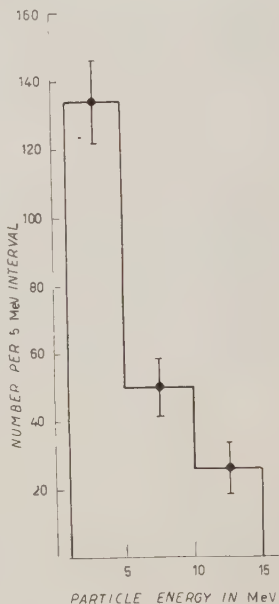


TABLE III. - *Fast Proton Data on Carbon.*

1. Number of prongs per star	0	1	2	3	4	5
2. Number of stars observed. Total 944. .	154	131	220	369	67	3
3. Proportion of stars showing recoil	0.36	0.14	0.04	—	—	—
4. α/p ratio	—	$.42 \pm .08$	$.38 \pm .04$	$1.55 \pm .08$	$.33 \pm .05$	—
5. Proportion of protons whose energy is estimated by range or by radius of curvature (a)	—	0.73	0.38	0.27	0.48	—
Id. id. including probable case with $E_p > 30$ MeV (b) . .	—	0.80	0.46	0.30	0.51	—
6. Average number of fast protons ($E_p > 30$ MeV) per meson star (a) .	—	$.05 \pm .02$	$.08 \pm .02$	$0.12 \pm .02$	$.09 \pm .04$	—
Id. id. including probable cases with $E_p > 30$ MeV (b) . .	—	$0.1 \pm .03$	$.13 \pm .03$	$0.19 \pm .03$	$.17 \pm .07$	—
7. Average number of fast protons ($E > 30$ MeV) per meson star, including all types of stars (a)						$0.08 \pm .01$
Id. id. including probable cases with ($E_p > 30$ MeV) (b)						$0.13 \pm .01$
8. Proportion of protons whose energy is estimated either by range or by radius of curvature (b)36
Id. id. including probable cases with ($E_p > 30$ MeV) (b)						.40

of a total of 243 identified α -particles stop in the gas and hence their energies could be estimated from the ranges. Fig. 8 gives the α -particle energy spectrum corrected for the geometry as explained in Appendix II. One striking feature about the spectrum is the preponderance of α -particles with energy less than 10 MeV. This low energy peak persists in spite of uncertainties introduced by the large geometric corrections. Such low energy α -particles indicate that most of the rest energy of the meson escapes in the form of high energy neutrons.

In 21 of the stars all three α -particles stopped in the gas of the chamber and so their energies could be estimated from their ranges. Assuming an average energy per bond of 2.4 MeV of the α -particles in the ^{12}C nucleus, the average excitation energy of the ^{12}C nucleus is found to be 21.3 MeV. It is known that from experiments ⁽²³⁾ on the disintegration of ^{12}C by 29 MeV protons the 3α -particle disintegration is the most frequent reaction observed. It is, therefore, possible that the reaction (3) might sometimes proceed by the indirect disintegration of ^{14}N via a residual excited ^{12}C .

The comparison of the α -spectrum of nitrogen with that of carbon is qualitatively significant. Similar results were obtained in the emulsion work of MEXON *et al.* The predominance of low energy α 's in N has been explained by the deuteron absorption model, most of the rest energy of the pion going to the loosely bound «deuteron» in ^{14}N , the residual ^{12}C fragment subsequently decaying into three low energy α -particles. An unpublished calculation of the «standard» spectrum in ^{14}N by CLARK and RUDDLESDEN gives a spectrum with contributions up to over 50 MeV.

3.2.4. Fast Protons Emitted in the π^- Disintegrations of Carbon and Nitrogen. — One of the clues to the mechanism of the π^- meson absorption in carbon and nitrogen can be obtained from a study of the protons of energy $E > 30$ MeV emitted in the disintegrations. Since the evaporation spectrum predicts essentially no protons of energy greater than 30 MeV for the nuclear excitation considered here, the emission of such energetic protons must be the result of a direct interaction between the meson and the absorbing nucleons which effectively take up the entire rest energy of the incident meson. Table III shows the results obtained on the fast protons emitted in carbon disintegrations. Row 5(b) includes all the measured protons plus those that have projected length $l > 3.5$ cm and whose deviation from straight path is less than 0.1 mm. The latter protons have an energy $E > 30$ MeV for the magnetic field employed and all exhibit relatively low ionization density. Row 6 gives the average number of fast protons per meson star and all the quoted errors are statistical. Row 7 shows the proportion of measured protons including all the stars. Row 8(a) gives the average number of fast protons per meson star considering all the meson stars. Row 8(b) includes the probable cases as explained above, plus all the measured protons. Our results indicate that about 10 percent of the absorptions in carbon lead to fast protons of energy $E > 30$ MeV. Table IV gives the results for the fast protons in the case of nitrogen.

TAMOR ⁽²⁴⁾ has made rough estimates of the percentage of fast protons of

⁽²³⁾ J. L. NEED: *Phys. Rev.*, **99**, 1356 (1955).

⁽²⁴⁾ S. TAMOR: *Phys. Rev.*, **77**, 412 (1950).

TABLE IV. - *Fast Proton Data on Nitrogen.*

1. Number of prongs per star	0	1	2	3	4	9
2. Number of stars observed, total 430 . .	59	63	63	146	67	9
3. Proportion of stars showing recoil	0.46	0.20	0.05	—	—	—
4. α/p ratio	—	$.47 \pm .13$	$.58 \pm .10$	7.43 ± 1.23	$1.0 \pm .09$	—
5. Proportion of protons whose energy is estimated either by range or by radius of curvature (a)	—	.72	.55	—	.23	—
Id. id. including probable cases with ($E_p > 30$ MeV) (b) . . .	—	.74	.57	—	.25	—
6. Average number of fast protons ($E_p > 30$ MeV) per meson star (a)	—	$.12 \pm .05$	$.02 \pm .02$	—	$.07 \pm .04$	—
Id. id. including probable cases with ($E_p > 30$ MeV) (b) . . .	—	$.16 \pm .08$	$.05 \pm .03$	—	$.11 \pm .05$	—
7. Average number of fast protons ($E_p > 30$ MeV) per meson star, including all types of stars (a)					$0.02 \pm .01$	
Id. id. including probable cases with $E_p > 30$ MeV (b) . . .					$0.04 \pm .02$	
8. Proportion of protons whose energy is estimated by range or radius of curvature (a)					0.43	
Id. id. including probable cases with $E_p > 30$ MeV (b) . . .					0.46	

energy greater than 30 MeV on the basis of two models. In one, the pion is absorbed primarily by two nucleons and the disintegration is a consequence of the subsequent collision of these nuclei. By a Monte Carlo type of calculation Tanor finds, in nitrogen, that 39 percent of the disintegrations lead to protons of energy greater than 30 MeV. In the second model the absorption leads to a fast neutron and a tritium recoil nucleus (multinucleon model).

The fast protons in this case arise mainly as a result of charge exchange component of the n-p scattering. Our results would seem to be in accord with the second model. However, the high percentage of fast protons calculated on the basis of the two nucleon model may be due to the neglect of the specific states involved in the absorption matrix element which favors absorption of the pion by an n-p pair as compared to that by a p-p pair. This would have the effect of a large reduction in the estimated number of fast protons. This point will be discussed more fully in Sect. 4.

3'2.5. Angular Distribution of Star Particles: Anisotropy of Disintegration. — For many of the stars where detailed identification is not possible, a technique is employed to display any possible correlation effects. When a π^- meson is absorbed by a nucleus such as carbon or nitrogen, the angular distribution of the emitted particles would very much depend on whether the energy distribution takes place in a random fashion or a special mechanism exists for the disintegration. In the former case, the particles would be evaporated from an excited compound nucleus while in the latter case, correlations exist between different emitted particles probably because of the occurrence of intermediate states.

Following a method employed by HODGSON⁽²⁵⁾, we proceed to examine the angular distribution of star particles in the following way. The method consists in measuring the least projected angle ζ between any two tracks in the plane normal to the axis of the cameras. If the particles are randomly emitted from a nucleus, the theoretical distribution of these angles, for an n-prong star, is given by

$$P(\zeta) d\zeta = n(n-1)/2\pi (1 - n\zeta/2\pi)^{n-2} d\zeta \quad \zeta < 2\pi/n$$

$$= 0 \quad \zeta > 2\pi/n$$

For a star of a given number of prongs, the least projected angle is measured and the distribution of these angles is compared with the above theoretical distribution. A marked difference between the two indicates anisotropy.

In the case of three prong stars in carbon, the least projected angle is first measured, considering all the tracks. The distribution so obtained is compared with the theoretical distribution and is shown in Fig. 9. The agreement between the two distributions is examined by the χ^2 -test. In applying the χ^2 -test^(26,27) the theoretical distribution is normalized in such a way that it

⁽²⁵⁾ P. E. HODGSON: *Phil. Mag.*, **43**, 190 (1952).

⁽²⁶⁾ A. G. WOTHING and J. GEFFNER: *Treatment of Experimental Data* (New York, 1943).

⁽²⁷⁾ *Biometrika Tables for Statisticians*, Volume I, Edited by E. S. PEARSON and H. O. HARTLEY.

contains the same number of events as the experimental distribution. This imposes one restrictive condition. To test whether there is any difference between the emission of α -particles and protons, the distribution of the least projected angles between the α -tracks is again checked.

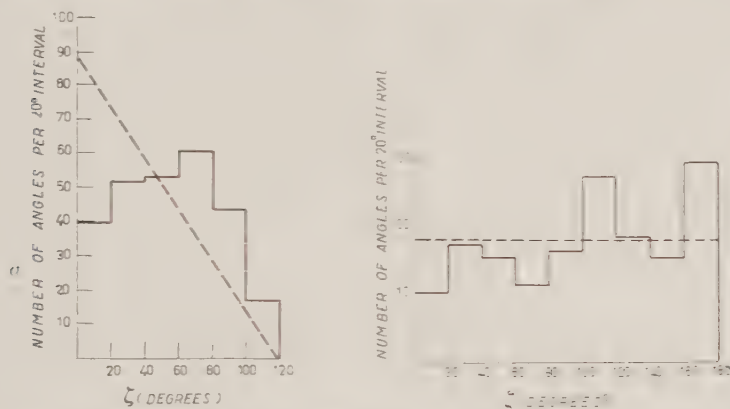


Fig. 9. - Least projected angular distribution in the case of *a* three and *b* two prong stars in carbon. The solid histogram represents the experimental distribution. The dashed line gives the distribution on the basis of simple evaporation of emitted particles.

Similarly, in the case of four prong stars of the $1\alpha 3p$ type the least projected angle is measured for all of the tracks and also for the proton tracks alone. For the two prong stars, only one set of least projected angles is possible. The results on χ^2 -probabilities are given in Table V. A probability less than 0.1 indicates a significant deviation from the assumed distribution. The anisotropy of emission is obvious from the low values for the χ^2 -probabilities.

The procedure is repeated for the stars in nitrogen and the results are included in Table V.

We conclude that there is a marked anisotropy in the distribution of emitted particles from the π^- meson absorption in carbon and nitrogen. Similar investigations⁽²⁷⁾ involving π^- stars in cosmic rays show that the emitted particles from stars without recoils (attributed to light elements) show a marked anisotropy in their angular distribution. Stars in heavy nuclei (Al, Br) on the other hand show no significant deviation from isotropy.

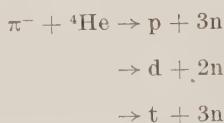
Since the negative pion is captured essentially at rest, the momentum in the center of mass system is zero and the emitted particles would be expected to show an isotropic angular distribution were the evaporation process responsible for the disintegration. The observed anisotropy in the angular distribution of the emitted particles would thus definitely exclude a simple evaporation model for the nuclear disintegrations observed in carbon and nitrogen.

TABLE V. - χ^2 -Probability Distributions in Carbon and Nitrogen.

Number of prongs	All tracks	α -tracks only	Protons only
(a) Carbon			
2	.015	—	—
2	> .00001	.003	—
4	.02	—	.32
(b) Nitrogen			
2	—	—	—
3	.0009	.0009	—
4	.009	—	—

A moderately excited nucleus, the residue of a two nucleon absorption process, would show correlation effects for specific modes of disintegration. As an extreme example, the indirect disintegration of ^{12}C would have strongly correlated α 's from ^8Be decay.

3'3. *Disintegration of ^4He .* - The capture of a slow negative pion by helium leads to the following reactions:



where p, d, t, and n stand for a proton, deuteron, triton, and neutron respectively. For reasons already discussed in Sect. 3'2.1 it was not feasible to separate the various isotopes of hydrogen on criteria based on ionization in identifying the one prong stars that occur in helium. All the prongs are classified as «protons». Where curvature measurement is possible, the average error in the determination of momentum amounts to about ± 10 percent. In Fig. 10 is shown a histogram giving the corrected energy distribution of the protons. The plot includes 80 measured events. The energy of 40 of these protons is estimated from the curvature while in 20 of the cases, the energy is determined from the range of the protons that stop in the gas of the chamber. This distribution is corrected for the inefficiency due to finite sensitive region as explained in Appendix II. Fig. 10 includes 20 events (identified as protons)

observed by LEAVITT⁽²⁸⁾ in an earlier investigation of π^- absorption in a high pressure helium filled cloud chamber. These events have been corrected for the geometry of the sensitive region in a manner similar to ours.

The experimental results are compared (Fig. 10) with the theory of Clark and Ruddelsden who calculate the energy spectra of protons emitted from ${}^4\text{He}$ as a result of π^- meson capture for (1) a meson-nucleon interaction $\sigma \cdot \nabla \psi(r_i)$ where $\psi(r_i)$ is the meson wave function (pseudoscalar) at the position of the i -th nucleon and σ is the nucleon spin operator, and (2) statistical phase space distribution of energy among the four nucleons. Neither theory agrees with the experimental results.

Although it is difficult in the present experiment to differentiate between the hydrogen isotopes, we can get an estimate of the probable number of tritons from the observed proton spectrum in the following way. If a triton is formed, it must have an energy of 30 MeV and therefore a momentum corresponding to a proton of 90 MeV kinetic energy. A 30 MeV triton has an ionization of about nine times that of a 90 MeV proton. There are two one prong events in which the energy of the particles, identified as protons, are 86 MeV and 101 MeV, one of which (energy 101 MeV) has an ionization a little heavy for a proton of that energy. This could possibly represent a triton. None of the unmeasurable fast prongs are compatible with this ionization. Thus the number of triton recoils may be of the order of or less than 1 in 60. It is interesting to compare our results with the frequency of triton

emission calculated by PETSCHKE⁽¹⁶⁾ and CLARK and RUDELSDEN⁽²⁰⁾. PETSCHKE finds that 22 percent of the absorptions of the π^- meson from mesic K -shell in helium lead to triton emission. The high frequency of triton emission, in disagreement with our results, has been attributed by PETSCHKE to the presence of high frequency Fourier components in the initial state of his helium

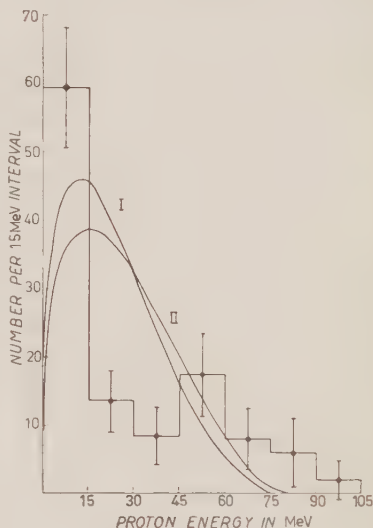


Fig. 10. — Energy spectrum of protons in the reaction: $\pi^- + {}^4\text{He} \rightarrow \text{p} + 3\text{n}$. The solid histogram represents the experimental distribution. Curve I is the proton energy distribution for interaction $\vec{\sigma} \cdot \vec{\nabla} \psi$ and Curve II gives the statistical spectrum, as calculated by CLARK and RUDELSDEN. The errors attached to the experimental points are statistical but corrected for the geometrical inefficiency.

(28) C. P. LEAVITT: *Thesis M.I.T.* (1951).

wavefunction. CLARK and RUDELSDEN using less carefully chosen Gaussian wave-function with a much lower average kinetic energy find that the probability of triton emission is about three percent ⁽²⁹⁾ which is (probably fortuitously) within range of our experimental value. Here again, the two nucleon model will give qualitative agreement with the data, since the « sticking factor » for the recoiling fast neutron will be small.

4. — Discussion of Results.

The absorption of slow negative pions in light elements such as helium, carbon, and nitrogen was investigated with a view to obtain information regarding the mechanism of disintegration of these nuclei.

In Sect. 3'3 we have shown that in the disintegration of helium by slow π^- meson, the triton emission is very small and that practically all the one prong stars are either protons or deuterons. Assuming that all the tracks are protons, we have compared the energy spectrum of protons with the spectrum obtained on the basis of (a) statistical phase space distribution of energy among the four nucleons and (b) non-relativistic expression of a meson nucleon interaction. The agreement of the experimental results with either theory is very poor.

The proton spectrum fits qualitatively with the « quasi-deuteron » model for high energy nuclear processes first employed in meson reactions by PERKINS ⁽³⁰⁾ and later elaborated in detail by BRUECKNER, SERBER and WATSON ⁽¹²⁾. A recent survey and interpretation of the experiments bearing on the correlation effects in nuclear wave functions has been given by BRUECKNER, EDEN and FRANCIS ⁽¹³⁾. According to the quasi-deuteron model we suppose that the π^- meson is initially absorbed by a pair of nucleons. For the absorption of the pion in helium, the wave function of the helium nucleus can be decomposed into a correlated pair factor either N-P or P-P and a residual factor. The absorption by an N-P pair gives rise to two fast neutrons.

To satisfy the laws of conservation of energy and momentum these two neutrons will emerge in opposite directions each with about half the available energy, i.e. 55 MeV. Since the helium nucleus is a strongly bound system, the primary absorption process would affect the remaining nucleons such that, in the case of absorption by an N-P pair, we expect to observe protons (deuterons also) of low energy characteristic of nuclear motions. On the other hand, the absorption by a P-P pair gives rise to a high energy proton which, for a stationary quasi-deuteron, would be 55 MeV. The relative probability of these

⁽²⁹⁾ S. N. RUDELSDEN: Private communication.

⁽³⁰⁾ D. H. PERKINS: *Phil. Mag.*, **40**, 601 (1949).

two processes is governed by statistical weight factors and by the relative magnitudes of the matrix elements for absorption by the nucleons involved. Although subsequent nuclear collisions and higher order correlations will introduce smearing effects, the presence of both the processes is suggested by the «proton» spectrum of Fig. 10 where we find a definite peak for proton energy less than 15 MeV (due to N-P pairs) and the suggestion of a peak for proton energy between 45 and 60 MeV (due to P-P pairs.)

For S -state nucleons, statistical weight factors due to spin and parity favor the N-P pairs by 3:1 if we assume that this goes principally from the 3S state of the two nucleons. (For capture in deuterium this is indeed the case). In addition, information on the matrix elements may be obtained from the inverse reaction: production of S wave mesons near threshold in N-P and P-P collisions. The most probable absorption mechanisms correspond to the following production processes:

(a) The absorption of the meson by an N-P pair, i.e. $\pi^- + N + P \rightarrow N + N$, corresponds to the inverse of the meson production in P-P collisions, i.e. $P + P \rightarrow N + P + \pi^+$, assuming charge symmetry in the production reaction. Considering the latter reaction, for the final nucleons in a 3S_1 state and therefore isotopic spin 0 and the meson being emitted in an S -state, the cross-section (near threshold) is given by $^{(31)} \sigma_{10} \sim 0.14 \eta$ where η is the maximum pion momentum in the center of mass system in units of $m_\pi c$. The contribution to the cross-section comes from the state $T=0$ for the final nucleons, with initial protons having $T=1$. We neglect the small $^{(31)} ^1S_0$ contribution.

(b) The absorption of the meson by a P-P pair corresponds to the inverse of the production reaction: $N + P \rightarrow P + P + \pi^-$. Considering the latter reaction for the 1S_0 state of the final protons and S state of the emitted meson, the initial state of the two nucleons must be a 3P_0 state and $T=1$. (For $T=0$ of initial nucleons the meson emission in S states is forbidden.) The cross-section near the threshold is given by $^{(31)} \sigma_{11} \sim .02 \eta^2$. Since $\sigma_{10} \gg \sigma_{11}$, we expect a large matrix element favoring N-P absorption from considerations of detailed balance. A similar conclusion was reached previously by PUPPI (?) in connection with the pion absorption in heavy nuclei. Thus, the proton spectrum in helium has a bearing on the relative strength of S wave meson production in nucleon-nucleon collisions where the isotopic spin I of the two nucleons undergoes, under the assumption of charge independence, the changes defined by $I = 1 \rightarrow I = 0$ and $I = 1 \rightarrow I = 1$. Both meson production and meson absorption experiments show that the transition $I = 1 \rightarrow I = 0$ predominates over the transition $I = 1 \rightarrow I = 1$. The explanation may reside in the increased enhancement brought about by the 3S_1 initial state over the

$^{(31)}$ A. H. ROSENFELD: *Phys. Rev.*, **96**, 139 (1954).

1S_0 initial state of the correlated pairs inside the nucleus. This may be influenced by the presence of the meson in the case of absorption. The contributions of 3S_1 state in the nitrogen ground state wave function may also account for the predominance of the 3α -reaction with small excitation.

In carbon, twenty-five percent of the π^- disintegrations follow the reaction

$\pi^- + ^{12}\text{C} \rightarrow 2\alpha + 1p + 3n$. Suppose that the carbon nucleus is composed of three α -clusters and that the π^- meson interacts with one of the α -clusters in a way similar to that found in the case of a helium nucleus. Then the proton spectrum in both cases should be similar. In Fig. 11 we have superimposed the proton spectrum obtained in helium on the proton spectrum obtained in the $2\alpha 1p$ -reaction in carbon, the spectra being normalized to include equal number of events. The low energy end of the spectra is the same in both cases to within statistical limits while for proton energy greater than 15 MeV no noticeable peak, such as is seen in the case of helium, is found. This disagreement is not significant because carbon is a bigger nucleus than helium, and the fast nucleons in the primary stage lose more energy in leaving the nucleus than in the case of helium. This would tend to wash out any peaks in the high energy part of the proton spectrum. The similarity of the proton spectrum in helium and carbon suggests

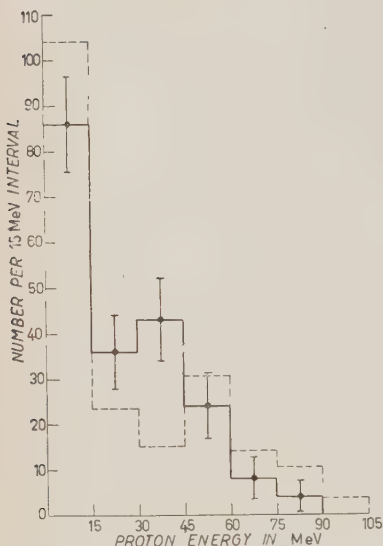


Fig. 11. — Comparison of energy spectra of protons in helium (dashed lines) and in carbon (solid lines). The errors attached to the solid histogram are statistical but corrected for the geometrical inefficiency.

that the primary stage in the absorption in carbon is the same as in the case of helium, namely absorption by a pair of nucleons in one of the α -clusters. In the subsequent disintegration, the α -particles receive a small fraction of the available energy. This is supported by the low observed average energy of the α -particles of about 7.5 MeV.

5. — Conclusions.

In carbon and nitrogen, the data point to a primary mechanism which is consistent with the absorption of the pion through a correlated pair of nucleons, more usually n - p pairs, leaving relative small excitation to the re-

mainder of the nucleus which shows strong preference to the break up into low energy α -particles. This is particularly seen in three prong stars, thus adding to the evidence for an α -particle structure to these nuclei. This is similar to what happens in mild photo nuclear ³²) as well as proton (²³) and neutron (³³) induced reactions in light nuclei. Additional support for the primary absorption process comes from the angular anisotropy of the emitted particles, from the generally low energy of α -particles emitted, especially in ¹⁴N, from the proton spectrum in ¹²C (2 α , 1p) and in ⁴He, and from the low probability of triton emission in ⁴He. Subsequent nuclear collisions of the nucleons involved in the primary stage will produce new nuclear reactions. The fraction of the time that this is expected to happen may be estimated (³⁴) and is of the order of 0.7 in the case of carbon. Thus, it is not surprising that a wide variety of star types are actually observed.

* * *

It is a pleasure to thank Messrs. M. C. RINEHART, K. C. ROGERS, and D. KOPPEL who have participated in the operation of the diffusion cloud chamber during cyclotron runs.

APPENDIX I

Technique of Measurements.

The methods of measurement are similar to those described in the previous investigations (¹⁴) from this laboratory. For those α -particles and protons which stop in the gas of the chamber, the energy is determined from range vs. energy curves drawn for the appropriate temperature and pressure of the gas employed. Use is made of the tables (³⁵) of range vs. energy calculated for paraffin in constructing similar curves for ethylene. For nitrogen, the ranges in air are employed, the error involved being small for our purposes. In the case of protons which do not stop in the gas but which exhibit an appreciable curvature, the energy is determined from the measured radius of curvature. The radii are measured by matching suitable arcs of circles of different radii drawn on thin lucite sheets.

The projected range of particles could be measured accurately to within a millimeter. The true ranges are then found from the dip angle of the tracks. The corrections due to magnification and reprojection are estimated to amount to ± 10 percent.

(³²) M. EDEN and V. L. TELEGI: *Helv. Phys. Acta*, **25**, 55 (1952).

(³³) G. M. FRYE, Jr., L. ROSEN and L. STEWART: *Phys. Rev.*, **99**, 1375 (1955).

(³⁴) S. FERNBACH, B. SERBER and T. TAYLOR: *Phys. Rev.*, **75**, 1352 (1949).

(³⁵) J. O. HIRSCHFELDER and MAGGE: *Phys. Rev.*, **73**, 207 (1948).

APPENDIX II

Geometrical Corrections.

The depth d , of the sensitive region in the present experiment is 5.0 cm and this introduces a bias in the energy spectrum of the emitted particles. To correct for this, we calculated the probability for the loss to observation of a charged particle (α -particle or proton) of a given length l , assuming that the particles are emitted isotropically at any given point in the sensitive region. If P is the probability for loss, we find the following expressions:

$$\begin{aligned} P &= 1 - d/2l & l > d, \\ &= l/2d. & l < d. \end{aligned}$$

To correct for the observed spectrum of α -particles or protons, the frequency of the events for each energy interval is divided by $1 - P$ depending on the length of the track. In applying the correction to the spectrum of the α -particles or protons that stop in the gas, the range of the track corresponding to the mid point of the energy grouping is taken. For the proton spectrum in the case of helium and carbon where the energy of the proton is estimated from its curvatures in the magnetic field, a minimum length of proton track for each energy interval in question is calculated for an average value of the field and a sagitta of 0.03 cm. The correction is computed using this minimum length.

The above correction factor takes into account only the loss of particles from the top and bottom of the sensitive region. To account for the loss from the sides of the chamber, the diametral plane of the sensitive region is divided up into zones and the geometrical efficiency factor for loss of particles in each zone is computed as above assuming the sides of the chamber to be approximated by an infinite plane. The effective efficiency factor is computed by weighting the efficiency factor for each zone by the area of the zone relative to that of the whole plane.

RIASSUNTO (*)

Si è studiato l'assorbimento dei pioni negativi lenti nei nuclei leggeri, elio, carbonio e azoto. Le reazioni dominanti osservate nei singoli casi sono state: (1) $\pi^- + {}^4\text{He} \rightarrow p + 3n$; (2) $\pi^- + {}^{12}\text{C} \rightarrow 2\alpha + 1p + 3n$; (3) $\pi^- + {}^{14}\text{N} \rightarrow 3\alpha + 2n$. Si sono prodotti e confrontati con la teoria di Clark e Ruddelsden le distribuzioni dei rami e gli spettri protonici e alfa. La frequenza di emissione α dà un forte appoggio qualitativo al modello a particelle α della struttura nucleare. Una prova a favore di tale modello è data dalla similarità degli spettri protonici nelle reazioni (1) e (2). La bassa energia media dei protoni in (1) e (2) e delle particelle α in (3) è a favore del modello di rinculo a due nucleoni nell'assorbimento primario. Nel caso (np), stati iniziali 3S_1 risultano favoriti rispetto a stati (pp) 1S_0 , d'accordo con la reazione inversa — la produzione di mesoni nelle collisione nucleone-nucleone.

(*) Traduzione a cura della Redazione.

Orbital Electron Capture in ^{179}Ta .

A. BISI, L. ZAPPA and E. ZIMMER (*)

Istituto di Fisica Sperimentale del Politecnico - Milano

(*) *Laboratori CISE - Milano*

(ricevuto l'11 Maggio 1956)

Summary. — The electron capture decay of ^{179}Ta has been investigated. No γ -rays were observed. The P_L/P_K capture ratio was measured and found to be $P_L/P_K = 1.4 \pm 0.4$. The corresponding transition energy is $E_0 = 94_{-4}^{+9}$ keV. By means of a coincidence method the L -fluorescence yield for transition to the L level following the K -capture was measured and found to be $\omega_{LK} = 0.17 \pm 0.02$.

1. — Introduction.

^{179}Ta was produced by WILKINSON ⁽¹⁾ on bombarding lutecium with α -particles, and hafnium and tantalum with protons. The decay ($T_{1/2} = 600$ d) was reported to occur through orbital electron capture. Weak γ -rays of 0.7 MeV energy and 0.1 MeV conversion electrons were observed by means of absorption methods.

Low-lying levels of ^{179}Hf are known to have energies of 0.215 and 0.375 MeV from the decay of ^{179m}Hf ⁽²⁾. Recently the Coulomb excitation of hafnium by 6 MeV α -particles ⁽³⁾ showed the existence of two levels at 0.119 and 0.260 MeV energy in ^{179}Hf .

In view of the lack of agreement between the above results, a detailed investigation of the radiations from ^{179}Ta and a determination of the atomic mass difference between ^{179}Ta and ^{179}Hf , seemed to us to be useful.

(1) G. WILKINSON: *Phys. Rev.*, **80**, 495 (1950).

(2) J. M. HOLLANDER, I. PERLMAN and G. T. SEABORG: *Rev. Mod. Phys.*, **25**, 469 (1953).

(3) N. P. HEYDENBURG and G. M. TEMMER: *Phys. Rev.*, **100**, 150 (1955).

2. - Measuring Techniques.

^{179}Ta was obtained by bombarding HfO_2 with 26 MeV deuterons in the Amsterdam cyclotron.

The bombarded hafnium oxide was fused with sodium pyrosulfate and some tantalum carrier (potassium tantalate) in a platinum crucible, until a complete fusion was obtained. The fusion product was then leached with water and filtered, and the insoluble residue (mainly hydrated tantalum pentoxide) was well washed and dissolved in a dilute solution of potassium hydroxide. The alkaline solution was centrifugated and the clear portion acidified. The precipitate of hydrated tantalum pentoxide was washed with water by decantation and centrifugation, until essentially free of extraneous soluble salts. The aqueous suspension was finally dried.

A γ -ray scintillation spectrometer and a proportional counter spectrometer were employed in investigating the radiations from ^{179}Ta . The pulse size was measured by means of a twenty channel electronic pulse analyzer ⁽⁴⁾. γ - γ and X- γ coincidence technique was used both between the proportional counter and the scintillation spectrometer ⁽⁵⁾ and between two scintillation spectrometers. The coincidence circuit was triggered only by the pulses belonging to a selected photopeak, by means of a single channel pulse height selector.

3. - Radiations from the Sample.

An inspection of the γ -radiations from the sample in the γ scintillation spectrometer showed the presence of a very intense peak at about 55 keV and a very faint peak at 740 keV. No other γ -rays were detected; in particular the 119 keV γ -ray arising from the de-excitation of the first rotational level of ^{179}Hf , if present, would have an intensity under $2 \cdot 10^{-4}$ times that of the 55 keV peak.

A careful measurement of the 55 keV peak energy was carried out in the proportional counter after calibrating the apparatus by means of the K_α X-radiations characteristic of Ag (22.10 keV), Eu (41.31 keV), Ta (57.11 keV) and Pt (66.25 keV). The previous values for K_α X-rays energy are the weighed means of the K_{α_1} and K_{α_2} energies according to the table given by FINE and HENDEE ⁽⁶⁾. In this way we have obtained the value $E = 55.4 \pm 0.2$ keV

⁽⁴⁾ E. GATTI: *Nuovo Cimento*, **11**, 153 (1954).

⁽⁵⁾ A. BISI, E. GERMAGNOLI and L. ZAPPA: to be published.

⁽⁶⁾ S. FINE and C. F. HENDE: *Nucleonics*, **13**, n. 3, 36 (1955).

which corresponds to the energy of the K_{α} X-radiation characteristic of Hf (55.36 keV).

At lower energies two peaks were observed, at 9.4 and 16.4 KeV respectively, the first of which was interpreted as due to the L X-radiations characteristic of Hf. No evidence of the second peak and, likewise, none of the 740 keV peak was found one year afterwards. Thus we believe that traces of niobium (²) were present in the samples as impurities.

The half-life of the K and L X-rays of Hf was not measured but the time decrease of their intensity observed through one year was consistent with a half-life of about 600 d as reported by WILKINSON (¹).

4. — Results.

4.1. L/K -capture ratio. — As no γ -rays arise from the decay of ^{179}Ta , the emission of the X-rays characteristic of Hf is only due to the electron capture decay. Therefore the relative intensities (I_L/I_K) of the L X- and K X-radiation are related to the relative amounts of L - (P_L) and K -capture (P_K) by the expression:

$$(1) \quad \frac{I_L}{I_K} = \left(\frac{P_L}{P_K} + n_{KL} \right) \frac{\bar{\omega}_L}{\omega_K},$$

where n_{KL} is the number of L -shell vacancies produced in the filling of a K -shell vacancy;

$\bar{\omega}_L$, a mean L -fluorescence yield which depends, evidently, on the excitation probabilities of the three L -subshells. Strictly speaking eq. (1) is a definition of $\bar{\omega}_L$ (⁷);

ω_K , the K -fluorescence yield of Hf.

In eq. (1) for n_{KL} and $\bar{\omega}_L$ we adopt the approximate values derived from plots given by ROBINSON and FINK (⁷)

$$n_{KL} = 0.81$$

$$\bar{\omega}_L = 0.20$$

and for ω_K the value $\omega_K = 0.94$ (⁸).

The ratio I_L/I_K was obtained from the spectra taken in the scintillation

(⁷) B. L. ROBINSON and R. W. FINK: *Rev. Mod. Phys.*, **27**, 424 (1955).

(⁸) I. BERGSTRÖM in K. SIEGBAHN: *Beta and Gamma-Ray Spectroscopy* (Amsterdam, 1955), p. 624.

and in the proportional counter spectrometer by integration of the areas under the peaks. Detection efficiencies and escape peak corrections were taken into account. We have found:

$$\frac{I_L}{I_K} = 0.46 \pm 0.04,$$

and then

$$(2) \quad \frac{P_L}{P_K} = 1.4 \pm 0.4.$$

The error in eq. (2) arises mostly from the estimated uncertainty in $\bar{\omega}_L$. As can be seen from eq. (3), however, it does not affect seriously the value of the transition energy.

The energy E_0 involved in the transition $^{179}\text{Ta} \rightarrow ^{179}\text{Hf}$ can be calculated according to the formula given by MARSHAK ⁽⁹⁾

$$(3) \quad \frac{P_L}{P_K} = \left(\frac{g_{L_I}}{g_K} \right)^2 \left(\frac{E_0 - E_L}{E_0 - E_K} \right)^2 \left(1 + \frac{f_{L_{II}}^2}{g_{L_I}^2} \right),$$

where E_L and E_K are the L - and the K -shell electron binding energies; $(g_{L_I}/g_K)^2$ and $(f_{L_{II}}/g_{L_I})^2$ are the ratios between L_I - and K -shell and between L_{II} - and L_I -shell electron densities at the nuclear radius. From

$$\left(\frac{g_{L_I}}{g_K} \right)^2 = 0.14^{(10)},$$

$$\left(\frac{f_{L_{II}}}{g_{L_I}} \right)^2 = \frac{3}{16} \left(\frac{Z - 4.15}{137.3} \right)^2 \quad (^9),$$

and with the known values of E_L and E_K we obtain for the transition energy:

$$E_0 = 94_{-4}^{+9} \text{ keV}.$$

4.2. *L-fluorescence yield arising from K vacancies.* — It is well known that L -shell ionization arises from reorganization of an atom ionized in the K -shell. A direct measurement of the L -fluorescence yield (ω_{L_K}) for transition to the L level following the K -capture can be made in a coincidence arrangement in which the K X-rays peak is used to trigger the coincidence circuit and the

(⁹) E. R. MARSHAK: *Phys. Rev.*, **61**, 431 (1942).

(¹⁰) M. E. ROSE and J. L. JACKSON: *Phys. Rev.*, **76**, 1540 (1949).

L X-rays spectrum is recorded. We have:

$$\frac{I_{KL}^*}{I_K^*} = n_{KL} \omega_{LK} \varepsilon_L,$$

where I_{KL}^* is the counting rate due to K X- L X coincidences and I_K^* the counting rate due to K X-rays; ε_L is the detection efficiency of the proportional counter spectrometer for L X-rays.

For Hf ($Z = 72$) we have obtained:

$$\omega_{LK} = 0.17 \pm 0.02.$$

This value is considerably lower than the total fluorescence yield obtained by LAY ⁽¹¹⁾ for fluorescent excitation ($\omega_L = 0.26$).

5. - Discussion.

The low value of the transition energy ($E_0 = 94$ keV) justifies the absence of the known γ -radiations from the excited levels of ^{179}Hf .

With $T_{\frac{1}{2}} = 600$ d, the $\log ft$ value of transition $^{179}\text{Ta} \rightarrow ^{179}\text{Hf}$ calculated according to the discussion given by MAJOR and BIEDENHARN ⁽¹²⁾, results to be

$$\log ft = 6.0.$$

This fact suggests that the transition can be classified as allowed ($\Delta I = 0, 1$; no) or first forbidden ($\Delta I = 0, 1$; yes).

As far as concerns spin and parity of the ground state involved in the transition, the following considerations can be made. For ^{179}Hf the value of the spin ($\frac{1}{2}$ or $\frac{3}{2}$) on the basis of previous estimates is somewhat doubtful ⁽¹³⁾. Quite recently SPECK and JENKINS ⁽¹⁴⁾ on the basis of the observed hyperfine structure using enriched isotopes, assigned the value $I = \frac{3}{2}$ to the ground state of ^{179}Hf . According to the classification of MOTTELSON and NILSSON ⁽¹⁵⁾ of the nucleonic states in deformed nuclei, the expected ground state spin and parity are $\frac{3}{2}^-$. Concerning ^{179}Ta , we observe that nuclei with odd protons from $Z = 65$ to $Z = 75$ have generally ground states $\frac{7}{2}^-$ or $\frac{5}{2}^-$ ⁽¹⁶⁾.

⁽¹¹⁾ M. LAY: *Zeits. f. Phys.*, **91**, 533 (1953).

⁽¹²⁾ J. K. MAJOR and L. C. BIEDENHARN: *Rev. Mod. Phys.*, **26**, 321 (1955).

⁽¹³⁾ J. E. MACK: *Rev. Mod. Phys.*, **22**, 64 (1950).

⁽¹⁴⁾ D. R. SPECK and F. A. JENKINS: *Phys. Rev.*, **101**, 1831 (1956).

⁽¹⁵⁾ B. E. MOTTELSON and S. G. NILSSON: *Phys. Rev.*, **99**, 1615 (1955).

⁽¹⁶⁾ M. GOEPPERT MAYER and J. H. D. JENSEN: *Elementary Theory of Nuclear Shell Structure* (New York, 1955), p. 71.

In view of all these facts the decay of ^{179}Ta appears very probably as a $\frac{7}{2}^{+} \rightarrow \frac{9}{2}^{+}$ transition.

* * *

Acknowledgement is due to Prof. G. Bolla for his kind interest.

RIASSUNTO

Si studia il decadimento per cattura elettronica orbitale del ^{179}Ta . Non si osserva emissione di raggi γ . Il rapporto tra la probabilità di cattura L e la probabilità di cattura K è $P_L/P_K = 1.4 \pm 0.4$ cui corrisponde un'energia di transizione $E_0 = 94_{-4}^{+9}$ keV. Applicando un metodo di coincidenza si determina il rendimento di fluorescenza L per transizioni al livello L che seguono la cattura K . Si è ottenuto $\omega_{LK} = 0.17 \pm 0.02$.

On the Nucleon-Nucleus Interaction.

W. E. FRAHN

*Nuclear Physics Division of the National Physical Laboratory,
C.S.I.R. - Pretoria, South Africa*

(ricevuto l'11 Maggio 1956)

Summary. — A phenomenological energy-dependent interaction is introduced to describe the modified propagation character of nucleons in nuclear matter and to account for the observed energy-dependence of the real part of the optical potential.

1. — Introduction.

The nucleon-nucleus interaction has been successfully treated in terms of the optical model, which represents the nucleus as a region with a static attractive potential $U(r)$. The relative motion is described by the Schrödinger equation

$$(1) \quad \frac{\hbar^2}{2m} \Delta \psi(\mathbf{r}) + E\psi(\mathbf{r}) = U(\mathbf{r})\psi(\mathbf{r}).$$

In general, the potential consists of a real and an imaginary part,

$$(2) \quad U(\mathbf{r}) = V(\mathbf{r}) + iW(\mathbf{r}),$$

the coherent (elastic scattering) and incoherent (absorptive) parts of the interaction thus being formally separated. In its simplest form, the optical model assumes a square-well potential for both of these parts

$$(3) \quad U = \begin{cases} -V_0(1 + i\zeta), & r < R \\ 0, & r > R \end{cases}$$

(R = nuclear radius).

This individual particle picture differs markedly from the statistical model for nuclear reactions, which is based on the assumption of strong coupling between nuclear particles. Considering the remarkable successes of both models in explaining the experimental data on nuclear scattering and reactions, the question arises of how to reconcile the opposite assumptions underlying these two interaction models.

Important progress regarding this problem has recently been achieved by BRUECKNER and his collaborators ⁽¹⁻³⁾ in their investigations on nuclear structure and nuclear saturation in terms of two-body forces. According to this approach, the motion of a nucleon through nuclear matter can be represented by a modified plane wave motion in a medium, characterized by a dispersion law

$$(4) \quad E_k = \frac{\hbar^2}{2m} k^2 + V(k),$$

the «optical» interaction potential being a function of the wave number k . The propagation character of a nucleon moving in the nuclear medium is altered as a result of its coherent interaction with the other nucleons. An equivalent interpretation, due to WHEELER, is to assign a reduced effective mass to the interacting nucleon. Thus, the passage of a strongly interacting nucleon through nuclear matter can be represented by the motion of an equivalent «free» nuclear particle with a modified mass. A general investigation into the relationship between nuclear models and the actual nucleus shows, that these modified nuclear particles play the role of nucleons in the independent particle models ⁽⁴⁾.

On the other hand, the optical model analysis ⁽⁵⁾ of nucleon-nucleus cross-section measurements ⁽⁶⁾ in the energy range 30 MeV to 400 MeV, exhibits a strong energy dependence of the real part of the optical potential. The interpretation of these results in terms of a complex nuclear refractive index showed, that the optical model with a static potential does not reproduce the measurements and that this disagreement is due to the real part of the refractive index. Therefore, the nucleon-nucleus interaction can apparently no longer be described in terms of a static potential.

For this reason, we shall investigate a generalized type of interaction, which

⁽¹⁾ K. A. BRUECKNER, C. A. LEVINSON and H. M. MAHMOUD: *Phys. Rev.*, **95**, 217 (1954).

⁽²⁾ K. A. BRUECKNER: *Phys. Rev.*, **96**, 508 (1954).

⁽³⁾ K. A. BRUECKNER: *Phys. Rev.*, **97**, 1353 (1955).

⁽⁴⁾ R. J. EDEN and N. C. FRANCIS: *Phys. Rev.*, **97**, 1366 (1955).

⁽⁵⁾ T. B. TAYLOR: *Phys. Rev.*, **92**, 831 (1953).

⁽⁶⁾ V. A. NEDZEL: *Phys. Rev.*, **94**, 174 (1954).

reproduces the results of BRUECKNER and also accounts qualitatively for the energy dependence of the real optical model parameters in the intermediate and higher energy regions.

2. — The Phenomenological Interaction.

According to the optical model, the plane wave representing a moving nucleon in nuclear matter will be scattered by the other nucleons. To the elastic part of this scattering correspond coherent scattered waves which superimpose on the original wave, thus forming a new plane wave with a modified phase velocity. The elementary scattered waves are determined by the individual nucleon-nucleon interactions. In his approach, BRUECKNER correlates the modified plane wave properties to the observed scattering phase shifts of the elastic nucleon-nucleon collisions, without needing specific assumptions about the elementary law of nucleon-nucleon interaction.

In the following we shall give an alternative description, assuming an explicit form of the nucleon-nucleus interaction. The static potential concept is obviously insufficient to represent the interaction arising from the effect of collisions on the wave function of the moving nucleon. Therefore, we will describe the relative nucleon motion by a generalized Schrödinger equation

$$(5) \quad \frac{\hbar^2}{2m} \Delta \psi(\mathbf{r}) + E \psi(\mathbf{r}) = \int K(\mathbf{r}, \mathbf{r}') \psi(\mathbf{r}') d\mathbf{r}',$$

with a non-static (« non-local ») interaction term, formally taking into account the correlation effects due to the many-body character of the interaction.

An interaction of this type is also suggested by the meson theory of nuclear forces in the non-adiabatic treatment of LEVY (7), which describes the elementary nucleon-nucleon interaction in terms of a non-local operator (8). It is, however, not yet possible to derive the complete form of this operator which, in Levy's treatment, is given only in terms of a power series in the coupling parameter.

In accordance with the single-particle models, we assume that the over-all effect of the elementary interactions will on the average result in a static potential $V(r)$ plus a « small » non-static correction. That is to say, we assume the interaction kernel of eq. (5) to be of the form

$$(6) \quad K(\mathbf{r}, \mathbf{r}') = V(r) f(\mathbf{r} - \mathbf{r}').$$

(7) M. LEVY: *Phys. Rev.*, **88**, 725 (1952).

(8) M. LEVY and R. E. MARSHAK: *Proc. Glasgow Conference* (1955).

Obviously, for $f(\mathbf{r} - \mathbf{r}') = \delta(\mathbf{r} - \mathbf{r}')$, eq. (5) reduces to the Schrödinger-equation (1) with static real potential $V(r)$. The «smallness» of the non-static correction means therefore, that we have to choose an approximation function of the δ -function for $f(\mathbf{r} - \mathbf{r}')$. As can be seen from their Fourier-transforms, these approximation functions act as a cut-off in the momentum distribution. Thus, such a choice for $f(\mathbf{r} - \mathbf{r}')$ qualitatively takes into account the most important property of the interaction arising from the effect of collisions on the wave function, viz. the rapid decrease of this effect with increasing relative momenta. As the momentum cut-off must be a smooth one, it seems reasonable, to choose for $f(\mathbf{r} - \mathbf{r}')$ the normalized Gaussian approximation to the δ -function with parameter r_0 :

$$(7) \quad f(\mathbf{r} - \mathbf{r}') = \pi^{-\frac{3}{2}} r_0^{-3} \exp \left[-\frac{(\mathbf{r} - \mathbf{r}')^2}{r_0^2} \right].$$

Equations of the general form (5) have been investigated by WHEELER⁽⁹⁾ to account for nuclear saturation. We shall point out in the next section, that the connection between Brueckner's «optical» treatment of the saturation problem in terms of two-body forces and Wheeler's in terms of a non-static interaction, also holds for the modified propagation properties of nucleons in nuclei, which follow from both treatments. The starting points of WHEELER's and BRUECKNER's works, although formally different, thus prove to be essentially equivalent.

Mathematically, the integro-differential equation (5) is equivalent to an ordinary differential equation of infinitely high order, thus leading to a velocity-dependent interaction. Physically, this means that the interaction is no longer independent of the state of the interacting system. The state-independence of the nuclear interaction, as assumed by the single-particle models, seems to be realized only approximately. A state dependent interaction of the form described by eq. (5) will phenomenologically take into account some of the collective aspects of the nuclear states which modify the single-particle motion in a nuclear medium.

3. — The Motion of Nuclear Particles in Nuclear Matter.

We consider the motion of a nucleon, as described by eq. (5), in an infinite nuclear medium, assuming a constant potential $V(r) = -V_0$. Eq. (5) then becomes translation-invariant, thus describing the motion of a «free» particle with modified propagation character. This can be seen by Fourier-trans-

⁽⁹⁾ J. A. WHEELER: *Phys. Rev.*, **50**, 643 (1936).

formation of eq. (5), which yields

$$(8) \quad \left(-\frac{\hbar^2}{2m} k^2 + E \right) \varphi(k) = -V_0 g(k) \varphi(k),$$

φ and g being the Fourier-transforms of ψ and f , respectively. Thus, the motion is equivalent to a free motion in a medium, characterized by a dispersion relation

$$(9) \quad E = \frac{\hbar^2}{2m} k^2 + V(k),$$

with $V(k) = -V_0 g(k)$. The effective nuclear potential is therefore a function of the momentum, if $f \neq \delta$.

For the special assumption (7) we obtain

$$(10) \quad g(k) = \exp \left[-\frac{1}{4} r_0^2 k^2 \right],$$

a Gaussian cut-off function for the higher relative momenta. With $r_0 k \ll 1$, we have

$$(11) \quad V(k) \approx -V_0 + \frac{1}{4} V_0 r_0^2 k^2,$$

and in this case, eq. (9) can be rewritten in the form

$$(12) \quad E + V_0 = \frac{\hbar^2}{2m^*} k^2,$$

with an effective mass

$$(13) \quad m^* = \frac{m}{1 + (r_0^2 V_0 / 2\hbar^2) m}.$$

Consequently, the motion in the nuclear medium, characterized by the optical relation (9), is approximately equivalent to the free motion of a nuclear particle with reduced mass $m^* < m$ in a constant static potential $-V_0$.

Brueckner's treatment gives the values

$$V_0 = 68 \quad \text{MeV}$$

$$m^* = 0.6 \, m,$$

which will be used here to fix the parameter of the phenomenological inter-

action. Inserting these values in (13) we get

$$(14) \quad r_0 = 0.65 \frac{\hbar}{\mu c},$$

for the range of the interaction kernel (7).

JOHNSON and TELLER⁽¹⁰⁾ have proposed a classical field theory of nuclear forces and had to add a velocity-dependent term to the interaction-Hamiltonian, to account for saturation and for the neutron-proton ratio in heavy nuclei. They derived an effective nucleon mass depending on the meson field amplitude, the meson mass and the coupling parameter of the velocity-dependent interaction. From comparison with empirical data, they obtained the mass ratio $m^*/m \approx 0.5$.

4. - Energy Dependence of the Real Optical Potential.

During the past few years, total neutron cross-sections have been measured on various nuclei. The results up to 410 MeV have been summarized by NEDZEL⁽⁶⁾. The analysis of these measurements, given by TAYLOR⁽⁵⁾, based on the optical model of FERNBACH, SERBER and TAYLOR⁽¹¹⁾, showed that the real part V of the optical potential is a monotonically decreasing function of the neutron energy E ranging from about 30 MeV for $E = 60$ MeV to about 10 MeV for $E = 300$ MeV. The elastic scattering of protons in the region between 5 and 30 MeV has recently been analyzed by MELKANOFF *et al.*⁽¹²⁾ in terms of the optical model and revealed a similar uniformly decreasing real part of the potential, which was found to be in accordance with an effective mass ratio $m^*/m \approx 0.5$.

To obtain the effective potential for a nucleon with energy E , we have to evaluate the function $k^2(E)$ from

$$(15) \quad E = \frac{\hbar^2}{2m} k^2 - V_0 \exp \left[-\frac{1}{4} r_0^2 k^2 \right],$$

and insert this into $V(k)$, yielding

$$(16) \quad V(E) = -V_0 \exp \left[-\frac{1}{4} r_0^2 k^2(E) \right].$$

This function, with the accepted values for V_0 and r_0 , is shown in Fig. 1.

⁽¹⁰⁾ M. E. JOHNSON and E. TELLER: *Phys. Rev.*, **98**, 783 (1955).

⁽¹¹⁾ S. FERNBACH, R. SERBER and T. B. TAYLOR: *Phys. Rev.*, **75**, 1352 (1949).

⁽¹²⁾ M. A. MELKANOFF, S. A. MOSZKOWSKI, J. NODVIK and D. S. SAXON: *Phys. Rev.*, **101**, 507 (1956).

The resulting values are in fair agreement with those following from TAYLOR's analysis in the region between $E \approx 60$ and $E \approx 200$ MeV. For higher energies (250–400 MeV) Taylor's function remains nearly constant at $V \approx 10$ MeV. In view of the qualitative nature of our results, which depend on the special cut-off function (7), a detailed comparison with those obtained from the experimental data, does not seem to be justified. Moreover, the relation (16) has been derived under the assumption of an infinite extension of the nuclear medium. Above $E \approx 300$ MeV, relativistic effects will become important. Nevertheless, the general trend of the energy dependence is fairly well represented.

An even better agreement exists with the values given by KIND and VILLI⁽¹³⁾, who approached the problem differently, using perturbation theory.

In the vicinity of $E = 0$, we obtain from (16):

$$(17) \quad V(E) \approx -44.2 \text{ MeV} + 0.3E.$$

For negative energies, the expansion of the exponential in (15) for $r_0 k \ll 1$ leads to

$$(18) \quad V(E) \approx -\frac{m^*}{m} V_0 + \left(1 - \frac{m^*}{m}\right) E = -41 \text{ MeV} + 0.4E,$$

the result obtained by BRUECKNER, EDEN and FRANCIS⁽¹⁴⁾ for the low neutron energy range (< 5 MeV).

5. — The Nuclear Refractive Index.

The optical properties of the nuclear medium can be represented by a complex refractive index. Its real part, n , is defined by the ratio of the internal and external wave numbers k_i and k_e ; its imaginary part is determined by the absorption coefficient.

To the observed energy dependence of the total neutron cross-sections

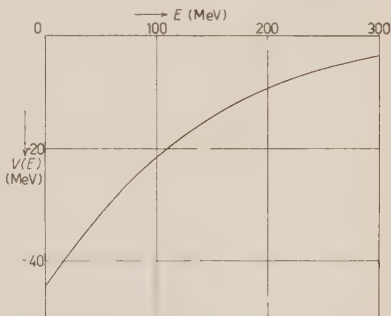


Fig. 1. — Real part of the optical potential as a function of energy.

(13) A. KIND and C. VILLI: *Nuovo Cimento*, **1**, 749 (1955).

(14) K. A. BRUECKNER, R. J. EDEN and N. C. FRANCIS: *Phys. Rev.*, **100**, 891 (1955).

corresponds a certain variation of the refractive index with energy. An analysis by JASTROW ⁽¹⁵⁾, showed that the optical model failed to reproduce this variation at intermediate energies. In this treatment, the absorption coefficient is given in terms of the total n-n and n-p cross-sections, for which the measured values have been inserted. The real part of the refractive index is given by

$$(19) \quad n - 1 = \frac{2\pi\rho}{k^2} f(0)$$

(ρ = nucleon density); thus it contains the forward scattering amplitudes $f(0)$, which depend on the particular nucleon-nucleon interaction assumed. It has, therefore, been concluded, that the disagreement is entirely due to the real part of the refractive index. This conclusion has been supported by measurement (cf. NEDZEL ⁽⁶⁾). In order to obtain agreement with experiment, the real part of the refractive index has to show a much more rapid decrease with energy than that following from the static potential model. This point has been discussed in detail by MEMMERT ⁽¹⁶⁾. This author has calculated the values of $n - 1$ required by the experimental data. In Jastrow's formula (19), the nucleon-nucleon forward scattering amplitude $f(0)$ should decrease rapidly with increasing energy. This behaviour can be explained in terms of Jastrow's « hard core » model.

The forward scattering amplitude can be related to the nucleon interaction potential. With a non-static interaction of type (5), using the kernel (7), one obtains the following ratio between the forward scattering amplitudes of the non-static and static cases in Born-approximation:

$$(20) \quad \frac{f^*(0)}{f(0)} \sim \exp \left[-\frac{1}{4} \gamma_0^2 k^2 \right].$$

A direct derivation of the real nuclear refractive index is obtained from the dispersion relation (15). Hence follows

$$(21) \quad k_i^2 - \frac{2m}{\hbar^2} V_0 \exp \left[-\frac{1}{4} \gamma_0^2 k_i^2 \right] = k_s^2.$$

This equation is only approximately correct, because (15) is the dispersion relation in an infinite nuclear medium and has to be corrected for a finite extension of the nucleus. This correction will, however, not affect the qualitative behaviour.

⁽¹⁵⁾ R. JASTROW: *Phys. Rev.*, **82**, 261 (1951).

⁽¹⁶⁾ G. MEMMERT: *Zeits. f. Phys.*, **134**, 42 (1952).

For the refractive index $n = k_i/k_e$ we obtain

$$(22) \quad n^2 - 1 = \frac{V_0}{E} \exp \left[-n^2 \frac{E}{E^*} \right],$$

where we have introduced the energy

$$(23) \quad E^* = \frac{2\hbar^2}{mr_0^2} - \frac{V_0}{(m/m^*)} - 1 = 1.5 V_0 = 102 \text{ MeV}.$$

Eq. (22) implicitly defines the refractive index as a function of the external nucleon energy. The resulting values are given by the full line in Fig. 2 in comparison with those obtained from the Fermi gas model (dashed line) according to

$$(24) \quad n^2 - 1 = \frac{V}{E},$$

with $V = 30 \text{ MeV}$.

For higher energies, the dependence is given by

$$(25) \quad n^2 \approx 1 + \frac{V_0}{E} \exp \left[-\frac{E}{E^*} \right],$$

equivalent to that following from (20). In the low-energy region we get

$$(26) \quad n^2 \approx \frac{m^*}{m} \left(1 + \frac{V_0}{E} \right).$$

Generally, the refractive index is related to the effective nuclear potential (16) by

$$(27) \quad E(n^2 - 1) = -V(E).$$

The values calculated from (22) are in fair agreement with those obtained by MEMMERT⁽¹⁶⁾ from his analysis of the neutron-cross section measurements.

6. - Summary and Discussion.

It has been shown, that the assumption of a non-static nucleon-nucleus interaction of the type (5), which is chosen so as to represent certain quali-

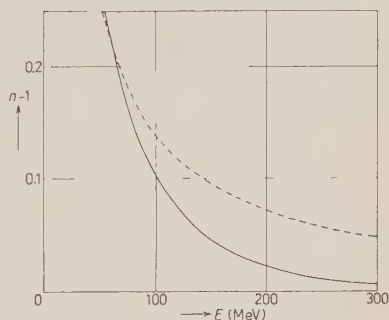


Fig. 2. - Real part of the nuclear refractive index, $n - 1$, as a function of energy.

tative features of the elastic nucleon-nucleon collisions in the nucleus, can account for both the modified motion of nucleons in a nuclear medium and the energy dependence of those optical model parameters, which describe the coherent (elastic) part of nuclear interaction.

Obviously, the results obtained are of a qualitative nature only, depending on the special form of the assumed phenomenological interaction. Therefore, the numerical values as given in Figs. 1 and 2, although in fair general agreement with experimental data, should by no means be taken too literally. They are intended only as an illustration of the general qualitative behaviour of the magnitudes discussed. The aim was to illustrate with a typical example how a non-local, state-dependent generalization of the static potential concept, as suggested by fundamental nuclear theory, could account for the intimate connection between the coherent nuclear effects, saturation properties, and the collective features of nuclear interactions.

* * *

The author would like to express his indebtedness to Dr. S. J. DU TOIT, head of the Nuclear Physics Division, for his interest in this work; Dr. I. J. VAN HEERDEN for discussion and the South African Council for Scientific and Industrial Research for permission to publish this paper.

RIASSUNTO (*)

Si introduce un'interazione fenomenologica dipendente dall'energia per descrivere il carattere modificato della propagazione dei nucleoni nella materia nucleare e per render conto della dipendenza dall'energia, osservata per la parte reale del potenziale ottico.

(*) *Traduzione a cura della Redazione.*

Differential Cross-Sections for Photoproduction of Positive Pions in Hydrogen.

I. — Low Energies.

M. BENEVENTANO (*), G. BERNARDINI (-), D. CARLSON-LEE (×),
G. STOPPINI (×) and L. TAU (*)

(ricevuto il 21 Maggio 1956)

Summary. — The cross-sections $\sigma(E_\gamma, \theta)$ for the reaction $p\gamma \rightarrow n^+$ have been measured near threshold as a function of photon energy and at four angles. See Table I. These results combined with previously known data, have given a fairly complete and accurate description of $\sigma(E_\gamma, \theta)$ between the limits $30^\circ \leq \theta \leq 180^\circ$ and $170 \leq E_\gamma \leq 270$ MeV. See Table II and Fig. 2. Writing $\sigma(E_\gamma, \theta) = W\{a_0 + a_1 \cos \theta + a_2 \cos^2 \theta\}$ with $W = \eta\omega\{1 + (\mu/E_i)v\}^{-1}\{1 + (\mu/E_f)\omega\}^{-1}$ (see formula (5)) the experimental data indicate that (Table III) a_0 is constant up to about $E_\gamma \simeq 260$ MeV; and that (Table V) the three a_i coefficients analyzed in terms of S and P waves give a very small spin flipping P -amplitude K . The presumption that the S amplitude E_1 is *mainly* due to the gauge invariance requirement is definitely not consistent with the data (see Table IV). A discussion based on the Kroll and Rudermann theorem leads to the conclusion that this inconsistency may be eliminated if allowance is made for the contribution of fairly large nucleon recoils. However, it turns out that only the changing sign part of these recoils is really large and apparently so up to terms of order higher than μ/M . The amount of the recoil at threshold is estimated and consequently a value for the pspv interaction constant is derived.

1. — Introduction.

1.1. — In the last few years a considerable amount of theoretical and experimental work has been done on the problem of photoproduction of pions in hydrogen.

(*) Istituto di Fisica dell'Università, Roma - Istituto Nazionale di Fisica Nucleare, Sezione di Roma.

(-) Physics Department, University of Illinois, Urbana, Illinois.

(×) Istituto di Fisica dell'Università, Roma - Istituto Nazionale di Fisica Nucleare, Sezione di Roma. Now at Physics Department, University of Illinois, Urbana, Illinois.

The theoretical work has been developed following several lines of approach. The simplest, called «phenomenological», has been worked out mainly by AIZU, FELD, FERMI and WATSON ⁽¹⁾. This analysis is phenomenological in the sense that it is based on the application of the *S*-matrix formalism ⁽²⁾ and time reversal, that is, on general conservation principles and the correlated selection rules. Thus it cannot be erroneous, with the possible exception of some oversimplification introduced in dealing with the several processes. For example, the limitation to the two lowest angular momentum states or the assumption of the existence of particular symmetries in the Hamiltonian.

As has been shown in detail by KAWAGUCHI and MINAMI, FERMI, WATSON ⁽¹⁾ and by GELL-MANN and WATSON ⁽³⁾, this interpretation of photopion processes establishes a direct connection between the photoproduction and pion-nucleon scattering. This connection is due to «cross-links» between the photon-nucleon and the pion-nucleon states. The strong interaction in the $I = \frac{3}{2}$, $J = \frac{3}{2}$ state (I = Isospin, J = total angular momentum) is accepted as experimentally verified by the pion-nucleon scattering experiments and then phenomenologically introduced through the scattering «channel» ⁽²⁾ also for pion-photo-production.

The charge independence principle is applied to the final state [WATSON ⁽¹⁾]. The Isospin is not conserved as far as concerns the photon absorption. Thus the absorbing e.m. source is not the physical ground state of the nucleon but the dynamical pion-nucleon system with its own e.m. properties corresponding to the two Isospin-substates $I = \frac{1}{2}$ and $I = \frac{3}{2}$.

This splitting into two independent Isospin-states follows from a first order approach to the electromagnetic interaction. The incident e.m. plane wave is thought to be decomposed into (an infinite number of) pure parity and angular momenta substates, i.e. in multipoles. The pion-nucleon system emphasizes, because of its e.m. structure, some of these e.m. poles. The strengths of these poles can be determined experimentally and they may be considered as the photon energy dependent parameters defining empirically

⁽¹⁾ B. T. FELD: *Phys. Rev.*, **89**, 330 (1953); K. AIZU: *Proceeding of the International Conference of Theor. Phys.*, Kyoto and Tokyo, 1953, p. 200; E. FERMI: 1954 Varenna Lecture, *Suppl. Nuovo Cimento*, **2**, 17 (1955); K. WATSON: *Phys. Rev.*, **95**, 228 (1954); see also K. A. BRUECKNER and K. M. WATSON: *Phys. Rev.*, **86**, 923 (1952); S. HAYAKAWA, M. KAWAGUCHI and S. MINAMI: *Prog. Theor. Phys.*, **12**, 355 (1954); **12**, 789 (1954).

⁽²⁾ A comprehensive account of this formalism with particular reference to nuclear reactions can be found in *Theoretical Nuclear Physics* by BLATT and WEISSKOPFF. A lucid presentation of the essentials of this formalism is given in FERMI's Varenna lectures.

⁽³⁾ M. GELL-MANN and K. M. WATSON: *Annual Review of Nuclear Science*, **4**, 219 (1954).

this e.m. structure of the pion-nucleon system. In that sense one might speak of the e.m. structure of the pion-nucleon system almost independently of any particular model, but because of its generality, the analysis introduces too many of this type of parameters whose energy dependence is a priori unknown. However, as will be shown, some rather interesting conclusions can be derived about these pole-strengths (see Part II).

1'2. - The other theoretical works have the aim of presenting a real theory capable of expressing the essential features of pion-nucleon scattering, photoproduction, nucleon interaction. The simplest and most successful theory of this type has been extensively worked out by CHEW, CHEW and Low (⁴). Recently a comprehensive and clear presentation of this theory has been published by WICK (⁵). It involves some very definite assumptions (a Yukawa type interaction with a finite-sized and infinitely heavy nucleon) and the calculations have only been carried out, up to now, with some approximation. However, it has the great advantage of introducing consistently very few parameters; mainly the renormalized coupling constant and the nucleon size or, equivalently, a pion-momentum cut-off.

In the discussion of the experimental data obtained near threshold (as that presented in this paper) a general theorem established by KROLL and RUDERMAN (⁶) is most interesting. The value of this theorem lies in the fact that it permits a proper estimate of the pion-nucleon interaction constant and indicates clearly the origin of all uncertainties included in any discussion of this type. Briefly this theorem, which will be extensively used in the following discussion, states: In the limit in which the total energy of the mesons goes to zero, the renormalized psp matrix H_r for photoproduction coincides with that H_{II} obtained in the same limit by the second order perturbative approximation. That is

$$(1) \quad \lim_{\mu \rightarrow 0} H_r = \lim_{\mu \rightarrow 0} H_{II} = \frac{eg_r}{2M} \frac{\sigma \cdot \epsilon}{\sqrt{\mu^2 + \omega^2}},$$

where ω is the total energy (in μ units) of the outgoing real pion and:

$\epsilon = 1/\sqrt{137}$ ($\hbar = c = 1$);

g_r = renormalized symmetric psp coupling constant;

σ = nucleon spin;

(⁴) G. F. CHEW: *Phys. Rev.*, **95**, 1669 (1954); G. F. CHEW and F. E. LOW: *Phys. Rev.*, **101** 1570, 1579 (1956).

nication.

(⁵) G. WICK: *Rev. Mod. Phys.*, **27**, 339 (1955).

(⁶) N. KROLL and M. RUDERMAN: *Phys. Rev.*, **93**, 233 (1954).

ϵ = photon polarization vector;

M = nucleon mass;

ν = photon energy-momentum (in μ units).

As a direct consequence of the theorem itself, one can write, in the real case in which μ has a finite value, the squares of the matrix element for the proton and neutron target cases as

$$(2) \quad \left\{ \begin{aligned} \langle p^\gamma | T_+ | n^+ \rangle^2 &= \frac{1}{\nu\omega} \left\{ G_{0s} + \omega \frac{\mu}{M} G_1 + H_1 \left(\omega \frac{\mu}{M} \right) \right\}, \\ \langle n^\gamma | T_- | p^- \rangle^2 &= \frac{1}{\nu\omega} \left\{ G_{0s} + \omega \frac{\mu}{M} G_2 + H_2 \left(\omega \frac{\mu}{M} \right) \right\}, \end{aligned} \right.$$

where G_1 and G_2 are independent from $\omega\mu/M$ and, at threshold, equal but with opposite signs. It has to be noticed that the first term includes S -waves only, and coincides with the so-called gauge invariance term first proposed by WENTZEL (7) which arises in any pseudovector coupling.

Precisely, as is well-known (8) this S -wave part arises from the pspv Hamiltonian extra term: $ie[\mathcal{A} \cdot (\text{pseudovectors independent of pion momentum})]$.

The e.m. structure of the nucleon has been the main object of a series of papers by SACHS *et al.* (9). In these papers the pion structure of the magnetic-moment of the nucleon, the neutron-proton mass difference etc. have been investigated, but a definite attempt to estimate quantitatively the photopion processes was not made and a simple comparison of the experiments with the theoretical prediction does not seem yet possible.

1'3. - The more recent experimental work on photoproduction in hydrogen offers today a rather satisfactory picture of the reaction

$$(3) \quad \gamma + p \rightarrow n + \pi^+,$$

up to about 450 MeV.

Precisely we refer to the experiments carried out in the following laboratories:

Berkeley. - STEINBERGER and BISHOP (10), using fast and delayed coinci-

(7) Unpublished. See FERMI's Varenna Lectures, ref. (6) and (29).

(8) G. F. CHEW, ref. (4); FERMI's Varenna lectures 1954, *Suppl. Nuovo Cimento*, **2**, 17 (1955); K. M. WATSON, ref. (1) and *Proceeding of the V Annual Rochester Conference*, p. 32, 1955.

(9) R. G. SACHS: *Phys. Rev.*, **95**, 1065 (1954); W. G. HOLLADAY and R. G. SACHS: *Phys. Rev.*, **96**, 810 (1954) and preprints.

(10) J. STEINBERGER and A. S. BISHOP: *Phys. Rev.*, **86**, 171 (1952).

dences, gave an excitation curve at 90° Lab for the photon energy interval 170 to 320 MeV, and an angular distribution at 255 MeV.

WHITE, JACOBSON and SCHULZ⁽¹¹⁾, repeated and extended the experiment using both emulsions and fast coincidences in the energy interval 200 to 300 MeV.

Somewhat later, JARMIE, REPP and WHITE⁽¹²⁾ added a determination of the cross section at 0° and 278 MeV.

California Institute of Technology. - WALKER, TEASDALE, PETERSON and VETTE⁽¹³⁾ analyzed reaction (3) with a large magnetic spectrometer and fast coincidences in the energy interval 200 to 170 MeV and the angular interval 12.5° to 180° Lab.

At the same time, TOLLESTRUP, KECK and WORLOCK⁽¹⁴⁾ carried out measurements with a scintillation counter telescope from 230 MeV, in the angular interval 24° to 160° Lab.

Cornell. - JENKINS, LUCKEY, PALFREY and WILSON⁽¹⁵⁾ measured, with thinwalled proportional counters in coincidence, three angular distributions covering six angles in the 40° to 180° angular interval at 200, 235 and 265 MeV.

Massachusetts Institute of Technology. - FELD, FRISCH, LEPOW, OSBORNE and CLARK⁽¹⁶⁾, with nuclear emulsion have given two excitation curves at 26° and 90° Lab in the energy interval 210 to 305 MeV.

Successively, JANES and KRAUSHAAR⁽¹⁷⁾ have completed, with counters, the excitation curve at 90° Lab for the photon energy interval 165 to 280 MeV.

Illinois. - BERNARDINI and GOLDWASSER⁽¹⁸⁾, using nuclear plates, have measured the angular distributions at 175, 185 and 195 MeV, for the angular interval 30° to 150° Lab.

LEISS, ROBINSON and PENNER⁽¹⁹⁾ have measured, by detecting the fast electrons from the $\pi \rightarrow \mu \rightarrow e$ chain, the total cross sections from threshold to 170 MeV.

⁽¹¹⁾ R. S. WHITE, M. J. JACOBSON and A. G. SCHULZ: *Phys. Rev.*, **88**, 836 (1952).

⁽¹²⁾ N. JARMIE, G. V. REPP and R. S. WHITE: *Phys. Rev.*, **91**, 1023 (1953).

⁽¹³⁾ R. L. WALKER, J. G. TEASDALE, V. Z. PETERSON and J. I. VETTE: *Phys. Rev.*, **99**, 210 (1955).

⁽¹⁴⁾ A. V. TOLLESTRUP, J. C. KECK and R. M. WORLOCK: *Phys. Rev.*, **99**, 220 (1955).

⁽¹⁵⁾ T. L. JENKINS, D. LUCKEY, T. R. PALFREY and R. R. WILSON: *Phys. Rev.*, **95**, 179 (1954).

⁽¹⁶⁾ B. T. FELD, D. H. FRISCH, I. L. LEBOW, L. S. OSBORNE and J. S. CLARK: *Phys. Rev.*, **85**, 680 (1952).

⁽¹⁷⁾ G. S. JANES and W. L. KRAUSHAAR: *Phys. Rev.*, **93**, 900 (1954).

⁽¹⁸⁾ G. BERNARDINI, E. L. GOLDWASSER: *Phys. Rev.*, **94**, 729 (1954).

⁽¹⁹⁾ J. E. LEISS, C. S. ROBINSON and S. PENNER: *Phys. Rev.*, **98**, 201 (1955).

LEISS and ROBINSON⁽²⁰⁾, with a counter telescope, measured the differential cross section from 195 to 300 MeV at 90°, 135° and 159° Lab.

1.4. — In part I of this work, we want to present a new and rather complete set of experimental data obtained with pellicle technique and concerning the less-known region between 170 and 230 MeV. A preliminary report on this material has been presented at the Pisa International Conference, 1955, (to be issued in *Suppl. Nuovo Cimento*). Then these data will be discussed mostly in connection with a proper estimate of the *S*-wave.

In part II, a multipole analysis and a discussion of the *P*-wave terms will be performed mostly concerned with the magnitude and energy dependence of the magnetic dipole and electric quadrupole of the pion-nucleon system.

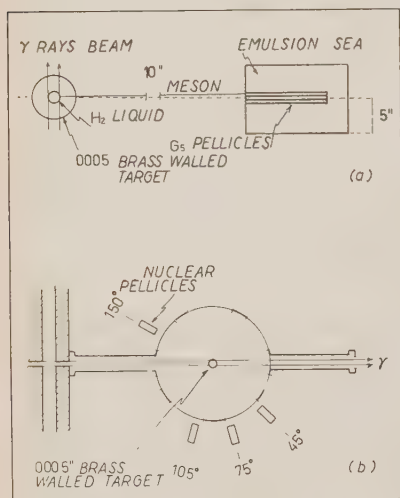


Fig. 1. *a*) Shows the blocks in which the pellicles were imbedded; *b*) Shows schematically the experimental set-up (horizontal-plane).

2. — Experimental Arrangement and Procedure.

The apparatus used in this experiment has already been described by BERNARDINI and GOLDWASSER⁽²¹⁾. Ilford G5 pellicles were exposed to the angles 45°, 75°, 105° and 150° around a liquid hydrogen target⁽²²⁾ irradiated by the bremsstrahlung beam of the Illinois 300 MeV betatron. The experimental set-up is sketched in Fig. 1*b*.

The photon beam was calibrated with the calorimetric method of KERST and EDWARDS⁽²³⁾. The shape of the spectrum has been checked rather carefully by LEISS, YAMAGATA and HANSON⁽²⁴⁾. It agrees, within the limits of the pair-spectrometer resolution (≈ 2 MeV), with the Schiff spectrum⁽²⁵⁾.

The pion detectors are shown in detail in Fig. 1*a*; they consist of blocks of emulsion in which three pellicles were immersed. The twelve pellicles were

⁽²⁰⁾ J. E. LEISS and C. S. ROBINSON: *Phys. Rev.*, **95**, 638 (A) (1954).

⁽²¹⁾ G. BERNARDINI and E. L. GOLDWASSER: *Phys. Rev.*, **95**, 857 (1954).

⁽²²⁾ E. A. WHALIN Jr. and R. A. REITZ: *Rev. Sci. Instr.*, **26**, 59 (1955).

⁽²³⁾ P. D. EDWARDS, D. W. KERST: *Rev. Sci. Instr.*, **24**, 490 (1953).

⁽²⁴⁾ J. LEISS, T. YAMAGATA and A. O. HANSON: *Illinois Reports*, 1954.

⁽²⁵⁾ L. I. SCHIFF: *Phys. Rev.*, **83**, 252 (1951).

scanned in volume for the $\pi \rightarrow \mu$ decays. The effect of the surrounding emulsion was to compensate, at least for the energy interval considered here, for the effect of scattering losses, so that the effective solid angle is that given by the pellicle section. The effective thickness T of the pellicles has been measured using the relation $T = 2R/A$, where R is the average chord length of the decay μ 's, and A is the ratio of the total number of $\pi \rightarrow \mu$'s to those whose μ ends in the emulsion. Measurements of A and R agreed within statistical stragling for all pellicles, and the thickness found, $T = 535 \pm 12 \mu\text{m}$ is within the 10% tolerance given by Ilford for their 500 μm pellicles.

The advantage of this experimental arrangement are:

a) Continuous spectra of pions corresponding to the continuous photon spectrum. This fact eliminates the edge effects in the definition of the energy-intervals.

b) The nuclear absorption of pions in emulsions is well known (see later).

c) The pion energy is given by the range-energy relation (the range is given by the position of the $\pi \rightarrow \mu$ decay in the pellicle).

d) The number of doubtful cases is reduced to a minimum by tracing the secondaries.

The above method guarantees that most of the systematic corrections (see following section) are small and easily calculated. As a consequence it has been felt that this experimental arrangement was able to give dependable information on the energy dependence of the absolute cross sections.

Because of the strong background of electrons, the pellicles had to be strongly underdeveloped to improve the contrast. In order to obtain a rather high precision, i.e. good statistics, the main problem was that of combining a high speed scanning technique with high efficiency and accurate coordinate measurements. With several technical improvements in the microscope stages, and with the invaluable cooperation of an extremely well-trained crew of scanners, this aim was, to a considerable extent, achieved.

For a total of more than 14000 stopping pions, the emulsions were scanned twice in volume and, in all doubtful cases of confusion of a scattering-out with a decay, the secondaries were followed through in the adjacent emulsion. The average efficiency per scanning was about 90%, and the total efficiencies were 98-99%. A meson-per-meson control, including following through, was carried out by the authors. Since the efficiency falls off markedly near the two surfaces due to the difficulty of seeing and identifying short pieces of tracks, 20 μm was rejected at each surface.

3. — Sources of Errors, and Results.

The differential cross-sections as a function of Lab photon energy and C.M. angle are presented in Table I. The data at 93° are those of BERNARDINI and GOLDWASSER ⁽²¹⁾ revised by a more extensive scanning.

TABLE I. — C.M. Differential cross-sections in units 10^{-30} cm²/ster.

E_γ (MeV, Lab)	59°	93°	123°	159°
170	$5.2 \pm .4$	$5.4 \pm .4$	—	—
180	$6.5 \pm .5$	$7.5 \pm .4$	$7.6 \pm .5$	$6.6 \pm .9$
190	$7.2 \pm .5$	$9.1 \pm .5$	$8.7 \pm .6$	$7.5 \pm .6$
200	$8.0 \pm .6$	$9.8 \pm .6$	$10.5 \pm .6$	$9.5 \pm .7$
210	$10.0 \pm .7$	$12.2 \pm .7$	$10.7 \pm .7$	$10.7 \pm .8$
220	$9.7 \pm .9$	$13.4 \pm .7$	$12.1 \pm .8$	$12.1 \pm .8$
230	—	—	$15.4 \pm .9$	13.0 ± 1.0

The main corrections introduced into the final values are the following:

1) The pion background from the target walls, amounting to about 3%, has been subtracted. It has been measured both by counting the negative pions observed in the pellicles and directly by exploring pellicles exposed to an evacuated target.

2) The scanning efficiency is based on two independent and complete scannings, assuming for each observer that the probability of missing a $\pi \rightarrow \mu$ decay is independent of the peculiarities of the track. This correction was never more than 3%, usually about 1%.

3) Decays in flight ranged between 6 and 3%.

4) Nuclear interactions of the pions before ending. The cross sections for π^+ interactions in nuclear emulsions given by STORK ⁽²⁵⁾ have been used. They ranged, according to the pion energy, from 0 to 8%.

In the worst cases, the total correction does not surpass 15%, with an error which is about 20%. The errors given in Table I include those estimated for the above corrections plus the 2% error in the beam calibration and the error in the solid angle (+).

The energies of the pions have been determined from the observed position

⁽²⁵⁾ D. H. STORK: *Phys. Rev.*, **93**, 868 (1954).

(+) The error in the definition of the 20μ m region excluded at the top and bottom of the pellicles is negligible.

of the $\pi \rightarrow \mu$ decays. The errors introduced by the straggling and multiple scattering are negligible. These energies have been corrected for the energy losses suffered by the pions in crossing the liquid H_2 target and walls.

The results presented in Table I agree well with the Illinois results, that is, with the plate data of Bernardini and Goldwasser and with the backward angle counter measurements of Leiss and Robinson (²⁰). In spite of the quite different detection techniques used in these experiments, the deviations are systematically within the limits of the estimated errors.

Unfortunately, a reliable absolute comparison between our data and those previously obtained in other experiments is possible in only a few cases. Actually, only the Cornell calibration agrees within 2% with the absolute calibration performed by EDWARDS and KERST (²³). Particularly the Caltech monitoring system (^{13,14}) seems to be higher than Cornell by about 7% or more.

For this reason, in the following Table II only the Cornell and Illinois data have been included and averaged according to the total estimated errors. Data and results of other laboratories will be considered for comparison in a final discussion (see Part II).

4. - Partial-Wave Analysis of the Angular Distributions.

As already mentioned [see ref. (¹) and (³)] since the early works by AIZU, FIELD, WATSON and FERMI an analysis of photoproduction in terms of partial waves of definite angular momentum, isospin and parity has been done, more or less completely several times. In the present paper (Part I) we will not make practical use of the details of this analysis. Only a few points of it, which are more closely connected with the discussion of the experimental results, will be summarized for the convenience of the reader.

Actually in what follows we want to show that already the simple analysis in terms of spin and angular momenta limited to $l_{\pi} = 1$ runs into some definite difficulties. It appears that the simplest way of surpassing these difficulties may be found in the introduction of fairly large, but reasonable nucleon recoils.

It is always possible to write the differential cross section in the center of mass system as a function of the photon energy ν and emission angle θ in terms of a series

$$(4) \quad \frac{d\sigma}{d\Omega} = A_0(\nu) + A_1(\nu) \cos \theta + A_2(\nu) \cos^2 \theta + \dots,$$

which is equivalent to an expansion in spherical harmonics, that is, in partial waves corresponding to the various angular momenta.

As already mentioned, we shall be concerned with reaction (3) at not too

TABLE II. — *Center of mass differential*

E_γ (MeV, lab.)	40°	59°	75°	93°	107°
170	—	5.2 ± 0.4	—	5.4 ± 0.4	—
175	—	6.1 ± 0.7	—	6.4 ± 0.4	—
180	—	6.5 ± 0.5	—	7.5 ± 0.4	—
185	6.0 ± 1.4	6.3 ± 1.5	—	6.9 ± 0.8	—
190	—	7.2 ± 0.5	—	9.1 ± 0.5	—
195	7.9 ± 1.7	—	—	9.0 ± 0.7	8.9 ± 0.9
200	7.0 ± 1.1	8.5 ± 0.5	9.5 ± 1.3	9.8 ± 0.6	10.1 ± 0.8
210	—	10.0 ± 0.7	—	12.2 ± 0.7	12.5 ± 1.3
220	—	9.7 ± 0.9	—	13.4 ± 0.7	12.7 ± 1.0
230	—	—	—	—	—
235	9.7 ± 1.1	11.6 ± 1.0	13.3 ± 1.2	—	15.7 ± 0.9
265	8.0 ± 1.0	11.6 ± 1.1	18.2 ± 1.7	—	19.4 ± 1.0

high energies. By «not too high energies», we mean energies such that the multiple photo-production of pions is certainly impossible or negligible. According to the results of some preliminary experiments at Caltech and Stanford ⁽²⁷⁾ that means energies up to at least 400 MeV.

In the energy interval of 150 to 400 MeV the average e.m. size r of the nucleon seems to be $0.7(h/\mu c)$ ⁽²⁸⁾. The corresponding angular momenta of the photons are then $hl \approx (E_\gamma/c)r \leq 2\hbar$. The same conclusion is reached considering the pion angular momenta l_π ⁽³⁾.

It is well known that the previous considerations are connected with some more general speculation on the basis of which one should not expect, from experiments carried out at these energies, any particular information on the more intimate electromagnetic structure of the physical nucleon. Actually, as far as only these low values of the angular momenta are sufficient to describe the mean features of the photopion processes the photon interaction averages in space and time the charge and current distribution of the pion-nucleon system. As already mentioned, this information will be applied to the dynamical properties of the pion-nucleon system and particularly will include the $\frac{3}{2}$ Isospin state. Thus the e.m. pole strengths, which will be mentioned later, will by no means be those of the «frozen» static nucleon. In part II an attempt will be made to correlate these pole strengths with the e.m. constants defining the physical nucleon system.

Fig. 2 presents a plot of the data assembled in Table II. It appears that at each photon energy, the experimental points can be ranged pretty well

⁽²⁷⁾ *Proceedings of the V Annual Conference, Rochester, 1955.*

⁽²⁸⁾ R. HOFSTADTER: *Proceedings of the V Annual Rochester Conference, 1955.*

sections in units $10^{-30} \text{ cm}^2/\text{ster.}$

123°	135°	148°	159°	165°	180°
—	—	—	—	—	—
4 ± 0.7	—	—	—	—	—
6 ± 0.5	—	—	6.6 ± 0.9	—	—
4 ± 0.6	—	8.5 ± 1.3	8.2 ± 0.8	—	—
7 ± 0.6	—	—	7.5 ± 0.6	—	—
9 ± 1.0	—	9.9 ± 1.4	9.0 ± 1.2	—	—
5 ± 0.6	11.9 ± 1.9	—	9.5 ± 0.7	—	—
7 ± 0.7	—	13.7 ± 1.4	10.7 ± 0.8	—	—
1 ± 0.6	—	14.2 ± 1.4	12.1 ± 0.8	12.0 ± 1.2	—
4 ± 0.9	—	—	13.0 ± 1.0	—	—
—	14.8 ± 1.4	15.7 ± 1.1	15.8 ± 1.7	13.4 ± 0.9	11.3 ± 1.2
—	19.9 ± 1.8	18.4 ± 1.3	17.0 ± 2.4	16.9 ± 1.1	14.8 ± 1.5

around a curve resembling a parabola. Hence, we will start by considering as appropriate a partial wave analysis of the experimental data limited to the first three terms in Eq. (4), which is certainly sufficient if only S and P waves contribute to the process. It is still sufficient if one assumes that a D wave is present, but rather small and evident mostly through interference with the large S -wave. We will discuss later the possible contribution of this higher order wave.

For the time being, and for the sake of simplicity, we want to see first what conclusion can be derived from this approach.

Accordingly, standard best-fits to parabolas have been made of the data of Table II (Fig. 2). To visualize better the energy dependence of the A coefficients, the differential C.M.

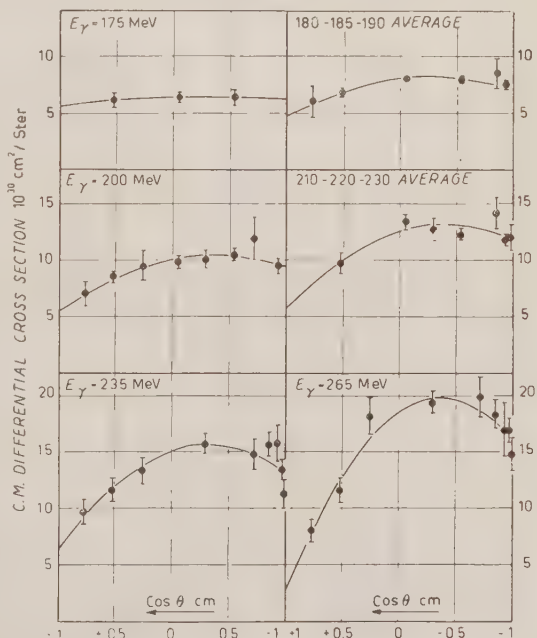


Fig. 2. — Plot of the experimental data of Table II and corresponding best fits of parabolas in $\cos \theta$.

cross section (4) can be written

$$\frac{d\sigma}{d\Omega} = W |T|^2,$$

where

$$(5) \quad W = \eta\omega \left(1 + \frac{\mu}{E_i} v\right)^{-1} \left(1 + \frac{\mu}{E_f} \omega\right)^{-1} \simeq \frac{\eta\omega}{\left(1 + \frac{\mu}{M} v\right)^2},$$

with $\hbar = c = 1$

and η = pion momentum in μc units
 ω = total pion energy in μc^2 units ($\mu c^2 = 139.7$ MeV)
 v = photon energy in μc^2
 E_i, E_f = initial and final total nucleon energy.

all in
center of mass
system

For the energy interval in consideration, we have assumed $E_i \simeq E_f \simeq M$. W is proportional to the density ϱ_F of the final states divided by the relative velocity v_r of the particles in the initial state. Actually

$$\frac{\varrho_F}{v_r} = \frac{\eta\omega\mu^2}{(2\pi)^3} \left(1 + \frac{\mu}{M} \omega\right)^{-1} \left(1 + \frac{\mu}{M} v\right)^{-1},$$

and $T = (\mu/2\pi)H$, where H is the usual matrix element (*).

W will be used instead of the pure statistical factor for the sake of simplicity in the numerical values of the coefficients. We write then

$$(6) \quad |T|^2 = \frac{A_0}{W} + \frac{A_1}{W} \cos \theta + \frac{A_2}{W} \cos^2 \theta = a_0 + a_1 \cos \theta + a_2 \cos^2 \theta.$$

The values of the a coefficients obtained by the best-fits are presented in Table III with the corresponding propagated errors. For convenience also the corresponding total cross-sections are given. The first fact to be noticed is that $a_0 = |T|_{90^\circ}^2$ seems to be constant. A best fit of a horizontal straight line gives

$$(7) \quad a_0 = (14.8 \pm 0.2) \cdot 10^{-30} \text{ cm}^2/\text{ster}.$$

(*) Frequently in recent literature on pion-physics it has been found more convenient to express the matrix element making explicit a factor which is simply $\chi = W/\nu\omega$. As can be seen (see for instance ref. (21)) this χ comes out more naturally than W in a S -matrix type (Møller) expression of the cross-section.

TABLE III. - (Units 10^{-30} cm²/ster).

E_{γ} (MeV, lab.)	W	a_0	a_1	a_2	σ_{total} . 10^{30} cm ²
170	.372	14.6 ± 1.1	—	—	—
175	.428	15.0 ± 0.9	-0.7 ± 2.1	-1.1 ± 5.4	78 ± 7
182.5	.509	14.4 ± 0.6	-2.0 ± 0.9	-2.4 ± 1.6	87 ± 3
192.5	.609	14.8 ± 0.5	$-2.7 \pm .09$	-4.5 ± 1.5	101 ± 4
200	.679	14.8 ± 0.6	-3.0 ± 0.8	-3.6 ± 1.6	116 ± 3
210	.770	15.3 ± 0.7	-2.2 ± 1.2	-4.0 ± 2.1	136 ± 5
220	.861	14.6 ± 0.6	-3.6 ± 1.2	-4.3 ± 1.7	142 ± 6
235	.995	14.9 ± 0.8	-3.4 ± 0.6	-5.1 ± 1.3	167 ± 5
265	1.255	$14.8 \pm .07$	-5.4 ± 0.6	-7.3 ± 1.1	195 ± 6

Because it is found that the internal deviations agree very well with the external one, we thus consider a_0 constant from threshold up to $E_{\gamma} \simeq 265$ MeV. Certainly this seems to be correct, within the limits of the rather small errors. See Fig. 3 (*).

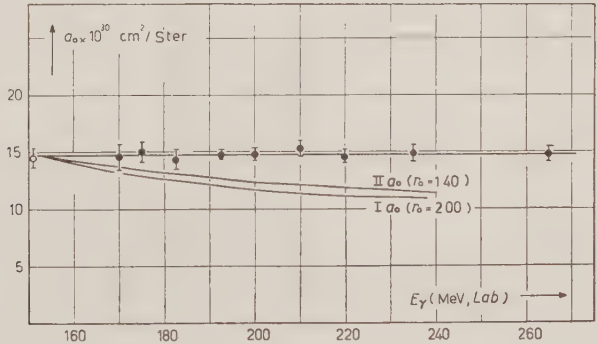


Fig. 3. - Plot of the a_0 coefficient (equ. (6)) versus photon energy.

This is an experimental fact. Because of its role in the following discussion we may add that all other now available experiments give confirmatory evidence; for instance, among those mentioned in the Introduction (and beside the Cornell one), those of the M.I.T. group (17) and Caltech (13,14) (+).

One may observe also that a_0 results (see later) from the summation of

(*) In Fig. 3 the point at $E_{\gamma} = 151.4$ ($\omega = 1$) is due to the threshold experiments of LEISS, PENNER and ROBINSON. Private communication by the authors. See *Washington meeting of the Am. Phys. Soc.*, 1956. The result (7) does not include this value.
(+) Apart from the systematic deviation already mentioned and probably due to the calibration.

several terms, the most important of which is supposed to be that originated by the matrix (1). Another term is the θ independent part of the P -wave, etc.

Unfortunately the other two coefficients a_1 and a_2 are not so well determined (see Fig. 4) but apart from the ν dependence of the S amplitude it is reasonable to believe that a_1 should depend upon η as $\eta^{\nu/2}$ if the a_2 dependence on η is as η'' . Very close to threshold ($E_\gamma \lesssim 180$) the experimental data are obviously unable even to suggest a guess on the behaviour of a_1 and a_2 :

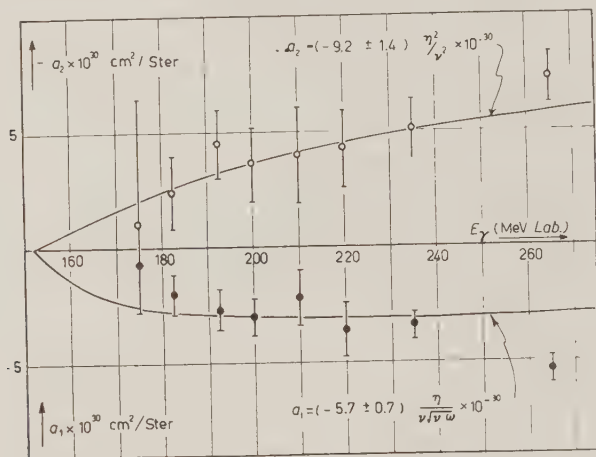


Fig. 4. — Plots of the coefficients, a_1 and a_2 (equ. (6)).

After a few trials it was found that the experimental dependence of the coefficients a_1 and a_2 on the photon energy may be represented (as shown in Fig. 4) by the following expressions:

$$a_1 = (-5.7 \pm 0.7) \frac{\eta}{\nu \sqrt{1-\omega}} \cdot 10^{-30} \text{ cm}^2/\text{ster},$$

$$a_2 = (-9.2 \pm 1.4) \frac{\eta^2}{\nu^2} \cdot 10^{-30} \text{ cm}^2/\text{ster}.$$

These energy dependencies are suggested by the second order perturbation theory, but, of course, here they should only be considered as a convenient empirical way of representing the data between the limits $180 \lesssim E_\gamma \lesssim 240$ MeV. Actually, from time to time (here, and in Part II), the previous values will be used in the discussion.

However it has to be stressed that in the following discussion this empirical representation of a_1 and a_2 does not imply any peculiar consequence. It has

been used only as a convenient way of taking the averaged values of a_1 and a_2 with reasonably estimated errors attached.

The only fact which will be substantially introduced into the discussion is the smallness of a_1 ; a fact again evidenced also by the results of other laboratories.

4.2. — For a full discussion of the a_i coefficients of Eq. (6) it is now convenient to introduce the e.m. multipoles. According to the assumptions, the transition matrix may be thought as split in partial matrices corresponding to transitions among substates of definite total angular momenta, $(J = \frac{1}{2}, \frac{3}{2})$. Further, the parity conservation selects the modes of absorption of the incident e.m. plane wave. In the limits of our assumptions, the relationships between the coefficients of (6) and the angular momenta involved can be explicitly written as follows:

$$(8) \quad \begin{cases} a_0 = E_1 E_1^* + a_{op} - \frac{1}{3} a_{sd}, \\ a_1 = -2 \operatorname{Re} (E_1^* K), \\ a_2 = K K^* - a_{op} + a_{sd}. \end{cases}$$

where $E_1 E_1^* = a_{os} = |S\text{-wave amplitude}|^2$,

$a_{op} = |P\text{-wave amplitude, non spin flipping (*) part}|^2$,

$K K^* = |P\text{-wave, spin flipping part}|^2$,

$a_{sd} = S\text{-}D \text{ interference.}$

The amplitudes can be expressed in terms of e.m. multipoles. The only possible poles involved in the reaction, for the above amplitudes, are those listed for convenience below.

<i>Pion-nucleon state</i>	<i>Photon pole</i>	<i>Parity</i>
$S_{\frac{1}{2}}$	$E_1(\frac{1}{2})$	—
$P_{\frac{1}{2}}$	$M_1(\frac{1}{2})$	+
$P_{\frac{3}{2}}$	$M_1(\frac{3}{2}), E_2(\frac{3}{2})$	+
$D_{\frac{3}{2}}$	$E_1(\frac{3}{2}), M_2(\frac{3}{2})$	—
$D_{\frac{5}{2}}$	$E_3(\frac{5}{2}), M_2(\frac{5}{2})$	—

(*) In the definition of spin flipping and non-flipping terms, we followed here the idea that the term which flips is that which corresponds to a transition to a final nucleon state with spin up (down) if initially the nucleon was down (up). The el. dipole term and all others able to interfere with it are, in that sense, spin flipping. However, frequently and more properly (for instance when many nucleons are present and governed by the action of the Pauli principle) it is correct to define as spin flipping all the interaction terms involving the operator σ , as for instance the term $\sigma \cdot (\mathbf{v} \times \boldsymbol{\epsilon}) \times \boldsymbol{\eta}$ which occurs (see later) in both the $M(\frac{1}{2})$ and $M(\frac{3}{2})$ induced transitions.

The symbol $E_1(\frac{1}{2})$ refers to the electric dipole transition with total $J = \frac{1}{2}$ angular momentum, (change in parity), $M_1(\frac{3}{2})$ refers to the magnetic dipole transition with total angular momentum, $J = \frac{3}{2}$ (no change in parity) etc.

Now, on the basis of the S -matrix formalism (see also later) it was originally pointed out by FERMI⁽²⁹⁾, GELL-MANN and WATSON⁽³⁾ that, at *low energies* ($E_\gamma \lesssim 240$ MeV) the matrices E_1 , M_1 etc., and hence E_1 , K etc. are *almost* real. Precisely the complex parts of each multipole matrix element are phase factors $\exp[ix_{2I,2J}]$ where $\alpha_{2I,2J}$ are (in Fermi's notation) the scattering phase shifts of the substates (I = Isotopic spin, J = total angular momentum) in which the pion may be produced. In the energy region of interest, where the largest phase shift is $\alpha_{33} \lesssim 10^\circ$, we can assume $\sin \alpha_{2I,2J} \simeq 0$.

In comparing our data with the set of equations (8), we start with the simplest approach, i.e. by assuming that a_{sd} is negligible *and* that the main part of the S -wave is due to the gauge-invariance term included in (2), i.e.: $G_{os}/\nu()$. As is shown by (2) this is equivalent to assuming that $M \rightarrow \infty$. In other words for the time being we assume $l_\pi \lesssim 1$ and we neglect the nucleon recoils. The coefficient G_{os} is supposed to be constant at least up to the point at which the Hamiltonian (1) still represents a good approximation ($\alpha_{33} \lesssim 90^\circ$, $E_\gamma \leq 350$ MeV).

In the limits of these assumptions, the value of G_{os} can be directly evaluated by the threshold value of a_0 and one has $G_{os} = (14.8 \pm 0.2)\nu_i \cdot 10^{-30}$ cm² where $\nu_i = .93$ is the center of mass threshold photon energy.

Equation (8) should then be written

$$(9) \quad \begin{cases} a_0 = \frac{G_{os}}{\nu()} + a_{op}, \\ a_1 = -2E_1K = -2\sqrt{\frac{G_{os}}{\nu()}}K, \\ a_2 = K^2 - a_{op}, \end{cases}$$

and one gets

$$(10) \quad K^2 = a_2 + a_{op} = a_0 + a_2 - \frac{G_{os}}{\nu()}.$$

This value, when substituted into the second eq. of (9) seems to be too large to be compatible with the experimental results. This is indicated in Table IV where the experimental values of a_1 listed in the first line are compared with those calculated by (10) and given in the second line. It turns out that the

⁽²⁹⁾ E. FERMI, unpublished: Dr. A. H. ROSENFELD kindly sent the authors a photostatic copy of the C-18 notes made by FERMI in preparation for the Summer Schools of Les Houches and Varenna, 1954.

TABLE IV. - (*Units* 10^{-30} cm²/ster).

E_γ (Mev, lab.)	a_1 (exper.)	a_1 (calc.)
175	-0.7 ± 2.1	-10.2 ± 12.0
182.5	-2.0 ± 0.9	-8.7 ± 3.9
192.5	-2.7 ± 0.9	-4.5 ± 6.5
200	-3.0 ± 0.8	-8.7 ± 3.4
210	-2.2 ± 1.2	-9.0 ± 3.9
220	-3.6 ± 1.2	-9.4 ± 2.1
235	-3.4 ± 0.6	-8.7 ± 2.0

probability of getting, as an experimental fluctuation, the a_1 (exp.) instead of the expected values a_1 (calc.) given by (10) is *less than* 10^{-5} .

It seems thus evident that the presumption of giving a consistent interpretation of the experimental data based on the oversimplified and overdetermined set of equations (9) should be abandoned.

A new parameter can plausibly be introduced into (9) either including, still according to expansion (6), an a_{sl} term as was done in (8), or a term which takes into account the nucleon recoils. The second does not exclude the first.

However, it should be pointed out that an a_{sl} term, in order to save the consistency of equations (9), cannot be too small. Precisely, a reasonable fit of the data gives a D -amplitude whose averaged value amounts to about 20% of the P -wave. This seems to be higher than the upper limit established by the scattering experiments⁽³⁰⁾.

Hence, the most plausible (*) introduction of higher order waves into (9) can be obtained by calling upon the direct photon interaction with the pion-current. This is the matrix

$$(11) \quad \mathcal{H} = -i \frac{2\pi ef}{\mu^2} \sqrt{\frac{2}{v\omega}} \frac{\boldsymbol{\sigma} \cdot (\boldsymbol{\eta} - \boldsymbol{v}) \boldsymbol{\epsilon} \cdot \boldsymbol{\eta}}{v^2(1 - v \cos \theta)}.$$

Here, besides the notations already used such as the nucleon spin $\boldsymbol{\sigma}$ and the photon polarization $\boldsymbol{\epsilon}$, we have v = pion velocity ($\hbar = c = 1$). Again

⁽³⁰⁾ L. FERRETTI, E. MANARESI, G. PUPPI, A. RANZI and G. QUARENI: *Nuovo Cimento*, **1**, 1239 (1955); M. O. STERN *et al.*: *Bull. Am. Phys. Soc.*, Z6, Series II, vol. 1, Jan., 1956.

(*) One may argue that the pion-scattering results do not rule out the possibility of some D -waves originated by $E_1(\frac{3}{2})$, $M_2(\frac{3}{2})$, etc. ... and not included in (11). This would be equivalent to the introduction of a strong contribution of the nucleon core structure. Considering that $1/\mu\nu > 1/M$ the use of (11) and the inclusion of nucleon recoils seems more plausible.

here the discussion concerns the low energies only. A more complete discussion of the influence of (11) on the features of photoproduction following the lines of Chew and Low papers (⁴) will be found in part II.

The operator (11) includes all orbital angular momenta. They are sizeable up to the higher orders so that it should be more correct to take into account the whole term without any limitations to the lower values of l_π . But this term, in our energy interval, gives appreciable deviations from the parabolic trend of the angular distributions only for the center of mass angles $\theta < 30^\circ$ (³¹). So the inclusion of \mathcal{H} in T can be accomplished, with a good approximation, taking into account only the projected S and P operators and that term of the angular momentum development of \mathcal{H} which originates in T^2 the S - D interference term. The details of this calculation are given for the convenience of the reader in the Appendix. The result is that, neglecting powers of r greater than two, the coefficients a_i must be written [see eq. (A.7) of the Appendix]

$$(12) \quad \begin{cases} a_0 = a_{os} + A, \\ a_1 = -2K'\sqrt{a_{os}}\left(1 - \frac{v^2}{3}\right), \\ a_2 = K'^2 - A, \end{cases}$$

where $a_{os} = G_{os}/v\omega$, K' is the phenomenological spin-flipping p -wave and A includes the phenomenological p -wave, the S - P and S - D interference term of the term (11) plus the interference between the phenomenological p -wave and the s -wave of the term (11). Because G_{os} is *a priori* known from the threshold extrapolation of the first equation, (12) is again a set of equations over-determinable with respect to the unknowns A and K' . So, by means of set (12), it is still possible to calculate a_1 in terms of a_0 and a_2 . The a_1 (calc.) in this case is, at 235 MeV, about 8% smaller than the corresponding value calculated neglecting the term (11) (see Table): this difference is smaller at lower energy. *In conclusion, one finds that, up to terms in v^2 , the introduction of (11) into T does not affect the energy dependence of the coefficients K and a_{op} to such an extent as to explain the above mentioned inconsistency.*

4.3. — The preceding considerations show that the introduction of the matrix (11) does not appreciably change the structure of set (9).

Moreover the previous discussion shows the opportunity of omitting the a_{s1} term in (8). Simultaneously the set of equations (8) may be solved at each energy interval, with respect to the unknowns E_1 , a_{op} and K ; i.e. it is possible

(³¹) K. M. WATSON, J. C. KECK, A. V. TOLLESTRUP and R. L. WALKER: *Phys. Rev.*, **101**, 1159 (1956).

to derive from the experimental values of the coefficients $a_i(\nu)$ the S term and the flipping and non flipping P terms. These terms are given in Table V.

TABLE V.

E_γ (MeV, lab.)	$E_1^2 \cdot 10^{30}$ cm ² /ster	$a_{op} \cdot 10^{30}$ cm ² /ster	$K \cdot 10^{15}$ $\sqrt{\text{cm}^2/\text{ster}}$
175	13.9 ± 4.7	1.1 ± 5.4	$.09 \pm .30$
182.5	11.9 ± 1.4	2.5 ± 1.6	$.29 \pm .12$
192.5	10.1 ± 1.3	4.7 ± 1.5	$.42 \pm .16$
200	11.0 ± 1.4	3.8 ± 1.7	$.45 \pm .13$
210	11.2 ± 1.7	4.1 ± 2.2	$.33 \pm .21$
220	10.0 ± 1.8	4.6 ± 2.0	$.57 \pm .22$
235	9.5 ± 0.9	5.4 ± 1.5	$.55 \pm .13$

Of course one should abandon the presumption of determining «a priori» by gauge invariance ($M \rightarrow \infty$) the full expression for E_1 .

To make clear a point of the following discussion and also for an argument developed in Part II, it has to be noticed that K^2 is very small in comparison with a_2 . This is again an experimental fact which comes directly from the smallness of a_1 and the large S -wave amplitude.

5. — The Nucleon Recoils.

5.1. — As a consequence of the preceding argument, one may consider, as a more plausible way of interpreting the experimental results, the introduction of appreciable nucleon recoils also at very low energies. The importance of these recoils is directly indicated by the values of the σ^-/σ^+ ratio of the cross sections of photoproduction of pions by neutrons and protons. The large value of this ratio also very near threshold ⁽³²⁾, shows for instance that G_1 and G_2 in eq. (2) cannot be negligible. More generally the σ^-/σ^+ ratio indicates the presence of a symmetric term in the matrix element. Consequently, also very close to threshold, set (9) is erroneous and one may write instead

$$(13) \quad \begin{cases} a_0^\pm = (S \mp R)^2 + a_{op}, \\ a_1^\pm = -2(S \mp R)K, \\ a_2 = K^2 - a_{op} \simeq -a_{op}. \end{cases}$$

⁽³²⁾ M. SANDS, J. G. TEASDALE and R. L. WALKER: *Phys. Rev.*, **95**, 592 (1954); M. BENEVENTANO, G. BERNARDINI, D. CARLSON-LEE, E. L. GOLDWASSER, G. STOPPINI: *Nuovo Cimento*, **12**, 156 (1954); D. CARLSON-LEE, G. STOPPINI and L. TAU: *Nuovo Cimento*, **2**, 162 (1955); M. BENEVENTANO, G. BERNARDINI, D. CARLSON-LEE, G. STOPPINI and L. TAU: *Proceeding of International Conference, Pisa, 1955*, and forthcoming paper in *Nuovo Cimento*.

Here R is a pure recoil term (i.e. $\lim_{M \rightarrow \infty} R = 0$) and is the part of the recoil which arises from that term of the Hamiltonian which is invariant with respect to rotations in isotopic spin space (*).

As far as the S term is concerned, according to the Kroll-Rudermann theorem, we know that at threshold

$$(14) \quad \lim_{(\mu/M) \rightarrow 0} S = \sqrt{\frac{\bar{G}_{os}}{\nu\omega}} = \frac{g_{os}}{\sqrt{\nu\omega}},$$

where $g_{os}/\sqrt{\nu\omega}$ is the numerical value of the matrix element arising from the gauge invariance transformation. Thus, because of the sumability of the currents one can write

$$(15) \quad S = \frac{g_{os}}{\sqrt{\nu\omega}} + \varrho,$$

where ϱ is the part of recoil arising from the term of the Hamiltonian which behaves as the third component of a isotopic spin vector⁽³³⁾. If one wants to extract explicitly the dependence of R and ϱ respect to $\omega^* = \omega\mu/M$, obviously one can always write

$$(16) \quad \left\{ \begin{array}{l} R = \frac{\mu}{M} \{R_0 + R_1\omega^* + R_2\omega^{*2} + \dots\}, \\ \varrho = \frac{\mu}{M} \{\varrho_0 + \varrho_1\omega^* + \varrho_2\omega^{*2} + \dots\}. \end{array} \right.$$

In a perturbative approximation of the PSPS renormalized theory, the coefficients of these power expansions would be constant⁽³⁴⁾, but we will consider them as unknown functions of the energy. Thus, close to the threshold,

$$\begin{aligned} (S - R)^2 &= \frac{1}{\nu\omega} \{g_{os} + \varrho\omega - R\omega\}^2 = \frac{1}{\nu\omega} \{g_{os} + \varrho_0\omega^* + \dots - R_0\omega^* - \dots\}^2 = \\ &= \frac{1}{\nu\omega} \{G_{os} + 2g_{os}(\varrho_0 - R_0)\omega^* + H_1\}, \end{aligned}$$

(*) Frequently the \pm sign instead of being applied to R is displaced to S . For instance, this is suggested by the idea that at the limits $\mu/M \rightarrow 0$ the proton neutron gauge invariance amplitudes should be opposite in sign. In what follows, it seemed more convenient to apply the sign to the recoil R .

⁽³³⁾ K. WATSON: *Phys. Rev.*, **85**, 852 (1952).

⁽³⁴⁾ A. KLEIN: *Phys. Rev.*, **99**, 998 (1955).

for positive pions, and

$$\begin{aligned}(S + R)^2 &= \frac{1}{\nu\omega} \{g_{0s} + \varrho\omega + R\omega\}^2 = \frac{1}{\nu\omega} \{g_{0s} + \varrho_0\omega^* + \dots + R_0\omega^* + \dots\}^2 = \\ &= \frac{1}{\nu\omega} \{G_{0s} + 2g_{0s}(\varrho_0 + R_0)\omega^* + H_2\},\end{aligned}$$

for negative pions. As a direct consequence of the Kroll-Rudermann theorem we obtain $\varrho_0(\omega \rightarrow 1) = 0$ and $G_1(\omega \rightarrow 1) = 2g_{0s}R_0(\omega \rightarrow 1)$.

Hence, at threshold, ϱ has to be an order in μ/M smaller than R and the changing sign part of the recoiling term is practically the first term of the R expansion (16). This conclusion may be considered correct as far as $G_1 \simeq -G_2$. Plausibly this is true also *near* threshold, that is in the energy interval considered in this paper. Thus it seems better to consider R instead of G_1 as done previously ⁽²¹⁾ because R includes automatically terms contained in H_1 and H_2 of eq. (2).

5.2. - Obviously in (13) only the s -wave recoils are considered. Thus one may expect that (13) gives the correct modification of set (9) only close to threshold. A simple consideration concerning the angular dependence of the ratio $\sigma^-(\theta)/\sigma^+(\theta)$ shows that it would be even better to say «quite close to threshold». Actually this ratio depends strongly on θ ⁽³²⁾ already at fairly low energies ($E_\gamma \simeq 250$ MeV) and its angular asymmetry is certainly due to *recoils* associated with p or higher order waves. As a matter of fact one may immediately verify without any assumption about the structure of the S and R terms that (13) is unable to account for this now mentioned asymmetry. Let us call r the value of $\sigma^-(\theta)/\sigma^+(\theta)$ at 90° center of mass: by the use of (13) (where $K = K^+ = K^-$ and $a_{op}^- = a_{op}^+$) one has, independently of the form of S and R ,

$$(17) \quad a_1^- = a_1^+ \sqrt{\frac{r - (a_{op}/a_0)}{1 - (a_{op}/a_0)}},$$

that is

$$(18) \quad \frac{\sigma^-(\theta)}{\sigma^+(\theta)} = \frac{ra_0 + a_1 \sqrt{\frac{r - (a_{op}/a_0)}{1 - (a_{op}/a_0)}} \cos \theta + a_2 \cos^2 \theta}{a_0 + a_1 \cos \theta + a_2 \cos^2 \theta}.$$

In Table VI the values of r are ranged versus photon energy E_γ and obviously since r decreases with E_γ the asymmetry indicated by (18) is just the opposite of the observed one (*). In the same table a few calculated and observed values

(*) At higher energies the discrepancy is worse. See ref. ⁽³²⁾.

TABLE VI.

E_γ (MeV, lab.)	r	59°		123°		159°	
		calc.	exper.	calc.	exper.	calc.	exper.
170	$1.50 \pm .15$	1.54	$1.67 \pm .19$	—	—	—	—
185	$1.41 \pm .07$	1.45	$1.26 \pm .08$	1.41	$1.40 \pm .07$	—	—
205	$1.15 \pm .06$	1.17	$1.21 \pm .09$	1.16	$1.31 \pm .08$	1.18	$1.42 \pm .09$
225	$1.12 \pm .06$	1.14	$1.07 \pm .10$	1.13	$1.34 \pm .07$	1.15	$1.44 \pm .08$

of σ/σ^+ are given for comparison. It seems then plausible that the observed asymmetry has its origin in the influence of some p -wave recoils. Actually it was found that an appreciable nucleon recoil in the K (spin-flipping) term such that $K^- = 1.5K^+$ is able to account for the observed angular distribution (*). It must be noted for the sake of consistency that this value of the ratio K^-/K^+ does not invalidate the condition $|K^-|^2 \ll a_2$.

Precisely, one sees ⁽³²⁾ that up to $E_\gamma \simeq 240$ MeV still $a_{op}^+ \simeq a_{op}^- \simeq -a_2$ with an error of $\sim 5\%$. Nucleon recoils as large as the K term itself were also introduced in KECK *et al.* ⁽³¹⁾. The previous discussion aims only to emphasize the timeliness of this point of view.

5.3. — A proper evaluation of R and S at threshold would be of great interest. With the well established constancy of a_0 , the knowledge of R and ϱ would permit, on the basis of the Kroll-Rudermann theorem, the proper determination of the interaction constant. However the preceding section points out that even if more extensive and more precise experimental results were available, the separation of the s -wave recoiling term would run into some difficulties. Precisely, this separation has to be based on an extrapolation to threshold of the σ^-/σ^+ ratio. But, from the high energy side the influence of p -waves recoils is already felt even at fairly low energies, while toward threshold the Coulomb effect (which is appreciable and vaguely known) diminishes the value of the deuterium experiment. However, if we consider only the 90° values of σ^-/σ^+ where interference effects disappear and with the limit-

(*) This point will be extensively discussed in a forthcoming paper (ref. ⁽³²⁾) and in Part II. Here one may observe that there are reasons to believe (see for instance ref. ⁽⁴⁾) that the quadrupole $E_2(\frac{3}{2})$ is rather small in comparison with M_1 . Hence near threshold, in order to make K small, $M_1(\frac{1}{2})$ and $M_1(\frac{3}{2})$ should be of the same magnitude, but not necessarily small. On the other hand they certainly contain the matrix element of the photon absorption due to the intrinsic magnetic moment of the nucleon. This is just a recoil term which changes sign with respect to the interchange of the proton and neutron. To introduce the required asymmetry in eq. (18) one should admit that the two recoils in $M_1(\frac{1}{2})$ and $M_1(\frac{3}{2})$ have different energy dependences. This seems plausible because of the quite different behaviour of the two phases α_{33} and α_{13} .

ation to an intermediate energy interval ($180 \text{ MeV} \lesssim E_\gamma \lesssim 240 \text{ MeV}$), one might think that the influence of the above mentioned errors can be attenuated.

Actually at 185, 205, 225 MeV photon energy the Coulomb corrections have been estimated to be respectively 7.4 and 3% (*). On the other hand, in the above energy interval, it can be considered as a good enough approximation to include the total effect of the p -wave recoil in the spin flipping part so one can write from (13)

$$(19) \quad R = \frac{1}{2}\sqrt{a_0} \left\{ \sqrt{r - \frac{a_{op}}{a_0}} - \sqrt{1 - \frac{a_{op}}{a_0}} \right\},$$

independently of any structure of S . In the sense clarified above one can think of r as a direct measure of R . In Table VII are listed some values of R corresponding to four different energies. From (19), R results a definitely decreasing function of the energy because experimentally r is just decreasing

TABLE VII. - (Units 10^{-15} cm).

E_γ (MeV, lab.)	R	S	$g_{\pi\pi}/\sqrt{\nu\omega}$
170	$.46 \pm .12$	$4.07 \pm .15$	$3.83 \pm .15$
185	$.39 \pm .06$	$3.86 \pm .14$	$3.82 \pm .14$
205	$.16 \pm .06$	$3.46 \pm .19$	$3.51 \pm .18$
225	$.14 \pm .06$	$3.31 \pm .23$	$3.25 \pm .23$

while a_{op} is increasing. It should be noted that this conclusion is based on two experimental results i.e. the constancy of a_0 , and the behaviour of σ^-/σ^+ at 90° where better data are available, and where Caltech results are in good agreement with ours.

(*) These figures are based on an rough estimate made by Professors G. F. CHEW and F. Low. Not published, see ref. (32).

Note added in proof.

At the CERN Conference—Geneva, June 1956—BALDIN reported a more accurate evaluation of the influence of the final states on the photopion production in deuterium. The conclusion seems to be (differently from the CHEW and Low estimate) that for the energies here considered the main correction to be taken into account is that due to the final two-nucleons state. As already pointed out by OREAR this correction tends to raise up instead to push down the value of the σ^-/σ^+ ratio for free nucleons, but again, at the energies here considered it is quite small (some percents).

Under the present circumstances it has been considered quite safe and more correct to neglect any type of correction. Of course this attitude would be wrong if values of σ^-/σ^+ ratio for photon energies lower than $E_\gamma \simeq 165 \text{ MeV}$ would have been included in the extrapolation to threshold, but this is not our case.

On the other hand

$$(20) \quad S = \frac{g_{os}}{\sqrt{\nu\omega}} + \varrho = \frac{\sqrt{a_0}}{2} \left\{ \sqrt{r - \frac{a_{op}}{a_0}} + \sqrt{1 - \frac{a_{op}}{a_0}} \right\}.$$

Because of the different energy dependence expected for the «static» term $g_{os}/\sqrt{\nu\omega}$ and for the «dynamic» one ϱ , it may be feasible to separate the two terms. According to the Kroll-Rudermann theorem this possibility of separation would allow a proper measurement of the interaction constant. Probably soon, very accurate measurements of a_0 , a_2 and r between $180 \div 240$ MeV will be possible. They would offer a way of determining each part of the s -wave matrix element, because of the smallness of the Coulomb corrections and because in this energy interval the P -wave recoil can be confined in the spin-flipping part and measured from the angular dependence of σ^-/σ^+ . Some values of S are given in Table VII, third column.

5.4. — At present the accuracy in the measurements of a_0 , a_2 and r is not sufficient for the above outlined analysis. Thus, for the time being, only a very crude treatment of the data seems to have some sense. Accordingly, we assume that ϱ is negligible with respect to R (i.e. we assume that in eq. (2) $H_1 = H_2$). This assumption, which is somewhat justified by the idea that, at threshold, ϱ should be an order smaller than R , is, as will be seen later, correct within the error limits. With this approximation the σ^-/σ^+ ratio at 90° centre of mass can be expressed as follows

$$(21) \quad r = \frac{1}{a_0} \left\{ \sqrt{\frac{a_0 \nu_0}{\nu\omega}} (1 + \sqrt{r_0}) - \sqrt{a_0 + a_2} \right\}^2 - \frac{a_2}{a_0},$$

where r_0 is the value of σ^-/σ^+ at threshold.

This formula is merely an *empirical* formula from which the influence of the pure P -wave term a_2 is properly subtracted. No particular assumptions are given as to the dependence of r or R on ω except the oversimplifications indicated previously. The purpose of using (21) is merely to find the upper energy limits for which the data can be used for the evaluation of $R(\omega - 1)$. In this sense, a first check of (21) is to find out up to what energy (18) gives, within the error limits, a constant value of r_0 . The r values obtained by the deuterium experiment (*) are given in Table VIII together with the corresponding values of r_0 .

(*) See ref. (32).

TABLE VIII.

E_γ (MeV, lab.)	170	185	205	225
r	$1.50 \pm .15$	$1.41 \pm .07$	$1.15 \pm .06$	$1.12 \pm .06$
r_0	$1.82 \pm .22$	$1.93 \pm .22$	$1.78 \pm .33$	$2.00 \pm .47$

From this table one has $r_0 = 1.87 \pm .13$. The corresponding trend of r is shown by the solid line of Fig. 5. From this, we can say that, up to $E_\gamma \simeq 240$ MeV, r depends essentially on the s -wave recoils and that the use of the empirical formula (21) is somewhat justified.

As was expected, when this value of r_0 is introduced in the expression for R and the corresponding R 's are used for set (8) the inconsistency presented in Table V is eliminated.

Knowing r_0 one is able to estimate R and g_{os} : With $r_0 = 1.87 \pm .13$ one finds

$$R(\omega = 1) = \frac{1}{2}\sqrt{a_0v_t}(\sqrt{r_0} - 1) = (.68 \pm .09) \cdot 10^{-15} \text{ cm} ,$$
$$g_{os} = \frac{1}{2}\sqrt{a_0v_t}(\sqrt{r_0} + 1) = (4.39 \pm .09) \cdot 10^{-15} \text{ cm} .$$

In Table VII, column 4, are given the values of S obtained directly from the g_0 , calculated above. It is seen that the S values of the third and fourth columns are practically coincident. This means that *within the error limits* q is negligible. This means also that *the clue for resolving the quite disturbing energy dependence indicated by (19) is not q but the neglected higher order terms of R .*

From the above value of G_{os} the interaction constant in the (PS, PV) coupling turns out to be

$$f^2 = g^2 \left(\frac{\mu}{2M} \right)^2 = .067 \pm .003 ,$$

where g , is the renormalized (PS, PS) interaction constant of equation (1). As is well known, the two constants are related through the equivalence theorem.

5.5. - The net result of the preceding analysis is merely the following: *the observed angular distributions for photopions produced by*

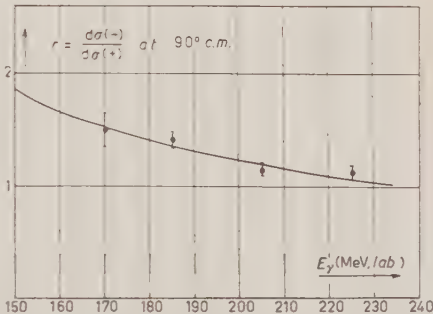


Fig. 5. - Plot of the ratio $r = \sigma^- / \sigma^+$ at 90° center of mass versus photon energy. The solid line is calculated by formula (21) using $r_0 = 1.87 \pm .13$ as threshold value.

protons can be explained by the use of an appropriate value of r_0 . This value was not picked up «ad hoc» but is the result of measurements on deuterium at energies where the influence of binding and Coulomb forces is supposed to be, within the limits of the experimental errors small and properly estimated. Further, the extrapolation to zero energy was based on the hydrogen experiment only.

This value of r_0 is very high. Particularly it is much higher than that predicted by the perturbation theory ⁽³⁴⁾. It is also higher than the value given by a straight linear extrapolation to zero of the deuterium σ^-/σ^+ ratio. Actually, the above mentioned linear extrapolation gives $r_0 = 1.65 \pm .15$. However, a large value of r_0 has the great advantage of making the analysis of the s -wave phase shifts ⁽³⁵⁾ more consistent. Precisely, one may apply again the Anderson-Fermi argument ⁽³⁶⁾. The difference lies now on the fact that (as indicated by Fig. 3) one may consider the extrapolated value of $(1/W)\sigma_r(p^\gamma|n^+)$ for $\eta \rightarrow 0$ which is now quite well determined.

The most recent value ⁽³⁷⁾ of the s -wave phase shifts is $(\alpha_1 - \alpha_3)/\eta = 0.27 \pm .03$.

The value of the Panofsky branching ratio suggested by recent experiments is ⁽³⁸⁾

$$\frac{\langle p^- | n^0 \rangle^2}{\langle p^- | n^\gamma \rangle^2} = 1.25.$$

The corresponding value of r_0 could be $r_0 = 2.11$ with an estimated error of about 25%. It is then consistent with the high value of r_0 previously mentioned.

An even better agreement between the values of r_0 given by scattering and photoproduction will be obtained using the argument recently developed by NOYES ⁽³⁵⁾.

It may be convenient to remember that because the approximation of cutting off the series development of (16) at the first term with $R_0 = \text{const.}$ (i.e. of putting $R = R_{0\mu}/M$) is inadequate (*), formula (19) does not aim at all to represent properly the energy dependence of R . It may be worthwhile to notice that independently of the value of R_0 , whether large or not, the approximation $R = R_{0\mu}/M = \text{const.}$ seems to be almost excluded by the fact that a_0 is constant up to 265 MeV. This is shown in Fig. 3 where curve II

⁽³⁵⁾ H. P. NOYES: *Phys. Rev.*, **101**, 320 (1956).

⁽³⁶⁾ H. L. ANDERSON and E. FERMI: *Phys. Rev.*, **86**, 794 (1952).

⁽³⁷⁾ L. LEDERMAN: *Phys. Rev.*, and *Proceedings VI Annual Rochester Conference*, April 1956.

⁽³⁸⁾ CASSEL and PANOFSKY: *Proceedings of VI Annual Rochester Conference*, 1956. It is likely that the total error is less than 20%.

Accordingly the NOYES argument the value of r_0 should be corrected as a consequence of the influence of the $\pi^+\pi^0$ mass difference on the total isospin conservation.

(*) Such an assumption was also followed recently by KLEIN.

represents the expected trend of a_0 when it is assumed $r_0 = 1.40$, while curve I is calculated taking $r_0 = 2.00$. Obviously, the introduction of p -wave recoils does not change this conclusion because, as long as K^2 is negligible or small, the p -wave included in a_0 is given directly by a_2 .

6. - Criticism and Conclusions.

In making some concluding remarks one may emphasize that the preceding discussion rests on some very simple considerations. Thus it would appear that the conclusions should be considered mostly correct. However, the second and third coefficient of (6), as already mentioned, and other parameters which have been analyzed during the discussion are subject to quite large errors. Thus one may feel that some systematic error which has been overlooked could make most of the points which have arisen in discussion meaningless.

Now it is clear that as far as concerns the experimental results, the discussion is based on the following points:

- 1) The constancy of a_0 .
- 2) The smallness of a_1 .
- 3) The large average value of σ^-/σ^+ around $E_Y \simeq 200$ MeV and the assumption that at this energy the corrections due to the (Coulomb) interaction cannot be higher than about 5%.

Beside the agreement with results of other experiments in support of the points 1) and 2) we may add that in this particular work the pion detection was practically independent of the Laboratory pion-energy and the same can be said for the deuterium experiment from which the value of r was derived. Actually the pellicles were quite uniform in background and development except at the forward angles or in the pellicle edges facing the target. Here the heavy background could have been somewhat dangerous in reducing the scanning efficiency. But at the forward angles this supposed error would increase apparently the forward-backward asymmetry and hence the apparent value of a_1 .

The edge effect actually would decrease the value of a_0 near threshold but it was confined in a very narrow region of the plates and its influence was certainly negligible. Anyhow, in the somewhat complementary experiment performed with *plates* by BERNARDINI and GOLDWASSER (see ref. (16) and forthcoming paper) a systematic error was expected in just the opposite direction and instead, the results of the two experiments are in excellent agreement.

One might also notice in Fig. 2 the slightly erratic distribution of experimental points at backward angles. We believe that this is due to the fact

that counter and pellicles experiments have been overlapped. At low energies and backward angles pion detection by counters is usually rather difficult. It has been checked that at $E_\gamma \approx 235$ if the 180° point is dropped, the behaviour of a_1 remains practically unchanged.

About point 3) independently of any calculations one may observe that the strongest influence of the Coulomb force is expected for the forward pion-angles because of the lower velocities of the corresponding recoiling nucleons. Instead the ratio σ^-/σ^+ is very large just for the backward pion angles where the kinematic energy of the recoiling nucleons is much larger than the deuterium binding energy even for photon-energies quite close to threshold.

Beside this point, one should admit that the quite large value of σ^-/σ^+ may be somewhat striking. At present it seems very difficult to find any plausible explanation of this fact.

However, it may be pointed out that several determinations of the interaction constant based on pion-nucleon scattering (*) systematically give a value of f^2 around 0.08 ± 0.01 . Instead, by using the value of r_0 imposed by perturbation theory (³⁴), i.e., $r_0 = 1.35$ the value of f^2 determined from the threshold cross-section of charged photopions drops to the very low value $f^2 = 0.056 \pm 0.005$.

* * *

This work was possible only with the invaluable and extremely friendly cooperation of all the Betatron group of the University of Illinois, Urbana, Illinois.

We want to express particularly our warm thanks to Professor A. O. HANSON, who in studying the photodisintegration of deuterium devised the pellicle experiment and to Professor E. L. GOLDWASSER and Dr. R. REITZ for their important contribution to the execution of the experiment itself. In the discussion and in the analysis of the data suggestions advice and criticisms by Professor GOLDWASSER have been most useful.

All the crew of the 300 MeV Bevatron were, as usual, extremely cooperative. To the Chief Engineer, Mr. T. ELFE, and to his mastery is due the good performance of the experiment.

The skilfulness and efficiency of all the Rome scanners and particularly of Mrs. O. MENDOLA, G. SALERNO and G. SANTACROCE was really remarkable.

(*) We refer here not only to quite a few of the most recent papers on the behaviour of α_{33} and to its connection with the Chew-Low scattering length extrapolation, but also to more recent works where the most general dispersion relationships have been used. See for instance ANDERSON, DAVIDOW and KRUSE: *Phys. Rev.*, **100**, 339 (1955), and the *Report of the VI Annual Rochester Conference*, 1956.

Quite frequently they told us how to improve the technique and speed of scanning.

During the discussion of the results the authors have been many times enlightened by suggestions, advice and criticism by Professors CHEW, LOW, TOUSCHEK and WATSON.

A critical reading of the manuscript by Professors CHEW and GOLDWASSER has been very useful and extremely appreciated.

APPENDIX

This appendix concerns the paragraph of the section on partial wave analysis. Its purpose is to give the derivation of the set (12) in some detail. In other words, we want to show that in the energy interval which has been considered, i.e. up to 230 MeV, the direct photon-pion current interaction expressed by the matrix (11) of the text, does not help in solving the contradictions found in comparing the set of equations (8) with the experimental data. The inclusion of (11) in the interaction does not affect any conclusion reached in the discussion.

The calculation involves practically only elementary algebra and is rather tedious. However, some of the conclusions reached in the paper may appear somewhat unorthodox. Thus it was felt that to facilitate any criticism it would have been better to display in full how the evaluations have been performed. As already quoted a similar evaluation was done by WALKER *et al.* ⁽¹⁾.

For the sake of simplicity we will consider at the moment only the matrix corresponding to the two following diagrams.

We then write

$$(A.1) \quad \mathcal{T} = i\alpha \left\{ \boldsymbol{\sigma} \cdot \boldsymbol{\epsilon} + \frac{\boldsymbol{\sigma} \cdot (\boldsymbol{v} - \boldsymbol{\eta}) \boldsymbol{\epsilon} \cdot \boldsymbol{\eta}}{v^2(1 - v \cos \theta)} \right\},$$

and, in order to compare this with the matrix element T given by (6) of the text, we must put:

$$\alpha = \frac{ef}{\mu} \sqrt{\frac{2}{v\omega}}.$$

In other words to avoid useless complications in performing the evaluations, we start by considering only the first order PS(PV) operator and a nucleon mass $M \rightarrow \infty$. In this way we shall obtain the corrections required by the phenomenological matrix when the operator (11) is added.

Now, (A.1) can be expanded in angular momentum eigenfunctions.

$$(A.2) \quad \mathcal{T} = \sum_{l, |m| \leq l} c_{l,m} Y_{l,m},$$



where

$$c_{l,m} = \frac{\int d\Omega \mathcal{T} Y_{l,m}^*}{\int d\Omega Y_{l,m} Y_{l,m}^*},$$

and one has

$$c_{0,0} = i\alpha\sqrt{4\pi} \left[1 - \frac{v^2}{4} F(v) \right] \boldsymbol{\sigma} \cdot \boldsymbol{\epsilon}, \quad c_{1,1} = -c_{1,-1} = -i\alpha \sqrt{\frac{2\pi}{3}} \frac{v}{v} \boldsymbol{\sigma} \cdot \mathbf{v},$$

$$c_{1,0} = -i\alpha \frac{\sqrt{3\pi}}{2} v^2 G(v) \boldsymbol{\sigma} \cdot \boldsymbol{\epsilon}, \quad c_{2,0} = -i\alpha \frac{\sqrt{5\pi}}{4} v^2 H(v) \boldsymbol{\sigma} \cdot \boldsymbol{\epsilon},$$

where $F(v)$, $G(v)$ and $H(v)$ are the following functions:

$$F(v) = \int_{-1}^1 \frac{1-x^2}{1-vx} dx, \quad G(v) = \int_{-1}^1 \frac{x(1-x^2)}{1-vx} dx, \quad H(v) = \int_{-1}^1 \frac{(1-x^2)(3x^2-1)}{1-vx} dx.$$

In order to avoid useless complications, we consider for the moment, only S and P waves. We will add later the S - D interference, the only one contribution of D waves allowed by our approximations. They consist in dropping all terms higher than $\cos^2 \theta$ in the cross section and powers higher than v^2 in the pion velocity. Keeping in mind these limitations, (A.2) is written

$$\mathcal{T} = ie_1 \boldsymbol{\sigma} \cdot \boldsymbol{\epsilon} - \frac{m_1}{v\eta} [\mathbf{v} \times \boldsymbol{\epsilon} \cdot \boldsymbol{\eta} - i \boldsymbol{\sigma} \cdot (\mathbf{v} \times \boldsymbol{\epsilon}) \times \boldsymbol{\eta}] - \frac{m_3}{v\eta} [2\mathbf{v} \times \boldsymbol{\epsilon} \cdot \boldsymbol{\eta} + i \boldsymbol{\sigma} \cdot (\mathbf{v} \times \boldsymbol{\epsilon}) \times \boldsymbol{\eta}] +$$

$$+ i \frac{e_2}{v\eta} \frac{1}{2} [(\boldsymbol{\sigma} \cdot \mathbf{v})(\boldsymbol{\epsilon} \cdot \boldsymbol{\eta}) + (\boldsymbol{\sigma} \cdot \boldsymbol{\epsilon})(\mathbf{v} \cdot \boldsymbol{\eta})],$$

where

$$e_1 = \alpha \left(1 - \frac{v^2}{4} F \right) = \text{electric dipole amplitude}, \quad (J = \frac{1}{2}),$$

$$m_1 = -\alpha \frac{v}{3} \left(1 + \frac{3}{4} vG \right) = \text{magnetic dipole amplitude}, \quad (J = \frac{1}{2}),$$

$$m_3 = \alpha \frac{v}{6} \left(1 + \frac{3}{4} vG \right) = \text{magnetic dipole amplitude}, \quad (J = \frac{3}{2}),$$

$$e_2 = \alpha v \left(1 - \frac{3}{4} vG \right) = \text{electric quadrupole amplitude}. \quad (J = \frac{3}{2}).$$

It is immediately seen that

$$F - vG = \frac{4}{3},$$

then putting $\Delta = 3F/4$ one has

$$(A.3) \quad \begin{cases} e_1 = \alpha \left(1 - \frac{v^2}{3} \Delta \right), \\ m_1 = \frac{2}{3} v \Delta, \\ m_3 = \frac{2}{6} v \Delta, \\ e_2 = \alpha v (2 - \Delta), \end{cases}$$

where

$$\Delta = \frac{3}{4} \frac{1}{v^3} \left\{ 2v - (1 - v^2) \ln \frac{1 + v}{1 - v} \right\}.$$

According to the previously mentioned approximations (which are allowed in the energy range here considered) (A.3) give us the corrections which should be included in the standard phenomenological multipole analysis when the operator (11) is *explicitly* added to the matrix T .

In other words the explicit inclusion of the S and P projections of the « photoelectric » operator (11) of text in the standard phenomenological matrix (see reference ⁽³⁾), gives for the full transition matrix, the expression:

$$\begin{aligned} T = iE_1 \boldsymbol{\sigma} \cdot \boldsymbol{\epsilon} - \frac{M_1}{v\eta} [\mathbf{v} \times \boldsymbol{\epsilon} \cdot \boldsymbol{\eta} - i\boldsymbol{\sigma} \cdot (\mathbf{v} \times \boldsymbol{\epsilon}) \times \boldsymbol{\eta}] - \frac{M_3}{v\eta} [2\mathbf{v} \times \boldsymbol{\epsilon} \cdot \boldsymbol{\eta} + i\boldsymbol{\sigma} \cdot (\mathbf{v} \times \boldsymbol{\epsilon}) \times \boldsymbol{\eta}] + \\ + i \frac{E_2}{v\eta} \frac{1}{2} [(\boldsymbol{\sigma} \cdot \mathbf{v})(\boldsymbol{\epsilon} \cdot \boldsymbol{\eta}) + (\boldsymbol{\sigma} \cdot \boldsymbol{\epsilon})(\mathbf{v} \cdot \boldsymbol{\eta})], \end{aligned}$$

where in place of the usual phenomenological multipole amplitudes

$$E'_1 + \alpha, \quad M'_1, \quad M'_3, \quad E'_2,$$

we have now

$$(A.4) \quad \begin{cases} E_1 = E'_1 + \alpha \left(1 - \frac{v^2}{3} \Delta \right), & M_1 = M'_1 - \alpha \frac{v}{3} \Delta, \\ M_3 = M'_3 + \alpha \frac{v}{6} \Delta, & E_2 = E'_2 + \alpha v (2 - \Delta), \end{cases}$$

where with the notations used in text

$$\alpha = \frac{g_{os}}{\sqrt{v\omega}}, \quad E'_1 = -R.$$

This is correct only as far as S and P waves are considered. If instead one includes the S - D interference, but neglects the pure D term $|\sum c_{2m} Y_{2m}|^2$

and its interferences with p -wave, the a_i coefficients are those given by (8) in the text (where the multipole amplitudes are given by (A.4)) and

$$a_{sz} = -\alpha \frac{15}{8} v^2 H(v) E_1.$$

Thus one has

$$(A.5) \quad \begin{cases} X = X' + \alpha \frac{v}{2}, \\ Y = Y' - \alpha \frac{v}{2}, \\ K = K' + \alpha v(\Delta - 1), \end{cases}$$

where X' , Y' , and K' are the (phenomenological) multipole linear combinations

$$X' = \frac{2}{3} M'_3 + \frac{1}{4} E'_2 \quad \text{etc.},$$

introduced by Fermi [see for instance GELL-MANN and WATSON, ref. (3)]. Thus finally, in the approximation $\sin \alpha_{2f,2f} \simeq 0$

$$\begin{aligned} a_0 &= \left[E'_1 + \alpha \left(1 - \frac{v^2}{3} \Delta \right) \right]^2 + a'_{op} + \alpha^2 \frac{v^2}{2} + \alpha v(X' - Y') + \frac{5}{8} \alpha v^2 H \left[E'_1 + \alpha \left(1 - \frac{v^2}{3} \Delta \right) \right], \\ a_1 &= -2(E'_1 + \alpha)K' + \frac{2}{3} \alpha v^2 K' \Delta - 2(E' + \alpha) \alpha v(\Delta - 1) + \frac{2}{3} \alpha^2 v^3 \Delta(\Delta - 1), \\ a_2 &= K'^2 - a'_{op} + \alpha^2 v^2 (\Delta - 1)^2 + 2\alpha K' v(\Delta - 1) - \alpha^2 \frac{v^2}{2} - \\ &\quad - \alpha v(X' - Y') - \frac{15}{8} \alpha v^2 H \left[E'_1 + \alpha \left(1 - \frac{v^2}{3} \Delta \right) \right]. \end{aligned}$$

At low energies, i.e. neglecting v^3 and higher powers one has

$$\Delta \simeq 1, \quad H \simeq -\frac{8}{15},$$

and

$$(A.6) \quad \begin{cases} a_0 = a'_{os} + a'_{op} + \alpha^2 \frac{v^2}{2} - \alpha v^2 \sqrt{a'_{os}} + \alpha v(X' - Y'), \\ a_1 = a'_1 + \frac{2}{3} \alpha v^2 K', \\ a_2 = K'^2 - a'_{op} - \alpha^2 \frac{v^2}{2} - \alpha v(X' - Y') + \alpha v^2 \sqrt{a'_{os}}, \end{cases}$$

where

$$a'_{os} = (\alpha + E'_1)^2.$$

2) To discuss now the inconsistency shown by the overdetermined set of equations (9) of text, let us start by assuming that the S -recoil is negligible, i.e. $-E'_1 = R = 0$. The set (A.6) becomes

$$(A.7) \quad \begin{cases} a_0 = \alpha^2 + a'_{op} - \alpha^2 \frac{v^2}{2} - \alpha v(X' - Y'), \\ a_1 = -2\alpha K'(1 - \frac{1}{3}v^2), \\ a_2 = K'^2 - a'_{op} + \alpha^2 \frac{v^2}{2} - \alpha v(X' - Y'). \end{cases}$$

Hence

$$a_0 + a_2 = \alpha^2 + K'^2.$$

Finally, solving this equation for K' and putting the obtained expression in the second eq. of (A.7), one has

$$a_1 \text{ (calc.)} = -2\alpha\sqrt{a_0 + a_2 - \alpha^2} + \frac{2}{3}\alpha v^2\sqrt{a_0 + a_2 - \alpha^2}.$$

This a_1 differs from the a_1 obtainable from (9) of text by the additional term $+\frac{2}{3}\alpha v^2\sqrt{a_0 + a_2 - \alpha^2}$. It is due to the direct photoelectric effect given by the operator (11). At the highest energy here considered it amounts to 8%. This is equivalent to saying that adding this term (but neglecting R) a_1 (calc.) is still ~ 2.7 times bigger than the averaged experimental value. In other words the inclusion of the interaction (11) brings down a_1 (calc.) from $\sim 3a_1$ (exp.) to $\sim 2.7a_1$ (exp.). It has to be noticed that K' remains very small.

Actually from (A.5) one has

$$K^2 = K'^2 + \alpha^2 v^2 (\Delta - 1)^2 + 2\alpha v K' (\Delta - 1),$$

and the values of K given in Table V remain practically unchanged.

It is clear that the «photoelectric» term up to ~ 235 MeV modifies the structure of the a_i coefficients but leaves practically unchanged their relationships and the corresponding equations used in the text.

3) If one completes now the analysis introducing the nucleon recoils, one has for the positive pions (with very good approximation)

$$a_0^+ = (\alpha + E'_1)^2 + a_{os}^+,$$

$$a_1^+ = -2\left[E'_1 + \alpha\left(1 - \frac{v^2}{3}\right)\right]K'^+,$$

$$a_2^+ = -a_{op}^+ = -a_{op}^{\prime+} - \alpha^2 \frac{v^2}{2} - \alpha v(X'^+ - Y'^+) + \alpha v^2(\alpha + E'_1),$$

and, in our approximation, for negative ones,

$$a_0^- = (x - E_1')^2 + a_{0p}^-,$$

$$a_1^- = -2 \left[E_1' + x \left(1 - \frac{r^2}{3} \right) \right] K'^-,$$

$$a_2^- = -a_{0p}^- = -a_{0p}'^- - x^2 \frac{r^2}{2} - x r (X'^- - Y'^-) + x r^2 (x - E_1').$$

Now, our approximation in the p -wave recoil implies $X^- = X^+$ and $Y^- = Y^+$ (from which $a_{0p}'^- = a_{0p}'^+ = -a_2$) so, with a little algebra, one has

$$E_1' = -R = \frac{\sqrt{a_0}}{2} \left\{ \left| 1 + \frac{a_2}{a_0} \right| \sqrt{r + \frac{a_2}{a_0}} \right\},$$

which is identical in respect to the a_i coefficients with (19) in the text.

Consequently the values of R remain unchanged by the introduction of the matrix (11) of the text. The same conclusion is obviously reached if one considers the procedure applied to extrapolate at threshold the value of the π^-/π^+ ratio.

It is worth mentioning that all these conclusions are reached just because we included systematically also the a_{s1} term as required by the expression of $d\sigma/d\Omega$ up to $\cos^2 \theta$.

RIASSUNTO (*)

La sezione d'urto $\sigma(E_\gamma, \theta)$ per la reazione $p \rightarrow n^+$ è stata misurata in prossimità della soglia in funzione dell'energia fotonica e sotto quattro angoli. Vedi Tab. I. I risultati ottenuti combinati con dati precedentemente noti hanno fornito una descrizione abbastanza completa ed esatta di $\sigma(E_\gamma, \theta)$ tra i limiti $30^\circ \leq \theta \leq 180^\circ$ e $170 \leq E_\gamma \leq 270$ MeV. Vedi Tab. II e Fig. 2. Scrivendo $\sigma(E_\gamma, \theta) = W \{ a_0 + a_1 \cos \theta + a_2 \cos^2 \theta \}$ con $W = n\omega \{ 1 + (\mu/E_i) \}^{-1} \{ 1 + (\mu/E_f) \omega \}^{-1}$ (vedi formula (5)), i dati sperimentali indicano che (Tab. III) a_0 è costante fino a circa $E_\gamma \simeq 260$ MeV, e che (Tab. V) i tre coefficienti a_i analizzati in termini di onde S e P danno una piccolissima ampiezza P di spin-flipping, K . La presunzione che l'ampiezza SE , sia principalmente dovuta all'imposizione dell'invarianza di gauge non si accorda in alcun modo coi dati (vedi Tab. IV). Una discussione basata sul teorema di Kroll e Rudermann porta alla conclusione che questa incongruenza può essere eliminata se si tien conto del contributo di rinculi nucleonici abbastanza energici. Tuttavia, risulta che solo la parte di tali rinculi che cambia di segno è realmente energetica ed apparentemente tale fino a termini di ordine superiore a μ/M . Si valuta la quantità di rinculo alla soglia e se ne deriva un valore per la costante di interazione psv .

(*) Traduzione a cura della Redazione.

The Application of Charge Independence to the Nuclear Capture of Negative K-Mesons (*).

M. KOSHIBA

Department of Physics, University of Chicago - Chicago, Illinois

(ricevuto il 21 Maggio 1956)

Summary. — The results of the charge independence hypothesis are compared with the existing experimental data on the nuclear capture of negative K-mesons. The comparison of the calculated Σ^-/Σ^+ and π^-/π^+ emission ratios with the experimental ones strongly suggest the dominance of the $T=1$ state ⁽¹⁾ over the $T=0$ state in the primary act. Furthermore, the π^-/π^+ emission ratio is shown to give an estimate of the branching ratio between Σ emission and Λ^0 emission, which is free from the ambiguities due to the secondary absorption of the products of the primary act or due to the difficulties of detecting neutral particles and is only slightly affected by secondary charge exchange scatterings of the product particles. The preliminary value thus determined by using the experimental data thus far available for the π^-/π^+ emission ratio, suggests that Σ emission is more favored than Λ^0 emission in the primary act. The implications of measuring the positive-to-negative ratio of high energy π -mesons emitted from K^- captures is discussed in some detail and a few experiments are proposed in this connection.

1. — Introduction.

The hypothesis of charge independence has been extensively investigated in various fields of nuclear science. Especially it is worth mentioning that in the scattering of π -mesons by nucleons only one, $T=\frac{3}{2}$, of the possible two states, $T=\frac{3}{2}$ and $T=\frac{1}{2}$, was found to be dominant, at least up to the so-called

(*) Supported in part by a joint program of the U.S. Office of Naval Research and the U.S. Atomic Energy Commission.

⁽¹⁾ We designate the total isotopic spin by T and the isotopic spin of individual particles by τ .

resonance at a π -meson energy of some 180 MeV ⁽²⁾. The hypothesis has also been extended to the reactions of newly discovered particles ⁽³⁻¹²⁾ other than nucleons and π -mesons. The motivation of the present work lies in the following considerations.

The τ -spin ⁽¹⁾ formalism incorporated with the strangeness selection rule seems to be successful in classifying new particles, as well as in explaining the strong and weak interactions ⁽¹³⁾. In other words, we can assign appropriate τ -spins to new particles in such a way that the assigned τ -spin of a particle is consistent with its observed charge multiplicity and at the same time the total isotopic spin, T , can be conserved in the strong reactions. (Also in weak interactions, where the situations in selection rules are naturally much more complicated, there has been some attempt to introduce a selection rule on the change of the total isotopic spin ⁽¹⁴⁾. However, as was the case in β -decay, the easiest to approach would be the strong (allowed) interactions.) If the total isotopic spin, T , is actually conserved in strong reactions, we can have some additional restrictions on the charge states of the product particles ^(8,9-12). In general, however, they are not sufficient to make a unique prediction as to the charge state of the product particles. This is so because even after the application of the charge independence there is, in general, more than one (complex) matrix element corresponding to states of different total isotopic spin or of different symmetry properties. The situation in π -meson-nucleon scattering, mentioned at the beginning of this section, was quite favorable since the experiment showed that only one of the possible states was predominant.

The experimental data on the nuclear capture of negative K -mesons are being rapidly accumulated and this reaction is one of the best investigated experimentally among the strong interactions. The comparison between the

⁽²⁾ K. A. BRUECKNER: *Phys. Rev.*, **83**, 106 (1952).

⁽³⁾ T. NAKANO and K. NISHIJIMA: *Prog. Theor. Phys.*, **10**, 581 (1953); M. GELL-MANN: *Phys. Rev.*, **93**, 933 (1953).

⁽⁴⁾ A. PAIS: *Proc. of the Fifth Annual Rochester Conference*, 1955.

⁽⁵⁾ R. H. DALITZ: *Phys. Rev.*, **99**, 1475 (1955).

⁽⁶⁾ A. PAIS and R. SERBER: *Phys. Rev.*, **99**, 1551 (1955).

⁽⁷⁾ R. G. SACHS: *Phys. Rev.*, **99**, 1573 (1955).

⁽⁸⁾ T. D. LEE: *Phys. Rev.*, **99**, 338 (1955).

⁽⁹⁾ K. M. CASE, R. KARPLUS and C. N. YANG: *Phys. Rev.*, **101**, 358 (1956).

⁽¹⁰⁾ K. M. CASE, R. KARPLUS and C. N. YANG: *Phys. Rev.*, **101**, 874 (1956).

⁽¹¹⁾ M. GOLDBABER: *Phys. Rev.*, **101**, 434 (1956).

⁽¹²⁾ D. FELDMANN: *UCRL* 3168 (1955).

⁽¹³⁾ « Strong » (« weak ») means the strangeness is (is not) conserved in the reaction. (See reference ⁽³⁾).

⁽¹⁴⁾ G. TAKEDA: *Phys. Rev.*, **101**, 1547 (1956); G. WENTZEL: *Phys. Rev.*, **101**, 1215 (1956).

experiments and the results of charge independence may reveal a similar situation as in the case of π -meson nucleon scattering, that is, the predominance of a single state. It will be shown that this is actually the case.

2. — Nuclear Capture of Negative K-Mesons.

Naturally the easiest and most direct comparison will be possible if the experimental data of negative K-meson capture by a single nucleon or by a deuteron is available. Even in these reactions, however, the experimental difficulties associated with the observation of neutral particles, π^0 , Σ^0 and Λ^0 , or with the inaccessibility of a free neutron target will obscure the analysis in terms of charge independence and the analysis itself would in general serve just to barely see whether the experiment is consistent, or inconsistent with the hypothesis. The experimental data on the nuclear capture of K-mesons at our disposal consist mainly of those obtained by means of photographic emulsions, thus implying that we have to expect a considerable modification of the primary product particles due to secondary processes in the nucleus absorption or charge exchange scattering. Therefore, we have to be careful in choosing the quantities on which the comparison between the calculation and the experiment should be made.

Now the strangeness selection rules allow us to confine ourselves to the following reactions:



and similarly for captures by still more nucleons. From the consideration of the available phase space volume, it is expected that the reactions (1')

and (2') are less favored than the corresponding reactions (1) and (2) unless there is some selection rule to make it otherwise. A selection rule of this sort has not been inferred thus far from any experiment or from any theory. We accordingly consider (1) and (2) as the most likely reactions. Furthermore, the Σ 's from reactions (2) have much more energy than those from (1) and we know experimentally that the emission of Σ 's of energy corresponding to the reactions (2) is very rare, so that we can take as of primary importance only reactions (1). There is another experimental indication that the reactions (1) are the main processes of K^- nuclear capture; that is, the percentage of π -emission is quite consistent with the assumption that a π -meson is always emitted in K^- capture. This will be discussed in a later section.

If we assign $\frac{1}{2}$, 1, and 0 for the τ -spins of K^- , Σ and Λ^0 , respectively, we can see immediately from the reactions (1) that Σ 's can be produced both in $T=1$ and 0 states of the K^- -nucleon system, while Λ^0 's can be produced only in the $T=1$ state. Therefore, if the $T=0$ state happens to be the dominant one in the reactions (1), Λ^0 must be considered as a product of some secondary reactions, such as $\Sigma + \text{nucleon} \rightarrow \Lambda^0 + \text{nucleon}$ and we will have equal probabilities for having Σ^+ , Σ^0 , Σ^- , π^0 , π^- and π^+ in the primary K^- capture process since the state of $T=0$ has no preferential direction in isotopic spin space. If, on the other hand, the state $T=1$ were of primary importance we should expect more Σ^- 's (π^- 's) than Σ^+ 's (π^+ 's) coming from K^- -neutron reactions.

The above qualitative considerations can be seen clearly if we write down the matrix element corresponding to each reaction in (1):

$$(1a') \quad \frac{1}{2}M_1 + \frac{1}{\sqrt{6}}M_0,$$

$$(1b') \quad -\frac{1}{\sqrt{6}}M_0,$$

$$(1c') \quad -\frac{1}{2}M_1 + \frac{1}{\sqrt{6}}M_0,$$

$$(1d') \quad -\frac{1}{\sqrt{2}}M_1,$$

$$(1e') \quad +\frac{1}{\sqrt{2}}M_1,$$

$$(1f') \quad \frac{1}{\sqrt{2}}N_1,$$

$$(1g') \quad N_1,$$

where M_1 , M_0 and N_1 are the transition matrix elements from $(K + \text{nucleon})$ to $(\Sigma + \pi)$ in $T=1$, $T=0$ states and from $(K + \text{nucleon})$ to $(\Lambda^0 + \pi)$ in the $T=1$ state, respectively.

In order to make quantitative comparison with experiment, we have to specify the charge state of the nucleus by which the K^- is captured. For the sake of simplicity, we assume that the nucleus is self-conjugate; i.e. the number of protons in the nucleus is equal to that of neutrons. This is justified for C, N, O nuclei in the emulsion but not for heavier nuclei, Ag or Br. The problem of the effect of the neutron excess in silver or bromine nuclei on our results will be qualitatively discussed in the last section in conjunction with other effects such as that of the Coulomb field. Furthermore, we treat the problem in two extremities, that is in the pure $T=1$ and in the pure $T=0$ state. The interference between these two states will also be discussed in the last section and will be shown not to alter seriously the conclusions arrived at in this work.

Now we have specified the dominant channel state as well as the charge state of the capturing nucleus and we can obtain the charge state of the product particles of the primary K^- -capture process.

The results are:

for the $T=0$ channel

$$\left\{ \begin{array}{ll} \Sigma^+ & \frac{1}{3} \\ \Sigma^0 & \frac{1}{3} \\ \Sigma^- & \frac{1}{3} \\ \Lambda^0 & 0 \end{array} \right. \quad \left\{ \begin{array}{ll} \pi^+ & \frac{1}{3} \\ \pi^0 & \frac{1}{3} \\ \pi^- & \frac{1}{3} \end{array} \right.$$

and for the $T=1$ channel

$$\left\{ \begin{array}{ll} \Sigma^+ & (1-m)/12 \\ \Sigma^0 & (1-m)/6 \\ \Sigma^- & (1-m)/4 \\ \Lambda^0 & (1+m)/2 \end{array} \right. \quad \left\{ \begin{array}{ll} \pi^+ & (1-m)/12 \\ \pi^0 & \frac{1}{3} \\ \pi^- & (7+m)/12 \end{array} \right.$$

where in the $T=1$ channel, the branching ratio to Σ and to Λ^0 emission is given by $(1-m)/(1+m)$.

These individual percentages of occurrence are, however, not best suited for comparisons with the experimental results since we have to expect deviations from the above due to secondary absorptions of charge exchange scat-

terings by other nucleons in the nucleus. The ratio of positive to negative particles of the same kind is not affected by the secondary absorption as long as the nucleus is self conjugate and this ratio is readily observable experimentally. Therefore, we take Σ^-/Σ^+ and π^-/π^+ as quantities to be compared with the experimental data and calculate the effect on them of secondary charge-exchange scattering.

In the case of the $T=0$ channel, these ratios are always equal to unity, irrespective of the number of charge-exchange scatterings they underwent before escaping the nucleus, since we assumed a self-conjugate nucleus and we have an equal number of positive and negative particles to start with.

The situation in the case of the $T=1$ channel is not so simple. In the scattering of Σ particles by a nucleon two states are possible, $T=\frac{3}{2}$ and $T=\frac{1}{2}$; the former state is not possible in the reaction $\Sigma + (\text{nucleon}) \rightarrow \Lambda^0 + (\text{nucleon})$. If we assume that all the Σ 's produced in the primary act have been scattered once by a nucleon, the ratio Σ^-/Σ^+ changes from its original values of 3 to

$$\begin{aligned} 17/7 & \quad \text{after } T=\frac{3}{2} \text{ scattering} \\ (85-13n)/(35-11n) & \quad \text{after } T=\frac{1}{2} \text{ scattering} \end{aligned}$$

where n is defined by

$$\frac{(\Sigma + \text{nucleon}) \rightarrow (\Sigma + \text{nucleon})}{(\Sigma + \text{nucleon}) \rightarrow (\Lambda_0 + \text{nucleon})} = \frac{(1-n)}{(1+n)},$$

in the $T=\frac{1}{2}$ state. Because of the small energies, ~ 10 MeV, of Σ 's and because of the Pauli principle on the scattered nucleon, the scattering mean free path will not be so small in the nucleus as to necessitate the consideration of more than one scattering.

As to the scattering of π -mesons by a nucleon, we know that it occurs through the $T=\frac{3}{2}$ state. The π -meson energy is about 140 MeV and 80 MeV when produced by K^- -capture with Λ^0 - and Σ^- -emission, respectively. The ratio (π^-/π^+) of $(7+m)/(1-m)$ changes to

$$\frac{(39+5m)}{(9-5m)}, \quad \text{for singly scattered } \pi\text{-mesons,}$$

$$\frac{(219+25m)}{(69-25m)}, \quad \text{for doubly scattered } \pi\text{-mesons,}$$

$$\frac{(1239+125m)}{(489-125m)}, \quad \text{for triply scattered } \pi\text{-mesons,}$$

and so on. More specifically, the percentages of π^- , π^0 and π^+ in the unscattered, singly scattered, doubly scattered, etc., meson groups are given in Table I.

TABLE I. — *Distribution in charge states of π -mesons after scatterings by nucleons. The π -mesons are produced through the $T=1$ channel.*

	Unscattered	Singly scattered	Doubly scattered	Triply scattered
π^-	$\frac{7+m}{12}$	$\frac{39+5m}{72}$	$\frac{219+25m}{432}$	$\frac{1239+125m}{2592}$
π^0	$\frac{1}{3}$	$\frac{1}{3}$	$\frac{1}{3}$	$\frac{1}{3}$
π^+	$\frac{1-m}{12}$	$\frac{9-5m}{72}$	$\frac{69-25m}{432}$	$\frac{489-125m}{2592}$

The quantity to be compared with the experimental data is

$$(\pi^-/\pi^+)_{\text{effective}} = \frac{\sum_i x^-(i)N(i)}{\sum_i x^+(i)N(i)},$$

where $N(i)$ is the percentage of π -mesons scattered i times before escaping the nucleus and $x^-(i)$ ($x^+(i)$) is the percentage of the negative (positive) mesons in the i -th generation. $x^-(i)$'s are given in Table I and $N(i)$'s must be determined according to the experimental conditions, for example, the energy range of the π -mesons of which the charges have been identified.

The simplest comparison will be obtained if we have experimental data on the charges of fast mesons of energy greater than about 70 MeV. However, in emulsion work thus far carried out, we know only the charges of slow π -mesons stopped in the emulsion. The $N(i)$'s corresponding to this group of π -mesons are not easy to estimate and we simply give the preliminary comparison in the next section.

3. — Comparison with the Experiments.

In the previous section we have derived the Σ^-/Σ^+ and the π^-/π^+ ratios on the basis of charge independence. The experimental results are summarized in Table II.

TABLE II. - *Experimental Results on K⁻ Captures.*

The numbers of cases where Σ^- , π^- are emitted from K⁻ capture are tabulated. The number in parenthesis is the number of probable cases. We note that the Berkeley and Brookhaven groups employ the track following scanning procedure while others employ the area scanning procedure.

	Berkeley (¹⁹)	Brookhaven (¹⁸)	Chicago (²¹)	Wisconsin (²⁰)	Total
Σ^-	7	2 + (1)	4 + (3)	12 + (3)	25 + (7)
Σ^+	6 + (1)	1	3	15	25 + (1)
Σ^\pm	0	2	0	5	7
π^-	10 + (2)	2 + (1)	1	0	13 + (3)
π^+	3 + (2)	0	0	1	4 + (2)
π^\pm	20	14	19	63	116
Total	133	39	70	207	449

In comparing the numbers of Σ^- and Σ^+ we have to make a correction for the low efficiency of detection of Σ^- , i.e. for the number of Σ^- stopping without giving rise to a visible star at its end. This correction was done by FRY and others (²¹) by observing slow electrons at the ends of some Σ^- -particles and by assuming that the percentage of associated slow electrons in the Σ^- -stopping was the same as in the case of μ^- stopping where it was found to be 25%. Their result was a total of 24 Σ^- 's compared with 15 Σ^+ 's, thus giving the ratio Σ^+/Σ^- of 1.6. (*). In the present analysis, we use the following method to correct for those Σ^- stoppings without visible prongs. Except for the case of Σ^- stopping with no visible prong at the end, we have some experimental information on the prong distribution of the Σ^- capture stars. Naturally we have to expect that there must have been experimental detection bias in favor

(¹⁸) J. HORNBOSTEL and E. O. SALANT: to appear in *Phys. Rev.*, April 15 (1956). The author is grateful to them for furnishing their results before publication.

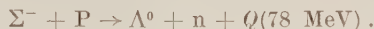
(¹⁹) F. H. WEBB, W. W. CHUPP, G. GOLDBABER and S. GOLDBABER; to be published. The author is indebted to them for giving him their data before publication.

(²⁰) J. FRY *et al.*: *Phys. Rev.*, **100**, 950 (1955). Also a private communication for which the author is grateful to him.

(²¹) D. HASKIN, T. BOWEN and M. SCHEIN: to appear in *Phys. Rev.*

(*) The direct application of their method to the whole data in Table II gives the ratio of 49/25 \sim 2.

of stars of more prongs. However, if we restrict ourselves to those Σ^- 's which were emitted from K^- -capture, the prong distribution would not be distorted so much by this detection bias, except of course for zero prong stars, since one would investigate the prongs of K^- capture stars much more carefully to identify them. This prong distribution gives a measure of the excitation energy of the residual nucleus when a Σ^- was captured. The experimental prong distribution of Σ^- capture stars, with the primary Σ^- from K^- capture, indicates that it is quite consistent with the primary absorption process of



Actually the excitation energy estimated from the ratio of one to two prong stars is about 55 MeV. This reduction of the excitation energy compared with the available total energy is quite understandable since the excitation of the residual nucleus is mainly caused by the secondary interactions of the product particles and for a particle energy of some 40 MeV, which the neutron or Λ^0 can have in the above reaction, the Pauli exclusion principle will reduce the cross-section considerably. (Also in π^- capture stars the excitation energy which fits the experimental prong distribution is smaller than the available energy of 140 MeV).

Now using the excitation energy which gives the observed ratio of one to two prong Σ^- -capture stars we can estimate the number of zero prong Σ^- capture stars. The corrected number of Σ^- is 78, thus giving a value of 3.1 to the ratio Σ^-/Σ^+ . (If we, instead, take as an extremity 78 MeV excitation, this ratio becomes 1.7.) This value is well above the unity which one would obtain if the primary K^- capture process occurred only through the $T=0$ channel. Unfortunately, one cannot deduce the branching ratio of $\Sigma^+(\text{nucleon})$ to $\Sigma^+(\text{nucleon})$ and $(\Lambda^0+\text{nucleon})$ from this comparison, since, besides the uncertainty due to the statistical error in the experimental value, the effect of this branching on Σ^-/Σ^+ is rather small and will be masked easily by a small amount of $T=0$ state admixture.

Going now to the π^-/π^+ ratio we first note that the π -mesons of identified charges are all of low energy, presumably smaller than 40 MeV which corresponds to a range of 2.7 cm in the photographic emulsion. This implies those mesons have been scattered at least once before escaping the nucleus. Hence, those charge identified π -mesons are the admixture of the singly, doubly, etc., scattered ones. It is, however, very difficult to make estimates of the percentages of these π -meson groups for a specified energy region. Therefore, we proceed in the following way. Our aim is the effective scattering mean free path of π -mesons in the nuclear matter. We know the absorption mean free path, λ_a , of the π -mesons emitted from the K^- capture, namely from the observed percentage of the π -meson emissions in Brookhaven and Berkeley

experiments where the scanning procedure of presumably uniform detection efficiency is employed, we obtain 1.02 for the ratio $\langle l \rangle / \lambda_a$, where $\langle l \rangle$ is the average distance of traversal in the nucleus and λ_a should be understood as the absorption mean free path averaged over the successive collisions of π -mesons of degrading energies. This ratio is quite reasonable in view of our knowledge of the nuclear radius and the other experimental determinations of λ_a ⁽¹⁵⁾. The scattering mean free path, λ_s , can, in principle, be calculated assuming, for example, the Goldberger model ⁽¹⁵⁾. However, we do not follow this approach since the calculation with the actually observed π -nucleon cross-section will be almost forbiddingly tedious. Instead, we note the energy dependence of λ_a and λ_s ⁽¹⁶⁾ and the ratio of λ_a/λ_s observed experimentally to

be $\frac{1}{2}$ at 40 MeV by TENNEY and TINLOT ⁽¹⁷⁾. If we take into account the large energy degradation of scattered π -mesons, and thus the reduction in the scattering cross-section for the next collision, the estimate of λ_a/λ_s to be from 2 to $\frac{1}{2}$ would not be much different from reality. The results of assuming $\lambda_a/\lambda_s = 2, 1$, and $\frac{1}{2}$ are shown in Fig. 1. The experimental results are $\pi^-/\pi^+ = 13/4$. Therefore, the comparison of π^-/π^+ ratio not only confirms the predominance of the $T=1$ state which was indicated from the Σ^-/Σ^+ data but also seems to suggest a slightly negative value of m implying that Σ 's are produced more than Λ 's in the primary act of K^- -capture process.

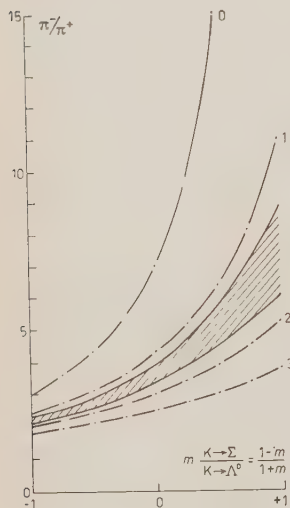


Fig. 1. — The ratio of π^- to π^+ as a function of the branching parameter which is defined by

$$\frac{K^- + N \rightarrow \Sigma^{\pm 0} + \pi^{\pm 0}}{K^- + N \rightarrow \Lambda^0 + \pi^0} = \frac{1 - m}{1 + m}.$$

The curves 0, 1, 2 and 3 represent the ratios of π^- to π^+ after 0, 1, 2 and 3 scatterings before escaping the nucleus, respectively. The shaded area is a superposition of the curves 1, 2 and 3 with the assumption of λ absorption/ λ scattering from $\frac{1}{2}$ to 2.

⁽¹⁵⁾ M. L. GOLDBERGER: *Phys. Rev.*, **74**, 1269 (1948); M. H. JOHNSON: *Phys. Rev.*, **85**, 510 (1951).

⁽¹⁶⁾ R. M. FRANK, J. L. GAMMEL and K. WATSON: *Phys. Rev.*, **101**, 891 (1956); K. WATSON: *Am. Journ. Phys.*, **21**, 659 (1953).

⁽¹⁷⁾ F. H. TENNEY and J. TINLOT: *Phys. Rev.*, **92**, 974 (1953); A. M. SHAPIRO: *Phys. Rev.*, **84**, 1063 (1951); H. BYFIELD, J. KESSLER and L. M. LEDERMAN: *Phys. Rev.*, **86**, 17 (1952); J. F. TRACY: *Phys. Rev.*, **91**, 960 (1953); G. BERNARDINI and F. LEVY: *Phys. Rev.*, **84**, 610 (1951).

As was mentioned at the beginning of this section, the experimental determination of the charges of the fast π -mesons, $\gtrsim 70$ MeV, from K^- -capture gives information on the Σ to Λ^0 emission ratio which would be much less affected by the secondary charge exchange scatterings. This will most easily be carried out by cloud chambers in magnetic field.

Before concluding this analysis, some additional remarks may be needed concerning the interference between different T -states, the effect of Coulomb attraction in the case of K^- -capture by protons, and the neutron excess of the capturing nuclei. We have treated the two isotopic spin states separately without considering the possible interference effect. This can be justified ad hoc by comparison with the experimental Σ^+/Σ^- and π^+/π^- ratios; namely the inspection of matrix elements in the previous section immediately leads to the conclusion that the interference of the two states affect these two ratios in opposite directions, while experimentally the predominance of the $T=1$ state is confirmed by both of these ratios. Hence the possibility of the interpretation of the experimental results in terms of the interference effect seems to be excluded. As to the enhancement of capture probability by a proton as compared with that by a neutron, we may note that the capturing nucleon is in Fermi motion so that the effect will not be as large as in the case of capture by a free nucleon at rest. Furthermore, if this effect were important, we should have obtained the experimental results closer to the results of the $T=0$ act. Finally, the neutron excess of the capturing nuclei would not give the modification of the results by much more than 10 percent as long as protons and neutrons are more or less similarly distributed inside the nucleus. If this neutron excess effect was quite appreciable due to some difference in the densities of protons and of neutrons, say at the periphery of the nucleus, then it could give rise to increases of both of the ratios, Σ^+/Σ^- and π^+/π^- . However, the mere fact that the neutron excess effect is appreciable would indicate a large interaction in the $T=1$ state since the system of K^- and neutron is a pure $T=1$ state.

* * *

The author is grateful to Professor M. SCHEIN for his stimulating discussions throughout this work as well as for furnishing him his experimental results before publication. Thanks are also due Professor Y. NAMBU for his valuable discussions.

Note Added.

After this analysis was worked out the author was informed of Dr. S. WHITE's work on K^- -capture at Berkeley. (F. C. GILBERT, C. E. VIOLET and R. S. WHITE) Upon his request, Dr. WHITE kindly furnished the data before publication for

which the author is very grateful. The results are 4 Σ^+ 's (Event No. 36 was omitted since it would correspond to two nucleon captures which was not considered in this work), no Σ^- , 10 π^- stoppings, no π^+ stoppings, and 13 π^\pm mesons out of 74 cases. These results seem to have rather different characteristics from the ones listed in Table II and are rather similar to the results of the Sidney group (private communication to Professor M. SCHEIN); that is, a very large π^-/π^+ ratio and no cases of Σ^- emission. If these are real, one might think we would have to conclude that the $T=0$ state interferes with the $T=1$ state constructively in the $\Sigma^++\pi^-$ case and destructively in the $\Sigma^-+\pi^+$ case. However, for a completely destructive interference so as to have no π^+ -mesons, we should have $\frac{1}{2}$ for the Σ^-/Σ^+ ratio which is quite contrary to the results of other data in Table II. Therefore, the interference effect cannot account for the difficulty and one will instead be led to retain the predominance of the $T=1$ state which is required by the Σ^-/Σ^+ ratio of better statistics (the inclusion of WHITE's data and that of the Sidney group changes the experimental value of Σ^-/Σ^+ to 2.7 which still strongly suggests the dominance of $T=1$ state) and to explain the π^-/π^+ ratio in terms of Σ to Λ^0 emission ratio. The ratio π^-/π^+ after including his data and that of the Sidney group (6 π^- 's and 0 π^+) becomes 29/3, which in turn indicates the overwhelming Λ^0 emissions compared with Σ emission (at least 5 to 1) for any reasonable choice of the scattering mean free path. However, his stopping π^- 's have rather large energies, (half of them had energies above 40 MeV); therefore, we can expect some contribution of unscattered π -mesons which will raise the ratio considerably. The unscattered π -meson can have energies from 49 to 94 MeV in case of $\Sigma+\pi$ because of the Fermi motion of the capturing nucleon. If we want to estimate the Σ to Λ^0 emission ratio from the observation of the π^-/π^+ ratio, obviously experimental data of much better statistics are needed. However, the conclusion of the predominant $T=1$ state seems to have been reasonably well established.

RIASSUNTO (*)

Si confrontano i risultati dell'ipotesi dell'indipendenza della carica con i dati sperimentali esistenti sulla cattura nucleare dei mesoni K negativi. Dal confronto dei rapporti d'emissione Σ^-/Σ^+ calcolati con quelli sperimentali emerge la predominanza dello stato $T=1$ sullo stato $T=0$ nell'atto primario. Inoltre si dimostra che il rapporto d'emissione π^-/π^+ da una stima della « branching ratio » fra emissione F ed emissione Λ^0 esente dalle ambiguità dovute all'assorbimento secondario dei prodotti dell'atto primario o dovute alla difficoltà di svelare particelle neutre e solo debolmente influenzata dagli scattering secondari per scambi di carica delle particelle prodotte. Il valore preliminare così determinato servendosi dei dati sperimentali finora disponibili per il rapporto d'emissione π^-/π^+ , fa ritenere che l'emissione Σ sia favorita nell'atto primario rispetto all'emissione Λ^0 . Si discutono dettagliatamente le questioni che sorgono dalla misura del rapporto fra pioni positivi e negativi di alta energia emessi nelle catture K^- e a tale proposito si propongono alcune esperienze.

(*) Traduzione a cura della Redazione.

Meson Nucleon S Scattering and Crossing Theorem (*).

A. MARTIN

École Normale Supérieure, Université de Paris

(ricevuto il 21 Maggio 1956)

Summary. — It is noticed that the low energy S wave calculations of meson nucleon scattering cannot be very satisfactory if they do not obey the « crossing theorem ». It may be interesting to modify the iteration treatments in order to satisfy the symmetry requirements. For this purpose the series of scattering processes considered is completed by a new series in which the initial meson and the final meson are exchanged. In this way, we generalize Lévy's covariant treatment of S wave scattering. The result of the calculation is deeply modified by the introduction of these new processes. It is not possible to get a quantitative agreement with experiment. The signs of the phase shifts, however, are correct near $G^2/4\pi = 15$. The approximations used in solving the integral equations are discussed by comparison with other calculations.

1. — Introduction.

Several theoretical attempts have been made to explain meson nucleon scattering. It is well known that the P wave behavior can be correctly described by different methods (¹⁻⁷). The S wave calculations (^{1,2,6,8-10}) however

(*) A preliminary report of the present work has been already given at the International Conference on Elementary Particles (Pisa, July 1955).

(1) F. J. DYSON, M. ROSS, E. E. SALPETER, S. S. SCHWEBER, M. K. SUNDARESAN, W. M. VISSCHER and H. A. BETHE: *Phys. Rev.*, **95**, 1644 (1954).

(2) M. H. KALOS and R. H. DALITZ: *Phys. Rev.*, **100**, 1515 (1955).

(3) G. F. CHEW: *Phys. Rev.*, **95**, 1669 (1954).

(4) G. F. CHEW: *Proc. of the Pisa Conf. on Elementary Particles* (to be published).

(5) G. C. WICK: *Rev. Mod. Phys.*, **27**, 339 (1955).

(6) M. CINI and S. FUBINI: *Nuovo Cimento*, **11**, 142 (1954); L. SARTORI and V. WATAGHIN: *Nuovo Cimento*, **12**, 260 (1954).

are still in an unsatisfactory state. According to the latest interpretation of experimental data ⁽¹¹⁾ the two S phase shifts exhibit a linear dependence on the meson momentum up to energies of the order of 200 MeV. It seems very important to explain their low energy behavior, and especially, the difference between the two corresponding scattering lengths. GELL-MANN and GOLD-

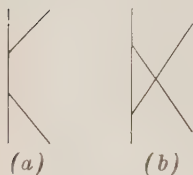


Fig. 1.

BERGER ⁽¹²⁾ have shown that, when all scattering processes are taken into account, the S phase shifts obey the so-called Crossing Theorem which states that in the limit $k \rightarrow 0$ $\mu/M \rightarrow 0$ the ratio $(\alpha_1 - \alpha_3)/k$ goes to zero. Any treatment of S scattering which gives for this ratio a non vanishing limit cannot be very satisfactory, at least at low energies, since the actual ratio μ/M is rather small (0.147). The theorem is deduced from the fact that to every process one can associate a « crossed » process

in which the initial and final meson lines have been exchanged (see Fig. 1). It will be shown that the amplitude for the second process is connected to the amplitude for the first process by the equation:

$$(1) \quad a'_{ij}(p_1, p_2, p_3, p_4) = a_{ij}(p_1, -p_4, p_3, -p_2).$$

For zero energy and zero meson mass the sum of these amplitudes becomes $a_{ij}(p, 0, p, 0) + a_{ij}(p, 0, p, 0)$ and since, on invariance grounds, $a_{ij} = A \delta_{ij} + B[\tau_i, \tau_j]$, the sum is independent of the isotopic spin state ⁽¹³⁾.

A covariant calculation up to a given order in the coupling constant satisfies automatically these symmetry requirements; such a calculation has been made by H. W. WYLD JR. up to fourth order ⁽¹⁴⁾. But treatments using iterations of elementary processes such as a Bethe-Salpeter or Tamm-Dancoff equation violate the symmetry theorem. However the relative success of these methods and the failure of perturbation expansions make it interesting to modify the iteration treatments in order to take into account the crossed processes.

(7) D. ITO and H. TANAKA: *Prog. Theor. Phys.*, **12**, 105 (1954).

(8) M. M. LÉVY and R. E. MARSHAK: *Nuovo Cimento*, **11**, 366 (1954).

(9) M. M. LÉVY: *Phys. Rev.*, **94**, 460 (1954) (referred to as A in the present paper)

(10) M. M. LÉVY: *Phys. Rev.*, **98**, 1470 (1955) (referred to as B in the present paper).

(11) J. OREAR: *Phys. Rev.*, **100**, 288 (1955).

(12) M. GELL-MANN and M. L. GOLDBERGER: *Proc. of the Fourth Annual Rochester Conf. on High Energy Nuclear Physics*.

(13) This property becomes evident if the matrix element for scattering is expressed in terms of Heisenberg operators (F. E. LOW: *Phys. Rev.*, **97**, 1392 (1955)).

(14) H. W. WYLD JR.: *Thesis*, University of Chicago, 1955.

Starting from a given series of terms, we can add a new series containing the corresponding crossed terms. It will be shown that the Feynmann two body kernel for the second series can be directly deduced from the kernel corresponding to the first series. Besides it may be shown that the « crossed » kernel obeys an integral equation, whilst the corresponding part of the wave function does not.

The present work starts from the covariant treatment proposed by M. LÉVY in two papers ^(9,10). This treatment used a Bethe-Salpeter equation with, as irreducible processes, the two second order terms. In A a general formalism was given. In B the difficulties arising from overlapping divergences were examined and an approximate solution, adapted to S scattering, was given.

2. — Notations. Connection between the Feynman Kernels and the Wave Function.

In principle we use the same notations as A and B . However, for the sake of completeness we give them here again.

The volume element is chosen:

$$d^4p = dp_1 dp_2 dp_3 dp_4 = i dp_1 dp_2 dp_3 dp_0.$$

The propagator are defined by:
and

$$(2) \quad \left\{ \begin{array}{l} K_N(p) = -i(\gamma p + M - i\varepsilon)^{-1}, \quad K_M(p) = -(p^2 + \mu^2 - i\varepsilon)^{-1}, \\ K_M^{ij}(x_1 x_2) = (2\pi)^{-4} \int K_M(p) \exp[ip(x_1 - x_2)] d^4p \delta_{ij}, \\ K_N(x_1 x_2) = (2\pi)^{-4} \int K_N(p) \exp[ip(x_1 - x_2)] d^4p. \end{array} \right.$$

We define the two body kernel in momentum space:

$$(3) \quad K_x^{ij}(p_1, p_2; p_3, p_4) = \int K_x^{ij}(x_1, x_2; x_3, x_4) \cdot \exp[-i(p_1 x_1 + p_2 x_2) + i(p_3 x_3 + p_4 x_4)] d^4x_1 d^4x_2 d^4x_3 d^4x_4,$$

where 1 and 3 are nucleon indices, and 2 and 4 are meson indices.

In particular, to

$$K_0^{ij}(x_1, x_2; x_3, x_4) = K_N(x_1, x_2) K_M^{ij}(x_2, x_4)$$

corresponds

$$K_0^{ij}(p_1, p_2; p_3, p_4) = K_N(p_1) K_M(p_2) \delta(p_1 - p_3) \delta(p_2 - p_4) \delta_{ij}.$$

The wave functions are defined by:

$$(4) \quad \left\{ \begin{array}{l} \psi_0(1, 2) = \lim_{\substack{t_3 \rightarrow -\infty \\ t_4 \rightarrow -\infty}} \int K_N(1, 3) K_M(2, 4) \gamma_4 \psi_0(3, 4) \mathbf{d}^3\mathbf{d}^4, \\ \varphi_x(1, 2) = \lim_{\substack{t_3 \rightarrow -\infty \\ t_4 \rightarrow -\infty}} \int K_x(1, 2; 3, 4) \gamma_4 \psi_0(3, 4) \mathbf{d}^3\mathbf{d}^4, \end{array} \right.$$

and in momentum space:

$$(5) \quad \varphi_x(p_1, p_2) = \int \exp[-i(p_1 x_1 + p_2 x_2)] \psi_x(x_1, x_2) \mathbf{d}^4 x_1 \mathbf{d}^4 x_2.$$

If we assume for the free wave function in momentum space the following form:

$$(6) \quad \varphi_{0j}(p_1, p_2) = (2\pi)^4 \Phi_{0j}(p_N, p_M) \delta(p_1 - p_N) \delta(p_2 - p_M),$$

where $\Phi_{0j}(p_N, p_M)$ obeys the free equations, then it can be shown that

$$(7) \quad q_x^i(p_1, p_2) = \frac{1}{(2\pi)^4} \lim_{\substack{p_3 \rightarrow p_N \\ p_4 \rightarrow p_M}} [K_x^{ij}(p_1, p_2; p_3, p_4) K_N^{-1}(p_3) K_M^{-1}(p_4)] \Phi_{0j}(p_N, p_M).$$

Taking into account the energy-momentum conservation we can write:

$$(8) \quad \varphi_x^i(p_1, p_2) = \delta(p_N + p_M - p_1 - p_2) \Phi_x^i(-p_2, p_N + p_M).$$

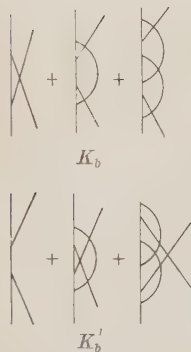


Fig. 2.

3. - Classification of Scattering Processes.

We first take into account the iterations of graphs (a) and (b) (Fig. 1). Iteration of graph (a) gives a series of finite processes K_b (Fig. 2); the remaining terms give rise to K_a , which can be written in terms of two vertex parts Γ_N and Γ_M and a nucleon modified propagator $K'_N = K_N(1 - \sum K_N)^{-1}$ (see Fig. 3). We now add the corresponding crossed graphs, which lead to the kernels K'_b (Fig. 2) and K'_a (Fig. 3). We notice that in the sum $K_a + K_b + K'_a + K'_b$ the zero order and second order terms appear twice; therefore the correct Feynman

amplitude is

$$(9) \quad K_a + K_b + K'_a + K'_b - (a) - (b) - K_0.$$

The wave function can be correspondingly split in several parts, ψ_a , ψ_b , ψ'_a , ψ'_b , etc...

4. — Calculation of Finite Processes.

q_b has been calculated in B . In order to calculate K'_b and consequently φ'_b , we first establish the mathematical correspondence between K_b and K'_b . Consider a given scattering process X . We can always write

$$(10) \quad K_X^{ij}(1, 2; 3, 4) = \\ = \int K_N(1, 5) K_M^{ii}(2, 6) F^{ij}(5, 6, 7, 8) K_N(7, 3) K_M^{jj}(8, 4) d5 d6 d7 d8,$$

and exchanging the initial and final meson lines,

$$(11) \quad K_X^{ij}(1, 2; 3, 4) = \\ = \int K_N(1, 5) K_M^{ii}(2, 8) F^{ij}(5, 6, 7, 8) K_N(7, 3) K_M^{jj}(6, 4) d5 d6 d7 d8.$$

Use of the equality: $K_M^{ii}(1, 2) = K_M^{jj}(2, 1)$ and of the commutation properties of K_M leads to the equation

$$(12) \quad K_X^{ij}(1, 2; 3, 4) = K_X^{ij}(1, 4; 3, 2)$$

which becomes in momentum space:

$$(13) \quad K_X^{ij}(p_1, p_2; p_3, p_4) = K_X^{ij}(p_1, -p_4; p_3, -p_2).$$

Hence K'_b can be deduced from K_b . Unfortunately the knowledge of q_b is not sufficient to determine completely K_b . We must therefore solve the following integral equation:

$$(14) \quad K_b^{ij}(p_1, p_2; p_3, p_4) = (2\pi)^6 K_N(p_1) K_M(p_2) \delta(p_1 - p_3) \delta(p_2 - p_4) \delta_{ij} - \\ - \tau_i \tau_j \frac{iG^2}{(2\pi)^4} K_N(p_1) K_M(p_2) \gamma_5 \int K_N(p_1 - p) \gamma_5 K_b^{ij}(p_1 - p, p; p_3, p_4) d^4 p.$$

This equation can be made separable by use of the approximation proposed

in B . It consists in replacing $\gamma_5 K_N(p_1 - p)\gamma_5 = K_N(-p_1 + p)$ by

$$(15) \quad K_N(-(p_1 + p_2) + p_2) K_N^{-1}(-(p_1 + p_2)) K_N(-(p_1 + p_2) + p).$$

This approximation is valid when p or p_2 (meson momenta) is small compared to the total energy-impulsion $p_1 + p_2 = P$, but cannot be applied to $L \neq 0$ phase shift calculations, since it destroys the correlation between the spatial directions of the mesons. The error can be estimated of order $(\varepsilon/M)^2$ where ε is the total meson energy and M the nucleon mass. Equation (14) then becomes:

$$(16) \quad K_b^{ij}(p_1, p_2; p_3, p_4) = (2\pi)^8 K_N(p_1) K_M(p_2) \delta(p_1 - p_3) \delta(p_2 - p_4) \delta_{ij} - \\ - \frac{iG^2}{(2\pi)^4} \tau_i \tau_j K_N(p_1) K_M(p_2) K_N(-p_1) K_N^{-1}(-p_1 - p_2) C_b^{ij}(P, p_3, p_4),$$

where

$$(17) \quad C_b^{ij} = \int K_N(-P + p) K_b^{ij}(P - p, p; p_3, p_4) d^4p.$$

The C_b^{ij} obey a system of algebraic equations:

$$(18) \quad C_b^{ij} = \lambda \delta_{ij} \mu \tau_i \tau_j C_b^{ij},$$

where

$$(19) \quad \begin{cases} \lambda = (2\pi)^8 K_N(-p_3) K_N(p_3) K_M(p_4) \delta(P - p_3 - p_4), \\ \mu = -\frac{G^2}{4\pi} Q(P), \end{cases}$$

$Q(P)$ is a convergent integral defined in II.

Solving this system we obtain

$$(20) \quad K_b^{ij}(p_1, p_2; p_3, p_4) = (2\pi)^8 K_N(p_1) K_M(p_2) \delta(P - p_3 - p_4) \delta(p_2 - p_4) \delta_{ij} - \\ - iG^2 (2\pi)^4 K_N(p_1) K_N(-p_1) K_M(p_2) K_N^{-1}(-P) \frac{\tau_j \tau_i - 2(G^2/4\pi)Q(P)\delta_{ij}}{[1 + 2(G^2/4\pi)Q(P)][1 - (G^2/4\pi)Q(P)]} \cdot \\ \cdot K_N(p_3) K_N(-p_3) K_M(p_4) \delta(P - p_3 - p_4).$$

The corresponding part of the wave function is given by

$$\varphi_b^i(p_1, p_2) = \delta(P - p_N - p_M) \Phi_b^i(-p_2, P),$$

where

$$(21) \quad \Phi_b^i(p, P) = (2\pi)^4 \delta(p - k) \Phi_0^i(P + k, -k) - \\ - iG^2 K_N(P + p) K_N(-P - p) K_M(-p) K_N^{-1}(-P) \frac{\tau_j \tau_i - 2(G^2/4\pi) Q(P) \delta_{ij}}{[1 + 2(G^2/4\pi) Q(P)][1 - (G^2/4\pi) Q(P)]} \cdot \\ \cdot K_N(-P - k) \Phi_0^i(P + k, -k).$$

The operator $\tau_j \tau_i$ has the following eigenvalues:

$$T_b^{\frac{3}{2}} = +2,$$

$$T_b^{\frac{1}{2}} = -1.$$

This remark enables us to write the preceding equation in the following form:

$$(22) \quad \left\{ \begin{array}{l} \Phi_b^{\frac{3}{2}}(p, P) = (2\pi)^4 \delta(p - k) \Phi_0^{\frac{3}{2}}(P + k, -k) \\ - 2iG^2 K_N(P + p) K_N(-P - p) K_M(-p) K_N^{-1}(-P) \frac{1}{1 + 2(G^2/4\pi) Q(P)} \cdot \\ \cdot K_N(-P - k) \Phi_0^{\frac{3}{2}}(P + k, -k), \\ \Phi_b^{\frac{1}{2}}(p, P) = (2\pi)^4 \delta(p - k) \Phi_0^{\frac{1}{2}}(P + k, -k) - \\ - (-1) iG^2 K_N(P + p) K_N(-P - p) K_M(-p) K_N^{-1}(-P) \frac{1}{1 - (G^2/4\pi) Q(P)} \cdot \\ \cdot K_N(-P - k) \Phi_0^{\frac{1}{2}}(P + k, -k). \end{array} \right.$$

These expressions coincide with those given in B.

Equation (13) gives us now K'_b . Let us put

$$II = p_1 - p_4 = P + p_2 + p_4$$

(II plays the same role in K'_b as P does in K_b). We obtain:

$$(23) \quad K_b'^{ij}(p_1, p_2; p_3, p_4) = (2\pi)^4 K_N(p_1) K_M(p_2) \delta(P - p_3 - p_4) \delta(p_2 - p_4) \delta_{ij} - \\ - iG^2 (2\pi)^4 K_N(p_1) K_N(-p_1) K_M(p_4) K_N^{-1}(-II) \frac{\tau_j \tau_i - 2(G^2/4\pi) Q(II) \delta_{ij}}{[1 + 2(G^2/4\pi) Q(II)][1 - (G^2/4\pi) Q(II)]} \cdot \\ \cdot K_N(p_3) K_N(-p_3) K_M(-p_2) \delta(P - p_3 - p_4).$$

The corresponding part of the wave function can be written:

$$(24) \quad \Phi'_b(p, P) = (2\pi)^4 \delta(p - k) \Phi_0(P + k, -k) - \\ - iG^2 K_N(P + p) K_N(-P - p) K_M(-p) K_N^{-1}(-II) \frac{T_A - 2(G^2/4\pi) Q(II)}{[1 + 2(G^2/4\pi) Q(II)][1 - (G^2/4\pi) Q(II)]} \cdot \\ \cdot K_N(-P - k) \Phi_0(P + k, -k),$$

where $T_a^{\frac{3}{2}} = 0$, $T_a^{\frac{1}{2}} = 3$ are the eigenvalues of the operator $\tau_i \tau_j$.

5. — Calculation of K'_a and K'_a .

These two kernels can be written in terms of the vertex parts Γ_α and Γ_β and of the modified propagator K'_N (see Fig. 3). In principle all these quantities are given in *B*. However, we can no longer take the renormalization prescriptions used in *B*. These prescriptions were as follows:

$$(25) \quad (\Gamma_{5\alpha})_c = \gamma_5 \frac{\Gamma_\alpha(p, q)}{\Gamma_\alpha(p_0, p'_0)},$$

where $i\gamma p'_0 + M = 0$, $(p'_0 - p_0)^2 + \mu^2 = 0$, (to the right),

$$(25') \quad (\Gamma_{5\beta})_c = \frac{\Gamma_\beta(p, q)}{\Gamma_\beta(p'_0, p_0)} \gamma_5,$$

where $i\gamma p'_0 + m = 0$, $(p_0 - p'_0)^2 + \mu^2 = 0$ (to the left).

So that when we apply Γ_α to the initial free state:

$$\Gamma_\alpha = 1$$

and when we apply Γ_β to the left to the final free state:

$$\Gamma_\beta = 1.$$

Unfortunately we need a more complete knowledge of the vertex parts in order to calculate K'_a . Γ_α and Γ_β obey integral equations which can be solved by replacement of their exact kernel by a separable one. The divergent solution thus obtained can be made finite by a special prescription adapted to the approximation, completely different from the one used in *B*.

For instance, Γ'_α defined by $\Gamma'_{5\alpha} = \tau_i \gamma_5 \Gamma'_\alpha$ obeys the following integral equation:

$$(27) \quad \Gamma'_\alpha(P, P+p) = 1 + \frac{iG^2}{(2\pi)^4} \int \Gamma_\alpha(P, P+k) K_N(P+k) K_M(-k) \gamma_5 K_N(P+p+k) \gamma_5 d^4k.$$

The substitution (15):

$$\gamma_5 K_N(P+p+k) \gamma_5 \rightarrow K_N(-P-k) K_N^{-1}(-P) K_N(-P-p),$$

makes the integral equation separable. We then can write:

$$(28) \quad \Gamma_{\alpha}(P, P+p) = 1 + \frac{iG^2}{(2\pi)^4} C(P) K_N^{-1}(-P) K_N(-P-p),$$

with

$$(29) \quad C(P) = \int \Gamma_{\alpha}(P, P+p) K_N(P+p) K_N(-P-p) K_M(-p) d^4p.$$

The solution is as follows:

$$(30) \quad \Gamma_{\alpha}(P, P+p) = 1 + \frac{iG^2}{(2\pi)^4} \frac{I(P^2)}{1 - (G^2/4\pi)Q(P)} K_N^{-1}(-P) K_N(-P-p),$$

$Q(P)$ is a convergent integral already encountered.

$$(31) \quad I(P^2) = \int K_N(P+p) K_N(-P-p) K_M(-p) d^4p,$$

is a logarithmically divergent quantity.

We formally develop Γ_{α} in a power series of $G^2/4\pi$ and follow Salam's prescriptions for the renormalization of divergent integrals. Consequently, in every term of the series $I(P^2)$ is replaced by $I(P^2) - I(P_0^2)$ with $P_0^2 + M^2 = 0$. Summing the renormalized series we get the following result:

$$(32) \quad \Gamma_{\alpha}(P, P+p) = 1 + \frac{G^2}{4\pi} \frac{F(P^2)}{1 - (G^2/4\pi)Q(P)} K_N^{-1}(-P) K_N(-P-p),$$

where

$$(33) \quad F(P^2) = \frac{I(P^2) - I(-M^2)}{4\pi^3 i} = \frac{1}{4\pi} \int_0^1 \log \frac{D}{D_0} dx$$

$$D = M^2 x + \mu^2(1-x) + P^2 x(1-x), \quad D_0 = D(-M^2)$$

(this integral has been defined in B).

A symmetric treatment applied to Γ_{β} gives:

$$(34) \quad \Gamma_{\beta c}(P+p, P) = 1 - \frac{G^2}{4\pi} K_N(-P-p) K_N^{-1}(-P) \frac{F(P^2)}{1 - (G^2/4\pi)Q(P)}.$$

The modified propagator K'_N can be directly taken from B:

$$K'_N = K_N / (1 - \Sigma K_N),$$

with

$$(35) \quad \Sigma_c(P) = \Sigma_{0c} - 3 \left(\frac{G^2}{4\pi} \right)^2 K_N^{-1}(P) \frac{F^2(P^2)}{1 - (G^2/4\pi)Q(-P)},$$

where Σ_{0c} is the second order term calculated by BRUECKNER, GELL-MANN and GOLDBERGER ⁽¹⁵⁾.

The following exact relations between unrenormalized quantities show the self-consistency of our approximations:

$$(36) \quad \Sigma(P) = - \frac{iG^2}{(2\pi)^4} \tau_i \gamma_5 \int K_N(P+p) K_M(-p) \tau_i \gamma_5 \Gamma_\beta(P+p, P) d^4p,$$

$$(36') \quad \Sigma(P) = - \frac{iG^2}{(2\pi)^4} \tau_i \gamma_5 \int \Gamma_\alpha(P, P+p) K_N(P+p) K_M(-p) \tau_i \gamma_5 d^4p,$$

$$(37) \quad \frac{\partial \Sigma(P)}{\partial G^2} = - \frac{3i}{(2\pi)^4} \gamma_5 \int \Gamma_\alpha(P, P+p) K_N(P+p) K_M(-p) \Gamma_\beta(P+p, P) d^4p,$$

and:

$$(38) \quad \frac{1}{(2\pi)^8} \tau_i \gamma_5 \int K_b^{ij}(P'+p', -p'; P+p, -p) K_N^{-1}(P+p) K_M^{-1}(-p) dP' dp' = \\ = \Gamma_{5\alpha}^i(P, P+p),$$

$$(38') \quad \frac{1}{(2\pi)^8} K_N^{-1}(P+p) K_M^{-1}(p) \int K_b^{ij}(P+p, -p; P'+p', -p') \tau_i \gamma_5 dP' dp' = \\ = \Gamma_{5\beta}^i(P+p, P).$$

Use of the above given expressions for K'_N and Γ enables to construct K'_a and K'_n :

$$(39) \quad K_a^{ij}(p_1, p_2; p_3, p_4) = -iG^2(2\pi)^4 K_N(p_1) K_M(p_2) \Gamma_{5\beta}^i(p_1, p_1+p_2) K_N'(p_1+p_2) \cdot \\ \cdot \Gamma_{5\alpha}^j(p_1+p_2, p_3) K_N(p_3) K_M(p_4) \delta(p_1+p_2-p_3-p_4)$$

and

$$(40) \quad K_n^{ij}(p_1, p_2; p_3, p_4) = -iG^2(2\pi)^4 K_N(p_1) K_M(p_2) \Gamma_{5\beta}^j(p_1, p_1-p_1) K_N'(p_1-p_1) \cdot \\ \cdot \Gamma_{5\alpha}^i(p_3-p_2, p_3) K_N(p_3) K_M(p_4) \delta(p_1+p_2-p_3-p_4).$$

By the standard technique we obtain the corresponding parts of the wave

⁽¹⁵⁾ K. A. BRUECKNER, M. GELL-MANN and L. M. GOLDBERGER: *Phys. Rev.*, **90**, 476 (1953).

function:

$$(41) \quad \Phi_a(p, P) = -iG^2 T_a K_N(P+p) K_M(-p) \Gamma_\beta(P+p, p) \cdot \\ \cdot K'_N(-P) \Gamma_\alpha(P, P+k) \Phi_0(P+k, -k),$$

$$(42) \quad \Phi'_a(p, P) = -iG^2 T_b K_N(P+p) K_M(-p) \Gamma_\beta(P+p, \Pi) \cdot \\ \cdot K'_N(-\Pi) \Gamma_\alpha(\Pi, P+k) \Phi_0(P+k, -k)$$

where $\Pi = P + p + k$.

6. — Relation between the Wave Function and the Phase Shifts.

In the center of masses system ($P = p_1 + p_2 = 0, 0, 0, iP_0$) the wave function can be written,

$$(43) \quad \Phi(p, P) = (2\pi)^4 \Phi_0(P+k, -k) \delta(p - k) - \\ - i K_N(P-p) K_N(P+p) K_M(-p) f(i\gamma P, i\gamma p_k, i\gamma k) \Phi_0(P+k, -k).$$

The wave function for equal times is obtained by integration over p_0 . If we only retain the terms contributing to the asymptotic form we get

$$(44) \quad \Phi(\mathbf{p}) = (2\pi)^3 \delta(\mathbf{p} - \mathbf{k}) \Phi_0(P+k, -k) - \frac{1}{4E_k \omega_k (E_p + \omega_p - P_0)} \cdot \\ \cdot f(i\gamma P, i\gamma p_k, i\gamma k) \Phi_0(P+k, -k),$$

where $p_k = \mathbf{p}_k$, $-\omega_k$ and $|\mathbf{p}| = |\mathbf{k}|$.

Multiplying by the positive energy normalized spinors $u_+^*(\mathbf{p})$ to the left and $u_+(\mathbf{p})$ to the right respectively we obtain an equation for a spin dependent amplitude $b_+(\mathbf{p})$:

$$(45) \quad b_+(\mathbf{p}) = (2\pi)^3 \delta(\mathbf{p} - \mathbf{k}) C \frac{1}{4E_k \omega_k (E_p + \omega_p - P_0)} \cdot \\ \cdot \left[F(\mathbf{p}_k \cdot \mathbf{k}) + \frac{(\boldsymbol{\sigma} \cdot \mathbf{p}_k)(\boldsymbol{\sigma} \cdot \mathbf{k})}{k^2} H(\mathbf{p}_k \cdot \mathbf{k}) \right],$$

with the following connection with the preceding equation:

$$(46) \quad \begin{cases} \Phi(\mathbf{p}) \text{ asymptotic} = (\chi_+^* b_+(\mathbf{p}) \chi_k) u_+(\mathbf{p}) \\ \Phi_0(P+k, -k) = C u_+(\mathbf{k}) \end{cases}$$

and

$$(47) \quad u_{+}^{*}(\mathbf{p})f(i\gamma P, i\gamma p_k, i\gamma k)u_{+}(\mathbf{k}) = \chi_p^{*} \left[F(\mathbf{p}_k \cdot \mathbf{k}) + \frac{(\boldsymbol{\sigma} \cdot \mathbf{p}_k)(\boldsymbol{\sigma} \cdot \mathbf{k})}{k^2} H(\mathbf{p}_k \cdot \mathbf{k}) \right] \chi_k,$$

where χ_p and χ_k are the two component spin wave functions corresponding to $u(\mathbf{p})$ and $u(\mathbf{k})$. In the calculation of F and H , use is made of the Dirac equations

$$[i\gamma(P + k) + M]u(\mathbf{k}) = 0$$

$$u(\mathbf{p})[i\gamma(P + p) + M] = 0$$

and of the matrix elements:

$$u^{*}(\mathbf{p})u(\mathbf{k}) = \chi_p^{*} \left[1 + \frac{(\boldsymbol{\sigma} \cdot \mathbf{p})(\boldsymbol{\sigma} \cdot \mathbf{k})}{(E_k + M)^2} \right] \frac{E_k + M}{2E_k} \chi_k,$$

$$u^{*}(\mathbf{p})\gamma_4 u(\mathbf{k}) = \chi_p^{*} \left[1 - \frac{(\boldsymbol{\sigma} \cdot \mathbf{p})(\boldsymbol{\sigma} \cdot \mathbf{k})}{(E_k + M)^2} \right] \frac{E_k + M}{2E_k} \chi_k,$$

F and H can be developed in Legendre polynomials:

$$(48) \quad \begin{cases} F = F_0 + F_1 P_1(\cos(\mathbf{p} \cdot \mathbf{k})) + F_2 P_2(\cos(\mathbf{p} \cdot \mathbf{k})) + \dots \\ H = H_0 + H_1 P_1(\cos(\mathbf{p} \cdot \mathbf{k})) + H_2 P_2(\cos(\mathbf{p} \cdot \mathbf{k})) + \dots \end{cases}$$

Transforming the equation for b_{+} to configuration space we obtain the following phase shifts:

$$(49) \quad \begin{cases} S \text{ wave:} & \text{tg } \alpha_x = -\frac{k}{8\pi P_0} \left[F_0 + \frac{H_1}{3} \right], \\ P \text{ wave:} & \begin{cases} \text{tg } \alpha_{x1} = -\frac{k}{8\pi P_0} \left[\frac{F_1}{3} + H_0 \right], \\ \text{tg } \alpha_{x3} = -\frac{k}{8\pi P_0} \left[\frac{F_1}{3} + \frac{H_2}{5} \right], \end{cases} \end{cases}$$

where x is the isotopic spin index.

We notice that the S phase shift is just proportional to the mean value over the angles of the quantity

$$u_{+}^{*}(\mathbf{p})f_{\omega}(i\gamma P, i\gamma p_k, i\gamma k)u_{+}(\mathbf{k}),$$

where $u_+(p)$ and $u_+(k)$ correspond to the same spin state.

$$(50) \quad \begin{aligned} \operatorname{tg} \alpha_x &= -\frac{k}{8\pi P_0} \langle u_+^*(\mathbf{p}) f(i\gamma P, i\gamma p_k, i\gamma k) u_+(\mathbf{k}) \rangle = \\ &= \frac{k}{8\pi P_0} \left\langle F(\mathbf{p} \cdot \mathbf{k}) + \frac{\mathbf{p} \cdot \mathbf{k}}{k^2} H(\mathbf{p} \cdot \mathbf{k}) \right\rangle. \end{aligned}$$

These formulae show that the different contributions of the wave function to the tangents of the phase-shifts will be additive.

Since the wave function can be written:

$$(51) \quad \Phi = \Phi_0 + (\Phi_b - \Phi_0) + \Phi_a + (\Phi'_b - \Phi_0) + \Phi'_a - (\Phi_b - \Phi_0)_{\text{Born}} - (\Phi'_b - \Phi_0)_{\text{Born}}$$

the corresponding phase shifts are given by:

$$(52) \quad \operatorname{tg} \alpha = (\operatorname{tg} \alpha)_a + (\operatorname{tg} \alpha)_b + (\operatorname{tg} \alpha)_a' + (\operatorname{tg} \alpha)_b' - (\operatorname{tg} \alpha)_b_{\text{Born}} - (\operatorname{tg} \alpha)_b'_{\text{Born}}.$$

Relatively simple expressions may be derived for $(\operatorname{tg} \alpha)_a$ and $(\operatorname{tg} \alpha)_b$. This fact comes from the structure of f_a and f_b .

$$(53) \quad f_{a \text{ or } b} = \psi_1(i\gamma(P+p)) \times \psi_2(i\gamma(P+k)).$$

Consequently, by use of the Dirac equation, it can be shown that:

$$(54) \quad u_+^*(\mathbf{p}) f_{a \text{ or } b} u_+(\mathbf{k}) = \chi_p^* \left[(F_0) + \frac{(\boldsymbol{\sigma} \cdot \mathbf{p})(\boldsymbol{\sigma} \cdot \mathbf{k})}{k^2} (H_0) \right] \chi_k,$$

where F_0 and H_0 do not depend on the angle $(\mathbf{p} \cdot \mathbf{k})$. We have obtained

$$(55) \quad \begin{aligned} (\operatorname{tg} \alpha)_a &= -k T_a \frac{G^2}{4\pi} \frac{(E_k + M)}{2P_0(P_0 + M)} \left[1 - \frac{G^2}{4\pi} \frac{M + P_0}{2E_k} \frac{F(P^2)}{1 - (G^2/4\pi) \Delta_b(P_0)} \right] \cdot \\ &\cdot \left[1 - \frac{G^2}{4\pi} \frac{M + P_0}{2M} \frac{F(P^2)}{1 - (G^2/4\pi) \Delta_b(P_0)} \right] \frac{1}{1 + (G^2/4\pi) \Delta_a(P_0)}, \end{aligned}$$

and (this is exactly the expression given in B):

$$(56) \quad (\operatorname{tg} \alpha)_b = -\frac{k}{2M} T_b \frac{G^2}{4\pi} \frac{(M + P_0)(E_k + M)}{4E_k P_0} \frac{1}{1 + (G^2/4\pi) T_b \Delta_b(P_0)}.$$

Unfortunately it is not possible to give explicit expressions for $(\operatorname{tg} \alpha)_a'$ and $(\operatorname{tg} \alpha)_b'$ since f_a' and f_b' are functions of $i\gamma(P+p+k) = i\gamma\Pi$. Starting from

$$(58) \quad \begin{aligned} f_a' &= G^2 T_b K_N^{-1}(-P-p) \Gamma_\beta(P+p, \Pi) K_N'(-\Pi) \Gamma_\alpha(\Pi, P+k), \\ f_b' &= G^2 K_N^{-1}(-P) \left[1 + \frac{T_a - (G^2/4\pi) Q(\Pi)}{2(G^2/4\pi) Q(\Pi)} \right] \frac{(-i)}{(2M)}, \end{aligned}$$

it is possible to calculate numerically the corresponding contributions to the phase shifts. Evaluation of the matrix elements for three angles (0° , 90° , 180°) is sufficient to give a correct mean value (up to energies of the order of 200 MeV).

In the low energy limit, however, considerable simplifications arise. In this limit

$$P = (0, 0, 0, i(M + \mu))$$

$$\Pi = (0, 0, 0, i(M - \mu))$$

$$k = p = (0, 0, 0, -i\mu).$$

γ_4 is consequently the only Dirac matrix appearing in f_a and f_b , and, since in this limit $u_+(\mathbf{p})u_+(\mathbf{k}) = u_+(\mathbf{p})\gamma_4 u_+(\mathbf{k}) = 1$, the evaluation of the phase shifts is straightforward.

The low energy results are:

$$\begin{aligned} (60) \quad \text{tg } \alpha_1 = & -\frac{k}{2M} \frac{G^2}{4\pi} - \frac{2M + \mu}{2(M + \mu)} \left[\frac{1}{1 - (G^2/4\pi)\Delta_b(M + \mu)} - 1 \right] + \\ & + \frac{2M - \mu}{2(M + \mu)} \left[\frac{3}{1 + 2(G^2/4\pi)\Delta_b(M - \mu)} \frac{2(G^2/4\pi)\Delta_b(M - \mu)}{1 - (G^2/4\pi)\Delta_b(M - \mu)} - 3 \right] + \\ & + \frac{2M^2}{(2M + \mu)(M + \mu)} \frac{1}{3} \left[1 - \frac{G^2}{4\pi} \frac{2M + \mu}{2M} \frac{F[-(M + \mu)^2]}{1 - (G^2/4\pi)\Delta_b(M + \mu)} \right]^2 \frac{1}{1 + (G^2/4\pi)\Delta_a(M + \mu)} - \\ & - \frac{2M^2}{(2M - \mu)(M + \mu)} \left[1 - \frac{G^2}{4\pi} \frac{2M - \mu}{2M} \frac{F[-(M - \mu)^2]}{1 - (G^2/4\pi)\Delta_b(M - \mu)} \right]^2 \frac{1}{1 + (G^2/4\pi)\Delta_a(M - \mu)}, \\ (61) \quad \text{tg } \alpha_3 = & -\frac{k}{2M} \frac{G^2}{4\pi} + \frac{2M + \mu}{2(M + \mu)} 2 \left[\frac{1}{1 - 2(G^2/4\pi)\Delta_b(M - \mu)} - 1 \right] - \\ & - \frac{2M - \mu}{2(M + \mu)} \frac{2(G^2/4\pi)\Delta_b(M - \mu)}{[1 + 2(G^2/4\pi)\Delta_b(M - \mu)][1 - (G^2/4\pi)\Delta_b(M - \mu)]} + \\ & + \frac{2M^2}{(M + \mu)(2M - \mu)} 2 \left[1 - \frac{G^2}{4\pi} \frac{2M - \mu}{2M} \frac{F[-(M - \mu)^2]}{1 - (G^2/4\pi)\Delta_b(M - \mu)} \right]^2 \frac{1}{1 + (G^2/4\pi)\Delta_a(M - \mu)}. \end{aligned}$$

7. - Results and Discussion.

7.1. Comparison with experiment.

a) Low energy limit. - We have plotted $\alpha_1(\mu/k)(G^2/4\pi)^{-1}$ and $\alpha_3(\mu/k)(G^2/4\pi)^{-1}$ against $G^2/4\pi$ (Fig. 4).

In the whole range of values of $G^2/4\pi$ no quantitative agreement is obtained with the experimental data which are according to OREAR⁽¹¹⁾:

$$\alpha_1 = 0.16 \, k/\mu, \quad \alpha_3 = -0.11 \, k/\mu.$$

In the region $13 < G^2/4\pi < 17$ the signs and ratios of the two phase shifts are correct but their magnitude is about ten times the experimental value. We notice that the value $G^2/4\pi = 15$ ($f^2/4\pi = 0.08$) is precisely the coupling constant proposed by BETHE, DYSON *et al.* ^(1,2), and by CHEW ⁽⁴⁾ to explain

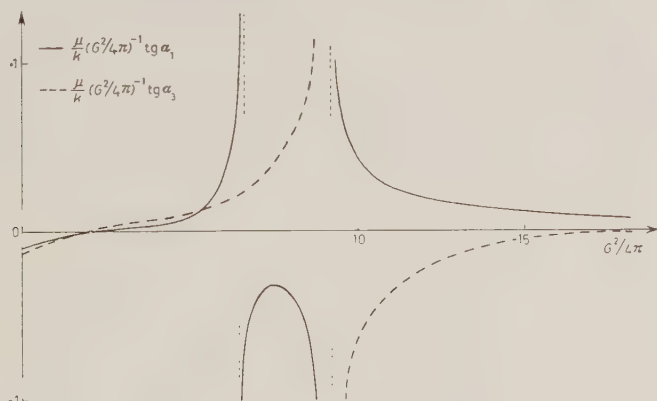


Fig. 4.

P wave scattering. One may tentatively say that the discrepancy in magnitude could be accounted for by some pair damping. On the other hand, meson-meson scattering has been neglected and its influence on S scattering is certainly important ⁽¹⁶⁾.

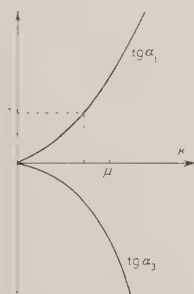


Fig. 5.

b) Energy dependance of the phase shifts. — The errors introduced by the approximation are of order $(\omega/M)^2$ so that the energy dependence of the phase shifts should not be taken too seriously. We have carried out numerical calculations up to energies of the order of 150 MeV for $G^2/4\pi = 16$ (Fig. 5). The smoothness of the curves near zero energy justifies the low energy calculation. The sign of the $T = \frac{1}{2}$ phase shift remains positive, in contradiction with B ; but we know, from Orear's latest analysis of experimental data that the energy dependence of the S phase shifts might well be purely linear.

7.2. Internal consistency of the calculation. — In this study we shall not investigate the influence of the neglected processes (meson-meson interaction,

⁽¹⁶⁾ A calculation is made on this subject by G. BONNEVAY at the University of Paris.

higher order irreducible—in the Bethe Salpeter sense—processes), but rather we shall try to see to what extent it is permissible to replace the exact kernel of our integral equations by a separable one.

a) Dependence on $G^2/4\pi$. — We first examine the limit $G^2/4\pi \rightarrow 0$. This gives us an interesting test of our approximations since $(\text{tg } \alpha)_a$ and $(\text{tg } \alpha)_b'$, $(\text{tg } \alpha)_a'$ and $(\text{tg } \alpha)_b$ should be rigorously equal in this limit, because they correspond to the same graphs. In fact they slightly differ since K_b and K_b' are calculated with use of the approximate kernel. Calculations have been made for $k = 0$ and $k = 2\mu$. It is seen (Table I) that the agreement is good in the low energy limit, but becomes poor when the energy increases, as it was anticipated.

TABLE I.

	$k = 0$	$k = 2\mu$
$\lim_{G^2/4\pi \rightarrow 0} \frac{(\text{tg } \alpha)_b}{(\text{tg } \alpha)_a'}$	0.993	0.985
$\lim_{G^2/4\pi \rightarrow 0} \frac{(\text{tg } \alpha)_b'}{(\text{tg } \alpha)_a}$	0.995	0.974

A noticeable feature of the dependence of the phase shifts on $G^2/4\pi$ is the appearance of « resonances » for certain values of the coupling constant. Four resonances are expected, corresponding, in the low energy limit, to

$$\begin{aligned}
 1 - (G^2/4\pi) \Delta_b(M + \mu) &= 0, & 1 - (G^2/4\pi) \Delta_b(M - \mu) &= 0 \\
 1 + (G^2/4\pi) \Delta_a(M + \mu) &= 0, & 1 + (G^2/4\pi) \Delta_a(M - \mu) &= 0.
 \end{aligned}$$

In fact, the first two resonances cancel in the sums $(\text{tg } \alpha)_a + (\text{tg } \alpha)_b$ and $(\text{tg } \alpha)_a' + (\text{tg } \alpha)_b'$. We shall try to see whether this cancellation is a consequence of our approximation or not.

The answer can be found in the following way: we formally express Γ, Γ_μ, K_N' and consequently K_a in terms of

$$(61) \quad K_b^{ij}(P+p, -p; P'+p', -p') = \bar{K}_b^{ij}(P+p, -p; P'+p', -p') \delta(P - P').$$

Suppose now that \bar{K}_b has a pole in isotopic spin state $\frac{1}{2}$, for some value of P independent of p and p' . An approximate expression of \bar{K}_a can be given, near this pole. Under the assumption that K_b has a separable form,

$$(62) \quad (\bar{K}_b - \bar{K}_0)^{ij} = \Phi(p, P) F^{ij}(P) \Phi(p', P),$$

it can be shown that, near the pole,

$$(63) \quad \bar{K}_a = -\bar{K}_b$$

in isotopic state $\frac{1}{2}$. Therefore the cancellation is a consequence of our approximations. Fortunately these hidden poles are outside the interesting range of values of $G^2/4\pi$.

b) Low energy limit. — We first verify that when $\mu/M \rightarrow 0$ ($\alpha_1 - \alpha_3)/k \rightarrow 0$. This is a consequence of the following equations:

$$(64) \quad \left\{ \begin{array}{l} A_b(M + \mu) \rightarrow A_b(M) = \frac{1}{2\pi} \leftarrow A_b(M - \mu), \\ A_a(M + \mu) \rightarrow A_a(M) \leftarrow A_a(M - \mu), \\ F[-(M + \mu)^2] \rightarrow 0, \\ F[-(M - \mu)^2] \rightarrow 0. \end{array} \right.$$

Our results can be compared with other calculations among which should be mentioned Wyld's calculations up to fourth order⁽¹¹⁾ and calculation of α_3 by the Tamm-Dancoff method by BETHE *et al.*⁽¹²⁾.

In order to compare our results with Wyld's calculation we develop α_1 and α_3 up to the fourth order:

$$(65) \quad \left\{ \begin{array}{l} \alpha_1 = -(k/M)(G^2/4\pi)(0.747 - 0.49 G^2/4\pi) + \dots \\ \alpha_3 = -(k/M)(G^2/4\pi)(0.94 - 0.584 G^2/4\pi) + \dots \end{array} \right.$$

Wyld's results are the following:

$$(66) \quad \left\{ \begin{array}{l} \alpha_1 = -(k/M)(G'^2/4\pi)(0.75 - 0.25 G'^2/4\pi) \\ \alpha_3 = -(k/M)(G'^2/4\pi)(0.94 - 0.40 G'^2/4\pi). \end{array} \right.$$

The two calculations take into account the same graphs but the renormalization prescriptions of the vertex parts are different. In principle the second order radiative correction to the vertex parts is determined up to an arbitrary constant. We can compare the vertex parts for $p = p' = P_0 = (0, 0, 0, iM)$.

In our calculation

$$(67) \quad A_{5\alpha}(P_0, P_0) = A_{5\beta}(P_0, P_0) = 0,$$

while Wyld gives

$$(68) \quad A_5(P_0, P_0) = \gamma_5(G^2/4\pi)(1/2\pi) \int \frac{M^2 x^2 dx}{M^2 x^2 + \mu^2(1-x)} - \gamma_5(G^2/4\pi)C.$$

The correspondence is thereby completely determined. Comparison of the sum of all processes up to fourth order in the two cases gives the following connection between the coupling constants:

$$(69) \quad (G'^2/4\pi) - (G^2/4\pi) = -2C(G^2/4\pi)^2 + \dots$$

and using numerical values

$$(69') \quad (G'^2/4\pi) = (G^2/4\pi)(1 - 0.264G^2/4\pi).$$

Wyld's results can be rewritten in terms of our coupling constant:

$$(70) \quad \begin{cases} \alpha_1 = -\frac{k}{M} \frac{G^2}{4\pi} \left(0.75 - \frac{G^2}{4\pi} 0.45 \right), \\ \alpha_3 = -\frac{k}{M} \frac{G^2}{4\pi} \left(0.94 - \frac{G^2}{4\pi} 0.64 \right). \end{cases}$$

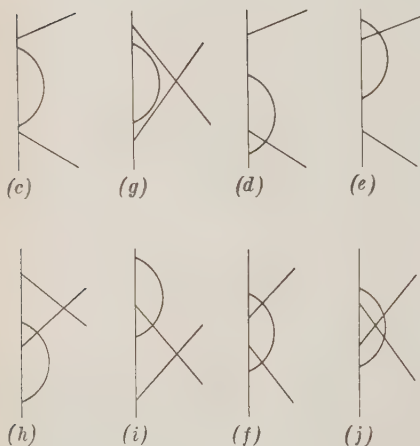


Fig. 6.

The agreement with the present calculation is rather good. However the discrepancy of about 10% in the fourth order coefficients gives a quite important contribution for large coupling constants. This discrepancy could be expected, since integrations over intermediate meson momenta extend to infinity while the approximate kernel is only valid for small momenta.

It may be interesting to make a term to term comparison of contributions of the different graphs to the phase shifts.

Hereafter we denote the fourth order graphs by the same letters as WYLD (Fig. 6); the contributions are divided by $(1/\pi)(G^2/4\pi)^2(k/M)$.

1) Finite processes:

$$(71) \quad \left\{ \begin{array}{ll} \text{graph (f)} & \begin{array}{ll} \text{exact calculation} & \text{present calculation} \\ 0.32 \quad (T=\frac{1}{2}) & 0.27 \quad (T=\frac{1}{2}) \\ -0.64 \quad (T=\frac{3}{2}) & -0.54 \quad (T=\frac{3}{2}) \end{array} \\ \text{graph (j)} & \begin{array}{ll} 0.64 \quad (T=\frac{1}{2}) & 0.734 \quad (T=\frac{1}{2}) \\ 0.26 \quad (T=\frac{3}{2}) & 0.294 \quad (T=\frac{3}{2}) \end{array} \end{array} \right.$$

It is seen that the ratio crossed graph/uncrossed graph is slightly increased in our calculation. If this is true to all orders, it may explain why we find a too large value for α_1 .

2) Self energies (graphs (c) and (g)). The two calculations give identical results, because the second order part of Σ was calculated exactly.

3) Vertex parts.

Since our renormalization method is adapted to our approximation, it is not very easy to compare our prescription with another one. The exact prescription following as closely as possible our procedure seems to be

$$\begin{aligned}
 (72) \quad & A_{5c}(p, p') = A_5(p, p') - A_5(p_0, p'_0) \\
 & p_0 = p'_0 \\
 & \begin{array}{cc}
 -i\gamma p_0 + m = 0 & + i\gamma p'_0 + m = 0 \\
 \text{to the left} & \text{to the right}
 \end{array}
 \end{aligned}$$

Such a prescription is particularly well adapted to an S wave calculation since the radiative corrections vanish in pair terms at zero energy if the meson mass is neglected. Wyld's definition is the following:

$$\begin{aligned}
 (73) \quad & A_{5c}(p, p') = A_5(p, p') - A_5(p_0, p'_0) \\
 & p_0 = p'_0 \\
 & \begin{array}{cc}
 i\gamma p_0 + m = 0 & i\gamma p'_0 + m = 0 \\
 \text{to the left} & \text{to the right}
 \end{array}
 \end{aligned}$$

Subtracting $A_5(0\ 0\ 0\ iM, 0\ 0\ 0\ iM)$ we obtain the *exact* second order radiative correction to the vertex in S state, with *our* renormalization prescription:

$$(74) \quad \left\{ \begin{array}{l} A_5(0\ 0\ 0\ i(M+\mu), 0\ 0\ 0\ iM) = \gamma_5 0.085 (G^2/4\pi) \quad (\text{graphs (d) and (e)}) \\ A_5(0\ 0\ 0\ i(M-\mu), 0\ 0\ 0\ iM) = -\gamma_5 0.030 (G^2/4\pi) \quad (\text{graphs (h) and (j)}) \end{array} \right.$$

Our calculation gives:

$$(75) \quad \left\{ \begin{array}{l} A_{5x}(i(M+\mu), iM) = -\gamma_5 (G^2/4\pi) F(-(M+\mu)^2) (2M+\mu/2M) = \\ \hspace{25em} = \gamma_5 0.0759 (G^2/4\pi) \\ A_{5x}(i(M-\mu), iM) = -\gamma_5 (G^2/4\pi) F(-(M-\mu)^2) (2M-\mu/2M) = \\ \hspace{25em} = -\gamma_5 0.0194 (G^2/4\pi) . \end{array} \right.$$

The agreement is poor but does not affect too much the total result because these terms are small. The discrepancy probably comes from the fact that

certain approximations which are permissible in convergent integrals cannot be crudely made in divergent integrals. To second order, our treatment leads to replace the exact second order term:

$$(76) \quad \gamma_5 \frac{iG^2}{(2\pi)^4} \cdot \int [K_N(p+k)K_N(-p'-k)K_M(-k) - K_N(p'_0+k)K_N(-p'_0-k)K_M(-k)] d^4k,$$

by

$$(77) \quad \gamma_5 \frac{iG^2}{(2\pi)^4} \cdot \int [K_N(p+k)K_N(-p-k)K_M(-k) - K_N(p'_0+k)K_N(-p'_0-k)K_M(-k)] d^4k \cdot K_N^{-1}(-p)K_N(-p').$$

A more correct evaluation consists in writing the exact term:

$$(78) \quad \left\{ \begin{aligned} & \gamma_5 \frac{iG^2}{(2\pi)^4} \cdot \int [K_N(p+k)K_N(-p'-k)K_M(-k) - K_N(p+k)K_N(-p-k)K_M(-k)] d^4k, \\ & + \gamma_5 \frac{iG^2}{(2\pi)^4} \cdot \int [K_N(p+k)K_N(-p-k)K_M(-k) - K_N(p'_0+k)K_N(-p'_0-k)K_M(-k)] d^4k. \end{aligned} \right.$$

The first integral is convergent and an approximation can be made for small momentum change of the nucleon:

$$(79) \quad K_N(-p'-k) - K_N(-p-k) \cong K_N(-p-k) \gamma \cdot (p-p') K_N(-p-k).$$

The second integral is known. The result is

$$(80) \quad A_{5a}(p, q) = -\gamma_5 \frac{G^2}{4\pi} \left[F(p^2) - i\gamma(q-p)Q(p) - \frac{1}{i\gamma p + M} \right],$$

(Q has been defined earlier), instead of

$$(81) \quad A_{5a}(p, q) = -\gamma_5 \frac{G^2}{4\pi} F(p^2) - \frac{1}{i\gamma p + M} (-i\gamma q + M).$$

The two expressions are of the order of $\mu/M \log M/\mu$, while their difference is of the order of μ/M , which explains the discrepancy. We can check this new approximation by numerical evaluation. It gives:

$$(82) \quad \begin{cases} A_{1\alpha}[i(M + \mu), iM] = \gamma_5 \frac{G^2}{4\pi} 0.0833 \text{ the exact result being } 0.085, \\ A_{3\alpha}[i(M - \mu), iM] = -\gamma_5 \frac{G^2}{4\pi} 0.0302 \text{ the exact result being } -0.030. \end{cases}$$

Unfortunately this approximation cannot be extended to higher orders.

The present calculation can be compared, at least in isotopic spin state $\frac{3}{2}$, with the Tamm-Dancoff calculations ^(1,2). In order to make a consistent comparison, we only retain the K_b terms. Our results are the following:

$$(\alpha_3)_b = -(k/M) \cdot 61^\circ \quad \text{for } G^2/4\pi = 2,$$

$$(\alpha_3)_b = -(k/M) \cdot 122^\circ \quad \text{for } G^2/4\pi = 16.$$

KALOS and DALITZ give

$$(\alpha_3)_b = -(k/M) \cdot 60^\circ \quad \text{for } G^2/4\pi = 2,$$

$$(\alpha_3)_b = -(k/M) \cdot 150^\circ \quad \text{for } G^2/4\pi = 16.$$

The agreement is quite good.

Finally, the uncertainties due to the approximations do not permit us to draw very definite conclusions. However, the present calculation clearly shows the importance of the crossed graphs. We obtain the correct signs for the phase shifts and the discrepancy in magnitude might well be due to the approximation or to meson-meson scattering.

* * *

I am deeply indebted to Professor MAURICE LÉVY for proposing this subject and for numerous and helpful discussions.

RIASSUNTO (*)

Si nota che i calcoli dell'onda S di bassa energia dello scattering mesone-nucleone non possono dare risultati soddisfacenti se non rispettano il cosiddetto «teorema di cancellazione». Può essere opportuno modificare i procedimenti di iterazione per soddisfare alle condizioni di simmetria. A questo scopo si completa la serie dei processi di scattering considerati con una nuova serie nella quale i mesoni iniziale e finale sono scambiati. In tal modo si generalizza il trattamento covariante di Lévy dello scattering dell'onda S . L'introduzione di questi nuovi procedimenti modifica profondamente il risultato del calcolo. Non è possibile ottenere un accordo quantitativo con l'esperienza. I segni degli spostamenti di fase sono, tuttavia, corretti in prossimità di $G^2/4\pi = 15$. Si discutono le approssimazioni usate nella soluzione delle equazioni integrali confrontandole con altri calcoli.

(*) Traduzione a cura della Redazione.

Further Measurements on Charged V-Events.

W. A. COOPER, H. FILTHUTH, J. A. NEWTH and R. A. SALMERON (*)

CERN - Geneva

(ricevuto il 23 Maggio 1956)

Summary. — The decays of 150 charged V-particles from lead and copper have been observed in a magnetic cloud chamber. Among the slow charged V-events, which are all interpreted as K-mesons, the proportions of the different decay modes are in good agreement with the results given by nuclear emulsions. Our own evidence agrees with that of other experiments which suggests that an appreciable fraction of the charged V-events with high energy (> 1 GeV) are due to the decays of hyperons. Data on the positive to negative ratio of slow K-mesons are discussed and a partial explanation in terms of the energy dependence of the production cross-section is suggested. Among the 150 events, 3 are most easily interpreted as the decays of K_S^0 -mesons and 1 as the decay of a Σ^+ -particle. In addition 10 events are interpreted as the decays of τ -mesons, of which 1 is negative.

1. — Introduction.

In 1954, the Jungfraujoeh cloud chamber group published a paper (BUCHANAN *et al.* ⁽¹⁾) giving full measurements of 44 charged V-events observed in a magnet cloud chamber at an altitude of 3580 m. At that time there was little statistical information available about charged V-events and the interpretation of the measurements was limited by their inaccuracy and by the smallness of the sample of events.

Since the earlier paper was written, a great deal of information has been published by groups working on cosmic-ray V-particles. In addition, there

(*) On leave of absence during part of the work from the Centro Brasileiro de Pesquisas Físicas, Rio de Janeiro, Brazil.

(1) J. S. BUCHANAN, W. A. COOPER, D. D. MILLAR and J. A. NEWTH: *Phil. Mag.*, **45**, 1025 (1954).

are now available many measurements of heavy mesons and hyperons observed in large blocks of photographic emulsion exposed at great altitude. Finally, studies of heavy mesons produced by large accelerators are now appearing and many very precise measurements have been made on these particles. The following decay modes are now established:

- | | | |
|-----|---|--------------------------------|
| (1) | $K_{\mu 2} \rightarrow \mu + \nu$ | $(p^* = 238 \text{ MeV/c})$ |
| (2) | $K_{\pi 2} \rightarrow \pi + \pi^0$ | $(p^* = 205 \text{ MeV/c})$ |
| (3) | $K_{\mu 3} \rightarrow \mu + \pi^0 + ?$ | $(p^* \leq 218 \text{ MeV/c})$ |
| (4) | $K_{\rho} \rightarrow e + ? + ?$ | $(p^* \leq 246 \text{ MeV/c})$ |
| (5) | $\tau' \rightarrow \pi + 2\pi^0$ | $(p^* \leq 133 \text{ MeV/c})$ |
| (6) | $\tau \rightarrow 3\pi$ | $(p^* \leq 125 \text{ MeV/c})$ |
| (7) | $\Sigma^- \rightarrow \pi + \text{Nucleon}$ | $(p^* \sim 190 \text{ MeV/c})$ |
| (8) | $\Xi^- \rightarrow \pi^- + \Lambda^0$ | $(p^* \sim 120 \text{ MeV/c})$ |

The values of the momentum of the secondary in the centre of mass system are given in brackets.

In this paper we summarize the information we have obtained from a total of 150 charged V-events observed at the Jungfraujoch (including those reported by BUCHANAN *et al.*). We compare our results with those of other groups in an attempt to determine any residual points of disagreement. For brevity, we refer below to the paper of BUCHANAN *et al.* as paper I.

2. — Corrections to Earlier Measurements.

In paper I there were some errors that must be corrected. The first of these concerns the event RP 993, a positive K-meson apparently having a mass greater than $1100 m_e$. All the measurements on this event have recently been repeated and an arithmetic error in calculating the line of flight of the secondary particle has been found. As a consequence, the angle of decay is 107° and not 117° as originally stated, and the momentum of the secondary is 230 MeV/c and not 250 MeV/c .

These alterations make a significant change in the interpretation of the event. The mass of the primary particle, on the assumption that there is a single neutral secondary of zero rest mass is now found to be

- $(1100 \pm 55) m_e$ if the charged secondary is a μ -meson, or
 $(1060 \pm 60) m_e$ if the charged secondary is an electron.

Although the quoted errors are greater than standard deviations (as described in Table III of paper I) it is clear that the mass values are not incompatible with $965 m_e$. We conclude, therefore, that the event is not convincing evidence for a K-meson with mass greater than $965 m_e$.

The remaining errors are of less importance. The event QR 979 of paper I has been excluded from the present analysis since the intersection of the two tracks in this event occurs too near to the back of the illuminated volume of the cloud chamber for us to be certain that the tracks do not cross or originate from a nuclear interaction in the gas. Event RE 410 was listed as positive whereas it is, in fact, negative.

In addition, because of the importance of the positive excess among the V-particles, we have, in this paper, used a more stringent criterion for determining the signs of fast particles. Applying this criterion to the earlier events we find that five V^+ -events and one V^- -event should now be classed as of indeterminate sign. Making these corrections the numbers of positive, negative and indeterminate events in paper I are 23:12:8 rather than 29:13:2.

3. — General Survey of the Events.

Of the total of 150 charged V-events, 43 were reported in I and the remainder have been observed in the period up to October, 1955. The apparatus ⁽²⁾ has not been altered significantly. The total number of photographs taken is about 100 000. Of these, 35 000 were taken with a 13 mm copper plate across the centre of the cloud chamber and 10 000 with a 30 mm lead plate in the same position. Nineteen charged V-particles came from nuclear interactions in these two plates.

In addition to the 150 charged V-events, 10 events have been observed that are best interpreted as the decays of τ -mesons into three charged π -mesons. The numbers of positive and negative V-particles and τ -mesons are given in Table I.

One criterion for identifying a charged V-event has been made less strict than that used in paper I. The value of the transverse momentum ($P_2 \sin q$) of the secondary particle has been required to be greater than 50 MeV/c by at least one standard deviation. Previously a value of 100 MeV/c was required. Relaxing this criterion may allow a large-angle scatter of a fast particle by an argon nucleus to be misinterpreted as a V-event but the total number of such scatters expected in our experiment is about two.

It has been emphasized by the Ecole Polytechnique workers ⁽³⁾ that the

⁽²⁾ J. A. NEWTH: *Suppl. Nuovo Cimento*, **11**, 297 (1954).

⁽³⁾ R. ARMENTEROS, A. ASTIER, C. D'ANDLAU, B. GREGORY, A. HENDEL, F. MULLER, C. PEYROU and R. RAU: *Pisa Conference, mimeographed report* (1955).

TABLE. I - Sign distribution of charged V-particles observed in the Jungfrauoch cloud chamber.

Group of events	Positive	Negative	Doubtful sign	Total
Reported in Paper I (*) . .	23	12	8	43
Since Paper I	46	32	29	107
Total	69	44	37	150 (+)
$\tau \rightarrow 3\pi$	7	1	2	10
Charged V's produced in copper or lead plate	6	7	6	19

(*) See corrections in Sect. 2.

(+) The total of 150 charged V-particles includes the 19 produced in the plate.

sample of V-events identified with a magnet cloud chamber is limited by the cloud chamber performance in a very definite manner. In particular, the identification of small angle decays depends directly upon the maximum detectable momentum in the chamber. If the decay angle (φ) is small the condition $P_2 \sin \varphi > 50 \text{ MeV}/c$ can only be satisfied when the lower limit for P_2 is high. The result of this restriction is a strong bias against recognizing decays in which the angle is below some value characteristic of the apparatus. For our equipment we find empirically that very few events with φ less than 10° have been identified. This is shown by the histogram of decay angles given in Fig. 1.

The full significance of this limitation is seen when our events are compared with those reported by ARMENTEROS *et al.* (³). The median decay angle for our 69 positive events is 37° and for the 44 negative events it is 25° . The Ecole Polytechnique group found values of 18° for 54 positive events and 12° for 44 negative events. This difference is discussed fully when our results are compared with those of other groups.

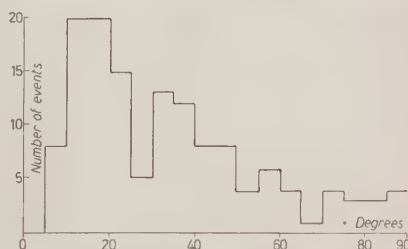


Fig. 1. - Histogram of decay angles for all the charged V-events observed in the Jungfrauoch cloud chamber.

4. — Dynamics of the Decays.

4.1. *Direct Mass Estimates.* — Of the 150 primary particles 20 had measurable momenta below 350 MeV/c and the masses of the particles could be estimated from the density of ionization in their tracks. For all 20 particles (14 positive and 6 negative) the estimated mass is consistent with a unique value near to $1000 m_e$. In addition, for 16 particles (12 positive and 4 negative) the upper limit to the estimate of mass is less than $2000 m_e$; these particles cannot, therefore be hyperons.

Nearly all the secondary particles could be light mesons but only three can be so identified from momentum and ionization. Three of the secondary particles are probably *not* light mesons; the events are discussed below.

In event SE 234 the secondary particle has a momentum of (460_{-90}^{+130}) MeV/c and its ionization is estimated to be between $2I_0$ and $3I_0$. Its mass is therefore between $1400 m_e$ and $2200 m_e$. This particle traverses the 13 mm copper plate in the cloud chamber and its momentum loss in the plate and its ionization below the plate are both compatible with the behaviour of a proton. The primary particle in this event has a track length of only 4 cm in the chamber and its momentum cannot be found. The angle of decay is 15° . It seems most reasonable to suggest that this event is a hyperon decay of the type

$$\Sigma^+ \rightarrow P + \pi^0 + 110 \text{ MeV}.$$

If this is correct the primary particle had a time of flight in the chamber of $1.5 \cdot 10^{-10}$ s.

In two events the secondary particles are apparently *lighter* than π^- or μ -mesons. SD 1472 is a photograph of poor contrast but the secondary momentum is only 30 MeV/c and a μ -meson of this momentum would have an ionization of $7.5 I_0$. We estimate the ionization from the photograph as $< 3I_0$. The second event is QM 861 which is reproduced in the plate. The relevant measurements are given in Table VI. If we assume that the event is the decay of a K-meson into a μ -meson, the ionization densities of the two tracks should be $2.2 I_0$ for the primary and $2.6 I_0$ for the secondary. From the photograph it appears that the secondary is less heavily ionizing than the primary and its mass should therefore be less than that of a μ -meson.

For neither of these two last events is the interpretation completely certain but, since the K_S^0 mode of decay is established, we much prefer to interpret the decays in this way.

4.2. *Transverse Momentum Distribution.* — In paper I distributions of the transverse momenta of the secondary particles were given in an attempt to

distinguish between 2- and 3-body decay schemes. The results were not significant and we do not consider it worth while to present further distributions of this type. TRILLING and LEIGHTON ⁽⁴⁾ have made a careful study of the experimental bias introduced into such distributions and there is no doubt that the histograms given in Fig. 1 of paper I were more affected by bias than was thought.

4.3. Determination of p^* . — Among the 150 events there are 26 where the momenta of both primary and secondary particles can be measured (15 positive and 11 negative). In these cases the secondary momentum (p^*) in the rest-frame of the primary has been calculated by assuming masses for the two particles. Table II lists the results obtained.

Of the 15 positively charged particles there are 11 which give values of p^* such that the decay could be that of a K_{π^2} or K_{μ^2} meson. The mean value of p^* for these 11 events is 203 MeV/c if the secondaries are π -mesons and 202 MeV/c if they are μ -mesons.

The negative particles give 10 such values out of 11 events and we find that the mean value of p^* is 209 MeV/c assuming π -meson secondaries and 194 MeV/c assuming μ -meson secondaries.

The events excluded when finding these mean values of p^* are the following:

- 1) Event QM 861 which is thought to be an example of $K_{\mu^2}^+$ -decay,
- 2) Two positive events (SN 184 and TF 289) for which the values of p^* are 115_{-17}^{+18} MeV/c and 135_{-15}^{+18} MeV/c,
- 3) The negative event SY 531 with a value of p^* of 109_{-10}^{+16} MeV/c,
- 4) Event RP 993.

5. — Mean Lifetime Estimates.

As in paper I, we have analyzed the distribution of our events in an attempt to determine the mean lifetime of the primary particles. The momenta of the primary particles were estimated where they could not be measured (see Fig. 2) and, for the purpose of calculation, the particles were all assumed to be K_{π^2} -mesons. The curves for K_{μ^2} -decay differ from these by about 10%. The time (t_i) that each particle spent in the cloud chamber was calculated together with the corresponding « potential » time (T_i) and these times were then

(4) G. H. TRILLING and R. B. LEIGHTON: *Phys. Rev.*, **100**, 1468 (1955).

TABLE II. — *The 26 events observed at the Jungfraujoch which give accurate measurements.* p_1 = momentum of primary particle, p_2 = momentum of secondary particle, φ = angle between the directions of primary and secondary, p_{π}^* = momentum of the secondary particle in the centre of mass system assuming that it is a π -meson, p_{μ}^* = momentum of the secondary particle in the centre of mass system assuming that it is a μ -meson, $p_{\pi \max}^*$ is obtained by altering p_1 , p_2 and φ in such a way as to increase p^* as much as possible while remaining compatible with their quoted errors, $p_{\pi \min}^*$ is made as small as possible in a similar way.

The events shown are those with $p_{\pi \max}^* - p_{\pi \min}^* < 2.0 \cdot 10^8$ eV/c. The errors in p_1 and p_2 are found from an m.d.m. calculated in the way described in Paper I. The mass $4.93 \cdot 10^8$ eV/c² was assumed for the primary particle in the calculation of p^* .

Event	Sign	p_1 10 ⁸ eV/c	p_2 10 ⁸ eV/c	φ degrees	p_{μ}^* 10 ⁸ eV/c	p_{π}^* 10 ⁸ eV/c	$p_{\pi \max}^*$ 10 ⁸ eV/c	$p_{\pi \min}^*$ 10 ⁸ eV/c
QD 138	+	1.9 \pm 0.3	2.0 \pm 0.3	47 \pm 3	1.82	1.80	2.21	1.52
QL 707	+	2.2 $\begin{smallmatrix} +0.6 \\ -0.5 \end{smallmatrix}$	2.7 $\begin{smallmatrix} +0.3 \\ -0.2 \end{smallmatrix}$	32 \pm 2	2.08	2.05	2.42	1.70
QM 861	+	3.4 \pm 0.3	0.66 \pm 0.08	82 \pm 2	1.02	1.18	1.28	1.08
RG 585	+	3.9 $\begin{smallmatrix} +2.3 \\ -1.0 \end{smallmatrix}$	1.2 \pm 0.2	75 \pm 1	1.34	1.42	2.42	1.20
RP 993	+	2.04 \pm 0.06	2.3 \pm 0.1	107 \pm 2	2.80	2.82	2.95	2.71
SC 226	+	2.8 $\begin{smallmatrix} +0.8 \\ -0.5 \end{smallmatrix}$	3.9 \pm 0.4	43 \pm 2	2.78	2.76	3.15	2.34
SF 1726	+	8.6 $\begin{smallmatrix} +7.0 \\ -3.0 \end{smallmatrix}$	2.7 $\begin{smallmatrix} +0.4 \\ -0.3 \end{smallmatrix}$	35 \pm 2	1.62	1.78	3.15	1.38
SN 146	+	2.2 \div 3.7	3.2 \pm 0.4	33 \pm 2	2.17	2.04	2.52	1.65
SN 814	+	2.5 \div 4.0	0.9 \pm 0.03	73 \pm 2	1.04	1.15	1.33	0.98
SQ 387	+	1.7 \div 2.2	2.4 $\begin{smallmatrix} +0.2 \\ -0.1 \end{smallmatrix}$	85 \pm 2	2.51	2.52	2.78	2.36
SS 242	+	2.0 $\begin{smallmatrix} +0.7 \\ -0.4 \end{smallmatrix}$	2.3 $\begin{smallmatrix} +1.3 \\ -0.6 \end{smallmatrix}$	41 \pm 1	1.73	1.70	2.45	1.13
SY 238	+	3.0 $\begin{smallmatrix} +0.6 \\ -0.4 \end{smallmatrix}$	3.7 $\begin{smallmatrix} +1.0 \\ -0.7 \end{smallmatrix}$	23 \pm 2	2.19	2.15	2.88	1.54
SZ 984	+	10.0 $\begin{smallmatrix} +4.0 \\ -2.0 \end{smallmatrix}$	2.5 $\begin{smallmatrix} +2.5 \\ -0.8 \end{smallmatrix}$	33 \pm 1	1.56	1.72	3.18	1.24
TC 1363	+	3.0 \pm 0.2	1.8 \pm 0.6	97 \pm 2	2.36	2.44	3.20	1.92
TF 289	+	1.9 \div 2.7	1.35 \pm 0.08	72 \pm 1	1.33	1.35	1.53	1.20

TABLE II (continued).

Event	Sign	p_1 10 ⁸ eV/c	p_2 10 ⁸ eV/c	φ degrees	p_μ^* 10 ⁸ eV/c	p_π^* 10 ⁸ eV/c	$p_{\pi\max}^*$ 10 ⁸ eV/c	$p_{\pi\min}^*$ 10 ⁸ eV/c
NJ 93	—	3.5 ± 0.5	$2.8 \pm \begin{smallmatrix} 1.1 \\ 0.6 \end{smallmatrix}$	53 ± 2	2.24	2.25	2.72	1.76
QG 66	—	$3.4 \pm \begin{smallmatrix} 0.5 \\ 0.5 \end{smallmatrix}$	$1.6 \pm \begin{smallmatrix} 0.3 \\ 0.2 \end{smallmatrix}$	88 ± 2	2.05	2.13	2.64	1.79
QH 425	—	$7.0 \pm \begin{smallmatrix} 2.0 \\ 1.5 \end{smallmatrix}$	1.4 ± 0.2	55 ± 2	1.60	1.81	2.56	1.35
RD 473	—	7.0 ± 1.0	2.1 ± 0.4	40 ± 1	1.45	1.55	2.11	1.21
RQ 461	—	$7.5 \pm \begin{smallmatrix} 2.5 \\ 1.5 \end{smallmatrix}$	3.2 ± 0.3	37 ± 1	1.98	2.03	2.21	1.85
SD 1314	—	2.4 ± 0.2	1.9 ± 0.2	78 ± 2	1.96	1.99	2.23	1.78
X 38	—	$2.5 \div 3.5$	3.0 ± 0.3	47 ± 3	2.24	2.23	2.51	1.97
ST 223	—	$1.5 \div 2.1$	1.7 ± 0.3	124 ± 3	2.24	2.30	2.80	1.80
SY 531	—	$2.2 \pm \begin{smallmatrix} 0.9 \\ 0.4 \end{smallmatrix}$	$0.66 \pm \begin{smallmatrix} 0.20 \\ 0.10 \end{smallmatrix}$	106 ± 2	0.99	1.09	1.25	0.89
TC 1546	—	$2.0 \div 3.0$	2.3 ± 0.2	66 ± 3	1.21	2.14	2.30	1.88
TC 1700	—	$2.0 \div 3.0$	$2.5 \pm \begin{smallmatrix} 0.3 \\ 0.2 \end{smallmatrix}$	74 ± 2	2.42	2.43	2.88	2.24

combined by BARTLETT's procedure⁽⁵⁾ to obtain an estimate of the decay constant ($1/\tau$) of the particles.

Because the charged V-events are certainly a mixture of different types of decay we made a large number of different classifications of the events in an attempt to select a group rich in short-lived particles. For every group the mean lifetime was estimated and for nearly every group the value of $1/\tau$ obtained was less than one standard deviation from zero. Some of the results are given in Table III.

Classification 4) in Table III is similar to one used by TRILLING and LEIGHTON⁽⁴⁾ and shows in the same way that there may be a short-lived component of the V-particles produced in the thin copper plate placed across the chamber. In assessing the significance of our result it should be borne in mind that we made about 20 different classifications of our events. Even if all the particles had a long mean lifetime, we expect to find a value of $1/\tau$ differing from zero by two or more standard deviations in one out of 30 *random* selections.

⁽⁵⁾ M. S. BARTLETT: *Phil. Mag.*, **44**, 249 and 1407 (1953).

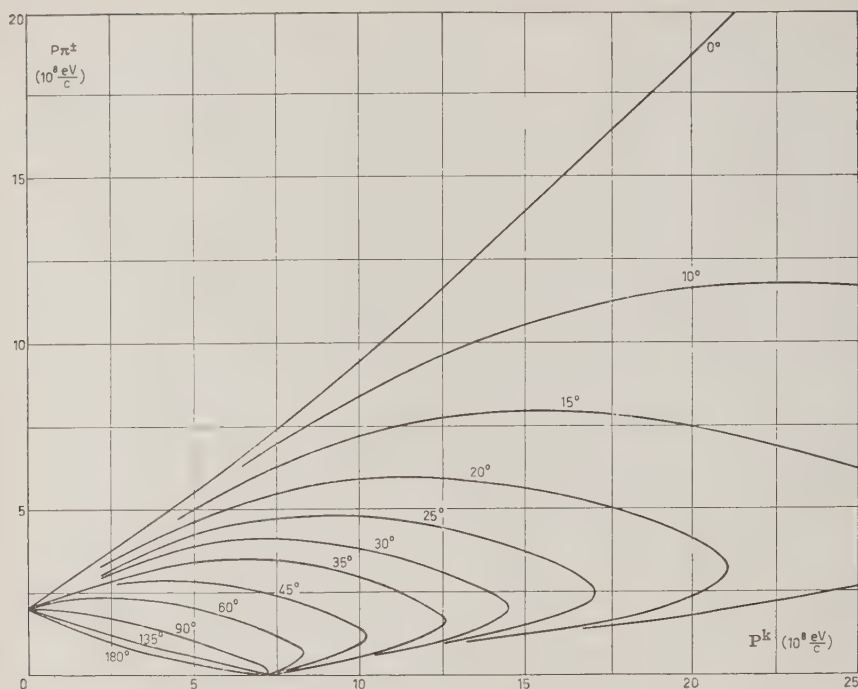


Fig. 2. — The relation between the momenta of primary and secondary particles and the decay angle for the $K_{\pi 2}$ -meson.

TABLE III. — *Lifetime Estimates.*

In the first three rows the times of flight have been obtained in cases where the primary momentum was unmeasured, by calculation from P_2 and φ assuming the decay of a $K_{\pi 2}$ (see Fig. 2). In the last row the decay $\Sigma \rightarrow \pi + \text{neutron}$ has been assumed.

Class of particles	Total	Positive	Negative	$1/\tau$ (10^{10} s^{-1})
1. All events, except 3 K_β	147	67	43	-0.003 ± 0.026
2. All events from copper plate	16	6	6	-0.06 ± 0.13
3. Events from copper plate excluding those which cannot be Σ^\pm	13	4	5	$+0.63 \pm 0.30$
4. As 3 but assuming all events to be Σ^\pm	13	4	5	$+0.64 \pm 0.29$

The only safe conclusion that can be drawn from this analysis is that a large fraction of the primary particles has a mean lifetime greater than $2 \cdot 10^{-9}$ s. There is an indication of some short-lived particles among the primaries coming from the copper plate but our evidence is far from conclusive.

6. — The Positive Excess.

In the past a great deal of apparently conflicting evidence has been published on the relative numbers of V^+ - and V^- -particles. Thanks largely to the work of the Paris group at the Ecole Polytechnique it seems now to be possible to fit all the published information into a relatively simple picture. Briefly, there is a large positive excess for the slow particles that are observed to decay in magnet cloud chambers. Among the high energy particles there is a negative excess. The extent to which this high-energy negative excess is apparent depends upon the performance of the apparatus since the decay angles are generally small in these events.

With our apparatus we find a large positive excess among the primaries with momenta below 600 MeV/c (31 positive and 12 negative). By contrast, at momenta above 1 GeV/c the numbers are 24 positive and 22 negative. In Table IV we compare these figures with those obtained in other experiments. Unfortunately, the intervals of momentum chosen for comparison are not constant but there is clear evidence of agreement in the main features.

It is safe to assume that the decays of slow V-particles are detected with high efficiency in all cloud chamber experiments. These particles can frequently be directly identified as K-mesons (a hyperon with momentum below 800 MeV/c is heavily ionizing) and we can conclude from the results quoted in Table IV that there is a positive excess of about 3.4 to 1 among the observed K-mesons with momenta less than, say, 600 MeV/c. The agreement between different cosmic ray cloud chamber experiments on this point is reasonably good.

Concerning the negative excess at high energies, the situation is less clear. Our own observations are not valuable because we identify so few events with decay angles less than 10° . The obvious explanation in terms of known particles is that Σ^- -decays are responsible for this excess. Owing to their short mean lifetime these particles are unlikely to decay inside a cloud chamber unless their momenta are several GeV/c and, at these momenta, a decay of the type $\Sigma^- \rightarrow N + \pi^- + 118 \text{ MeV}$ has an angle of less than 15° . If this explanation is correct, the negative excess may be partly or wholly an experimental bias since the decay of a Σ^+ -particle into a proton and a π^0 -meson is extremely difficult to recognize, the angle of decay being only about 2° for a Σ^+ with a momentum of 5 GeV/c.

We have little to contribute to the study of these fast particles and in the

TABLE IV. — *The momentum dependence of the ratio of positive to negative V-particles observed in various experiments.*

Group	Low momenta			High momenta		
	Class of particles	+	—	Class of particles	+	—
Cal. Tech. (4)	V^\pm with heavily ionizing primary	19	5	V^\pm with lightly ionizing primary	22	38
Princeton (13)	Measured events (+) $P_1 < 1 \text{ GeV/c}$	15	10	Measured events (+) $P_1 > 1 \text{ GeV/c}$	6	11
École Poly-technique (3)	Well measured events $P_1 < 1 \text{ GeV/c}$	20	4			
»	8 events, mean initial $P_1 \sim 0.5 \text{ GeV/c}$	22	2			
»	$\tau \rightarrow 3\pi$ $P_1 < 1 \text{ GeV/c}$	5	2	$\tau \rightarrow 3\pi$ $P_1 > 1 \text{ GeV/c}$	0	2
Jungfraujoch	Measured events (+) $P_1 < 0.6 \text{ GeV/c}$ (*)	31	12	Measured events (+) $P_1 > 1 \text{ GeV/c}$	24	22
»	$\tau \rightarrow 3\pi$ $P_1 < 1 \text{ GeV/c}$	6	0	$\tau \rightarrow 3\pi$ $P_1 > 1 \text{ GeV/c}$	1	1

(+) The primary momentum has in some cases been estimated from a measured secondary momentum and decay angle and the assumption of the $K\pi\pi$ decay mode (see Fig. 2).

(*) 6 positive and 2 negative events could be hyperon decays.

following sections we restrict our attention to the measurement and interpretation of the K-meson decays.

7. — The Decay Modes of the Slow Charged V-Particles.

It is possible to estimate the relative proportions of the different types of K-meson decay using the dynamical measurements reported in Sect. 4. The different modes of decay that have to be considered are (1)–(6) as listed in the introduction.

From magnet cloud chamber measurements it is hardly ever possible to obtain a value of p^* with a precision better than $\pm 10 \text{ MeV/c}$ and the errors are more usually $\pm 30 \text{ MeV/c}$. For this reason the only valuable classification is to make a broad division between those events with p^* near to 200 to 240 MeV/c and those with p^* significantly less than 200 MeV/c . We

class all p^* values where the quoted errors include part of the range from 190 MeV/c to 250 MeV/c as «normal». Values less than 190 MeV/c by at least one deviation are called «low». Clearly, the events with normal p^* will include some $K_{\mu 3^-}$ and K_{β^-} -decays but the events with low p^* should *not* include $K_{\mu 2^-}$ and $K_{\pi 2^-}$ -decays.

The numbers of normal and low p^* values from our 26 events were given in Sect. 4. In Table V we compare these with other results obtained from cosmic ray cloud chamber experiments.

From the table it seems that the events with low p^* form about 20% of the total of both positive and negative K-decays. In this 20% may be included some τ' -decays, $K_{\mu 3^-}$ -decays and K_{β^-} -decays. The number of τ' -decays can be found from the experimentally determined branching ratio (1:5) between the two modes of decay of positive τ -mesons ⁽⁶⁾.

TABLE V. — *Distribution of p^* values from various experiments.*

An event with low p^* is taken as one where the quoted range of errors does not include a value > 190 MeV/c. A normal value is taken as one where the quoted range of errors includes a value between 190 MeV/c and 250 MeV/c. The nature of the secondary particle assumed in calculating p^* is shown in brackets.

Group	Positive				Negative			
	Total	Normal	Low	Unweight- ed mean p^* (10^6 eV/c)	Total	Normal	Low	Unweight- ed mean p^* (10^6 eV/c)
Cal. Tech. ⁽⁴⁾	18	18	1	2.37 (π) 2.31 (μ)	6	6	0	2.06 (π) 2.00 (μ)
Princeton ⁽¹³⁾	13	9 (*)	2	2.13 (π)	10	7 (*)	1	2.31 (π)
École Poly- technique ⁽³⁾	14	8	6	2.10 (π) (μ)	8	5	3	2.56 (π) (μ)
Jungfraujoch	15	11 (+)	3	2.02 (π) 2.03 (μ)	11	10	1	2.09 (π) 1.94 (μ)
Total	61	46	12	—	35	28	5	—

(*) 2 events which may be due to hyperons are omitted.

(+) RP 993 is omitted.

⁽⁶⁾ J. CRUSSARD, V. FOUCHÉ, J. HENNESSY, G. KAYAS, L. LEPRINCE-RINGUET, D. MORELLET and F. RENARD: *Nuovo Cimento*, **3**, 731 (1956).

If we normalize to a total of 100 K-meson and τ -meson decays we now have the following estimate of their composition:

	positive	negative
« Normal » p^* events	70	79
Low p^* events other than τ' . . .	13	12
$\tau \rightarrow 3\pi$ decays	14	7
τ' -decays	3	2

The errors in these estimates are large and there is certainly no significant difference between the proportions for the positive and negative events.

It is only possible to proceed further with the analysis by making some assumption about the distribution of p^* values in the $K_{\mu 3}$ and K_{β} decay modes. Because of the inaccuracy of the measurements it is likely that the only values of p^* that are classified as « low » are values below 150 MeV/c (*). We may assume that about half the $K_{\mu 3}$ - and K_{β} -decays have p^* below 150 MeV/c and half above (†). This estimate is not unreasonable and the result of our analysis would not be changed greatly unless the proportion of decays with low p^* were, in fact, as low as one quarter. There is a bias favouring the inclusion of events with low p^* in our sample due to the requirement that the event should be well measured. The École Polytechnique group estimates (‡) that a low value of p^* is, *a priori*, twice as likely to be selected as a normal value. Taking this estimate and again normalizing to a total of 100 mesons we find the following figures for their composition:

	positive	negative
$K_{\mu 2}$ and $K_{\pi 2}$	63	71
$K_{\mu 3}$ and K_{β}	20	20
τ	14	7
τ'	3	2

From the information we have discussed here a further separation of the first two classes is not possible.

(*) The criteria for recognizing a charged V-event may prevent values of p^* less than 50 MeV/c from being recorded but, for the slow primary particles we consider, this effect is unlikely to be important as the V-events can frequently be identified without reference to the absolute value of the transverse momentum.

(†) C. M. YORK: *Phil. Mag.*, **43**, 935 (1952).



Plate 1. — A K-meson (travelling horizontally) decays into a particle which is probably lighter than a μ -meson.

The K_β mode of decay. — While we cannot deduce any reliable figure for the ratio of the numbers of $K_{\mu 3}$ and K_β -decays among the events there is some interest in recording the details of 3 events that are probably K_β -decays. Event QM 861 (Plate 1) is identified from the momentum and ionization of the secondary particle and has been discussed in Sect. 4. Event SD 1472 is also identified in this way but the photograph of this event is of poor quality. The third event (SO 333) is a negative V-event where only a lower limit can be set to the primary momentum. However, this sets a lower limit also to

TABLE VI. — K_β Events.

The p^* is calculated assuming $M_1 = 493 \text{ MeV}/c^2$ $M_2 = 0.51 \text{ MeV}/c^2$.

θ^* is the angle of emission of the secondary in the centre of mass system with respect to the direction of the primary in the laboratory system. The value $\theta^* = 175^\circ$ for event SO 333 is found assuming $p_1 = 10 \cdot 10^8 \text{ eV}/c$. p_1 , p_2 and φ are defined in the legend to Table II.

Event	Sign	P_1 ($10^8 \text{ eV}/c$)	P_2 ($10^8 \text{ eV}/c$)	φ Degrees	p^* ($10^8 \text{ eV}/c$)	θ^* Degrees
QM 861	+	3.5 ± 0.3	0.67 ± 0.06	82 ± 2	75 ± 9	112
SD 1472	+	$7.3^{+6.0}_{-2.3}$	0.3 ± 0.1	117 ± 5	73^{+90}_{-36}	158
SO 333	—	> 10	0.60 ± 0.02	163 ± 3	> 244	175

the value of p^* . If the secondary is a μ -meson this lower limit is $370 \text{ MeV}/c$ a value incompatible with the decay of any known particle. If the secondary is an electron the value of p^* is $> 244 \text{ MeV}/c$.

The details of the 3 presumed K_β -events are given in Table VI. In all three events the secondary was emitted backwards in the centre of mass system nearly along the primary line of flight. This is effectively a prerequisite for identifying a K_β -decay in flight. To our knowledge, no other examples of K_β -decay have been observed in cloud chamber experiments and we must regard our three events as a statistical fluctuation on a smaller expected number.

8. — Comparison with other Experiments.

8.1. *Relative abundances of the modes of decay.* — The figures given in Sect. 7 for the composition of the K-decays can be compared with the results obtained in several experiments using photographic emulsions. In Table VII this comparison is made.

The emulsion experiments are able to resolve the p^* distribution of the secondaries with far greater precision than is possible in the experiments we have so far considered. The value of the comparison made in Table VII is

TABLE VII. — *The relative frequencies of K-decay modes found in various experiments.*

	Emulsion evidence			Cloud chamber evidence	
	École Poly- technique ⁽⁶⁾	K-beam RITSON <i>et al.</i> ⁽⁸⁾	« G »-Stack ⁽⁹⁾	Positive	Negative
$K_{\mu 2}$	54	57	61	63	71
$K_{\pi 2}$	26	31	18		
$K_{\mu 3}$	4	1	3	20	20
K_{β}	8	2	8		
τ	7	7	8	14	7
τ'	1	2	2	3	2

that it suggests good agreement between all the observations made on the relative frequencies of the different K-decays.

In emulsions K^- -decays are not observed when the K-particles come to rest and no information is available on the different modes of K^- -decay other than that summarized in Sect. 7. It is possible that the K^- -meson decay modes are the same and have the same proportions as those of the K^+ -meson but there is some evidence against this simple view. This point is discussed further in §3 i) below.

§2. *The ratio of positive to negative K-mesons.* — The positive excess of 3.4:1 that was found in Sect. 6 is much less than the 10:1 found by the Padua group in the G-stack cosmic ray experiment ^(9,10). However, GEORGE *et al.* ⁽¹²⁾ find that 29% of the negative K-mesons which they observed stopping in

⁽⁸⁾ D. M. RITSON, A. PEVSNER, S. C. FUNG, M. WIDGOFF, G. T. ZORN, S. GOLDHABER and G. GOLDHABER: *Phys. Rev.*, **101**, 1085 (1956).

⁽⁹⁾ G-STACK COLLABORATION: *Nuovo Cimento*, **2**, 1063 (1955).

⁽¹⁰⁾ M. CECCARELLI, M. GRILLI, M. MERLIN, G. SALANDIN, and B. SECHI: *Pisa Conference, mimeographed report* (1955).

⁽¹¹⁾ M. SCHEIN, D. M. HASKIN and R. G. GLASSER: *Nuovo Cimento*, **3**, 131 (1956).

⁽¹²⁾ E. P. GEORGE, A. J. HERZ, J. H. NOON and N. SOLNTSEFF: *Nuovo Cimento*, **3**, 94 (1956).

emulsion placed in the K-meson beam from the Bevatron gave no star at the end of their track. Correcting the G-stack data for this loss would reduce their ratio from 10:1 to 7:1 but this is still incompatible with the mean value of 3.4:1 for events in cloud chambers. It is almost impossible to imagine how the cloud chamber result could be biased. Because the altitude at which the G-stack was exposed (27 km) is much greater than that at which the cloud chamber experiments were performed (3 km) the incident flux of particles is different in composition and mean energy in the two cases. This may well have caused a larger proportion of positive K-mesons to have been produced in the G-stack. The lower energies of the K-mesons observed in the G-stack may also affect, indirectly, the positive excess.

All the cosmic ray experiments find a much lower positive to negative ratio than that of 100:1 found in the K-meson beam produced by protons of 6 GeV incident on a copper target ⁽¹³⁾. A ratio of 100:1 is also found when the protons produce K-mesons directly in photographic emulsions ⁽⁶⁾. CECCARELLI *et al.* ⁽¹⁰⁾ after considering several possibilities explained the very high positive excess in the machine data by assuming a shorter lifetime for the majority of the negative K-particles. It now seems, however ⁽¹⁴⁾, that if there is a difference between the lifetimes of the K^+ - and K^- -mesons, it is insufficient to explain this effect. The next simplest explanation seems to be that depending on the different effective energies in the cosmic ray experiments and the machine experiments.

The production processes allowed by the scheme of Gell-Mann and Pais ⁽¹⁵⁾ and Nakano and Nishijima ⁽¹⁶⁾ are:

- (1) $\pi + N \rightarrow Y^{+,0} + K^{+,0} \dots \dots \dots (0.75 \text{ GeV})$
- (2) $N + N \rightarrow N + Y^{+,0} + K^{+,0} \dots \dots \dots (1.57 \text{ GeV})$
- (3) $\pi + N \rightarrow N + K^{+,0} + \bar{K}^{+,0} \dots \dots \dots (1.34 \text{ GeV})$
- (4) $N + N \rightarrow N + N + K^{+,0} + \bar{K}^{+,0} \dots \dots (2.48 \text{ GeV})$

The threshold energies in the laboratory system are given in brackets. Considering these reactions, we suggest that at higher energies the reactions (3) and (4) are more important than (1) and (2), whereas at lower energies such

⁽¹³⁾ W. W. CHUPP, S. GOLDBABER, G. GOLDBABER, W. R. JOHNSON and F. WEBB: *Pisa Conference, mimeographed report* (1955).

⁽¹⁴⁾ E. L. ILOFF, G. GOLDBABER, S. GOLDBABER, J. E. LANUTTI, F. C. GILBERT, C. E. VIOLET, R. S. WHITE, D. M. FOURNET, A. PEVSNER, D. RITSON and M. WIDGOTT: *UCRL*, 3323 (1956).

⁽¹⁵⁾ M. GELL-MANN and A. PAIS: *Glasgow Conference*, p. 342 (1954).

⁽¹⁶⁾ K. NISHIJIMA and T. NAKANO: *Prog. Theor. Phys.*, **10**, 581 (1953).

as given by 6.2 GeV protons, (2) is more important than (4). This involves a rather rapid increase with energy of the cross-sections for (3) and (4). If these cross-sections increase more rapidly than the cosmic ray spectrum falls, so that high energy interactions are important, the cosmic ray cloud chamber results can clearly be explained, since any positive to negative ratio greater than 1 can be obtained by a suitable combination of the processes (1) to (4).

8.3. *Further Comparison.* — In the above comparisons we have made some effort to emphasize the general agreement which exists between the experiments. There remain difficulties in some details.

i) If the positive excess is 3.4:1 the Ecole Polytechnique group should have observed 6 negative S -events while they have only found 2. Either this is a statistical fluctuation, in which case there is no evidence for the $K_{\mu 2}$ being only positive; or the $K_{\mu 2}$ is really only positive and the charged V -particles contain a component with a smaller positive excess than the S -particles.

ii) It is seen in Table V that the Ecole Polytechnique has an abnormally large fraction of events with low p^* . The effect seems too large to be due to better momentum resolution.

iii) The change of the positive to negative ratio with the energy of the charged V itself was explained in Sect. 6 by supposing an admixture of hyperons. However, the τ -mesons, which cannot be confused with hyperons, seem to show the same behaviour (see Table IV). If the K -mesons produced in high energy interactions have, themselves, high energies then an increase in the cross-section of processes (3) and (4) could cause a decrease in the positive excess though not a negative excess. Perhaps one observes a combination of both effects.

iv) ARNOLD *et al* ⁽¹⁷⁾ have found a short lifetime for a class of particles which are not hyperons. The classes were highly selected and therefore small and none of the lifetimes differs from infinity by as much as two standard deviations. Bearing in mind the difficulty (and sometimes the impossibility) of the correction procedure in such classes, the short lifetimes may not be significant.

v) In contrast to the results obtained with 6.2 GeV protons (which give 2 GeV available energy in the centre of mass system) SCHEIN *et al.* ⁽⁹⁾ find no positive excess for K -mesons produced by 4.6 GeV π -mesons (which give 2.2 GeV available energy in the centre of mass system) though the statistical significance is not discussed. His result may show that reaction (3) is already important at 2.2 GeV in the centre of mass system.

(17) W. H. ARNOLD, J. BALLAM and G. T. REYNOLDS: *Phys. Rev.*, **100**, 295 (1955).

9. — Interactions which Produce Charged V-Events.

We have found 19 V-particles which were clearly produced in the copper or lead plate. Table VIII summarizes the essential data on these events. It is noticeable that the number of heavy prongs of the interaction is always small, but this may be because some are stopped in the plate. Events SN 814 and SY 873 may represent large angle scattering of K-mesons with, in the case of SN 814, a charge exchange process. In the case of SS 678 a particle is scattered 8° in the plate and below it decays as a V^- -particle. The other features of the events are apparent from the table and it does not seem valuable at this stage to attempt any more elaborate discussion of them. In particular some of the V-particles are probably hyperons, so that the momentum spectrum, if evaluated, would be difficult to interpret.

TABLE VIII. — *Interactions producing charged V-particles inside the cloud chamber in copper and lead plates.*

N_h = number of heavily ionizing particles observed coming from the nuclear interaction.
 N_s = number of lightly ionizing particles observed coming from the nuclear interaction.

Event	Sign of V	Sign of primary	N_h	N_s	Event	Sign of V	Sign of primary	N_h	N_s
SL 496	+	0	4	6	ST 223 +	—	0	0	0
SN 814	+	0	0	0	SY 868	—	\pm	0	2
SO 1073	+	?	2	1	TH 759	—	\pm	0	2
SY 873	+	\pm	0	0	JB 127	—	?	0	1
SY 1058	+	?	2	4	JK 23	\pm	—	0	1
TJ 199	+	0	0	(15) *	QU 372	\pm	0	1	0
JB 127	—	?	0	1	SG 182	\pm	\pm	1	1
SG 35	—	\pm	3	2	X 43	\pm	?	1	1
SL 424	—	\pm	0	1	SJ 928	\pm	\pm	0	2
SL 990	—	\pm	0	(12) *	SS 678 \times	—	\pm	0	0

(*) Most of these particles are electrons.

(+) There may be secondary particles outside the illuminated volume.

(\times) See text.

10. — Conclusions.

We have attempted to combine our measurements of slow K-meson decays with others made in similar experiments and conclude that:

1) The positive excess of slow K-mesons (momentum < 600 MeV/c) observed under heavy material exposed to cosmic radiation is about 3.4:1 in cloud chamber experiments.

2) Our 150 events are only sufficient to give a lower limit ($2 \cdot 10^{-9}$ s) to the lifetime of charged V-particles.

3) About 20% of the K-mesons have values of μ^* significantly less than 200 MeV/c.

4) The relative frequencies of the different decay modes, so far as they can be separated, can be the same for both K^- and K^+ -mesons and the mean relative frequencies are

$K_{\mu 2}, K_{\pi 2}$	$K_{\mu 3}, K_{\beta}$	τ	τ'
67	20	10	3

These ratios are in good agreement with all the emulsion experiments made on positive K-mesons (both from machines and from cosmic radiation). Three events have been observed which are most easily interpreted as the decays of K_{β} -mesons. One of these is negatively charged.

5) It seems possible to account for all K-meson observations using only one mean lifetime (10^{-8} s) for both positive and negative particles. In this case we are led to suppose that the cross sections of the reactions

$$\begin{array}{ll}
 (1) \quad \pi + N \rightarrow Y + K & \\
 (2) \quad N + N \rightarrow N + Y + K & \left. \begin{array}{l} \\ \end{array} \right\} \text{ and } \begin{array}{l} (3) \quad \pi + N \rightarrow N + K + \bar{K} \\ (4) \quad N + N \rightarrow N + N + K + \bar{K} \end{array}
 \end{array}$$

vary differently with energy such that reactions (1) and (2) predominate at low energies, but at energies of several GeV, (3) and (4) become rather rapidly more important. Such a scheme would account for the observed values of the positive to negative ratio except for the difference between that observed in the G-stack and the mean value found in cosmic ray cloud chamber experiments.

* * *

We are grateful to the Administration of the Jungfraujoch Research Station and to the Manager, Mr. HANS WIEDERKEHR, for making our work there possible; also to the University of Manchester and in particular to Prof. G. D. ROCHESTER under whose auspices much of this work was carried out.

Most of the work has been financed by the British Department of Scientific and Industrial Research, from whom one of us (W.A.C.) has received a maintenance grant.

We are also indebted to the International Council of Scientific Unions for a grant toward the running expenses of the apparatus.

We are pleased to record the help of Mr. A. H. CHAPMAN, Mr. G. D. JAMES, Dr. E. G. MICHAELIS, Miss P. M. MILES and Mr. B. W. POWELL in obtaining the results presented in this paper, also to Dr. B. D'ESPAGNAT and Dr. J. PRENTKI for helpful discussions.

RIASSUNTO (*)

Si riportano i dati su 150 V cariche, generate in piombo e rame, osservate in camera a nebbia con campo magnetico. Le V cariche di bassa energia, interpretate tutte come mesoni K, mostrano una ripartizione nei differenti modi di decadimento che si accorda bene con i risultati forniti dalle osservazioni in emulsioni nucleari. Sono state trovate indicazioni di decadimenti iperonici nelle V cariche di alta energia (> 1 GeV) ed in quelle prodotte in rame. Si discute il rapporto tra il numero di K negativi e quello dei K positivi di bassa energia; viene suggerita una interpretazione in funzione di una dipendenza dall'energia della sezione d'urto per produzione. L'interpretazione più probabile di 3 dei 150 eventi è quella di mesoni K_S^0 , mentre altri 10 eventi sono interpretabili come decadimenti di mesoni τ , di cui uno negativo.

(*) Traduzione a cura della Redazione.

Coulomb Repulsion Integrals ($pp|pp$) and Bonding Power of an Atom in a Given Valence State.

L. PAOLONI

Istituto Superiore di Sanità, Laboratorio di Chimica Terapeutica - Roma

(ricevuto il 29 Maggio 1956)

Summary. — The semiempirical method, previously used by PARISER and PARR ⁽¹⁾, for evaluating ($pp|pp$) repulsion integrals has been generalized and extended to the whole set of the first and second row atoms, in their valence states purely p and hybridized sp . This generalization allowed us to obtain an energy measure of the bonding power of an atom in a given valence state, which appears adequate to solve some difficulties, pointed out by PRITCHARD and SKINNER ⁽³⁾, and originated from the comparison of the promotion energies with the behaviour of the O , N , S and P atoms in their isovalent hybrid states.

1. — A semiempirical modification of the Molecular Orbital (MO), Linear Combination of Atomic Orbitals (LCAO), method has been recently proposed by PARISER and PARR ⁽¹⁾ mainly for getting a simpler and better quantitative evaluation of electronic spectra of conjugated molecules. One of the most valuable simplifications was the empirical calculation of the Coulomb repulsion integrals for two electrons on the same atomic orbital χ_p

$$\int \chi_p^{(1)} \chi_p^{(2)} \frac{e^2}{r_{12}} \chi_p^{(1)} \chi_p^{(2)} dv_1 dv_2 = (pp|pp),$$

their value being obtained from the free atom valence state ionization poten-

⁽¹⁾ R. PARISER and R. G. PARR: *Journ. Chem. Phys.*, **21**, 466, 767 (1953).

tials, $-W_p$, and electron affinities, A_p , according to the relation

$$(1) \quad (pp|pp) = -W_p - A_p.$$

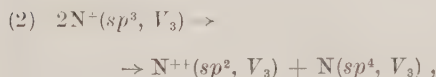
The numerical data, necessary for a wider extension of this method to organic molecules containing hetero-atoms, have been calculated by MULLIKEN ⁽²⁾ and later by PRITCHARD and SKINNER ⁽³⁾.

Equation (1) is not appropriate, however, to direct evaluation of $(pp|pp)$ when an electron pair in a given AO is conjugated to a π -electron system: indeed it was obtained by expressing $(pp|pp)$ as the net energy spent in a process like



with atoms and ions in the proper valence state, and where N^+ means the nitrogen atom as in the molecular core (*). When a substituent like $-NH_2$ is considered, the nitrogen atom enters into the molecular core as N^{++} .

In a recent paper on the structure of Melamine, together with Prof. DEWAR ⁽⁴⁾, we overcame this difficulty by considering the process



where the energy of the valence state $N^+(sp^3, V_3)$ was obtained by averaging between the energies of $N^+(sp^3, V_2)$ and $N^+(sp^3, V_4)$ states of pyridine-like and ammonium-like nitrogen respectively, assuming that the valence state energy of a conjugated $-NR_2$ (amino- or pyrrole-like) is intermediate between the other two.

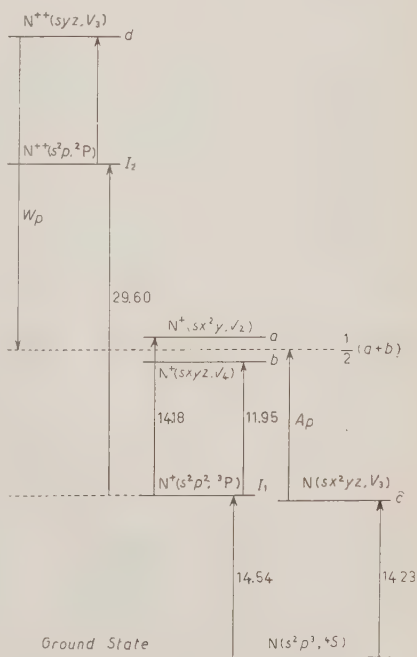


Fig. 1.

(2) R. S. MULLIKEN: *Journ. Chem. Phys.*, **2**, 782 (1934).

(3) H. O. PRITCHARD and H. A. SKINNER: *Chem. Rev.*, **55**, 745 (1955); *Trans. Faraday Soc.*, **49**, 1254 (1953).

(*) It is usual to name *core* what is obtained by removing all the π -electrons from the molecule, while leaving the atoms in their original equilibrium position.

(4) M. J. S. DEWAR and L. PAOLONI: *Trans. Faraday Soc.* (in press).

TABLE I. - Energy of each state above the ground state of the corresponding atoms or ions and

I_1		I_2		a	
$N^+ (s^2p^2, {}^3P)$	14.54	$N^{++} (s^2p^2, {}^2P)$	29.60	$N^+ (sx^2y, V_2)$	14.18
$O^+ (s^2p^3, {}^4S)$	13.61	$O^{++} (s^2p^2, {}^3P)$	35.15	$O^+ (s^2x^2y, V_1)$	4.17
				$O^+ (sx^2y^2, V_1)$	21.80
$P^+ (s^2p^3, {}^3P)$	10.55	$P^{++} (s^2p, {}^2P)$	19.65	$P^+ (sx^2y, V_2)$	9.40
$S^+ (s^2p^3, {}^4S)$	10.36	$S^{++} (s^2p^2, {}^3P)$	23.4	$S^+ (s^2x^2y, V_1)$	2.44
				$S^+ (sx^2y^2, V_1)$	12.34

Given the encouraging results thus obtained, an extension of this procedure was attempted for Oxygen, Sulphur and Phosphorus using valence state energies of PRITCHARD and SKINNER⁽³⁾. The results, collected in Table I, were obtained by evaluating W_p and A_p through the obvious relations (see Fig. 1)

$$(3) \quad W_p = -I_2 + \frac{1}{2}(a + b) - d$$

$$(4) \quad A_p = I_1 + \frac{1}{2}(a + b) - c$$

and then using eq. (1) (the meaning of the symbols is given in the heading of the table).

This procedure actually implies the following significance for W_p and $(pp|pp)$: the energy spent in a process like

$$(5) \quad N(sp^4, V_3) \rightarrow N^{++}(sp^2, V_3)$$

is the sum of the work done by the nuclear field in keeping the two π -electrons in the given AO, or $2W_p$; plus the Coulomb repulsion energy between the two electrons, $(pp|pp)$, in that AO, and in the field of N^{++} , viz:

$$(6) \quad 2W_p + (pp|pp) = -(I_1 + I_2) + c - d.$$

Such a relationship follows immediately also from eq. (1), (3) and (4). An obvious consequence of eq. (6) is that the quantity $2W_p + (pp|pp)$ depends only on the initial and final states of the process (5) and that the energy level of the intermediate state, introduced in eq. (3) and (4) as the average $\frac{1}{2}(a+b)$, play a role only in the partition of the total energy between W_p and $(pp|pp)$. Any error thus introduced in the W_p value through eq. (3) therefore brings an error in the repulsion energy. Now W_p and $(pp|pp)$ are used in the Pariser

integrals when the atom enters into the molecular «core» ionized twice. All values in eV.

b		c		d		$(pp pp)$
$(sxyz, V_4)$	11.95	N (s^2xyz, V_3)	1.19	N ⁺⁺ (xyz, V_3)	?	?
		N (sx^2yz, V_3)	14.23	N ⁺⁺ (syz, V_3)	11.20	14.36
(s^2xyz, V_3)	1.66	O (s^2x^2yz, V_2)	0.50	O ⁺⁺ (s^2xy, V_2)	0.65	16.86
(sx^2yz, V_3)	19.17	O (sx^2y^2z, V_2)	17.65	O ⁺⁺ (sy^2z, V_2)	18.36	16.58
$(sxyz, V_4)$	8.69	P (s^2xyz, V_3)	0.70	P ⁺⁺ (xyz, V_3)	?	?
		P (sx^2yz, V_3)	8.01	P ⁺⁺ (syz, V_3)	9.26	8.28
(s^2xyz, V_3)	0.92	S (s^2x^2yz, V_2)	0.30	S ⁺⁺ (s^2yz, V_2)	0.40	10.38
(sx^2yz, V_3)	11.0	S (sx^2y^2z, V_2)	9.39	S ⁺⁺ (sy^2z, V_2)	12.23	11.32

and Parr method ⁽¹⁾ both combined or separately, so that an evaluation of $(pp|pp)$ independently of W_p and A_p appears desirable, at least for ascertaining the reliability of the previously calculated values.

2. - To this purpose we have tried to understand the meaning of the difference between the *empirical* and *theoretical* values of $(pp|pp)$. The empirical value, which is obtained through eq. (1) differs from the theoretical one, which is obtained through the direct calculation of the integrals with the appropriate AO's, and is, in eV,

$$(7) \quad (pp|pp) = 5.324Z$$

when Slater $2p$ AO's are used. This difference was firstly pointed out by PARISER ⁽⁵⁾ and partly accounted for as the energy change accompanying the polarization of σ -electrons of the *core* atoms brought about as a consequence of the π -electrons migrations. Thinking this energy might be proportional to the effective charge Z of the atom and hence that it was possible to put the empirical integrals obtained from eq. (1) in a form analogous to eq. (7), we have tested the assumption on the whole set of first and second row atoms. The results, shown in Table II, indicate that such an assumption can be retained as a fairly good approximation, especially when one remembers that electron affinities A_p for Be, B, N, Mg, Al, Si, P and S are given with an error which «unlikely... is seriously in excess of ± 1 eV» ⁽³⁾. Among the first row atoms, considered only once ionized in the molecular *core*, the ratio of $(pp|pp)$ to the effective charge Z remains nearly constant around the averaged values 3.29₄ with a departure never exceeding $\pm 3\%$, irrespective

⁽⁵⁾ R. PARISER: *Journ. Chem. Phys.*, **21**, 568 (1953).

TABLE II. *Ratio of the $(pp|pp)$ integral to the effective charge Z of the atomic nucleus in the molecular « core ».*

Atom	Z	$(pp pp)$ eV	$\frac{(pp pp)}{Z}$	Atom	Z	$(pp pp)$ eV	$\frac{(pp pp)}{Z}$
Be (sp, V_2)	1.95	6.20	3.18	Mg (sp, V_2)	2.85	4.10	1.44
B (s^2p, V_1)	2.60	8.95	3.44	Al (s^2p, V_1)	3.50	6.03	1.72
B (sp^2, V_3)	2.60	8.41	3.23 ₅	Al (sp^2, V_3)	3.50	5.22	1.49
C (s^2p^2, V_2)	3.25	10.66	3.28	Si (s^2p^2, V_2)	4.15	7.19	1.75
C (sp^3, V_4)	3.25	10.84	3.33 ₅	Si (sp^3, V_4)	4.15	5.97	1.44
N (s^2p^3, V_3)	3.90	12.98	3.33	P (s^2p^3, V_3)	4.80	8.86	1.85
N (sp^4, V_3)	3.90	12.91	3.31	P (sp^4, V_3)	4.80	9.52	1.98
	4.25	14.36	3.38		5.15	8.28	1.61
O (s^2p^4, V_2)	4.55	14.58	3.20 ₅	S (s^2p^4, V_2)	5.45	9.80	1.80
	4.90	16.86	3.44		5.80	10.38	1.79
O (sp^5, V_2)	4.55	(12.91)*	(2.84)*	S (sp^5, V_2)	5.45	?	?
	4.90	16.58	3.38		5.80	11.32	1.95
F (s^2p^5, V_1)	5.20	17.33	3.33	Cl (s^2p^5, V_1)	6.10	11.27	1.85

(*) Values obtained through eq. (1) with W_p and A_p from P. & S. (2); (excepted some values taken from Table I).

(*) Values calculated with A_p given as uncertain by the above Authors.

of whether the valence state is purely p or hybridized (sp). The same holds when atoms enter into the molecular core ionized twice, despite the uncertainty in the integrals coming from the average term $\frac{1}{2}(a+b)$ in eq. (3) and (4). It seems legitimate, therefore, to use for the $(pp|pp)$ integrals of first row atoms, whatever their hybridization, the empirical relationship.

$$(8) \quad (pp|pp) = 3.29_4 Z.$$

It follows that $(pp|pp)$ values for N^{++} and O^{++} are 14.00 and 16.14 eV respectively, instead of the values recorded on Table I. Also the doubtful value 12.91 eV corresponding to $O(sp^5, V_2)$ can be substituted by 15.0 eV. This is equivalent to taking 2.76 eV as the electronaffinity of $O(sp^5, V_2)$ instead of the uncertain (3) value 4.85 eV.

The first thing one notices in the second row atoms is the change of the $(pp|pp)$ integrals as the valence state passes from a pure p to a hybridized (sp). The ratio between repulsion integrals and effective charge remains, however, within the limits $1.72 \div 1.85$ for all atoms with purely p bonding, ranging not more than 4% around the average 1.79_4 . It appears probable therefore that

for second row atoms in a pure p valence state the relationship

$$(pp|pp) = 1.79_4 Z$$

represents, at present, an useful approximation.

For the (sp) hybridized valence state of Mg, Al and Si the ratio remains nearly constant around 1.46. It is not so for P and S: the value 1.98 of P^+ , which agrees quite well with the value 1.95 of S^- (to which one can refer lacking the value of S^+) is to be compared with the value 1.61 of P^{++} . We regard this as anomalous because it alone contrasts with the other regularities. The averaging criterion probably does fail in this case: indeed the value of $\frac{1}{2}(a+b)$ necessary to keep the P^{++} 's ratio between 1.9 and 2.0 amounts to about 8.2 eV, and hence lies outside the interval of the actual values of a and b , 8.69 and 9.40 eV.

The only conclusion one can stress is that for the hybridized (sp) states of second row elements the repulsion energy of two electrons in the same AO is different from that of the corresponding p states: and more precisely it is lesser in the hybrids of Mg, Al and Si and higher in those of P and S.

3. — It seems that the above conclusion can throw some light on a difficulty pointed out by SKINNER and PRITCHARD⁽³⁾. They say (*Trans. Faraday Soc.*, l. c., p. 1260): « Yet despite that promotion energies are so much smaller in the second row elements, it seems that P and S are less inclined towards second order hybridization than are their first row analogues, and, as a corollary, that such hybridization is less effective in increasing orbital bonding power in the third quantum group ($3s$, $3p$) than in the second. This conclusion is not easy to accept. »

As SKINNER emphasized in a successive paper⁽⁶⁾ the difficulty lies in getting an energy measure of what they called the orbital bonding power. We have tried to obtain it by the following argument.

The total energy of an atom in a given valence state, approximated with the usual form of the hamiltonian, can be expressed as a sum of (i) mono-electronic terms, accounting for the nuclear field action on each electron; (ii) bi-electronic terms, accounting for the repulsion between electrons distributed among the various orbitals. This can be written

$$(9) \quad E_{\text{tot}} = \sum_{\nu} n_{\nu} W_{\nu} + \sum_{\nu \leq q} (pp|qq)$$

where p (and q) is referred to the orbitals actually occupied in the atom by $n_p = 1$ or 2 electrons, with $p = q$ only when $n_p = 2$. If we take the ground

(6) H. A. SKINNER: *Trans. Faraday Soc.*, **51**, 1036 (1955).

state of the free atom as the zero point of the energy and, considering only the outer electrons in the valence shell, we regard as constant or negligible the repulsions between electrons of different total quantum number (which is not a too severe limitation), then the energy E , of a given valence state above the ground state, can be decomposed into an attractive portion A and a repulsive portion R , both representing the variation of the corresponding terms of eq. (9) when the atom is promoted. The quantity E represents therefore the promotion energy and is approximately given by

$$(10) \quad E = A + R.$$

Let us now consider the ratio

$$(11) \quad B = \frac{A}{E}.$$

It follows from eq. (10) that $B \leq 1$ according as $R \geq 0$, i.e. according as the atom is promoted with an increase, without variation or with a decrease in the repulsive terms of eq. (9). If we do take B as a measure of the *bonding power* of the atom in that given valence state, in the sense that a higher ratio A/E corresponds to a higher bonding power, then it is easy to see that the difficulty referred to above does not persist any longer. The number of the bonding AO's does not change in the second order or isovalent hybridization: whence the atomic bonding power B can be divided in equal parts, each one being regarded as a measure of the orbital bonding power. Now such hybridization brings about a transition of a lone pair of electrons from a pure s to an (sp) orbital both for N and O in the first row and for P and S in the second row: but whereas in the formers the change is effected approximately without variation of the term (pp, pp), which is doubtless the most important of the repulsive terms, in the latter the isovalent hybridization increases (pp, pp) by about 10%.

The proposed criterion for the bonding power appears to be consistent with the principle of least energy and expresses the fact that a relative decrease in the repulsion energy produces a relative deepening in the total energy. If one takes into account all the conditions imposed on the building up of the molecule which are implied in the actual existence of a given valence state, then the bonding power of an atom in such a state will increase as the fractional amount of promotion energy spent in keeping the electron in the orbital in which it effects the bond (*).

(*) The atomic bonding power as defined in eq. (11) also agrees with common experience which, for example, predicts that the trivalent state of Al and tetravalent state of Si are the most bonding: the passage $V_1 \rightarrow V_3$ and $V_2 \rightarrow V_4$ respectively, produces indeed a decrease of (pp, pp) integrals of about 1 eV. Similar applications to other atomic states are straightforward.

4. — The form of the equations obtained above for the empirical ($pp|pp$) integrals suggests some further comments. Let us examine the difference between eq. (7) and (8), which may be written

$$(12) \quad (pp|pp)_{\text{theor}} - (pp|pp)_{\text{emp}} = 5.32_4 (Z - Z^*),$$

where Z^* is some kind of *true* effective charge of the atom in the molecular *core*. The Z^* values corresponding to the first row atoms collected on Table II are, in the order: 1.20, 1.60, 2.00, 2.40, 2.80, 3.20. These can be thought of as obtained with the same procedure of Slater's effective charges but by adding to his screening constants the quantities 0.75, 1.00, 1.25, 1.50, 1.75, 2.00 respectively. This seems an indication that the screening action of σ -electrons of the atoms in the molecular *core* increases along with the (Slater) effective charges of the atoms: indeed $0.75/1.95 = 1.00/2.60 = \dots = 2.00/5.20 = 0.38$ and finally

$$Z^* = \frac{3.294}{5.324} Z = (1 - 0.38)Z = 0.62Z.$$

In other words the empirical evaluation of ($pp|pp$) integrals proposed by PARISER and PARR (¹) appears equivalent to the introduction of a supplementary screening constant.

A correction of this kind has been used recently by OHNO and ITOH (²) in a study on electronic structure of ethylene; their evaluation of the atomic terms in ionic structures, although claimed as nonempirical, does not differ, in principle, from the PARISER and PARR procedure for ($pp|pp$) integrals.

* * *

A critical reading of the manuscript by Dr. CARL E. WULFMAN (Austin, Texas) is gratefully acknowledged.

(²) K. OHNO and T. ITOH; *Journ. Chem. Phys.*, **23**, 1468 (1955).

RIASSUNTO

Il metodo semiempirico usato da PARISER e PARR (¹) per il calcolo degli integrali di ripulsione ($pp|pp$) è stato generalizzato ed esteso agli atomi del primo e del secondo periodo nei loro stati di valenza puramente *p* ed ibridi *sp*. Questa generalizzazione ha permesso una definizione energetica del potere legante di un atomo, in un determinato stato di valenza, che sembra adeguata a risolvere alcune contraddizioni rilevate da altri autori (³) tra la scala delle energie di promozione ed il comportamento di certi atomi (O, N, S, P) in stati ibridi isovalenti.

Fast Photoneutrons from Bismuth.

F. FERRERO, A. O. HANSON (*), R. MALVANO and C. TRIBUNO

Istituto di Fisica dell'Università - Torino

Istituto Nazionale di Fisica Nucleare - Sezione di Torino

(ricevuto il 1° Giugno 1956)

Summary. — The excitation functions for fast photoneutrons from bismuth are observed with (n, p) detectors. These indicate that the fast neutrons are produced predominantly by photons in the region of the giant resonance giving further experimental evidence that the giant resonance can be attributed to strong individual particle transitions rather than a collective type of photon absorption resulting in a general nuclear heating. The experimental angular distribution of the fast neutron component from the giant resonance can be represented by a value of B/A of 0.9 ± 0.1 in agreement with that expected for shell model transitions. The relative number of fast neutrons was found to be about 7% of the total neutron yield. This is consistent with the idea that individual neutrons are excited from upper closed shell levels to levels in the continuum if one takes account of the interaction of the neutrons in these states with the rest of the nucleus, as in the model of Feshbach, Porter and Weisskopf.

1. — Introduction.

Previous work by PRICE ⁽¹⁾ indicated that about 20% of the neutrons from bismuth were in a group having an energy above that expected from the statistical model and that these had an angular distribution with a large $\sin^2 \theta$ component. Early theoretical work on the giant resonance considered the possibility of γ -ray absorption by a collective nuclear motion which results

(*) Fulbright scholar from the University of Illinois.

(1) G. A. PRICE: *Phys. Rev.*, **93**, 1279 (1954).

in a general heating of the nucleus and subsequent decay via the statistical model of the nucleus, but such models cannot easily explain a large anisotropic component of high energy neutrons and one needs to introduce transitions in which a single particle may carry off most of the available energy. Although a combination of these processes can in some sense explain the observed results, the purpose of the present work was to see if the results are consistent with an interpretation of the giant resonance as a collection of shell model transitions as has been discussed by WILKINSON⁽²⁾. From the latter point of view the giant resonance arises from the enhanced electric dipole transitions from the upper shell model states to unfilled states in the continuum. This point of view is also supported by the calculations of LEVINGER and KENT⁽³⁾ who showed that when the Pauli exclusion principle was taken into account 61% of the total oscillator strength was accounted for by transitions from the upper $1\frac{1}{2}$ shell of a $N = Z = 92$ nucleus.

In order to see if this point of view is borne out experimentally, it is of interest to try to answer, at least qualitatively, the following questions which were not clearly answered in the earlier experimental work.

Does the fast group of neutrons have the same giant resonance as that for the total neutron spectrum?

Is the angular distribution of the fast group of neutrons consistent with that expected from shell model ground states?

Is the observed fraction of neutrons in the fast group consistent with the assumption that the absorption of the photon results in a single particle transition?

We shall see that, with some qualifications, all these questions can be answered in the affirmative. It would, however, be desirable to have some more specific calculations.

2. - Experimental Methods and Results.

A bismuth cylinder, 2 cm in diameter and 2 cm thick was placed in a collimated X-ray beam from a Brown Boveri Betatron in Turin. The experimental arrangement is shown in Fig. 1. The Betatron was operated at a fixed amplitude of the magnetic field and the energy of the electrons at the time of expansion was determined by controlling the phase of the expander circuit. It is estimated that the energy spread of the electron energy was at the most about 0.3 MeV. The monitor was a parallel plate ionization chamber, connected to a Perucca electrometer, with about 5 cm of aluminum converter in

⁽²⁾ D. H. WILKINSON: *Proceedings of the Glasgow Conference on Nuclear and Meson Physics* (London, 1954).

⁽³⁾ J. S. LEVINGER and D. C. KENT: *Phys. Rev.*, **95**, 418 (1954).

front of the chamber. Its sensitivity has been calculated by FLOWERS, LAWSON and FOSSEY⁽⁴⁾ and for a bremsstrahlung spectrum varies from $3.31 \cdot 10^9$ MeV/cm esu at 10 MeV to $3.44 \cdot 10^9$ MeV/cm esu at 30 MeV.

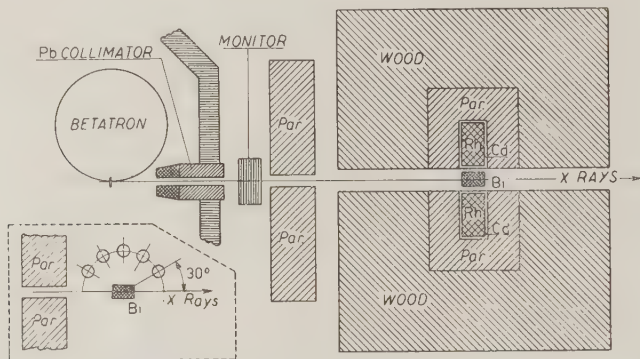


Fig. 1. - Schematic diagram of the general arrangement showing the paraffin moderated rhodium detector in place. Inset shows the arrangements with the (n, p) detectors.

The neutrons from bismuth were detected by the neutron induced radioactivity in three different substances. The 44 s activity in rhodium induced

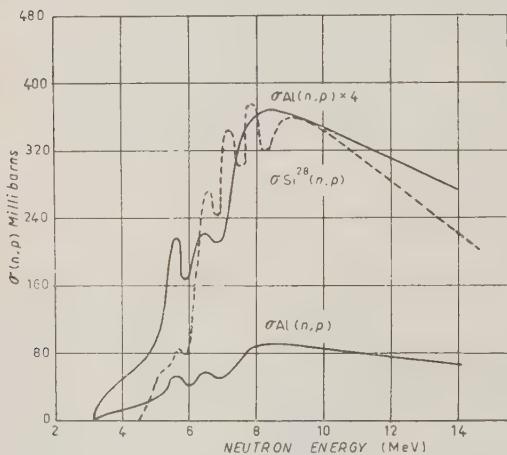


Fig. 2. - (n, p) cross sections for ^{27}Al and ^{28}Si .

by neutrons slowed down in the paraffin and wood is essentially a measure of the total neutron yield. It was found to be convenient to count this activity with the Geiger counters in place inside the paraffin block with the rhodium immediately surrounding the Geiger counters. The radioactivity was measured immediately after an irradiation of the sample by the X-rays from the Betatron. The more energetic neutrons were measured by the neutron induced activi-

(4) B. H. FLOWERS, J. D. LAWSON and E. B. FOSSEY: *Proc. Phys. Soc.*, **65** B, 286 (1952).

(5) U.S.A. ATOMIC ENERGY COMMISSION: *Neutron Cross Sections* (New York, 1955).

(6) I. B. MARION, R. M. BRUGGER and R. A. CHAPMAN: *Phys. Rev.*, **101**, 247 (1956).

ty in Aluminum and Silicon placed near the bismuth sample as shown in the inset in Fig. 1. In the work with these detectors it was found to be convenient to use the samples in powder form and to pour the powder into the jacket of a Geiger counter, adapted for counting liquids, immediately after the irradiation. The observed activities in these two elements are the 9.6 min activity from the $^{27}\text{Al}(n, p)^{27}\text{Mg}$ which has an effective threshold of about 3 MeV and the 2.4 min activity from the $^{28}\text{Si}(n, p)^{28}\text{Al}$ reaction which has an effective threshold of about 5 MeV. The measured cross-sections from aluminum (⁵) and silicon (⁶) are shown in Fig. 2.

2'1. *Excitation Curves.* Although it would be desirable to have the energy distribution of the neutrons at a number of Betatron energies, one can obtain some information about the behaviour of the high energy group with respect to the total neutron yield by comparing the neutron induced activity in the three detectors. The excitation curves for these three detectors are displayed in Fig. 3. In all cases the yields shown represent the difference obtained with and without the bismuth sample in the beam.

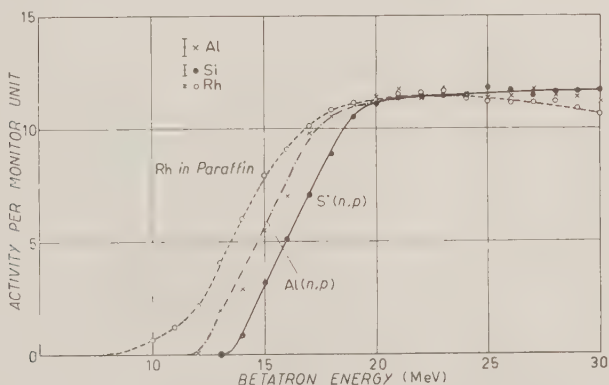


Fig. 3. — Photoneutron yields as a function of the betatron energy as obtained with three different detectors. Ordinates are arbitrarily normalized at 22 MeV.

In the case of the aluminum detector there was an appreciable 2.4 min activity induced by slow neutrons which was reduced by increasing the amount of paraffin between the Betatron and the sample and by covering the samples with cadmium. In the case of silicon some background activity was observed at energies above 20 MeV due to the $^{28}\text{Si}(\gamma, p)^{28}\text{Al}$ reaction.

This was apparently due to the scattering of the bremsstrahlung beam by the monitor and was largely eliminated by placing a block of lead between the silicon sample and the paraffin shield.

It is apparent that the large part of the yield in each case arises from photons below 20 MeV although the fact that the activity induced in silicon and aluminum remains above that for rhodium indicates that there are some fast neutrons which are produced by photons above that energy.

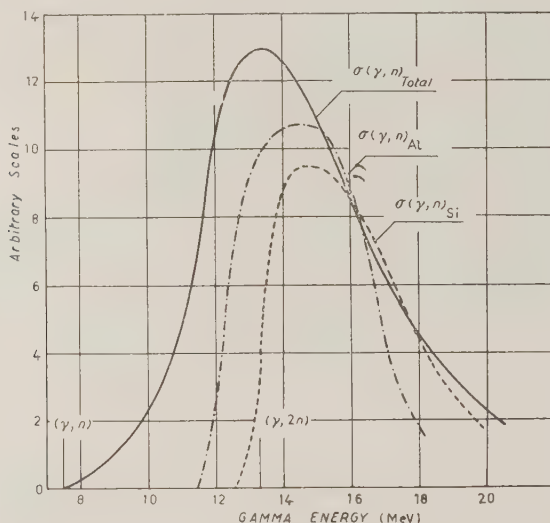


Fig. 4. — Photoneutron cross sections as observed with the three different detectors as a function of the photon energy. Scales for the ordinates are arbitrary.

Cross-sections for the activation of the various detectors were calculated from the curves in Fig. 3 using the photon difference method of KATZ and CAMERON⁽⁷⁾ and are shown in Fig. 4. The cross-section, as obtained with the Rh detector, is essentially that for neutron production since it has a sensitivity which is independent of the neutron energy, while those for the other two depend on the neutron spectrum from bismuth and on the energy sensitivity of the detectors.

The exact shape of these curves are not determined with great accuracy but they do indicate the regions of the greatest contributions to the cross-sections in each case. The cross section curve for Al is especially uncertain due to the large variation of the incremental activity from point to point. Since the cross-sections for the (n, p) reactions have been measured, it is interesting to compare the observed (γ, n) cross-sections as measured by these detectors with that calculated on the assumption that there is a fast group of neutrons which carry off all the available energy $(E_\gamma - E_{th})$ which has the

(7) L. KATZ and A. G. W. CAMERON: *Canad. Journ. of Phys.*, **29**, 518 (1951).

same excitation cross-section as that for the total neutrons. The existence of such a group of neutrons is indicated in the neutron spectrum of Price which is reproduced in Fig. 5. It is apparent that the threshold of the silicon detector is high enough to exclude any significant contribution of the high energy tail of the statistical distribution. The product of $\sigma(\gamma, n)_{\text{total}}$, as shown in Fig. 4, and $\sigma(n, p)_{\text{Si}}$ from Fig. 2 is shown in Fig. 6 where it is compared to $\sigma(\gamma, n)_e$ from Fig. 4. It is observed that the agreement between the observed and the calculated cross-sections is rather good. Similar calculations for the expected

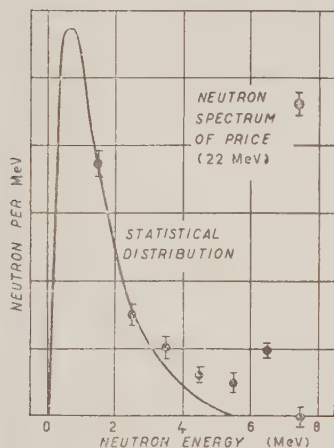


Fig. 5. - Energy spectrum of the photoneutrons from bismuth at 22 MeV as observed by PRICE.

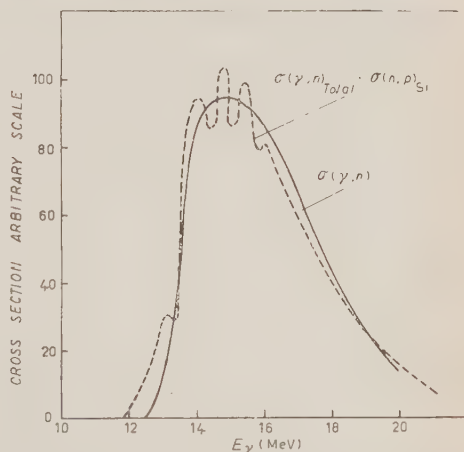


Fig. 6. - Calculated cross section for neutrons as detected by the Si(n, p) detector, on the assumption of a direct process, compared with the experimentally observed cross sections.

cross-sections for the Al detector indicates that the observed cross-section falls too fast at higher energy. The results do indicate, however, that the main contribution to the fast neutron yield takes place in the region of the giant resonance. It is, therefore, not necessary to assume that the fast neutron component is produced by a photon absorption process which is different from that responsible for the giant resonance.

2'2. Angular Distribution. - The experimental arrangement used in the measurement of the angular distribution was that shown in the inset of Fig. 1. The fast neutron detectors were placed at various angles at a distance of 4.5 cm from the effective center of the bismuth sample. These samples were counted by pouring the powders into the outer reservoir of a Geiger counter designed for counting liquids. The count obtained in this way

was considerably higher than that obtained with aluminum and quartz tubes, such as used by PRICE. In the usual run in which the sample was irradiated for about an half life and counted for a similar period, the net count would be more than 1000 counts. Such measurements were repeated at least 4 times for each point.

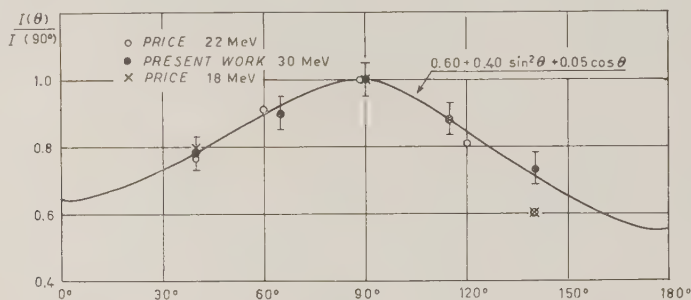


Fig. 7. - Angular distribution of neutrons from bismuth irradiated by 31 MeV bremsstrahlung as observed with the Al(n, p) detector.

The angular distribution as measured by the 9.6 min Al(n, p) activity for 30 MeV bremsstrahlung is shown in Fig. 7. The background activity with this detector is due to the 2.4 min slow neutron induced activity and does not vary appreciably with angle. The solid curve is a least square fit of the data with a function of the form $A + B \sin^2 \theta + C \cos \theta$. The value of B/A in this case is 0.67 ± 0.1 as compared to a value of 1 obtained by PRICE at 18 and 22 MeV. The angular distribution as measured by the 2.4 min Si(n, p) activity is shown in Fig. 8. The background without the bismuth in the beam was small but at 30 MeV there was a troublesome background

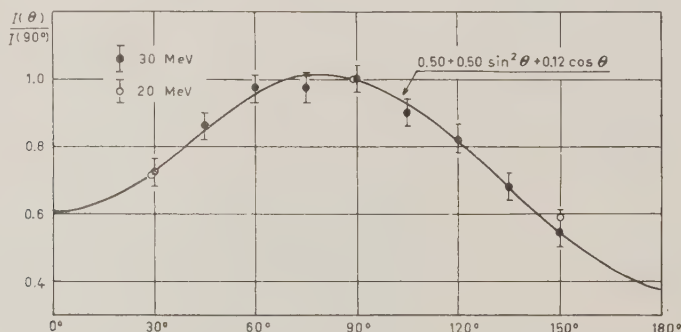


Fig. 8. - Angular distribution of neutrons from bismuth irradiated by 20 and 30 MeV bremsstrahlung as detected by the Si(n, p) detector.

at 30° due to the X-rays scattered by the bismuth giving rise to the same 2.4 min activity by the $^{29}\text{Si}(\gamma, p)^{28}\text{Al}$ reaction.

To estimate the effect of photon scattering at 30 MeV, the photon induced activities in copper and oxygen (H_2O) samples placed at the 30° position were compared to that induced in the direct beam with the bismuth sample removed. When the observed ratios of the scattered intensities are applied to the observed activity induced in Si in the direct beam, the fraction of the activity in Si at 30° which could be attributed to the scattered γ -rays was found to be 15 and 4 percent as calculated from copper and oxygen data respectively. Since the effective threshold for the $^{29}\text{Si}(\gamma, p)^{28}\text{Si}$ reaction lies midway between those for oxygen and copper, the average of these two values was used. It can be seen that the distribution is still quite asymmetrical. The value of B/A is 1.00 ± 0.1 .

At 20 MeV the betatron intensity was lower and it was more difficult to obtain good statistics. The points may be more significant, however, since the background was completely negligible and it is clear that at this energy the entire effect is contributed by photons from the region of the giant resonance. The three points obtained at this energy are also shown in Fig. 8 slightly displaced from the actual angles in order to avoid confusion. The value of B/A in this case is 0.9 ± 0.1 and is much lower than that obtained by PRICE with quartz detectors.

These values can also be compared with the work of JOHANSSON⁽⁸⁾. He found angular distributions which were symmetrical about 90° with values of B/A of 0.96 and 0.82 for Pb using ZnS plastic scintillators biased to detect neutrons above 5 and 10 MeV respectively. The bremsstrahlung energy, however, was 65 MeV and it was not clear that the major part of the neutrons was produced by photons in the region of the giant resonance.

An attempt was made to measure the angular distribution with the paraffin moderated Rh counters but, due to insufficient shielding, the background was too high to permit good measurements. The measurements, however, gave an upper limit of 10% for the anisotropic component.

2.3. Fraction of Neutrons in the Fast group. — The rough energy spectrum of Price shown in Fig. 5 indicates that about 16 percent of the neutrons are in the fast group above that of the neutrons expected on the basis of the statistical model.

In the present experiment the fraction of the neutrons in the fast group can be estimated by comparing the observed (n, p) activities with that calculated using the total photoneutron cross-section and the corresponding (n, p) cross-sections on the assumption that all neutrons have an energy of

(8) S. A. E. JOHANSSON: *Phys. Rev.*, **97**, 434 (1955).

($E_\gamma = 7.5$) MeV. The necessity of absolute measurements of counter sensitivity for the silicon sample was eliminated by observing the ^{28}Al activity produced by the $^{28}\text{Si}(\gamma, p)^{28}\text{Al}$ which has been studied previously by KATZ *et al.* (⁹). It is then only necessary to compare the observed (n, p) induced ^{28}Al activity measured in an identical sample and in the same counting geometry when irradiated with X-rays in the position of the bismuth sample. The ratio of the activity in a silicon sample placed 3 cm from the center of the bismuth at 26 MeV to that found with a similar sample directly in the beam at the same energy was 0.011 while that calculated on the assumption discussed above was 0.22. The observed (n, p) activity is therefore consistent with the assumption that 5% of the neutrons are emitted as fast neutrons, carrying away all the energy available.

The corresponding number calculated from the (n, p) induced activity in aluminum indicates that about 10% of the neutrons are in the fast group. It is expected that there will be some activity induced in Al by neutrons from the statistical distribution but a large contribution of isotropic neutrons from this distribution would considerably reduce the relative anisotropic component. It may be that the larger apparent yield from the Al detector is due to different counter efficiencies used in this work and in that used previously in the measurements of the (n, p) cross-sections.

It seems reasonable to say that the present work indicates that 7 : 3% of the neutrons are in the fast group. This is considerably less than that obtained from the earlier work and it would be desirable to have further measurements on this point.

3. - Discussion.

The fact that the fast group of neutrons with the anisotropic angular distribution is clearly associated with the giant resonance makes it interesting to see if the angular distribution and the fraction of neutrons in the fast group is quantitatively consistent with the assumption of shell model transitions.

First, it is clear that practically all photons absorbed through individual proton transitions lead to a general excitation of the nucleus since the protons have a very small probability of penetrating the Coulomb barrier. These transitions account for 50% of the total neutron yield but make no contribution to the characteristic fast neutron group. The remaining 50% of the transitions can be considered as electric dipole transitions from the upper closed neutron shells. The strongest of these are the $1\hbar^{9/2} \rightarrow 1i^{11/2}$ and the $1i^{13/2} \rightarrow 1j^{15/2}$

(⁹) L. KATZ, R. N. H. HASLAM, J. GOLDBERG and J. G. W. TAYLOR: *Canad. Journ. of Phys.*, **32**, 580 (1954).

transitions leading to final states in which the neutron has angular momenta of 6 and 7 respectively. The relatively large angular momentum barriers in these states increase their lifetime and make the consideration of the interaction of neutrons with the rest of the nucleus important. When such an interaction is introduced, the transitions from these upper states contribute largely to the statistical distribution and it is found that the largest contributions to the fast group of neutrons can be attributed to other transitions.

The angular distributions to be expected for simple electric dipole transitions from a state with angular momentum l to one with $l+1$ was shown by COURANT⁽¹⁰⁾ to be of the form $A+B\sin^2\theta$ where $B/A = (l+2)/2l$. The value to be expected from bismuth will depend on the relative contribution of various transitions to the fast neutron group.

The fraction of neutrons escaping directly without interaction with the rest of the nucleus can be expressed as $F = \Gamma_n/(\Gamma_n + \Gamma_a)$, where Γ_n is the width for neutron emission and Γ_a is the corresponding width for the absorption of the simple neutron state into a general excitation of the nucleus.

As a rough approximation for Γ_n one may use the relation⁽¹¹⁾ $\Gamma_n = 2k\gamma^2 T_{ln} \approx 3\hbar v T_{ln}/R$, where v is the neutron velocity, R is the conventional nuclear radius, and T_{ln} is the transmission of the angular momentum barrier⁽¹²⁾. For 7 MeV neutrons having no angular momentum the value of Γ_n is about 5 MeV. This value is reduced by the transmission factor for neutrons having angular momenta different from zero.

To obtain an estimate of Γ_a one may use the model of Feshbach, Porter and Weisskopf⁽¹³⁾ in which the potential for low energy neutrons is $V(1 - \zeta i) - 12(1 - 0.03i)$ MeV and the width for the absorption is $2\zeta V$. For a neutron energy E_n , which is comparable to the binding energy B , one expects the absorption to increase by a factor $((E_n - B)/B)^2$ which represents the dependence of the absorption on the excitation above the Fermi energy⁽¹⁴⁾. For a neutron of 7 MeV Γ_a is about 10 MeV.

In order to obtain an average value of B/A and F it is necessary to consider the enhancement factors for the possible photon transitions as well as the transmission of the angular momentum barrier by the outgoing neutron. The enhancement factors used are proportional to those given by WILKINSON⁽²⁾ and may not be strictly correct but these do take into account, at least qualitatively, the transfer of oscillator strengths from the transitions between lower

⁽¹⁰⁾ E. D. COURANT: *Phys. Rev.*, **82**, 703 (1951).

⁽¹¹⁾ J. M. BLATT and V. F. WEISSKOPF: *Theoretical Nuclear Physics* (London, 1952), p. 558.

⁽¹²⁾ M. LAX and H. FESHBACH: *Journ. Acoust. Soc. Am.*, **20**, 108 (1948). See also ref. ⁽¹¹⁾ page 361.

⁽¹³⁾ H. FESHBACH, C. E. PORTER and V. F. WEISSKOPF: *Phys. Rev.*, **96**, 448 (1954).

⁽¹⁴⁾ M. CINI and S. FUBINI: *Nuovo Cimento*, **2**, 75 (1955).

levels which are forbidden by the Pauli principle to the upper levels. The enhanced strengths (S) of various transitions, the neutron transmission factors, and the values of F and B/A are shown in Table I.

TABLE I. - *Shell model transitions in bismuth.*

Transition	l	l_n	n_s	ε	S	T_{ln}	F	N_f	B/A
$1i^{13/2} - 1j^{15/2}$	6	7	14	4.0	56	0.04	0.02	1.1	0.67
$1h^{9/2} - 1i^{17/2}$	5	6	10	3.0	30	0.14	0.07	2.1	0.70
$2f^{7/2} - 2g^{9/2}$	3	4	8	2.5	20	0.55	0.22	4.4	0.83
$2f^{5/2} - 2g^{7/2}$	3	4	6	2.0	12	0.55	0.22	2.6	0.83
$3p^{3/2} - 3d^{5/2}$	1	2	4	1.5	6	0.87	0.30	1.8	1.50
$3p^{1/2} - 3d^{3/2}$	1	2	2	1.0	2	0.87	0.30	0.6	1.50
Sum	—	—	44	—	126	—	—	12.6	—
Average	—	—	—	—	—	—	0.10	—	0.90

The headings of the various columns represent the initial (l) and final angular momentum (l_n), the number of neutrons in the shell (n_s), the enhancement factor (ε), the strength of the transition (S), the transmission of the angular momentum barrier (T_{ln}) for 7 MeV neutrons having angular momentum l_n , the fraction of neutrons escaping $F = T_{ln}/(T_{ln} + 2)$, the number of fast neutrons N_f ($S \times F$), and (B/A) the coefficient of the $\sin^2 \theta$ term of the angular distribution.

It is interesting to note that although the strongest photon absorption takes place in the upper shell it makes only a small contribution to the fast neutron group. The largest contribution comes from the $2f \rightarrow 2g$ transitions for which the angular momentum barrier is smaller. The average fraction of the neutrons which escape in these neutron transitions is seen to be 10% giving a fast component which is 5% of the total neutron yield. This estimate is in reasonable agreement with the observed value of 7% and it provides a way of understanding the relatively small fraction of neutrons in the fast group without the necessity of introducing a photon absorption of the co-operative type.

The average value of B/A obtained on the basis of the above model is seen to be 0.90 in agreement with the value observed at 20 MeV.

The measurements on the fast group of photoneutrons from bismuth are, therefore, consistent with the interpretation of the giant resonance as a col-

lection of individual particle transitions from initial shell model states to final states in the continuum.

In order to explain quantitatively the angular distribution and the yield of the fast neutron group one must take into account the absorption of the neutrons from the final single particle states into a general excitation of the (compound) nucleus.

* * *

We wish to express our appreciation to Prof. G. WATAGHIN, director of the Institute of Physics for his active support of this work and for useful discussions. One of us (A.O.H.) wishes to acknowledge the most enjoyable hospitality of the Institute during his stay in Italy.

RIASSUNTO

Si sono misurate con diversi tipi di rivelatori (n, p) le funzioni di eccitazione dei neutroni rapidi prodotti nella fotodisintegrazione del bismuto. Queste misure indicano che i neutroni rapidi sono essenzialmente prodotti nella regione della risonanza gigante, il che offre una ulteriore evidenza sperimentale all'ipotesi che la risonanza gigante sia un insieme di transizioni tra stati di un modello a particelle indipendenti piuttosto che un assorbimento di fotoni dovuto ad una vibrazione cooperativa dei nucleoni risultante in un generale riscaldamento del nucleo. La distribuzione angolare della componente veloce dei neutroni provenienti dalla risonanza gigante può essere rappresentata da un valore sperimentale di B/A dell'ordine 0.9 ± 0.1 in accordo col valore teorico per transizioni nel modello a shell. Si è trovato che il numero relativo di neutroni veloci è circa il 7% del numero totale dei neutroni emessi. Questo numero è in accordo con l'ipotesi che i singoli neutroni vengano eccitati da livelli appartenenti alla shell chiusa più esterna a livelli del continuo, sempre che si tenga conto dell'interazione dei neutroni in questi stati con il resto del nucleo come nel modello proposto da Feshbach, Porter e Weisskopf.

Pair Correlations in Dilute Gases at Low Temperatures.

J. M. BLATT

*The F.B.S. Falkiner Nuclear Research and Adolph Basser Computing Laboratories
School of Physics (*), The University of Sydney - Sydney, N.S.W.*

(ricevuto il 4 Giugno 1956)

Summary. — In classical statistical mechanics, the correlation function between pairs of gas particles in a dilute gas is given by $\exp[-\beta V(r)]$, where $\beta = 1/kT$ and $V(r)$ is the potential of the force between the two particles. This paper presents the corresponding quantum mechanical formulae, including the generalization to Bose-Einstein and Fermi-Dirac statistics. The quantum mechanical corrections are of major importance in the low-temperature region, where they change the correlation function qualitatively. In the absence of bound states, the quantum pair correlation function approaches a finite limit as the temperature approaches zero. Various approximation methods are developed for the pair correlation function, including an application of a variation principle for the inverse of an operator, due to Friedman.

1. — Introduction.

This paper is devoted to a discussion of the statistical mechanics of dilute gases at low temperatures, in the approximation in which 3-body and more complex collisions between gas particles can be neglected. This is the same approximation which gives the correct value for the second virial coefficient but incorrect values for the higher coefficients in the virial expansion. Alternatively, this paper may be considered an exact treatment of the statistical mechanics of a system of *two* gas particles enclosed in a large box with constant temperature walls, the box being empty otherwise.

(*) Also supported by the Nuclear Research Foundation within the University of Sydney.

The behaviour of dilute gases at low temperatures is an old subject ^(1,2), and no longer of major interest for its own sake. However, the methods used here to discuss this problem allow generalization to more interesting low-temperature systems.

The emphasis in the literature is primarily on the calculation of the second virial coefficient; this will form the subject of the following paper. In this paper, we make a detailed study of the pair correlation function in a dilute gas. We emphasize that effects due to the interposition of other particles between the particles of our pair are not considered in this treatment. Thus, in classical statistical mechanics, our pair correlation function is given simply by

$$(1.1) \quad q(r, \beta) = \exp [-\beta V(r)] \quad \text{classical,}$$

where $\beta = 1/kT$ and $V(r)$ is the potential of the force between the two particles. The classical result fails at low temperatures, and we are concerned with the quantum mechanical generalization of this correlation function, and with another correlation function, $q_p(r, t)$, which enters when the particles obey quantum (Bose-Einstein or Fermi-Dirac) statistics.

Our $q(r, \beta)$ is called $S(r)$ by UHLENBECK and BETH ^(2a), and is not introduced explicitly by GROPPER ^(2b) or GREEN ^(2d). The properties of this pair correlation function are not discussed at all, except for stating the obvious requirement

$$(1.2) \quad \lim_{\beta \rightarrow \infty} q(r, \beta) = 1, \quad \text{for all } \beta.$$

This is quite satisfactory if the virial coefficient is the main focus of interest. But in the generalization to other low-temperature phenomena, the pair correlation function itself is of more interest than the virial coefficient; this is so particularly because (as we shall show in the following paper) the main contribution to the virial coefficient at very low temperatures comes from values of the inter-particle separation r much larger than the range of the force between the particles, and hence also much larger than the normal inter-particle separations in denser systems such as liquids.

No numerical results are given in this paper. The formulae are too cumber-

(1) J. O. HIRSCHFELDER, C. F. CURTISS and R. B. BIRD: *Molecular Theory of Gases and Liquids* (New York, 1954); see chapter VI in particular.

(2) a) G. E. UHLENBECK and E. BETH: *Physica*, **3**, 729 (1936); **4**, 915 (1937); b) L. GROPPER: *Phys. Rev.*, **50**, 963 (1936); **51**, 1108 (1937); **55**, 1095 (1939); c) K. HUSIMI: *Proc. Phys.-Math. Soc. Japan*, **22**, 264 (1940); d) H. S. GREEN: *Proc. Phys. Soc. London*, A **45**, 1022 (1952).

(3) J. E. KILPATRICK, W. E. KELLER, E. F. HAMMEL and N. METROPOLIS: *Phys. Rev.*, **94**, 1103 (1954).

some to allow evaluation by desk computing methods, but are suitable for evaluation by electronic computers. A program for evaluating the second virial coefficient already exists⁽³⁾, and we intend to write a program for evaluating the pair correlation function as soon as the Sydney SILLIA⁴ comes into operation.

The general derivation given in Sect. 2 differs from the literature⁽²⁾ mostly through the more careful discussion of the contribution of the bound states; these are omitted completely by GROPPER and GREEN, and are treated in an ad hoc manner by UHLENBECK and BETH; these latter authors, however, do arrive at the correct final result. In our treatment the contribution of the bound states enters naturally as a consequence of the mathematics, and no special ad hoc treatment is necessary. For the same reason there is no difficulty about what normalization should be used.

The rest of the paper is devoted to a discussion of the properties of the pair correlation function, obtained through various approximation methods

2. - The Density Matrix of a Two-Particle System.

We consider two non-identical particles in a box. The density matrix is the matrix element of the statistical operator $\exp[-\beta H]$, where $\beta = (kT)^{-1}$ and H is the Hamiltonian of the system:

$$(2.1) \quad \begin{aligned} H &= -(\hbar^2/2m_1)\nabla_1^2 - (\hbar^2/2m_2)\nabla_2^2 + V(|\mathbf{r}_1 - \mathbf{r}_2|) = \\ &= -(\hbar^2/2M)\nabla_x^2 - (\hbar^2/2\mu)\nabla_r^2 + V(r), \end{aligned}$$

where \mathbf{x} is the coordinate of the centre of gravity, M the total mass, \mathbf{r} the relative co-ordinate, and μ the reduced mass. We write

$$(2.2) \quad \begin{aligned} U(\mathbf{x}, \mathbf{r}; \mathbf{x}', \mathbf{r}'; \beta) &= \langle \mathbf{r}_1 \mathbf{r}_2 | \exp[-\beta H] | \mathbf{r}'_1 \mathbf{r}'_2 \rangle = \langle \mathbf{x} \mathbf{r} | \exp[-\beta H] | \mathbf{x}' \mathbf{r}' \rangle = \\ &= U_0(\mathbf{x} - \mathbf{x}', \beta) G(\mathbf{r}, \mathbf{r}', \beta), \end{aligned}$$

where the factorized form is possible because the Hamiltonian for the centre-of-gravity motion commutes with the Hamiltonian for the relative motion⁽⁴⁾. The expression for U_0 is well known⁽²⁾

$$(2.3) \quad U_0(\mathbf{x} - \mathbf{x}', \beta) = (2\pi\hbar^2\beta/M)^{-\frac{3}{2}} \exp \left[-\frac{M|\mathbf{x} - \mathbf{x}'|^2}{2\hbar^2\beta} \right].$$

⁽⁴⁾ Strictly speaking, this is not true because of the fact that the system is enclosed in a box. However, the error involved here can be made arbitrarily small by letting the box become very large.

We shall be interested primarily in the function $G(\mathbf{r}, \mathbf{r}', \beta)$ defined by

$$(2.4) \quad G(\mathbf{r}, \mathbf{r}', \beta) = \langle \mathbf{r} | \exp[-\beta H_{\text{rel}}] | \mathbf{r}' \rangle$$

where H_{rel} is the Hamiltonian for the relative motion of the two particles, i.e., the last two terms in equation (2.1). G satisfies the differential equation

$$(2.5) \quad \partial G / \partial \beta = -H_{\text{rel}} G,$$

with the initial condition

$$(2.6) \quad \lim_{\beta \rightarrow 0} G(\mathbf{r}, \mathbf{r}', \beta) = \delta(\mathbf{r} - \mathbf{r}').$$

In the trivial case of no interaction between the particles, $V(r) = 0$, the solution of (2.5) and (2.6) is formally identical with (2.3), and is obtained from (2.3) by replacing M by μ , \mathbf{x} by \mathbf{r} , and \mathbf{x}' by \mathbf{r}' . We shall call this function $G_0(\mathbf{r}, \mathbf{r}', \beta)$,

$$(2.7) \quad G_0(\mathbf{r}, \mathbf{r}', \beta) = (2\pi\hbar^2\beta/\mu)^{-\frac{3}{2}} \exp\left[-\frac{\mu}{2\hbar^2\beta} |\mathbf{r} - \mathbf{r}'|^2\right].$$

It is easily verified that the total density matrix in this simple case assumes a factored form with one factor for each particle:

$$(2.8) \quad \langle \mathbf{r}_1 \mathbf{r}_2 | \exp[-\beta H] | \mathbf{r}'_1 \mathbf{r}'_2 \rangle = (2\pi\hbar^2\beta/m_1)^{-\frac{3}{2}} (2\pi\hbar^2\beta/m_2)^{-\frac{3}{2}} \cdot \exp\left[-\frac{m_1(\mathbf{r}_1 - \mathbf{r}'_1)^2 + m_2(\mathbf{r}_2 - \mathbf{r}'_2)^2}{2\hbar^2\beta}\right].$$

We now proceed to solve (2.5) in general. We introduce the following notation:

$$(2.9) \quad t = \hbar^2\beta/2\mu$$

$$(2.10) \quad W(r) = 2\mu V(r)/\hbar^2,$$

so that equation (2.5) assumes the form of a « heat-flow » equation with t as the « time »

$$(2.11) \quad \partial G / \partial t = \nabla^2 G - W(r)G$$

and the « free » solution (2.7) becomes

$$(2.7a) \quad G_0(\mathbf{r}, \mathbf{r}', t) = (4\pi t)^{-\frac{3}{2}} \exp\left[-\frac{(\mathbf{r} - \mathbf{r}')^2}{4t}\right].$$

We decompose G into spherical harmonics:

$$(2.12) \quad G(\mathbf{r}, \mathbf{r}', t) = \sum_{l=0}^{\infty} G_l(r, r', t) (rr')^{-1} Y_{10}(0) Y_{10}(\theta),$$

where θ is the angle between the vectors \mathbf{r} and \mathbf{r}' , and $Y_{lm}(\theta, \varphi)$ are the standard spherical harmonics ⁽⁵⁾. Equations (2.11) and (2.6) then split into separate equations, one for each value of l :

$$(2.13) \quad \partial G_l / \partial t = \partial^2 G_l / \partial r^2 - \left[\frac{l(l+1)}{r^2} + W(r) \right] G_l \equiv -H_l G_l,$$

$$(2.14) \quad \lim_{t \rightarrow 0} G_l(r, r', t) = \delta(r - r').$$

We now make a Laplace transform on the variable t , i.e. we introduce

$$(2.15) \quad Z_l(r, r', s) = \int_0^{\infty} \exp[-st] G_l(r, r', t) dt.$$

The differential equation for Z_l then becomes

$$(2.16) \quad H_l Z_l + s Z_l = \delta(r - r').$$

This equation must be solved subject to the boundary conditions:

$$(2.17) \quad Z_l(r, r', s) = 0 \quad \text{when } r = 0 \quad \text{and when } r \rightarrow \infty.$$

We introduce the regular and irregular solutions of the homogeneous equation corresponding to (2.16), i.e. of

$$(2.18) \quad H_l u_l(r, \sigma) + \sigma^2 u_l(r, \sigma) = 0,$$

where we write $s = \sigma^2$ for later convenience. The solution $u_l(r, \sigma)$ is defined by the conditions

$$(2.19) \quad u_l(r, \sigma) \rightarrow \exp[+\sigma r] \quad \text{for } r \text{ large}; \quad u_l(0, \sigma) = 0.$$

A linearly independent solution $v_l(r, \sigma)$ is defined by the condition

$$(2.20) \quad v_l(r, \sigma) \rightarrow \exp[-\sigma r] \quad \text{for } r \text{ large}.$$

⁽⁵⁾ E. U. CONDON and G. H. SHORTLEY: *The Theory of Atomic Spectra* (Cambridge 1935), chapter II.

This solution fails to vanish at the origin, of course, unless σ^2 assumes special values corresponding to energies of possible bound states; for our purposes we must exclude this possibility, i.e., we must choose the Laplace transform variable s in (2.15) such that $(\hbar^2/2\mu) \operatorname{Re}(s)$ is larger than the binding energy of the most strongly bound discrete energy level of the two-particle system ⁽⁶⁾. This is of course always possible.

We use the Wronskian identity

$$(2.21) \quad v_i(\partial u_i/\partial r) - u_i(\partial v_i/\partial r) = 2\sigma$$

which follows from the asymptotic forms (2.19), (2.20) together with the fact that the Wronskian is independent of r . We also introduce the notation

$$(2.22) \quad r_{>} = \text{Maximum}(r, r'), \quad r_{<} = \text{Minimum}(r, r').$$

The solution of (2.16) and (2.17) is then given by

$$(2.23) \quad Z_i(r, r', s) = \frac{1}{2}s^{-\frac{1}{2}}u_i(r_{<}, s^{\frac{1}{2}})v_i(r_{>}, s^{\frac{1}{2}}).$$

We now use the standard inversion formula for the Laplace transform (2.15), to get

$$(2.24) \quad G_i(r, r', t) = (2\pi i)^{-1} \int_C ds \exp[st] Z_i(r, r', s) = \\ = (2\pi i)^{-1} \int_{C'} d\sigma \exp[\sigma^2 t] u_i(r_{<}, \sigma) v_i(r_{>}, \sigma),$$

where C is the standard Bromwich contour and C' is its image in the plane of $\sigma = s^{\frac{1}{2}}$.

We now transform the contour so as to get (2.24) into purely real form. This means essentially taking the contour C' along the imaginary axis in the σ plane; however, care must be taken if there are bound states, so as not to lose their contribution. Suppose there exists a bound state with angular momentum l and energy

$$(2.25) \quad \epsilon_l^{(-)} = -(\hbar^2/2\mu)\sigma_1^2.$$

In that case, the solution $v_i(r, \sigma_1)$ not only vanishes at infinity but also becomes

⁽⁶⁾ As we shall see, this is merely the usual requirement on the Bromwich contour in the inversion of the Laplace transform, namely that the contour must run to the right of all singularities of the Laplace transform function $Z(s)$.

zero at $r = 0$. No solution $u_i(r, \sigma_1)$ satisfying the conditions (2.19) exists, and it is shown in appendix A that $u_i(r, \sigma)$, considered as a function of σ for fixed r , has a pole of first order at $\sigma = \sigma_1$, with residue proportional to $v_i(r, \sigma_1)$. More precisely, in the neighbourhood of $\sigma = \sigma_1$, $u_i(r, \sigma)$ is given by

$$(2.26) \quad u_i(r, \sigma) = (\sigma - \sigma_1)^{-1} \frac{v_i(r, \sigma_1)}{\int_0^\infty (v_i(r, \sigma_1))^2 dr} + \text{regular terms.}$$

When we substitute this result into (2.24), the contribution of the pole at $\sigma = \sigma_1$ becomes equal to

$$\exp[\sigma_1^2 t] \frac{v_i(r, \sigma_1) v_i(r', \sigma_1)}{\int_0^\infty (v_i(r, \sigma_1))^2 dr}.$$

We introduce a symbol for the *normalized* radial wave function of the i -th bound state with angular momentum l :

$$(2.27) \quad \psi_{ii}(r) = \frac{v_i(r, \sigma_1)}{\left(\int_0^\infty (v_i(r, \sigma_1))^2 dr \right)^{\frac{1}{2}}}.$$

In terms of this notation, the contribution of the i -th bound state to $G_i(r, r', t)$ is equal to

$$(2.28) \quad \exp[\sigma_1^2 t] \psi_{ii}(r) \psi_{ii}(r') = \exp[-\beta \epsilon_{ii}^-] \psi_{ii}(r) \psi_{ii}(r').$$

Having taken care of the contributions of the poles along the positive real axis in (2.24), the remainder can be evaluated by taking the contour C'' to lie along the imaginary axis in the σ -plane. We introduce the notation $\sigma = ik$ and the regular and irregular solutions of the Schrödinger wave equation:

$$(2.29) \quad \begin{cases} \varphi_i(r, k) = 0 & \text{at } r = 0, \\ \cong \sin(kr - \frac{1}{2}l\pi + \delta_i) & \text{for } kr \gg l, \end{cases}$$

$$(2.30) \quad \psi_i(r, k) \cong \cos(kr - \frac{1}{2}l\pi + \delta_i) \quad \text{for } kr \gg l.$$

In terms of these, we have

$$(2.31) \quad \begin{cases} u_i(r, ik) = 2i \exp[i(\frac{1}{2}l\pi - \delta_i)] \varphi_i(r, k) \\ u_i(r, -ik) = (u_i(r, ik))^* \end{cases} \quad k > 0$$

and

$$(2.32) \quad \begin{cases} v_i(r, ik) = \exp[-i(\frac{1}{2}l\pi - \delta_i)](\psi_i(r, k) - i\varphi_i(r, k)) & k > 0 \\ v_i(r, -ik) = (v_i(r, ik))^* . \end{cases}$$

Combining these results, we get the following expression for $G_i(r, r', t)$, (2.24):

$$(2.33) \quad G_i(r, r', t) = (2/\pi) \int_0^\infty \exp[-k^2 t] \varphi_i(r, k) \varphi_i(r', k) + \\ + \sum_i \exp[-\beta \epsilon_{ii}^{-1}] \psi_{ii}(r) \psi_{ii}(r') .$$

We now have a complete solution for the density matrix of our two-particle system, given by (2.2), (2.3), (2.12), and (2.33). In practice, of course, this solution can be used only in conjunction with a fast electronic computer. However, we shall develop approximation methods of various sorts, and we shall discuss the general behaviour of the solution in the limit of low temperatures. In the following paper we shall establish the connection with the calculation of the second virial coefficient.

Before proceeding, we indicate the changes necessary if the two particles are identical particles rather than distinguishable particles. Apart from the obvious $m_1 = m_2$, $\mu = \frac{1}{2}m_1$, we must take into account the statistics of the particles. The matrix element (2.2) involves the operator $\exp[-\beta H]$ acting on the unsymmetrized base function $\delta(\mathbf{r}_1 - \mathbf{r}') \delta(\mathbf{r}_2 - \mathbf{r}_2')$. We must now use base functions of proper symmetry, i.e., symmetric for Bose-Einstein statistics, anti-symmetric for Fermi-Dirac statistics. The normalized base functions are

$$2^{-\frac{1}{2}}(\delta(\mathbf{r}_1 - \mathbf{r}_1') \delta(\mathbf{r}_2 - \mathbf{r}_2') \pm \delta(\mathbf{r}_1 - \mathbf{r}_2') \delta(\mathbf{r}_2 - \mathbf{r}_1')) .$$

Using the fact that the Hamiltonian, and hence also the operator $\exp[-\beta H]$, is invariant under the exchange of the two particles, we get the following expression for the density matrix of a system of two identical particles:

$$(2.34) \quad \langle (\mathbf{r}_1 \mathbf{r}_2) | \exp[-\beta H] | (\mathbf{r}_1' \mathbf{r}_2') \rangle = \langle \mathbf{r}_1 \mathbf{r}_2 | \exp[-\beta H] | \mathbf{r}_1' \mathbf{r}_2' \rangle \pm \\ \pm \langle \mathbf{r}_1 \mathbf{r}_2 | \exp[-\beta H] | \mathbf{r}_2' \mathbf{r}_1' \rangle .$$

When we separate out the centre-of-gravity motion and use (2.12), we find that the effect of the quantum statistics is to restrict the sum over l to even values of l for Bose-Einstein statistics, odd values of l for Fermi-Dirac statistics. The two terms of (2.34) contribute equal amounts to those values of l which are retained in the sum (2.12).

3. -- Born Approximation to the Density Matrix.

Under certain conditions, namely if the influence of the forces between the particles are relatively unimportant, it possible to get an approximate form for the density matrix by expanding in powers of the potential. In this case it is easiest to proceed directly from the partial differential equation (2.11) for $G(\mathbf{r}, \mathbf{r}', t)$, rather than decomposing G into a sum over angular momenta l . We write

$$(3.1) \quad G(\mathbf{r}, \mathbf{r}', t) = G_0(\mathbf{r}, \mathbf{r}', t) + G_1(\mathbf{r}, \mathbf{r}', t) + \dots$$

where G_0 , (2.7), is the density matrix for the relative motion in the absence of interactions, and G_1 is linear in the potential. By equating terms of the same power of W in equation (2.11), we get the following equation for G_1 :

$$(3.2) \quad \partial G_1 / \partial t - \nabla^2 G_1 = -W(\mathbf{r}) G_0(\mathbf{r}, \mathbf{r}', t).$$

From its definition, $G_0(\mathbf{r}, \mathbf{r}', t)$ is the Green's function for the operator on the left side of (3.2), and we therefore have the immediate solution

$$(3.3) \quad G_1(\mathbf{r}, \mathbf{r}', t) = - \int_0^t dt' \int d^3 r'' G_0(\mathbf{r}, \mathbf{r}'', t') W(\mathbf{r}'') G_0(\mathbf{r}'', \mathbf{r}', t - t').$$

Since the «time» t occurs only in the known functions G_0 , the integration over t' can be performed once and for all. The easiest method consists in making a Laplace transform on t , and using the fact that the integral over t' is a convolution integral, for which the Laplace transform is simply the product of the original Laplace transforms; the inversion of the Laplace transform so obtained is trivial. The result is

$$(3.4) \quad G_1(\mathbf{r}, \mathbf{r}', t) = - \int d^3 r'' K(|\mathbf{r} - \mathbf{r}''|, |\mathbf{r}' - \mathbf{r}''|, t) W(\mathbf{r}''),$$

where

$$(3.5) \quad K(x, x', t) = \frac{x + x'}{(4\pi)^{3/2} t^{3/2} x x'} \exp \left[- \frac{(x + x')^2}{4t} \right].$$

One special case of interest is t very small, i.e., β very small or very high temperatures. In that case the Gaussian in (3.5) is very sharp, so that K_1 is practically zero unless $|\mathbf{r} - \mathbf{r}''| + |\mathbf{r}' - \mathbf{r}''| \cong 0$, i.e., unless $\mathbf{r} \cong \mathbf{r}' \cong \mathbf{r}''$. We can take $W(\mathbf{r}'') \cong W(\mathbf{r})$ outside the integral, and perform the integration

over \mathbf{r}'' ; this is done most easily by noticing that, for $W(\mathbf{r}'') = 1$, the integral (3.3) becomes equal to

$$(3.6) \quad G_0(\mathbf{r}, \mathbf{r}', t) \int_0^t dt' = t G_0(\mathbf{r}, \mathbf{r}', t).$$

We therefore get the following Born approximation expression for the density matrix at high temperatures

$$(3.7) \quad \begin{aligned} G(\mathbf{r}, \mathbf{r}', t) &= G_0(\mathbf{r}, \mathbf{r}', t) - t W G_0(\mathbf{r}, \mathbf{r}', t) + \dots \\ &= G_0(\mathbf{r}, \mathbf{r}', t) (1 - \beta V(\mathbf{r}) + \dots). \end{aligned}$$

It is easily recognized that this represents the first two terms in an expansion (in powers of the potential) of the « semi-classical » result

$$G(\mathbf{r}, \mathbf{r}', t) \cong \exp[-\beta V(\mathbf{r})] G_0(\mathbf{r}, \mathbf{r}', t).$$

Actually, this form as well as (3.7) violate a symmetry relation, according to which $G(\mathbf{r}, \mathbf{r}', t)$ must be symmetric in \mathbf{r} and \mathbf{r}' . The lack of symmetry arises because, when we took $W(\mathbf{r}'')$ outside the integral (3.4), we replaced \mathbf{r}'' by \mathbf{r} whereas we might just as well have replaced it by \mathbf{r}' . A reasonable compromise is therefore given by the following approximate form, valid at high enough temperatures:

$$(3.8) \quad G(\mathbf{r}, \mathbf{r}', t) \cong \exp[-\tfrac{1}{2}\beta(V(\mathbf{r}) + V(\mathbf{r}'))] G_0(\mathbf{r}, \mathbf{r}', t).$$

This approximation is good provided that $V(\mathbf{r})$ changes slowly over dimensions of the order of $t^{\frac{1}{2}}$. Once we get to low enough temperatures so that $t^{\frac{1}{2}}$ becomes of the order of magnitude of the range of the potential, the « smearing » of the potential implied by (3.4) must not be ignored.

In one respect (3.8) is much better than the Born approximation (3.4), at all temperatures: if the potential contains a repulsive core of great strength, the integral (3.1) gets a spuriously large contribution from the region of the core, whereas (3.8) becomes very small automatically whenever \mathbf{r} or \mathbf{r}' (or both) fall within the repulsive core. In the limiting case of an infinitely high repulsive core, (3.4) breaks down altogether whereas (3.8) gives at least qualitatively the right answer.

We now turn to the (for us more interesting) behaviour at extremely low temperatures. At first sight one might be tempted to conclude that the Born approximation fails completely in that region, by using the following argument: the approximation (3.1) is obtained by expanding the density matrix G in powers of the strength of the potential V , and retaining only the linear term.

This operation commutes with the operation of decomposing $G(\mathbf{r}, \mathbf{r}', t)$ into contributions from different angular momenta l , as was done to get (2.33). Hence (3.4) and (3.5) could also have been obtained by using the first Born approximation for the radial wave functions which appear in (2.33), and then performing the sum over l by means of standard identities for Bessel functions⁽⁷⁾. But it is clear from the integral in (2.33) that the main contributing region of wave numbers k is of the general order of $t^{-\frac{1}{2}}$, and hence shifts closer and closer to zero as the «time» t increases, i.e., as the temperature T approaches zero. The Born approximation is well-known to become invalid in the limit of zero energy, at least for $l = 0$. Hence we might try to conclude that (3.4) is of no use at very low temperatures.

The above argument is quite valid if we keep \mathbf{r} and \mathbf{r}' fixed while t increases indefinitely. However, another limiting process is possible, and is of considerable interest. Let us increase both \mathbf{r} and \mathbf{r}' as t increases, such that \mathbf{r} and \mathbf{r}' are always much larger than $t^{\frac{1}{2}}$. In that case the Gaussian factor in (3.5) is always very small, and hence the correction term $G_1(\mathbf{r}, \mathbf{r}', t)$, (3.4), is always small compared to $G_0(\mathbf{r}, \mathbf{r}', t)$. It is therefore at least plausible that the density matrix should be essentially equal to its «free» value, $G_0(\mathbf{r}, \mathbf{r}', t)$, in this region, no matter how large t is.

This is plausible physically as well: according to (3.4) and (3.5), the effect of the potential is «smeared» over distances of the order of $t^{\frac{1}{2}}$. Let b denote the «range» of the potential $V(r)$. Now consider values of \mathbf{r} and \mathbf{r}' such that

$$(3.9) \quad |\mathbf{r}| \gg b + t^{\frac{1}{2}}, \quad |\mathbf{r}'| \gg b + t^{\frac{1}{2}}.$$

For such values, the effect of the potential should not be felt at all, since insufficient «time» has elapsed for the effect of the potential to «diffuse» into the region of \mathbf{r} and \mathbf{r}' defined by (2.9). This argument is quite independent of the detailed validity of the Born approximation in the «interior» region, since the «heat flow» equation (2.11) was used in the «exterior» region only, where it reduces to the ordinary equation for heat conduction⁽⁸⁾.

However, there is one exception to this rule, which will be important later on. Consider the case $\mathbf{r}' = -\mathbf{r}$; then the Gaussian factor which appears in (3.4) and (3.5) is equal to $\exp[-r^2/t]$, and this is identical with the Gaussian factor $\exp[-(r-r')^2/4t]$ which appears in $G_0(\mathbf{r}, \mathbf{r}', t)$, for this case. Thus, although the «correction» term G_1 still goes down very rapidly, the function G_0 against which it must be compared decreases equally rapidly. To get a qualitative insight into what happens, consider the case $t^{\frac{1}{2}} \gg b$, i.e., the statistical «smearing» distance is much larger than the range of the force. We can then approximate the integral (3.4) by setting $\mathbf{r}'' = 0$ in the kernel K . This gives

(7) G. N. WATSON: *Bessel Functions* (Cambridge, 1948), see p. 366.

(8) H. S. CARSLAW: *Conduction of Heat in Solids* (New York, 1945).

the approximate result

$$(3.10) \quad G_1(\mathbf{r}, \mathbf{r}', t) \cong -K(r, r', t) \int d^3r'' W(\mathbf{r}'') = 4\pi f(0)K(r, r', t),$$

where $f(0)$ is the quantum mechanical amplitude of the scattered wave in the forward direction, $\theta = 0$, as calculated in the Born approximation. In the special case $\mathbf{r}' = -\mathbf{r}$ we therefore get

$$(3.11) \quad G_0(\mathbf{r}, -\mathbf{r}, t) + G_1(\mathbf{r}, -\mathbf{r}, t) + \dots = \\ = (4\pi t)^{-\frac{1}{2}} \exp[-r^2/t] \left(1 + \frac{2f(0)}{r} + \dots \right).$$

Thus the correction term is of relative order $f(0)/r$, rather than dropping off with r like a Gaussian.

This behaviour can be understood very simply in terms of our heat flow analogy. The density matrix $G(\mathbf{r}, \mathbf{r}', t)$ is the Green's function for the heat flow equation (2.11); a delta-function «heat pulse» is produced at the point \mathbf{r}' at «time» $t = 0$, and $G(\mathbf{r}, \mathbf{r}', t)$ then gives the «temperature» at position \mathbf{r} and «time» t ⁽⁹⁾. If \mathbf{r} and \mathbf{r}' are in arbitrary directions, the straight flow joining them does not pass through the origin: hence, as we increase the scale of \mathbf{r} and \mathbf{r}' jointly, the straight line connecting them moves farther and farther away from the region in which the potential acts. Since the heat pulse travels in a straight line, to a first approximation, the effect of the heat pulse is propagated according to the simple heat flow equation, i.e. $G(\mathbf{r}, \mathbf{r}', t)$ becomes asymptotically equal to $G_0(\mathbf{r}, \mathbf{r}', t)$. However, in the special case $\mathbf{r}' = -\mathbf{r}$, the straight line joining the two points passes through the origin, and hence the flow of heat is disturbed by the presence of the potential, no matter how large we make $|\mathbf{r}|$ and $|\mathbf{r}'|$. Since the potential «scatters» the heat pulse in all directions, but only the forward direction counts, the factor $f(0)/r$ becomes plausible as well. Indeed, it is possible that (3.11) is somewhat more accurate than the Born approximation on which it has been based so far; i.e., it may make sense to compute $f(0)$ by some method more accurate than the Born approximation (e.g., as a series over phase shifts), and substitute the result into (3.11). We need not follow this up for our present purpose.

We must still discuss the influence of the bound state terms in (2.33). Of course, the Born approximation does not yield bound states at all. But we now ask whether bound states, if they do occur, change the conditions under which the density matrix becomes essentially equal to the «free» density

⁽⁹⁾ We recall that this is purely an analogy; the «time» t is really $\hbar^2\beta/2\mu = \hbar^2/2\mu kT$, and the «temperature» for this heat flow equation has nothing to do with the actual physical temperature T , which determines the «time».

matrix $G_0(\mathbf{r}, \mathbf{r}', t)$. We shall see that they indeed do so. Let us assume that both r and r' are large enough so that the wave function of the bound state, $\psi_{ii}(r)$, already has its asymptotic form

$$(3.12) \quad \psi_{ii}(r) = N \exp[-\sigma r].$$

The normalization factor N depends upon the details of the wave function. We can find an order of magnitude estimate for N by assuming that the asymptotic form (3.12) is valid all the way in to $r = 0$. This gives

$$(3.13) \quad N \cong (2\sigma)^{-\frac{1}{2}}.$$

The contribution (2.28) of the bound state reduces to $N^2 \exp[\sigma^2 t - \sigma r - \sigma r']$. Using the estimate (3.13), combining with (2.21), and assuming $l = 0$ for simplicity, we get the following approximate value for the contribution of the bound state to the density matrix:

$$(3.14) \quad (4\pi r r')^{-1} N^2 \exp[\sigma^2 t - \sigma r - \sigma r'] \cong (8\pi \sigma r r')^{-1} \exp[\sigma^2 t - \sigma r - \sigma r'].$$

We want this to be small compared to the «free» density matrix $G_0(\mathbf{r}, \mathbf{r}', t)$; since the exponentials are by far the most rapidly varying factors, the condition becomes

$$(3.15) \quad \exp[\sigma^2 t - \sigma r - \sigma r'] \ll \exp\left[-\frac{(\mathbf{r} - \mathbf{r}')^2}{4t}\right],$$

or

$$(3.15a) \quad \sigma^2 t - \sigma(r + r') \ll -\frac{(\mathbf{r} - \mathbf{r}')^2}{4t}.$$

In the special case $\mathbf{r} = \mathbf{r}'$ the condition becomes

$$(3.16) \quad r \gg \frac{1}{2}\sigma t.$$

This condition differs from (3.9); it is less stringent for small t , more stringent for large t ; it can always be fulfilled, however, by choosing r large enough.

The situation is quite different for $\mathbf{r} = -\mathbf{r}'$; condition (3.15a) then reduces to

$$\sigma^2 t - 2\sigma r + r^2/t = (\sigma t^{\frac{1}{2}} - r t^{-\frac{1}{2}})^2 \ll 0$$

and this can obviously not be fulfilled. Thus for $\mathbf{r}' = -\mathbf{r}$ the asymptotic behaviour of the density matrix $G(r, r', t)$ is determined by the bound states; it reduces to the «free» density matrix plus correction terms, equation (3.11), only in the absence of bound states.

4. A Low-Temperature Expansion for the Density Matrix.

We shall now obtain an expansion for the density matrix $G(\mathbf{r}, \mathbf{r}', t)$ which is useful in the low-temperature region. The «time» t , (2.9), is dimensionally the square of a length. The length in question is the reduced de Broglie wave length of the relative motion of the two particles, if the energy of relative motion is equal to $\beta^{-1} = kT$ ⁽¹⁰⁾. The parameters defining the convergence of the expansion we shall now derive are the ratios $r/t^{\frac{1}{2}}$ and $r'/t^{\frac{1}{2}}$, both of which must be small compared to 1. Thus this expansion complements the results of Sect. 3, which apply when $r/t^{\frac{1}{2}}$ and $r'/t^{\frac{1}{2}}$ are large compared to 1.

At liquid helium temperatures, and with masses m_1, m_2 equal to the mass of a helium atom, the length $t^{\frac{1}{2}}$ is roughly $2.5 \cdot 10^{-8}$ cm which is about equal to the range of the *repulsive* force. Hence it is necessary to go to much lower temperatures, of the order of 0.1 K, before the expansion derived below becomes useful quantitatively. However, it is instructive qualitatively, and will be used in the next section in conjunction with a variational principle for the density matrix.

We start from equation (2.33) and ignore the bound state contributions for the moment. The radial wave functions $\varphi_l(r, k)$ can be expanded in power series in k , with coefficients which are functions of r only, as follows:

$$(4.1) \quad \varphi_l(r, k) = k^{l+1}(\varphi_{l0}(r) + k^2\varphi_{l1}(r) + k^4\varphi_{l2}(r) + \dots).$$

When we substitute this expansion into the integral in (2.33), we get integrals of the form

$$(4.2) \quad (2/\pi) \int_0^\infty \exp[-k^2 t] k^{2N} dk = (4\pi t^3)^{-\frac{1}{2}} \frac{(2N-1)!!}{(2t)^{N+1}},$$

where the «double factorial» is defined by

$$(4.3) \quad (2N-1)!! = 1 \cdot 3 \cdot 5 \cdot \dots \cdot (2N-1).$$

The result, ignoring bound state terms, is

$$(4.4) \quad G_l(r, r', t) = (4\pi t^3)^{-\frac{1}{2}} \sum_{N=0}^{\infty} \frac{(2l+2N+1)!!}{(2t)^{l+N}} \sum_{n+n'=N} \varphi_{ln}(r) \varphi_{ln'}(r').$$

⁽¹⁰⁾ Unfortunately the quantity of the dimension of a length commonly employed in the literature [see reference ⁽¹⁾] is not $t^{\frac{1}{2}}$, but rather $\lambda = (2\pi t)^{\frac{1}{2}}$. We have found, consistently, that the extra factor $(2\pi)^{\frac{1}{2}}$ in the conventional definition is misleading, the true «smearing distance» being $t^{\frac{1}{2}}$ rather than the conventional λ . In view of the fact that $t^{\frac{1}{2}}$ has a rather slow temperature dependence, this extra factor $(2\pi)^{\frac{1}{2}}$ represents a change of a factor 6 in the temperature at which certain estimates become valid.

We substitute this into (2.12) to get

$$(4.5) \quad G(\mathbf{r}, \mathbf{r}', t) = (4\pi t)^{-\frac{3}{2}} \sum_{M=0}^{\infty} \frac{(2M+1)!!}{(2t)^M} S_M(\mathbf{r}, \mathbf{r}'),$$

where

$$(4.6) \quad S_M(\mathbf{r}, \mathbf{r}') = \frac{4\pi}{rr'} \sum_{l+n+n'=M} \varphi_{ln}(r) \varphi_{ln'}(r) Y_{l0}(0) Y_{n0}(\vartheta),$$

ϑ being the angle between the vectors \mathbf{r} and \mathbf{r}' .

We are particularly interested in the leading term of this expansion, i.e., the term $M=0$, and hence $l=n=n'=0$ in (4.6). This term gives the approximate result

$$(4.7) \quad G(\mathbf{r}, \mathbf{r}', t) \cong (4\pi t)^{-\frac{3}{2}} \frac{\varphi_{00}(r) \varphi_{00}(r')}{rr'},$$

which is valid in the absence of bound states under the condition $r/t^{\frac{1}{2}} \ll 1$ and $r'/t^{\frac{1}{2}} \ll 1$.

The function $\varphi_{00}(r)$ is the radial wave function for S -wave scattering in the limit of zero kinetic energy of relative motion. This function is well known in scattering theory⁽¹¹⁾; its asymptotic form for r larger than the range of the potential b is

$$(4.8) \quad \varphi_{00}(r) = r - a \quad \text{for } r > b,$$

where a is the «scattering length». Substituting this into (4.7) we get

$$(4.9) \quad G(\mathbf{r}, \mathbf{r}', t) = (4\pi t)^{-\frac{3}{2}} \left(1 - \frac{a}{r}\right) \left(1 - \frac{a}{r'}\right) \quad \text{for } b < r \ll t^{\frac{1}{2}}, \quad b < r' \ll t^{\frac{1}{2}}.$$

For $r \ll t^{\frac{1}{2}}$ and $r' \ll t^{\frac{1}{2}}$, the «free» density matrix $G_0(\mathbf{r}, \mathbf{r}', t)$ is approximately equal to $(4\pi t)^{-\frac{3}{2}}$. We therefore get the following result in the absence of bound states:

$$(4.10) \quad \lim_{t \rightarrow \infty} \frac{G(\mathbf{r}, \mathbf{r}', t)}{G_0(\mathbf{r}, \mathbf{r}', t)} = \frac{\varphi_{00}(r) \varphi_{00}(r')}{rr'}.$$

That is, the effect of the potential, in the limit of zero temperature T , or infinite «time» t , is to multiply the density matrix by a *temperature-independent* factor. This contrasts sharply with the behaviour of the semi-classical approx-

⁽¹¹⁾ J. M. BLATT and V. F. WEISSKOPF: *Theoretical Nuclear Physics* (New York, 1952); see chapter II and the references quoted there.

imation (3.8), in which the ratio (4.10) is an exponential function which becomes *infinite* for values of r and r' at which the potential V is attractive. Thus, in the absence of bound states, the quantum mechanical «smearing» is so effective that the infinitely high classical peak reduces to the mild, finite peak (4.10). It should be noted that (4.10) is correct in the limit $t \rightarrow \infty$, r and r' fixed. For finite but large t , r and r' must be less than $t^{\frac{1}{2}}$ in order that (4.10) be a good approximation. Thus the approach to the limit (4.10) is not uniform in the variables r and r' .

We remark that in the special case $\mathbf{r}' = -\mathbf{r}$ (4.10) joins smoothly on to the «exterior region» result (3.11); this can be seen from the fact that ⁽¹¹⁾

$$(4.11) \quad \lim_{k \rightarrow 0} f(\theta) = -a.$$

On the other hand, for $\mathbf{r}' = \mathbf{r}$ the ratio G/G_0 approaches unity in the exterior region much faster than (4.10) would indicate, so that (4.10) does not join smoothly onto the result for the exterior region.

So far we have assumed that there are no bound states of the two-particle system. According to (2.33) the bound states, if any, contribute factors with exponential temperature dependence, which dominate the density matrix in the extreme low temperature limit. Of all the bound states, the one with the highest binding energy eventually dominates. This is normally an S -state; let its energy be $\epsilon_0^{(-)}$, the superscript serving as a reminder that this is a negative quantity. Then in the limit of very large t , we get from (2.12) and (2.33)

$$(4.12) \quad G(\mathbf{r}, \mathbf{r}', t) \cong \frac{\psi_0(r)\psi_0(r')}{4\pi r r'} \exp[-\beta \epsilon_0^{(-)}],$$

instead of (4.7). Thus, in the presence of bound states, the density matrix does have an exponential temperature dependence at extremely low temperatures, but the exponent is independent of r and r' , the dependence on r and r' arising through the wave functions which appear as multipliers of the exponential. This must be compared with the classical $\exp[-\beta V(r)]$ where the r -dependence is in the exponent.

5. - Variation Principle for the Density Matrix.

We return to the fundamental differential equation (2.11) for $G(\mathbf{r}, \mathbf{r}', t)$. If we define G to be zero when t is negative, we can rewrite this differential equation in the form

$$(5.1) \quad (\partial/\partial t - \nabla_r^2 + W(r)) G(\mathbf{r}, \mathbf{r}', t) = \delta(\mathbf{r} - \mathbf{r}') \delta(t).$$

Let us define the more general function $K(\mathbf{r}, \mathbf{r}', t, t')$ by

$$(5.2) \quad K(\mathbf{r}, \mathbf{r}', t, t') = G(\mathbf{r}, \mathbf{r}', t - t')$$

and the linear but non-Hermitean operator \mathcal{A} by

$$(5.3) \quad \mathcal{A} = \partial/\partial t - \nabla_{\mathbf{r}}^2 + W(\mathbf{r}).$$

If we then consider K as the kernel of a linear operator \mathcal{K} , we see that (5.1) becomes the operator relation

$$(5.4) \quad \mathcal{A}\mathcal{K} = \mathbf{1},$$

where $\mathbf{1}$ is the unit operator, with kernel

$$(5.5) \quad \langle \mathbf{r}, t | \mathbf{1} | \mathbf{r}', t' \rangle = \delta(\mathbf{r} - \mathbf{r}') \delta(t - t').$$

We are now in a position to use the Friedman variation principle⁽¹²⁾ for the inverse of an operator. This reads, in our case, as follows:

$$(5.6) \quad \langle \mathbf{r}, t | \mathcal{K} | \mathbf{r}', t' \rangle = \frac{\langle \mathbf{r}, t | \mathcal{K} | \mathbf{r}', t' \rangle^2}{\langle \mathbf{r}, t | \mathcal{K} \mathcal{A} \mathcal{K} | \mathbf{r}', t' \rangle}.$$

If \mathcal{K} on the right hand side of the equation is the exact inverse operator to \mathcal{A} , then (5.6) is an identity. Putting a trial operator for \mathcal{K} into the expression on the right hand side of (5.6), we get an improved value for the matrix elements of \mathcal{K} , this value being variationally correct.

Returning now to the function $G(\mathbf{r}, \mathbf{r}', t)$ by means of (5.2), (5.6) becomes

$$(5.7) \quad G(\mathbf{r}, \mathbf{r}', t) = \frac{(G(\mathbf{r}, \mathbf{r}', t))^2}{\int_0^t dt'' \int d^3r'' G(\mathbf{r}, \mathbf{r}'', t - t'') (\partial/\partial t'' - \nabla_{\mathbf{r}''}^2 + W(\mathbf{r}'')) G(\mathbf{r}'', \mathbf{r}', t'') }.$$

As a first approximation, we may insert as trial function the density matrix $G_0(\mathbf{r}, \mathbf{r}', t)$, (2.7), in the absence of a potential. (5.7) then reduces to

$$(5.8) \quad G(\mathbf{r}, \mathbf{r}', t) \cong \frac{(G_0(\mathbf{r}, \mathbf{r}', t))^2}{G_0(\mathbf{r}, \mathbf{r}', t) - G_1(\mathbf{r}, \mathbf{r}', t)},$$

(12) F. L. FRIEDMAN: *M.I.T. thesis* (unpublished); the proof is reproduced in a paper on shower theory, M. H. KALOS and J. M. BLATT: *Austr. Journ. of Phys.*, **7**, 543 (1954), see Appendix III of that paper.

where G_1 is the Born approximation correction to G_0 , defined by (3.4) and (3.5). If we assume that G_1 is much smaller than G_0 , and expand the denominator of (5.8), we get the Born approximation (3.1). However, since (5.8) was derived variationally, it is generally a better approximation than (3.1), and takes no more work to compute. For example, a large repulsive potential will make (3.1) negative within its range, whereas (5.8) stays positive but becomes very small, as it should. However, even (5.8) breaks down for an infinite repulsive core.

A better approximation in the intermediate temperature region could presumably be obtained by inserting the approximation (3.8) as a trial function on the right hand side of (5.7). However, the integrations become difficult, and we shall not pursue this subject farther.

Of much more interest to us is an approximation valid in the extremely low temperature region. To do this, we construct a trial function by the use of (4.10). That is, our trial function is

$$(5.9) \quad G_{\text{trial}}(\mathbf{r}, \mathbf{r}', t) = R_0(r) R_0(r') G_0(\mathbf{r}, \mathbf{r}', t),$$

where

$$(5.10) \quad R_0(r) = r^{-1} \varphi_{00}(r).$$

In other words, $R_0(r)$ is the actual radial wave function of the S -state at zero energy, rather than r times that wave function. From (4.8) we see that for large r , $R_0(r)$ is given by

$$(5.11) \quad R_0(r) = 1 - a/r \quad (\text{for large } r).$$

Thus our trial function (5.9) behaves correctly for $r, r' \ll t^{\frac{1}{2}}$, and also for very large r, r' . The trial function is of course quite wrong for small t (high temperatures) within the range of the potential.

In substituting (5.9) on the left side of (5.7), we can use the fact that $G_0(\mathbf{r}, \mathbf{r}', t)$ satisfies the equation

$$(5.12) \quad (-\nabla_r^2 + \partial/\partial t) G_0(\mathbf{r}, \mathbf{r}', t) = \delta(\mathbf{r} - \mathbf{r}') \delta(t)$$

and $R_0(r)$ satisfies the equation

$$(5.13) \quad (-\nabla_r^2 + W(r)) R_0(r) = 0.$$

The denominator of (5.7) then assumes the form

$$(5.14) \quad D = R_0(r) (R_0(r'))^3 G_0(\mathbf{r}, \mathbf{r}', t) - \\ - R_0(r) R_0(r') \int_0^t dt'' \int d^3r'' G_0(\mathbf{r}, \mathbf{r}'', t - t'') \nabla_{r''} R_0^2(r'') \cdot \nabla_{r''} G_0(\mathbf{r}'', \mathbf{r}', t'').$$

It is easy to show that a trial function symmetric in \mathbf{r} and \mathbf{r}' makes the denominator D of (5.7) a symmetric function of \mathbf{r} and \mathbf{r}' , the only additional proviso being that the trial function must vanish for negative values of the variable t (as we have assumed all along). Therefore we rewrite (5.14) in a way in which the symmetry between \mathbf{r} and \mathbf{r}' becomes manifest, namely

$$(5.15) \quad D = \frac{1}{2}D(\mathbf{r}, \mathbf{r}', t) + \frac{1}{2}D(\mathbf{r}', \mathbf{r}, t) = \frac{1}{2}(R_0^2(r) + R_0^2(r'))R_0(r)R_0(r')G_0(\mathbf{r}, \mathbf{r}', t) - \\ - \frac{1}{2}R_0(r)R_0(r') \int_0^t dt'' \int d^3r'' \nabla_{r''} R_0^2(r'') \cdot \nabla_{r''} [G_0(\mathbf{r}, \mathbf{r}'', t-t'')G_0(\mathbf{r}'', \mathbf{r}', t'')].$$

The integration over t'' can be done explicitly, and leads to the function K defined by (3.4) and (3.5). Furthermore, it is advantageous to take out a common factor $R_0(r)R_0(r')G_0(\mathbf{r}, \mathbf{r}', t)$, since this is just the trial function and hence cancels against one of the factors in the numerator of (5.7). We therefore define the kernel M by

$$(5.16a) \quad M(\mathbf{r} - \mathbf{r}'', \mathbf{r}' - \mathbf{r}'', t) = \frac{K(|\mathbf{r} - \mathbf{r}''|, |\mathbf{r}' - \mathbf{r}''|, t)}{G_0(\mathbf{r}, \mathbf{r}', t)},$$

$$(5.16b) \quad M(\mathbf{s}, \mathbf{s}', t) = \left(\frac{1}{4\pi|\mathbf{s}|} + \frac{1}{4\pi|\mathbf{s}'|} \right) \exp \left[\frac{(\mathbf{s} - \mathbf{s}')^2 - (|\mathbf{s}| + |\mathbf{s}'|)^2}{4t} \right],$$

and get the following result for the iterated density matrix:

$$(5.17) \quad G_{\text{iterated}} = G_{\text{trial}}/F,$$

where

$$(5.18) \quad F(\mathbf{r}, \mathbf{r}', t) = \frac{1}{2}(R_0^2(r) + R_0^2(r')) - \frac{1}{2} \int d^3r'' \nabla_{r''} R_0^2(r'') \cdot \\ \cdot \nabla_{r''} M(\mathbf{r} - \mathbf{r}'', \mathbf{r}' - \mathbf{r}'', t).$$

We now transform this expression for F in such a way that it becomes apparent that F approaches unity for $r, r' \ll t^{\frac{1}{2}}$, as of course it must according to (4.10), (5.9), and (5.17). The kernel M has singular points at $\mathbf{r}'' = \mathbf{r}$ and $\mathbf{r}'' = \mathbf{r}'$. We therefore write it in such a way that the singularity appears explicitly:

$$(5.19a) \quad M(\mathbf{s}, \mathbf{s}', t) = (4\pi|\mathbf{s}|)^{-1} + (4\pi|\mathbf{s}'|)^{-1} - M_1(\mathbf{s}, \mathbf{s}', t),$$

$$(5.19b) \quad M_1(\mathbf{s}, \mathbf{s}', t) = \left(\frac{1}{4\pi|\mathbf{s}|} + \frac{1}{4\pi|\mathbf{s}'|} \right) \left(1 - \exp \left[\frac{(\mathbf{s} - \mathbf{s}')^2 - (|\mathbf{s}| + |\mathbf{s}'|)^2}{4t} \right] \right).$$

The part of the integral not involving the regular kernel M_1 can be done immediately. We integrate by parts, and get contributions from surface integrals at infinity and around the points $\mathbf{r}'' = \mathbf{r}$ and $\mathbf{r}'' = \mathbf{r}'$. The surface integral at infinity gives 1, since $R_0(r)$ approaches 1 for large r . The surface integrals around the excluded points give a result which cancels exactly the first term on the right hand side of (5.18). We therefore get a transformed expression for F :

$$(5.20) \quad F(\mathbf{r}, \mathbf{r}', t) = 1 + \frac{1}{2} \int d^3r'' \nabla_{r''} R_0^2(r'') \cdot \nabla_{r''} M_1(\mathbf{r} - \mathbf{r}'', \mathbf{r}' - \mathbf{r}'', t).$$

We now integrate by parts once more. In order to avoid getting contributions from the surface at infinity, we replace $R_0^2(r'')$ by $R_0^2(r'') - 1$, which vanishes at infinity; this replacement obviously does not change the integral in (5.20), but has the result that the surface at infinity does not contribute in the integration by parts. There is no need to exclude little spheres around the points $\mathbf{r}'' = \mathbf{r}$ and $\mathbf{r}'' = \mathbf{r}'$, since the kernel M_1 is regular at those points, anyway. We therefore get our final result in the form

$$(5.21) \quad F(\mathbf{r}, \mathbf{r}', t) = 1 - \frac{1}{2} \int d^3r'' (R_0^2(r'') - 1) \nabla_{r''}^2 M_1(\mathbf{r} - \mathbf{r}'', \mathbf{r}' - \mathbf{r}'', t).$$

Although it is not obvious at this stage that the integral approaches zero as t approaches infinity (\mathbf{r} and \mathbf{r}' being kept fixed), we shall show that it does so for some special cases, later on. Equations (5.17) and (5.21) give a reasonable approximation to the exact density matrix $G(\mathbf{r}, \mathbf{r}', t)$ at very low temperatures (very high values of t).

6. — The q Function.

In the discussion of more complicated systems, BUTLER and FRIEDMAN⁽¹³⁾ found it expedient to write the density matrix as a product of two factors, one of which is the density matrix in the absence of interactions, the other indicating the modifications due to the interactions between the particles. In this section we shall be interested in the diagonal element of the density matrix, which we write in the form

$$(6.1) \quad \langle \mathbf{r}_1 \mathbf{r}_2 | \exp[-\beta H] | \mathbf{r}_1 \mathbf{r}_2 \rangle = \langle \mathbf{r}_1 \mathbf{r}_2 | \exp[-\beta H_0] | \mathbf{r}_1 \mathbf{r}_2 \rangle q(r_{12}, t)$$

where H_0 is the Hamiltonian in the absence of interactions between the part-

(13) S. T. BUTLER and M. H. FRIEDMAN: *Phys. Rev.*, **98**, 287 (1955).

icles, i.e., the kinetic energy only. Combining (2.2), (2.4), and (2.7), we get the following definition of the q function:

$$(6.2) \quad q(r, t) = \frac{G(\mathbf{r}, \mathbf{r}, t)}{G_0(\mathbf{r}, \mathbf{r}, t)} = (4\pi t)^{\frac{3}{2}} G(\mathbf{r}, \mathbf{r}, t).$$

Combining this with the general solution (2.12) and (2.33), we get an explicit expression for the q function:

$$(6.3) \quad q(r, t) = \frac{(4\pi t^{\frac{3}{2}})^{\frac{1}{2}}}{r^2} \sum_{l=0}^{\infty} (2l+1) \left(\frac{2}{\pi} \int_0^{\infty} \exp[-k^2 t] q_l^2(r, k) dk + \sum_i \exp[-\beta \varepsilon_{ii}^{(-)}] \psi_{ii}^2(r) \right).$$

In this form the q function can be computed directly with the help of a high speed digital machine, and we intend to do so as soon as the Sydney SILLIAC comes into operation. Meanwhile, however, in order to get a qualitative feeling for the behaviour of this function, we shall specialize the results obtained so far for the general density matrix $G(\mathbf{r}, \mathbf{r}', t)$ to this special case.

The Born approximation (3.1), (3.4), and (3.5) leads to the result

$$(6.4) \quad q(r, t) = 1 + \chi(r, t)$$

where $\chi(r, t)$ is given by

$$(6.5) \quad \chi(r, t) = - (2\pi)^{-1} \int \frac{\exp[-(\mathbf{r} - \mathbf{r}')^2/t]}{|\mathbf{r} - \mathbf{r}'|} W(\mathbf{r}') d^3 r'. \quad (\text{Born approx.})$$

The assumption of a central force, i.e. $W(\mathbf{r}')$ a function of $|\mathbf{r}'|$ only, allows us to perform the integration over angles explicitly. The result is

$$(6.6) \quad \chi(r, t) = - \int K_1(r, r', t) W(r') r'^2 dr',$$

where

$$(6.7) \quad K_1(r, r', t) = \frac{(\pi t)^{\frac{1}{2}}}{2rr'} \left(\operatorname{erf} \left(\frac{r+r'}{t^{\frac{1}{2}}} \right) - \operatorname{erf} \left(\frac{|r-r'|}{t^{\frac{1}{2}}} \right) \right),$$

$\operatorname{erf}(z)$ being the conventional error function⁽¹⁴⁾.

In the limit of very high temperatures (very small t) it follows from (3.7), and can also be shown directly from (6.6) and (6.7), that $\chi(r, t)$ approaches:

⁽¹⁴⁾ E. JAHNKE and F. EMDE: *Tables of Functions* (New York, 1943).

the form:

$$(6.8) \quad \chi(r, t) \cong -tW(r) = -\beta V(r) \quad (\text{small } t, \text{ Born approx.})$$

Hence in this limit (6.4) gives the Born approximation to the classical result

$$(6.9) \quad q(r, t) = \exp[-tW(r)] = \exp[-\beta V(r)] \quad (\text{classical}).$$

The arguments in Sect. 3 show that the q function approaches 1 rapidly for $r \gg t^{\frac{1}{2}}$ if there are no bound states; in the presence of bound states, the q function still approaches 1 for large r , but the region of validity is now given by two conditions, (3.9) and (3.16), the latter becoming more stringent at very low temperatures.

The low temperature expansion discussed in Sect. 4 gives the following result:

$$(6.10) \quad q(r, t) = \sum_{M=0}^{\infty} \frac{(2M+1)!!}{(2t)^M} S_M(\mathbf{r}, \mathbf{r}),$$

where

$$(6.11) \quad S_M(\mathbf{r}, \mathbf{r}) = r^{-2} \sum_{l=0, 2, 4, \dots, M} (2l+1) \varphi_{ln}(r) \varphi_{ln'}(r)$$

and in particular

$$(6.12) \quad \lim_{t \rightarrow \infty} q(r, t) = S_0(\mathbf{r}, \mathbf{r}) = (\varphi_{00}(r)/r)^2 = (R_0(r))^2.$$

This result, valid in the absence of bound states, shows first of all that the q function approaches a finite limiting form at very low temperatures, and secondly confirms the conjecture of FEYNMAN⁽¹⁵⁾ that this limiting form is given by the square of the wave function of the ground state of the system (in the case of no bound states, this means the S -state at zero energy; when there are bound states, their contributions must be added to the expansion (6.10); there are then terms exponential in t , with the leading term multiplied by the square of the ground state wave function).

It is easy to see, for example by considering the special case of a purely repulsive hard core interaction (no attraction outside) that the expansion (6.10) converges too slowly at liquid helium temperatures to be of much practical use, even for values of r just outside the core. The limiting form (6.12) is approached only at appreciably lower temperatures, less than 10^{-1} degrees Kelvin.

Going on to the results from the variation principle, Sect. 5, the improved

(15) R. P. FEYNMAN: *Phys. Rev.*, **91**, 1291 (1953).

Born approximation (5.8) leads to

$$(6.13) \quad g(r, t) = (1 - \chi(r, t))^{-1} \quad (\text{improved Born approx.})$$

where $\chi(r, t)$ is given by (6.6) and (6.7). (6.13) is a much better approximation than (6.4) if the potential has a strongly repulsive region; there (6.4) becomes negative whereas (6.13) stays positive but approaches zero, which is at least qualitatively the proper behaviour.

Of more interest to us is the variational result applicable at low temperatures, given by (5.9), (5.17), and (5.21). This gives for the q -function:

$$(6.14) \quad q(r, t) = \frac{(R_0(r))^2}{P(r, t)},$$

where

$$(6.15) \quad \begin{aligned} F(r, t) = F(\mathbf{r}, \mathbf{r}, t) &= 1 - \frac{1}{2} \int d^3r'' (R_0^2(r'') - 1) \nabla_{r''}^2 M_1(\mathbf{r} - \mathbf{r}'', \mathbf{r} - \mathbf{r}'', t) = \\ &= 1 - (2\pi t)^{-1} \int d^3r'' (R_0^2(r'') - 1) (1 - 2(\mathbf{r} - \mathbf{r}'')^2/t) \frac{\exp[-(\mathbf{r} - \mathbf{r}'')^2/t]}{r - r''}. \end{aligned}$$

The integrations over the solid angle can be performed explicitly, and yield

$$(6.16) \quad \begin{aligned} F(r, t) &= 1 + (tr)^{-1} \int_0^\infty dr' r' (R_0^2(r') - 1) (|r - r'| \exp[-(r - r')^2/t] - \\ &\quad - (r + r') \exp[-(r + r')^2/t]). \end{aligned}$$

This expression is suitable for direct evaluation by hand computing methods, if necessary. Since our main interest is in the qualitative behaviour of the q -function we shall investigate the behaviour of (6.16) for two extreme regions of r only, namely $r \gg t^{\frac{1}{2}}$ and $r \ll t^{\frac{1}{2}}$. For $r \gg t^{\frac{1}{2}}$, the main contribution to the integral comes from the region r' near r ; we assume also that $R_0(r')$ can be replaced by its asymptotic form, (5.11), valid outside the range of the potential. The term $\exp[-(r + r')^2/t]$ can be neglected compared to the other exponential, so we finally get (b = range of potential)

$$(6.17) \quad F(r, t) \cong 1 + (tr)^{-1} \int_b^\infty dr' (-2a + a^2/r') |r - r'| \exp[-(r - r')^2/t].$$

For the term $(-2a)$ we can replace the limits of integration by $-\infty$ to $+\infty$ within the limits of our approximation, and we then get $-2a/r$. We expand

the term a^2/r' in a power series in the variable $r - r'$, and keep the first two non-vanishing contributions. The result is

$$(6.18) \quad \begin{aligned} F(r, t) &\cong 1 - 2a/r + a^2/r^2 + a^2t/r^4 + \dots \\ &= R_0^2(r) + a^2t/r^4 \dots \end{aligned} \quad \text{for } r \gg t^{\frac{1}{2}}.$$

When we combine this with (6.14), we see that the iterated q function approaches 1 for $r \gg t^{\frac{1}{2}}$ much more rapidly than the trial function $R_0^2(r)$ did. Actually, the q function should approach 1 exponentially for $r \gg t^{\frac{1}{2}}$, but the variation principle has obviously produced a correction in the desired direction.

The discussion of the opposite limiting case, $r \ll t^{\frac{1}{2}}$, is much more involved and we shall give only the outline of the calculation. Starting from (6.16), we split the range of integration into two regions, $r' < r$ and $r' > r$. For $r' < r$, we expand the exponentials in power series, and keep only the leading term. The corresponding contribution is

$$(6.19a) \quad - (2/tr) \int_0^r r'^2 (R_0^2(r') - 1) dr'.$$

In the region $r' > r$, we write

$$(6.20) \quad R_0^2(r') - 1 = (R_0^2(r') - (1 - a/r')^2) - 2a/r' + (a/r')^2.$$

The difference in brackets vanishes outside the range of the potential. Hence, if this range b is much less than $t^{\frac{1}{2}}$ (as we shall assume henceforth), we can also expand the exponentials for this contribution, the leading term giving

$$(6.19b) \quad - (2/t) \int_r^\infty r' (R_0^2(r') - (1 - a/r')^2) dr'.$$

As regards the remainder of (6.20), we cannot expand the exponentials in (6.16), but must evaluate the integrals directly. The term $-2a/r'$ then leads to the contribution

$$(6.19c) \quad - (a/r)(1 - \exp[-4r^2/t]) \cong -4ar/t$$

whereas the term $+(a/r')^2$ leads to the result

$$(a^2/t) \left(\frac{1}{x_0} \int_0^{2x_0} \exp[-x^2] dx - \int_{-\infty}^{\infty} x^{-1} (\exp[-(x-x_0)^2] + \exp[-(x+x_0)^2]) dx \right),$$

where $x_0 = r/t^{1/2} \ll 1$. The first integral gives 2 as the leading contribution; in the second integral we write

$$\exp[-(x-x_0)^2] + \exp[-(x+x_0)^2] = 2 \exp[-x_0^2] \cosh(2x_0x) \exp[-x^2]$$

and expand in powers of x_0^2 , again keeping only the leading term. This leads to the integral

$$\int_{x_0}^{\infty} (2/x) \exp[-x^2] dx = -\text{Ei}(-x_0^2) = \ln(t/r^2) - C + \text{order}(r^2/t),$$

where $\text{Ei}(z)$ is the standard exponential integral⁽¹³⁾, and $C = 0.5772$, is Euler's constant. Thus, finally, the contribution from the term $(a/r')^2$ in (6.20) to the integral (6.16) is

$$(6.19d) \quad (a^2/t)(2 + C - \ln(t/r^2) + \text{order}(r^2/t)).$$

Combining the various contributions (6.19), we get our final result in the form

$$(6.21) \quad F(r, t) = 1 - \frac{a^2}{t} \ln\left(\frac{t}{r^2}\right) + \frac{v(r)}{t} + \text{order}(1/t^2), \quad [\text{for } r \ll t^{1/2}],$$

where

$$(6.22) \quad v(r) = (2 + C)a^2 - 4ar - 2 \int_r^{\infty} r'(R_0^2(r') - (1 - a/r')^2) dr' - \\ - (2/r) \int_0^r r'^2 (R_0^2(r') - 1) dr'.$$

This combined with (6.14) shows, as expected, that the q function approaches the value $R_0^2(r)$ in the limit of very large t . The logarithmic term in (6.12) is probably spurious, i.e., a result of the approximation used for the trial function (5.9); we believe that $F(r, t)$ should really allow a power series expansion in t^{-1} , at least for small r . The logarithmic divergence of $F(r, t)$ near $r = 0$ which seems to appear in (6.21) is actually cancelled by a similar logarithmic term arising from the first integral on the right of (6.22), so that $r = 0$ is a regular point of this expansion.

It should be noticed that terms of order a^2/t appear here where a is the scattering length. Higher order terms contain a^3/t^2 etc.; hence this expansion converges poorly if the scattering length is large in absolute value, i.e., if we are close to a scattering resonance at zero energy. Apparently this is the case

for the interaction between two helium atoms ^(3,16). This implies that the region of temperatures in which (6.21) and (6.22) represent a reasonable approximation for helium gas is even lower than the $T < 0.1$ K mentioned before, and is therefore of no interest from a practical point of view.

Since the difficulty arises as a result of the S -wave part of the density matrix (only this part shows the zero energy resonance) it should be possible to treat this part more directly. We have succeeded in doing so, by assuming a specific form for the potential, with 3 adjustable parameters (a core radius, and well depth and range of the attraction outside the core). However, the S -wave does not become really dominant until temperatures less than 0.1 °K are considered, and we therefore do not reproduce this rather lengthy calculation here.

We emphasize that, while the expansion (6.21) and (6.22) does not converge very well, this does not affect the usefulness of the general variational formula (6.16). Indeed, we believe that (6.14) and (6.16) give a reasonable approximation to the correct q function even in the liquid helium temperature range. We intend to check this numerically after the SILLIAC¹ comes into operation, by comparing this variational approximation with the exact result computed directly from equation (2.33).

Meanwhile, we recapitulate the salient properties of the q -function at low temperatures: in the absence of bound states, it approaches the square of the S -state radial wave function at zero energy for $r \ll t^{\frac{1}{2}}$, and approaches 1 very rapidly (exponentially) for $r \gg t^{\frac{1}{2}}$. Bound states contribute additional terms as shown in (6.3); these terms eventually dominate the q -function for small values of r , but for very large values of r (the condition is (3.16) now) the q -function still approaches unity.

7. - The q_p Function.

If the two particles in our system are identical particles, the density matrix is given by (2.34). The diagonal element of this matrix is

$$(7.1) \quad \langle (\mathbf{r}_1 \mathbf{r}_2) | \exp[-\beta H] | (\mathbf{r}_1 \mathbf{r}_2) \rangle = \langle \mathbf{r}_1 \mathbf{r}_2 | \exp[-\beta H] | \mathbf{r}_1 \mathbf{r}_2 \rangle \pm \\ \pm \langle \mathbf{r}_1 \mathbf{r}_2 | \exp[-\beta H] | \mathbf{r}_2 \mathbf{r}_1 \rangle$$

where the plus sign is used for Bose-Einstein statistics, the minus sign for Fermi-Dirac statistics. BUTLER and FEEDMAN ⁽¹³⁾ write the second term on

⁽¹⁶⁾ J. E. KILPATRICK, W. E. KELLER and E. F. HAMMEL: *Phys. Rev.*, **97**, 9 (1955).

the right side of (7.1) in the form

$$(7.2) \quad \langle \mathbf{r}_1 \mathbf{r}_2 | \exp[-\beta H] | \mathbf{r}_2 \mathbf{r}_1 \rangle = q_P(r_{12}, t) \langle \mathbf{r}_1 \mathbf{r}_2 | \exp[-\beta H_0] | \mathbf{r}_2 \mathbf{r}_1 \rangle$$

where the subscript « P » denotes the permutation in question (in our case the only permutation other than the identity is the interchange of the two particles), and H_0 is the unperturbed Hamiltonian (kinetic energy only). Combining (2.2), (2.4) and (2.7), we get the following definition of the q_P function:

$$(7.3) \quad q_P(r, t) = \frac{G(\mathbf{r}, -\mathbf{r}, t)}{G_0(\mathbf{r}, -\mathbf{r}, t)} = (4\pi t)^{\frac{3}{2}} \exp[r^2/t] G(\mathbf{r}, -\mathbf{r}, t).$$

Combining this with the general solution (2.12) and (2.33), we get an explicit expression for the q_P function:

$$(7.4) \quad q_P(r, t) = \frac{(4\pi t^3)^{\frac{1}{2}}}{r^2} \exp[r^2/t] \sum_{l=0}^{\infty} (-1)^l (2l+1) \cdot \left(\frac{2}{\pi} \int_0^{\infty} \exp[-k^2 t] q_l^2(r, k) dk + \sum_i \exp[-\beta \epsilon_i^{(-)}] \psi_{r_i}^2(r) \right).$$

Comparing with (6.3), we see that the difference between the q function and the q_P function is twofold: the alternating signs in the sum over l in (7.4), and the extra factor $\exp[r^2/t]$ in (7.4). At first sight, we might think that this Gaussian factor will dominate the q_P function for values of $r \gg t^{\frac{1}{2}}$. However, the discussion in Sect. 3, especially equation (3.11), has shown that in the absence of bound states this Gaussian factor is cancelled exactly, and indeed the Born approximation gives for large values of r , that is $r \gg t^{\frac{1}{2}}$,

$$(7.5) \quad q_P(r, t) = 1 + \frac{2f(0)}{r} + \dots \quad \text{for } r \gg t^{\frac{1}{2}}, \text{ no bound states,}$$

where $f(0)$ is the value of the quantum mechanical scattering amplitude, $f(\theta)$, in the forward direction, $\theta = 0$.

On the other hand, we have also shown in Sect. 3 that the presence of bound states changes the picture completely. The behaviour of the q_P function for large values of r is then determined by the factor $\exp[r^2/t]$ in (7.4), because the bound states have wave functions which decrease only exponentially, like $\exp[-\sigma r]$, for large values of r .

In their analysis, BUTLER and FRIEDMAN⁽¹³⁾ make the approximation

$$(7.6) \quad q_P(r, t) \cong q(r, t).$$

This approximation is reasonable, and expected to yield at least qualitatively correct results, if there are no bound states. If bound states do exist, however, the approximation (7.6) is qualitatively wrong and should not be used. The « tail » of the second term in (7.1) is then not Gaussian, $\exp[-r^2/t] = -\exp[-2\pi r^2/\lambda^2]$, but exponential, $\exp[-2\sigma r]$, with the coefficient in the exponent determined by the binding energy of the bound state⁽¹⁷⁾.

We now specialize the various approximation methods given earlier for the density matrix to the q_P function. The *Born approximation* is given by (3.1), (3.4), and (3.5); in combination with (7.3) we get

$$(7.7) \quad q_P(r, t) = 1 + \frac{G_1(\mathbf{r}, -\mathbf{r}, t)}{G_0(\mathbf{r}, -\mathbf{r}, t)} = 1 + \chi_P(r, t),$$

where

$$(7.8) \quad \chi_P(r, t) = - \int d^3r' \left(\frac{1}{4\pi|\mathbf{r}-\mathbf{r}'|} + \frac{1}{4\pi|\mathbf{r}+\mathbf{r}'|} \right) \cdot \exp \left[\frac{r^2}{t} - \frac{(|\mathbf{r}-\mathbf{r}'| + |\mathbf{r}+\mathbf{r}'|)^2}{4t} \right] W(r').$$

Since we assume a central force field, the angle integrations over \mathbf{r}' can be done once and for all. This is carried through in Appendix B. The result is

$$(7.9) \quad \chi_P(r, t) = - \int_0^\infty K_2(r, r', t) W(r') r'^2 dr',$$

where

$$(7.10) \quad K_2(r, r', t) = \frac{2t^{\frac{1}{2}}}{r r'} \exp \left[-\frac{r'^2}{t} \right] \int_0^{r < t^{\frac{1}{2}}} \exp[y^2] dy.$$

⁽¹⁷⁾ In this connection, we also mention that the approximation of replacing equation (22) by equation (23) in reference ⁽¹²⁾ is of insufficient accuracy quantitatively, although the qualitative conclusions drawn from that approximation are unaffected. Equation (23) of reference ⁽¹²⁾ is equivalent to the following approximation for the q function:

$$q(r, t) = \exp[-\beta H] \cdot 1.$$

In the limit of very large t , and no bound states, this gives

$$\lim_{t \rightarrow \infty} q(r, t) = R_0(r)$$

instead of the correct result (6.12). However, qualitatively these two functions behave, in the same way: zero inside a repulsive core, a maximum in the attractive region and a limiting value 1 for large r .

The lack of symmetry between r and r' in the kernel (7.10) is the result of the division by $G_0(\mathbf{r}, -\mathbf{r}, t)$ in the defining equation (7.7). $r_<$ is defined by (2.22).

In the low temperature limiting case of a force range $b \ll t^{\frac{1}{2}}$ and $r > b$, we can replace r by r' in the significant region for the integral (7.9), and we can replace K_2 by its limiting form for $r_< = r' \ll t^{\frac{1}{2}}$, namely $K_2(r, r', t) \cong 2/r$. This gives

$$(7.11) \quad \chi_P(r, t) \cong -2r^{-1} \int_0^\infty W(r') r'^2 dr' = + \frac{2f(0)}{r},$$

where $f(0)$ is the forward scattering amplitude in the Born approximation. Combination of (7.7) and (7.11) gives the result (7.5) which was derived more simply earlier.

The second limiting case of interest is the high temperature region, i.e. $r \gg t^{\frac{1}{2}}$ and force range b also much greater than $t^{\frac{1}{2}}$. It is easy to see that a good approximation for $\chi_P(r, t)$ is then given by

$$(7.12) \quad \chi_P(r, t) \cong - (t/r) \int_0^r W(r') dr'. \quad \text{for } r \gg t^{\frac{1}{2}}, b \gg t^{\frac{1}{2}}.$$

However, in any practical application this function is multiplied by the Gaussian factor $\exp[-r^2/t]$, which is by assumption very small. Thus the entire effect of the quantum statistics is small at high temperatures, which is of course a well known result.

We now turn to the low-temperature expansion discussed in Sect. 4. This gives the result

$$(7.13) \quad q_P(r, t) = \exp[r^2/t] \sum_{M=0}^{\infty} \frac{(2M+1)!!}{(2t)^M} S_M(\mathbf{r}, -\mathbf{r}),$$

where

$$(7.14) \quad S_M(\mathbf{r}, -\mathbf{r}) = r^{-2} \sum_{l+n+m=M} (-1)^l (2l+1) \varphi_{ln}(r) \varphi_{lm}(r).$$

It would perhaps be more in the spirit of this expansion also to expand the factor $\exp[r^2/t]$ in (7.13), and to collect terms of the same power in t^{-1} . However, the steps are trivial and we shall not state the result explicitly. (7.13) and (7.14) give the following limiting behaviour at very low temperatures (r being kept constant during the limiting process)

$$(7.15) \quad \lim_{t \rightarrow \infty} q_P(r, t) = r^{-2} \varphi_{00}^2(r) = (R_0(r))^2.$$

That is, the q_p function approaches the same limit as the q function.

Finally, we consider the results from the variation principle, Sect. 5. The improved Born approximation, (5.8) leads to

$$(7.16) \quad q_p(r, t) = \frac{1}{1 - \chi_p(r, t)} \quad (\text{improved Born app.}),$$

where χ_p is given by (7.9) and (7.10). Just as in the q function, the improvement over the straightforward Born approximation is most noticeable if the potential contains a strongly repulsive region. In such a region (7.16) stays positive but becomes very small, whereas the Born approximation (7.7) becomes negative and therefore qualitatively wrong.

The trial function adapted to the low-temperature region, (5.9), leads to (5.17) and (5.21). The corresponding result for the q_p function is

$$(7.17) \quad q_p(r, t) = \frac{(R_0(r))^2}{F_p(r, t)},$$

where

$$(7.18) \quad F_p(r, t) = 1 - \frac{1}{2} \int d^3r' (R_0^2(r') - 1) \nabla_{r'}^2 M_1(\mathbf{r} - \mathbf{r}', -\mathbf{r} - \mathbf{r}', t).$$

The angle integrations are done as in Appendix B, the Laplacean being performed afterwards; since the other factor is independent of angles, the differentiations with respect to the angles implied by the Laplacean give zero upon integration over angles. We then get

$$(7.19) \quad \begin{aligned} F_p(r, t) &= 1 - \frac{1}{2} \int_0^\infty dr' r' (R_0^2(r') - 1) \frac{\partial^2}{\partial r'^2} \left(r' \left(\frac{2r_{<}}{rr'} - K_2(r, r', t) \right) \right) \\ &= 1 - (2/rt) \int_0^r (R_0^2(r') - 1) r'^2 dr' - t^{-1} \int_0^\infty (R_0^2(r') - 1) \left(1 - \frac{2r'^2}{t} \right) K_2(r, r', t) r'^2 dr'. \end{aligned}$$

In this form the result can be evaluated by hand computing methods if necessary, but machine computation is definitely preferable. By arguments very similar to the ones employed near the end of Sect. 6, we can show that $F_p(r, t)$ approaches 1 in the region $r \ll t^{1/2}$, $b \ll t^{1/2}$, thereby recovering the limiting behaviour (7.15) of the correct solution, as well as of the trial function. The only difference is that now there are correction terms of order $a/t^{1/2}$ where a is the scattering length, in addition to terms of orders t^{-1} and $t^{-1} \ln(t)$. Until numerical computations of the correct q_p function are available, it is

difficult to assess the accuracy of this variational result, but at least the limiting behaviour is correct.

We mention, finally, that the various approximate results for the q_p function obtained in this section are valid only if there are no bound states of the two-particle system. If bound states do exist, they dominate the behaviour of the q_p function at low temperatures, and must be considered explicitly.

* * *

We would like to thank Drs. S. T. BUTLER and M. R. SCHAFFROTH for many very valuable discussions.

APPENDIX A

The Residue of $u(r, \sigma)$ at a Value of σ corresponding to a Bound State.

In Sect. 2, we have defined two linearly independent solutions of the radial Schrödinger equation (2.18) by the conditions (2.19) and (2.20). The solution $v(r, \sigma)$ approaches the wave function of the bound state as σ approaches the value σ_1 given by (2.25). The solution $u(r, \sigma)$ does not exist in that limit.

We start by establishing a general relation between $u(r, \sigma)$ and $v(r, \sigma)$ for σ not equal to σ_1 . $u(r, \sigma)$ satisfies the differential equation

$$(A.1) \quad -\frac{d^2 u}{dr^2} + \left(\frac{l(l+1)}{r^2} + W(r) + \sigma^2 \right) u = 0,$$

and we know another solution, $v(r, \sigma)$, of this same equation. Using standard methods from the theory of differential equations⁽¹⁸⁾ we can write the general solution of (A.1) in the form

$$(A.2) \quad Av(r, \sigma) + Bv(r, \sigma) \int_0^r \frac{dr'}{v^2(r', \sigma)},$$

where A and B are arbitrary constants. We now adjust A and B so as to get the solution $u(r, \sigma)$ defined by (2.19). Since u vanishes at $r = 0$, we must set $A = 0$. When we go to large r , the main contribution to the integral comes from r' close to r , because of (2.20). Substituting the limiting form $v(r, \sigma) = \exp[-\sigma r]$ into (A.2), we find that B must be set equal to 2σ in order to

⁽¹⁸⁾ L. C. INCE: *Ordinary Differential Equations* (New York, 1944), Section 5.22.

make (A.2) approach $\exp[+\sigma r]$. Our desired relation is therefore:

$$(A.3) \quad u(r, \sigma) = 2\sigma v(r, \sigma) \int_0^r \frac{dr'}{v^2(r', \sigma)}.$$

Next we investigate the behaviour of (A.3) as σ approaches a pole σ_1 . Since $v(0, \sigma_1) = 0$, and $v(r, \sigma_1)$ behaves for small r like r^{l+1} , the integral (A.3) diverges at its lower limit when σ approaches σ_1 .

For the sake of simplicity, we carry through the development for the special case $l = 0$, and indicate at the end the modifications required for other values of l . We assume that σ lies close to a pole σ_1 , and write

$$(A.4) \quad \sigma - \sigma_1 = \varepsilon,$$

$$(A.5) \quad v(r, \sigma) = v(r, \sigma_1 + \varepsilon) = v(r, \sigma_1) + \varepsilon w(r) + \dots$$

Since the divergence of the integral in (A.3) occurs at the lower limit, we need the behaviour of $v(r, \sigma_1)$ and of $w(r)$ near $r = 0$. For $l = 0$ we have

$$(A.6) \quad v(r, \sigma_1) = ar + \dots \quad w(r) = b + \dots \quad \text{for small } r,$$

where a and b are constants. Substitution into (A.3) yields

$$(A.7) \quad \lim_{\varepsilon \rightarrow 0} (\varepsilon u(r, \sigma_1 + \varepsilon)) = \frac{2\sigma_1 v(r, \sigma_1)}{ab}.$$

This is the desired residue, and it merely remains to find a general expression for the product ab . To do this, we notice that the Wronskian of $v(r, \sigma_1)$ and $w(r)$ at $r = 0$ is equal to ab :

$$(A.8) \quad (w(dv/dr) - v(dw/dr))_{r=0} = ab.$$

The differential equation satisfied by w can be found by setting $\sigma = \sigma_1 + \varepsilon$ in (A.1), substituting (A.5) for the unknown solution, and equating terms of order ε . The result is

$$(A.9) \quad -\frac{d^2 w}{dr^2} + \left(\frac{l(l+1)}{r^2} + W(r) + \sigma_1^2 \right) w = -2\sigma_1 v(r, \sigma_1).$$

From this and the differential equation satisfied by $v(r, \sigma_1)$, i.e., equation (A.1) with $\sigma = \sigma_1$, we immediately get the Wronskian relation

$$(A.10) \quad (w(dv/dr) - v(dw/dr)) - ab = -2\sigma_1 \int_0^r v^2(r', \sigma_1) dr'.$$

It remains to show that the bracketed term on the left side approaches zero as r approaches infinity. To do this, we compare the defining equation (A.5)

with the asymptotic form of $v(r, \sigma)$ for large r :

$$(A.11) \quad v(r, \sigma_1 + \varepsilon) \cong \exp [-(\sigma_1 + \varepsilon)r] = v(r, \sigma_1) + \varepsilon w(r) + \text{Order}(\varepsilon^2).$$

This shows that the asymptotic form of $w(r)$ for large r is given by

$$(A.12) \quad w(r) \cong -r \exp [-(\sigma_1 r)] \quad \text{for large } r.$$

Letting r approach infinity in (A.10) and combining with (A.7) we get the desired result

$$(A.13) \quad \lim_{\varepsilon \rightarrow 0} (\varepsilon u(r, \sigma_1 + \varepsilon)) = \frac{v(r, \sigma_1)}{\int_0^\infty v^2(r', \sigma_1) dr'}.$$

For non-zero values of l , the only change is in the behaviour of $v(r, \sigma_1)$ and $w(r)$ near $r = 0$, i.e., in equation (A.6). If we write

$$(A.6') \quad v_l(r, \sigma_1) = ar^{l+1} + \dots \quad w_l(r) = \frac{br^{-l}}{2l+1} + \dots \quad (\text{for small } r),$$

the rest of the proof goes through without change. The proportionality of $v_l(r, \sigma_1)$ to r^{l+1} is well known, and the fact that $w_l(r)$ is proportional to r^{-l} can be shown easily from the differential equations.

APPENDIX B

Evaluation of an Integral.

We wish to perform the integration over angles in (7.8). By symmetry, the terms $|\mathbf{r} - \mathbf{r}'|^{-1}$ and $|\mathbf{r} + \mathbf{r}'|^{-1}$ give the same result, so we consider only one of them, and multiply the result by two. Choosing the direction of \mathbf{r} as our z -axis, the integration over the polar angle φ gives a factor 2π . Instead of the polar angle θ we introduce the variable

$$(B.1) \quad p = (r^2 + r'^2 - 2rr' \cos \theta)^{\frac{1}{2}},$$

to get

$$(B.2) \quad \chi_P(r, t) = - \int_0^\infty dr' (r'/r) W(r') \exp \left[\frac{r^2 - r'^2}{2t} \right] \int_{|\mathbf{r}-\mathbf{r}'|}^{\mathbf{r}+\mathbf{r}'} dp \cdot \exp [-(p/2t)(2r^2 + 2r'^2 - p^2)^{\frac{1}{2}}].$$

In the integral over p we now introduce the notation

$$(B.3) \quad a^2 = 2r^2 + 2r'^2,$$

and the new variable of integration μ through

$$(B.4) \quad p = a \sin \mu .$$

This gives

$$(B.5) \quad \chi_p(r, t) = - \int_0^\infty dr' (ar'/r) W(r') \exp \left[\frac{r^2 - r'^2}{2t} \right] J(a^2/2t) ,$$

where

$$(B.6) \quad J(x) = \int_{\mu_0}^{\mu_1} d\mu \cos \mu \exp [-x \sin \mu \cos \mu]$$

$$\sin \mu_0 = |r - r'|/a \quad \sin \mu_1 = (r + r')/a .$$

It is important for the evaluation of this integral to notice that the angles μ_0 and μ_1 add up to a right angle. That is, the triangle with sides $|r - r'|$, $r + r'$, and a is a right triangle. If we replace the variable μ in the integral (B.6) by the variable $\gamma = \frac{1}{2}\pi - \mu$, we obtain

$$(B.7) \quad J(x) = \int_{\mu_0}^{\mu_1} d\mu \sin \mu \exp [-x \sin \mu \cos \mu] .$$

We now set up a differential equation for $J(x)$. To do this we differentiate with respect to x under the sign of integration, to get

$$\begin{aligned} dJ/dx &= - \int_{\mu_0}^{\mu_1} \exp [-x \sin \mu \cos \mu] \sin \mu \cos^2 \mu d\mu = \\ &= - \frac{1}{2} \int_{\mu_0}^{\mu_1} \exp [-x \sin \mu \cos \mu] \sin \mu d\mu - \\ &= - \frac{1}{2} \int_{\mu_0}^{\mu_1} \exp [-x \sin \mu \cos \mu] \sin \mu d(\sin \mu \cos \mu) . \end{aligned}$$

The first integral on the last line is just $J(x)$ itself, because of (B.7). The second integral can be transformed through an integration by parts:

$$\begin{aligned} (2x)^{-1} \int_{\mu_0}^{\mu_1} \sin \mu \frac{d}{d\mu} (\exp [-x \sin \mu \cos \mu]) d\mu &= \\ &= (2x)^{-1} (\sin \mu_1 - \sin \mu_0) \exp [-x \sin \mu_0 \cos \mu_0] - 2(x)^{-1} J(x) . \end{aligned}$$

Here we have again made use of the fact that $\mu_0 + \mu_1 = \frac{1}{2}\pi$, so that $\sin \mu_1 \cos \mu_1 = \sin \mu_0 \cos \mu_0$. Combining terms, we get the following differential equation for $J(x)$:

$$(B.8) \quad dJ/dx + \frac{1}{2}(1+x^{-1})J(x) = \frac{\sin \mu_1 - \sin \mu_0}{2x} \exp[-x \sin \mu_0 \cos \mu_0].$$

This must be solved subject to the initial condition

$$(B.9) \quad J(0) = \int_{\mu_0}^{\mu_1} \cos \mu \, d\mu = \sin \mu_1 - \sin \mu_0 = \frac{2r_{<}}{a}.$$

Since this is a first order linear differential equation, the solution is immediate, and is given by

$$(B.10) \quad J(x) = \frac{1}{2}(\sin \mu_1 - \sin \mu_0)x^{-\frac{1}{2}} \exp\left[-\frac{1}{2}x\right] \int_0^x y^{-\frac{1}{2}} \exp\left[\frac{1}{2}y - y \sin \mu_0 \cos \mu_0\right] dy - \\ = (2/x)^{\frac{1}{2}} \exp\left[-\frac{1}{2}x\right] \int_0^{(2x)^{\frac{1}{2}}(r_{<}/a)} \exp[z^2] dz.$$

Substitution of this result into (B.5) then yields the desired formulae (7.9) and (7.10).

RIASSUNTO (*)

Nella meccanica statistica classica, la funzione di correlazione tra coppie di particelle del gas in un gas diluito è data da $\exp[-\beta V(r)]$, dove $\beta = 1/kT$ e $V(r)$ è il potenziale della forza tra le due particelle. Il presente lavoro espone le corrispondenti formule della meccanica quantistica, compresa la generalizzazione alle statistiche di Bose-Einstein e di Fermi-Dirac. Le correzioni introdotte dalla meccanica quantistica sono particolarmente importanti nella regione delle basse temperature, dove modificano qualitativamente la funzione di correlazione. In assenza di stati legati, la funzione di correlazione delle coppie si approssima ad un limite finito coll'approssimarsi a zero della temperatura. Si sviluppano vari metodi di approssimazione per la funzione di correlazione delle coppie, ivi compresa un'applicazione di un principio variazionale per l'inverso di un operatore, dovuta a FRIEDMAN.

(*) Traduzione a cura della Redazione.

The Second Virial Coefficient Near Absolute Zero.

J. M. BLATT

*The F.B.S. Falkiner Nuclear Research and Adolph Basser Computing Laboratories
School of Physics (*), The University of Sydney - Sydney, N.S.W.*

(ricevuto il 4 Giugno 1956)

Summary. — A new proof of the quantum mechanical formula for the second virial coefficient is followed by a discussion of the behaviour of this coefficient in the limit of very low temperatures. Comparison is made with earlier work.

1. — Introduction.

At very low temperatures the second virial coefficient of a gas cannot be computed from the classical expression ⁽¹⁾

$$(1.1) \quad B = -2\pi \int_0^{\infty} (q(r) - 1) r^2 dr,$$

where

$$(1.2) \quad q(r, \beta) = \exp[-\beta V(r)] \quad (\text{classical})$$

is the classical value of the pair correlation function in a dilute gas; here $\beta = 1/kT$ and $V(r)$ is the potential of the force between the particles. Rather, it is necessary to use quantum mechanical expressions for the pair correlations, and to take account of the quantum statistics of the particles.

Although there is considerable literature on this subject, the matter is not in a completely satisfactory state. The derivations of GROPPER ⁽²⁾ and

(*) Also supported by the Nuclear Research Foundation within the University of Sydney.

⁽¹⁾ J. O. HIRSCHFELDER, C. F. CURTISS and R. B. BIRD: *Molecular Theory of Gases and Liquids* (New York, 1954); see Chapter VI in particular.

⁽²⁾ L. GROPPER: *Phys. Rev.*, **50**, 963 (1936); **51**, 1108 (1937); **55**, 1095 (1939).

GREEN ⁽³⁾ give results which agree with that of UHLENBECK and BETH ⁽⁴⁾ only if two gas particles cannot form a stable molecule. The contribution of bound states (stable molecules) does not appear in the results of GROPPER and GREEN; UHLENBECK and BETH do include such contributions, but by means of an ad hoc argument; in particular the normalization coefficient in front of this contribution is only made plausible, not derived directly from first principles.

Sect. 2 of this paper is devoted to a mathematical derivation of the formula of Uhlenbeck and Beth starting from the results of the preceding paper ⁽⁵⁾ on the quantum mechanical pair correlation function. Sect. 3 is devoted to the discussion of the extreme low-temperature limit; the results are the same as the ones obtained by UHLENBECK and BETH, but we gain some qualitative insight regarding the region of r which makes the main contribution to the integral (1.1). Unlike the classical case, this is *not* the region of r in which the potential is most strongly attractive, but rather is outside the range of the potential altogether. Furthermore, the asymptotic formulas are shown to be of little practical use even at liquid helium temperatures.

The asymptotic formulas given by GREEN ⁽³⁾ are discussed in Sect. 4. They agree with UHLENBECK and BETH as long as there are no bound states.

Since the extreme asymptotic formulas cannot be used until very low temperatures are reached, an alternative approach is desirable. This can be achieved by the use of the «effective range» expansion for the scattering phase shifts ⁽⁶⁾. This is carried out explicitly for the S -wave contribution to the second virial coefficient, in Sect. 5.

No numerical results are given in this paper, primarily because the evaluation of the exact expression for the second virial coefficient is already coded for an electronic computer ⁽⁷⁾.

2. - Derivation of the Formula for the Second Virial Coefficient in Terms of Phase Shifts.

The second virial coefficient is given by ⁽⁴⁾

$$(2.1) \quad B_{\pm} = B \pm B',$$

⁽³⁾ H. S. GREEN: *Proc. Phys. Soc. London*, A **45**, 1022 (1952).

⁽⁴⁾ G. E. UHLENBECK and E. BETH: *Physica*, **3**, 729 (1936); **4**, 915 (1937).

⁽⁵⁾ J. M. BLATT: Henceforth this paper will be called «I», and equations in I will be denoted by (I, ...).

⁽⁶⁾ J. M. BLATT and V. F. WEISSKOPF: *Theoretical Nuclear Physics* (New York, 1952); see chapter II and the references quoted there.

⁽⁷⁾ J. E. KILPATRICK, W. E. KELLER, E. F. HAMMEL and N. METROPOLIS: *Phys. Rev.*, **94**, 1103 (1954).

where the $+$ sign holds for Bose-Einstein statistics, the $-$ sign for Fermi-Dirac statistics, and the quantities B and B' are expressible in terms of the pair correlation functions $q(r, t)$ and $q_p(r, t)$ defined in I:

$$(2.2) \quad B = \frac{1}{2} \int d^3r (1 - q(r, t)),$$

$$(2.3) \quad B' = -\frac{1}{2} \int d^3r q_p(r, t) \exp[-r^2/t].$$

Here « t » is related to the temperature through

$$(2.4) \quad t = \hbar^2/mkT = \hbar^2\beta/m,$$

m being the mass of each gas particle.

We shall use the expressions for q and q_p derived in I, and transform the result so as to yield the usual expression^(1,4), for the second virial coefficient.

We start with formula (2.2). The function $q(r, t)$ is given by equation (I, 6.3). In the special case of no force between the particles (ideal gas), the wave function $\varphi_l(r, k)$ reduces to the regular solution of the free wave equation

$$(2.5) \quad F_l(r, k) = (\frac{1}{2}\pi kr)^{\frac{1}{2}} J_{l+\frac{1}{2}}(kr)$$

and (I, 6.3) reduces to the identity⁽⁶⁾.

$$(2.6) \quad 1 = (4\pi t^3)^{\frac{1}{2}} r^{-2} \sum_{l=0}^{\infty} (2l+1)(2/\pi) \int_0^{\infty} \exp[-k^2 t] F_l^2(r, k) dk.$$

We then obtain

$$(2.7) \quad 1 - q(r, t) = (4\pi t^3)^{\frac{1}{2}} r^{-2} (2/\pi) \sum_{l=0}^{\infty} (2l+1) \int_0^{\infty} \exp[-k^2 t] (F_l^2(r, k) - \varphi_l^2(r, k)) dk.$$

Substitution into (2.2) gives

$$(2.8) \quad B = \sum_{l=0}^{\infty} B_l,$$

with

$$(2.9) \quad B_l = 4(4\pi t^3)^{\frac{1}{2}} (2l+1) \int_0^{\infty} dr \int_0^{\infty} dk \exp[-k^2 t] (F_l^2(r, k) - \varphi_l^2(r, k)) - \\ - 2\pi(4\pi t^3)^{\frac{1}{2}} (2l+1) \sum_i \exp[-\beta \varepsilon_{il}^{(-)}].$$

(*) This identity can be derived by performing the sum over l first, using formula (9) on p. 366 of WATSON: *Bessel Functions* (Cambridge, 1948).

The contribution from the bound states has been evaluated by noticing that the $\psi_i(r)$ in (I, 6.3) is by definition the *normalized* wave function of the i -th bound state of angular momentum l , so that the integration over r gives unity.

The continuum contribution must be handled carefully, since it is not permissible to interchange the orders of integration over r and k . We therefore integrate over r to some large value $r = R$, and afterwards let R approach infinity. It is shown in Appendix A that the following is an identity (δ_i is the scattering phase shift):

$$(2.10) \quad 2 \int_0^R (F_l^2(r, k) - q_l^2(r, k)) dr = \frac{d\delta_i}{dk} + \frac{1}{2} \sin(2kR + 2\delta_i) - \frac{1}{2} \sin(2kR).$$

For any finite R we can interchange the orders of integration over r and k , and we obtain

$$(2.11) \quad \int_0^R dr \int_0^\infty dk \exp[-k^2 t] (F_l^2(r, k) - q_l^2(r, k)) = \\ = -\frac{1}{2} \int_0^\infty dk \exp[-k^2 t] (d\delta_i/dk) + \frac{1}{4} \int_0^\infty dk \exp[-k^2 t] (\sin(2kR + 2\delta_i) - \sin(2kR)).$$

We need the limit of this as R approaches infinity. The integrals in which R occurs explicitly may be considered to be Fourier integral transforms of certain functions of k , the transform variable being $p = 2R$. By the Riemann-Lebesgue lemma, these integrals approach zero as R approaches infinity, at least as fast as R^{-1} . The conditions of the lemma are not stringent at all and are certainly satisfied by such smooth functions of k as $\exp[-k^2 t] \sin(2\delta_i)$, $\exp[-k^2 t] \cos(2\delta_i)$, and $\exp[-k^2 t]$.

We therefore get an expression for B as follows:

$$(2.12) \quad B = -2(4\pi t)^{\frac{1}{2}} \sum_{l=0}^{\infty} (2l+1) \left(\pi \sum_i \exp[-\beta \varepsilon_i^{(l)}] + \int_0^\infty dk \exp[-k^2 t] (d\delta_i/dk) \right).$$

Next we perform a similar transformation on B' , (2.3). The function $q_\rho(r, t)$ is given by equation (I, 7.4). For the ideal gas we get the identity

$$(2.13) \quad q_\rho(r, t) = 1 = (4\pi t)^{\frac{1}{2}} r^{-2} \exp[r^2/t] \sum_{l=0}^{\infty} (-1)^l (2l+1) (2/\pi) \int_0^\infty \exp[-k^2 t] F_l^2(r, k) dk.$$

We add and subtract 1 from $q_p(r, t)$ in (2.3) to get

$$(2.14) \quad B' = \frac{1}{2} \int d^3r (1 - q_p(r, t)) \exp[-r^2/t] - \frac{1}{2} \int d^3r \exp[-r^2/t].$$

The second integral represents the second virial coefficient of an ideal (Bose-Einstein or Fermi-Dirac) gas, and is equal to $\frac{1}{2}(\pi t)^{\frac{3}{2}} = 2^{-\frac{3}{2}} \lambda^3$ where $\lambda = (2\pi t)^{\frac{1}{2}}$ is the conventional ⁽¹⁾ quantity of the dimension of a length. The first integral can be transformed in exactly the same way as B_l , and gives the same result as B_l , (2.12), except for a factor $(-1)^l$. Thus in the total second virial coefficient, (2.1), these contributions cancel for odd (even) l , and add up for even (odd) l , depending upon the statistics. The final result is

$$(2.15) \quad B_{\pm} = \mp \frac{1}{2}(\pi t)^{\frac{3}{2}} - (4\pi t)^{\frac{3}{2}} \sum_{l=0}^{\infty} \sum_i' (2l+1) \exp[-\beta \epsilon_{li}'] - \\ - (4\pi t)^{\frac{3}{2}} \sum_{l=0}^{\infty} (2l+1) \int_0^{\infty} dk \exp[-k^2 t] \frac{1}{\pi} \frac{d\delta_l}{dk}.$$

This is identically the same result which is obtained by the more usual approach ^(1,4); the primes on the sums over l mean even l only for Bose-Einstein statistics, odd l only for Fermi-Dirac statistics.

3. - Behaviour at very Low Temperatures.

We now investigate the behaviour of the virial coefficient (2.15) at extremely low temperatures (as we shall see later, these temperatures are not practical for dilute gases). First of all, if bound states exist, it is apparent from (2.15) that they dominate the low temperature virial coefficient. This is also obvious physically, since the formation of « molecules » becomes more and more important as the temperature is lowered; eventually most of the gas consists of molecules (assuming always that the density is kept low enough that formation of the liquid state does not occur). It is clear that the virial series is not well adapted to such a case.

In the absence of bound states (i.e., for sufficiently weak attractive forces between the particles of the gas), we must estimate the integrals in (2.15). It is well known from the quantum mechanical theory of scattering that the phase shift $\delta_l(k)$ is proportional to k^{2l+1} for low values of k . We write

$$(3.1) \quad \delta_l(k) = - \frac{(ka_l)^{2l+1}}{(2l+1)!!} (1 + \text{Order}(k^2)),$$

where a_l is a constant (for a given potential) which we shall call the « scattering length of order l » and the double factorial is defined by

$$(3.2) \quad (2l+1)!! = 1 \cdot 3 \cdot 5 \cdot \dots \cdot (2l+1).$$

At very low temperatures, and hence very large t , the main contribution to the integral in (2.15) comes from very small values of k , namely $k \lesssim t^{-\frac{1}{2}}$. We can therefore use the asymptotic form (3.1), to get the following leading term for the contribution of a given l in the absence of bound states:

$$(3.3) \quad 2B_l = 4\pi(2l+1)a_l t \left(\frac{a_l^3}{2t} \right)^l (1 + \text{Order}(1/t)).$$

In the limit of very large t , the most important contribution is the S -wave, $l=0$, with

$$(3.4) \quad 2B_0 = 4\pi a_0 t + \dots$$

For Bose-Einstein statistics, therefore, the behaviour of the second virial coefficient at very low temperatures, in the absence of bound states, is given by

$$(3.5) \quad B_+ = -\frac{1}{2}(\pi t)^{\frac{3}{2}} + 4\pi a_0 t + \text{Order}(1).$$

The asymptotic behaviour is different for Fermi-Dirac statistics where the lowest contributing l is the P -wave, $l=1$. We get, again in the absence of bound states

$$(3.6) \quad B_- = +\frac{1}{2}(\pi t)^{\frac{3}{2}} + 6\pi a_1^2 + \text{Order}(t^{-1}).$$

We observe that the ideal gas term, $\mp \frac{1}{2}(\pi t)^{\frac{3}{2}}$, dominates for sufficiently low temperatures over the effects of the interparticle potential, unless the potential is sufficiently attractive to produce bound states.

These results agree, except for notation, with the results of UHLENBECK and BETH ⁽¹⁾, and we shall see that they also agree with the results of GREEN ⁽³⁾ provided there are no bound states.

It is of interest, however, to find out which region of r contributes most to the second virial coefficient. Consider the integral (2.2); the function $q(r, t)$ which appears in the integrand has been studied in I. At very low temperatures, $q(r, t)$ has the following behaviour:

$$(3.7a) \quad q(r, t) \cong (R_0(r))^2 \quad \text{for } r \ll t^{\frac{1}{2}}, t \text{ large}$$

$$(3.7b) \quad q(r, t) \cong 1 \quad \text{for } r \gg t^{\frac{1}{2}}, t \text{ large}$$

The transition between these two regions is rather sharp. For qualitative arguments, therefore, we replace $q(r, t)$ by (3.7a) for $r \leq t^{\frac{1}{2}}$, by (3.7b) for $r > t^{\frac{1}{2}}$. Furthermore, we assume that $t^{\frac{1}{2}}$ is much larger than the range of the potential $V(r)$, so that we can replace the zero energy S -wave radial wave function $R_0(r)$ by

$$(3.8) \quad R_0(r) = 1 - (a_0/r), \quad \text{for } r > b.$$

Substitution in (2.2) yields the approximate form

$$(3.9) \quad 2B_0 \cong \int_0^{t^{\frac{1}{2}}} (1 - R_0^2) 4\pi r^2 dr \cong \int_b^{t^{\frac{1}{2}}} (2a_0 r - a) 4\pi dr = 4\pi a_0 t + \text{Order}(1).$$

This is precisely the asymptotic form (3.4), and we see from this qualitative derivation that the main contribution to the integral comes from the region $r \sim t^{\frac{1}{2}}$, *not* from the region in which the potential $V(r)$ is most strongly attractive. This is quite different from the classical expression for the second virial coefficient, and accounts at least to some extent for the fact that the quantum mechanical second virial coefficient at low temperatures is not very sensitive to the details of the potential $V(r)$ (7).

4. - Comparison with Green's Calculation.

We are now in a position to compare our results with those of GREEN (3). Green starts from the same expressions we use, (2.1) to (2.3), but treats them in a different way. He expands the pair correlation function in a power series in the inter-particle potential, and then operates formally with this series. This is equivalent, in quantum mechanical terminology, to working with infinitely many terms of the Born expansion, and should therefore give correct results whenever the Born expansion for the wave function converges. This is indeed the case: Green's final results are equivalent to ours *if there are no bound states*. If bound states do exist, Green's formulation fails to include their contribution; this is understandable because the Born expansion fails to converge to the correct solution in that case.

It is of some interest to show the equivalence between Green's formulas and our asymptotic expressions in more detail. By looking at Green's formulas (23) and (24), it is apparent that his function $\tau(r)$ is the radial wave function of the S -state in the limit of zero energy, and is identical with the function $R_0(r)$ defined by (I, 4.1), (I, 5.10), and (I, 5.11). Green's equations corresponding to our (3.4) are his formulas (15) and (16), which become in our

notation

$$(4.1) \quad 2B_0 = t \int d^3r W(r) R_0(r) + \dots$$

We write the integral in terms of $\varphi_{00}(r) = rR_0(r)$ and make use of the wave equation for $\varphi_{00}(r)$

$$(4.2) \quad d^2\varphi_{00}/dr^2 = W(r)\varphi_{00}(r)$$

in order to get

$$(4.3) \quad 2B_0 = 4\pi t \int_0^\infty r \frac{d^2\varphi_{00}}{dr^2} dr.$$

Since the asymptotic form of $\varphi_{00}(r)$ for large r is $r - a_0$, a_0 being the S -wave scattering length which appears in (3.1) (for $l = 0$) and in (3.4), we write

$$(4.4) \quad \varphi_{00}(r) = r - a_0 + g(r), \quad d^2\varphi_{00}/dr^2 = d^2g/dr^2.$$

The function $g(r)$ defined this way vanishes at infinity, and is equal to a_0 when $r = 0$ (since φ_{00} must vanish at the origin). Substituting (4.4) into (4.3) and carrying out an integration by parts yields

$$(4.5) \quad 2B_0 = 4\pi t(g(0) - g(\infty)) = 4\pi ta_0,$$

which is identical with our result (3.4).

If one expands the phase shift $\delta_l(k)$ in a power series in k^2 , with leading term given by (3.1), the result for the second virial coefficient, is a power series in t^{-1} . There are no logarithmic terms in t , nor does $t^{\frac{1}{2}}$ appear explicitly. We do not know the cause of the difference between this and Green's equation (19), but in any case these expansions converge disappointingly slowly at reasonable temperatures. Fig. 1 of reference (5) shows that the calculation of DE BOER and MICHELS (9) has only moderate accuracy, in spite of the fact that they included phase shifts for $l \leq 6$. Clearly an asymptotic form which is derived from the S -wave only is not even qualitatively correct at liquid helium temperatures. We cannot agree with Green's surmise that the asymptotic form is sufficient at temperatures slightly below 1 °K.

(9) J. DE BOER and A. MICHELS: *Physica*, **6**, 409 (1939).

5. - Effective Range Approximation.

In scattering theory it is shown ⁽⁶⁾ that the following expansion for the *S*-wave phase shift yields an excellent approximation for low values of the wave number *k*:

$$(5.1) \quad k \cot \delta_0 = -1/a_0 + \frac{1}{2}r_0k^2 + \text{Order}(k^4)$$

where a_0 is the *S*-wave scattering length and r_0 is called the « effective range ». Similar expansions hold for higher values of *l*. The first non-*S*-wave contribution to the virial coefficient of a Bose-Einstein gas is the *D*-wave, $l = 2$. Equation (3.3) shows that this contribution goes to zero in the low-temperature limit, and so do the contributions from $l = 4, 6, \dots$. Thus the *S*-wave does determine the virial coefficient completely, at sufficiently low temperatures, and we shall use (5.1) to get an asymptotic result which converges better than (3.4), and reduces to (3.4) at extremely low temperatures.

It follows from (5.1) that

$$(5.2) \quad \frac{d\delta_0}{dk} \cong -a_0 \frac{1 + \frac{1}{2}r_0a_0k^2}{(1 - \frac{1}{2}r_0a_0k^2)^2 + (a_0k)^2}.$$

We substitute this into the integral (2.12) for $l = 0$. We expand (5.2) into partial fractions; the zeros of the denominator of (5.2) shall be called $-\mu^2$ and $-\nu^2$, respectively; they are given by

$$(5.3) \quad \mu^2 = (2/r_0^2)(1 - r_0/a_0 + (1 - 2r_0/a_0)^{\frac{1}{2}})$$

$$(5.4) \quad \nu^2 = (2/r_0^2)(1 - r_0/a_0 - (1 - 2r_0/a_0)^{\frac{1}{2}}).$$

We then get, in the absence of bound states,

$$(5.5) \quad 2B_0 \cong 8 \left(\frac{\pi t^3}{a_0(a_0 - 2r_0)} \right)^{\frac{1}{2}} \int_0^{\infty} dk \exp[-k^2 t] \left(\frac{1 - \frac{1}{2}r_0a_0\mu^2}{k^2 + \mu^2} - \frac{1 - \frac{1}{2}r_0a_0\nu^2}{k^2 + \nu^2} \right).$$

At this point we use the definite integral

$$(5.6) \quad J(x) = \frac{2}{\pi} \int_0^{\infty} \frac{\exp[-xz^2]}{z^2 + 1} dz = e^x (1 - \operatorname{erf}(x^{\frac{1}{2}})),$$

to get our asymptotic formula:

$$(5.7) \quad 2B_0 \cong 4\pi \left(\frac{\pi t^3}{a_0(a_0 - 2r_0)} \right)^{\frac{1}{2}} ((\mu^{-1} - \frac{1}{2}r_0a_0\mu)J(\mu^2t) - (\nu^{-1} - \frac{1}{2}r_0a_0\nu)J(\nu^2t)).$$

The less accurate asymptotic form (3.4) can be obtained from (5.7) by using the limiting form

$$(5.8) \quad J(x) = (\pi x)^{-\frac{1}{2}} \quad \text{for large } x.$$

However, this is not accurate unless the argument of J is indeed large. By looking at (5.4), we see that ν^2 is approximately equal to $(a_0)^{-2}$ provided the scattering length a_0 is large (this is apparently the case for helium) ⁽¹⁰⁾. Thus the argument $\nu^2 t$ is of the order of t/a_0^2 . At liquid helium temperatures $t^{\frac{1}{2}}$ is of the border of a few Angström units, very much less than the absolute value of a_0 . One would have to go to temperatures of the order of 10^{-3} °K before (3.4), and hence (3.5), becomes a good approximation for helium. This point is quite apart from the question of the contribution of higher values of l .

* * *

We would like to thank Dr. S. T. BUTLER, Dr. M. R. SCHAFROTH, and Professor H. S. GREEN for valuable discussions concerning this paper.

APPENDIX A

Proof of Equation (2.10).

The differential equation satisfied by the radial wave function $\varphi_l(r, k)$ is

$$(A.1) \quad (\text{d}^2\varphi/\text{d}r^2) + \left(k^2 - \frac{l(l+1)}{r^2}\right)\varphi = W\varphi.$$

We write down the same equation for a neighbouring value of k , say $k + \varepsilon$, multiply (A.1) by $\varphi(r, k + \varepsilon)$, the other equation by $\varphi(r, k)$, and subtract. The result is

$$(A.2) \quad \frac{\text{d}}{\text{d}r} [\varphi(r, k + \varepsilon)\varphi'(r, k) - \varphi(r, k)\varphi'(r, k + \varepsilon)] = (2\varepsilon k + \varepsilon^2)\varphi(r, k)\varphi(r, k + \varepsilon),$$

where the dash denotes differentiation with respect to r . Since the « free » radial

⁽¹⁰⁾ Although the comparison of calculated second virial coefficients with experimental values does not allow us to determine whether a bound state of two helium atoms exists, the comparison does show that the absolute value of the scattering length is very large compared to usual atomic dimensions. That is, the potential either barely fails to allow a bound state, or else is barely strong enough to allow one. In the first case the scattering length is large and negative, in the second case, large and positive.

wave function $F_i(r, k)$ satisfies (A.1) with $W(r) = 0$, we also have

$$(A.3) \quad \frac{d}{dr} (F(r, k + \varepsilon)F'(r, k) - F(r, k)F'(r, k + \varepsilon)) = (2\varepsilon k + \varepsilon^2)F(r, k)F(r, k + \varepsilon).$$

We subtract (A.2) from (A.3) and integrate the result over r from $r = 0$ to $r = R$. Furthermore, we keep only the first order terms in ε . This gives

$$(A.4) \quad 2\varepsilon k \int_0^R (F^2(r, k) - \varphi^2(r, k)) dr = F(R, k + \varepsilon)F'(R, k) - F(R, k)F'(R, k + \varepsilon) - \\ - \varphi(R, k + \varepsilon)\varphi'(R, k) + \varphi(R, k)\varphi'(R, k + \varepsilon) + \text{Order}(\varepsilon^2).$$

The contribution of the lower limit, $r = 0$, to the right hand side of (A.4) vanishes because both F and φ vanish at $r = 0$. We now use the asymptotic forms, valid for $kR \gg l$ and $R \gg b$, the range of the potential:

$$(A.5) \quad F_i(r, k) \cong \sin(kr - \frac{1}{2}l\pi), \quad \varphi_i(r, k) \cong \sin(kr - \frac{1}{2}l\pi + \delta_i(k)).$$

We expand the right hand side of (A.4) in powers of ε , keeping only the linear term. The result is equation (2.10) of the text.

RIASSUNTO (*)

Una nuova dimostrazione della formula della meccanica quantistica per il secondo coefficiente del viriale è seguita da una discussione del comportamento di tale coefficiente al limite delle bassissime temperature. Si fanno dei confronti con lavori precedenti.

(*) Traduzione a cura della Redazione.

Non-Linear Effects in the Vacuum Polarization.

A. MINGUZZI

Istituto di Fisica dell'Università - Bologna

Istituto Nazionale di Fisica Nucleare - Gruppo di Bologna

(ricevuto il 4 Giugno 1956)

Summary. — We have investigated the vacuum polarization current arising from the superposition of a constant electromagnetic field $\mathbf{e} \cdot \mathbf{h} = 0$, $h^2 - e^2 > 0$, with a small arbitrarily varying field, without resorting to a power series development in the constant field. The energy density of a photon field in the constant field is also given.

1. — Introduction.

In this paper we have investigated the vacuum polarization current arising from the superposition of a small arbitrarily varying electromagnetic field with a constant electromagnetic field, which in a particular frame becomes a constant magnetic field, h_{12} , pointing in the x_3 -direction. The effect of the latter field consists only in a modification of the vacuum current caused by the former field. This is because a magnetic field is incapable of polarizing the matter vacuum. In this specific situation one can calculate the vacuum current without resorting to its series development in the magnetic field. Some difficulties met in discussing the gauge invariance properties of the vacuum current, have been completely removed using an extension of a procedure suggested by J. SCHWINGER ⁽¹⁾. The vacuum current can be expressed covariantly as sum of three terms, one of which depends only on the current associated with the varying field and the other two depend in a gauge invariant manner on the derivatives of the same field. The charge renormalization procedure affects only the first term. If the small field is interpreted as the quantized field associated with a photon field, the current terms depending on the derivatives give rise to additional terms in the Hamiltonian which describe the coupling between the photons and the magnetic field.

⁽¹⁾ J. SCHWINGER: *Phys. Rev.*, **82**, 664 (1951). See especially Appendix A.

The full Hamiltonian will be invariant with respect to translation in space and time, but not invariant with respect to rotations around the axis forming a non vanishing angle with the magnetic field direction. If, for instance, a photon with a definite linear momentum and definite circular polarisation enters the magnetic field region perpendicularly, it will leave out the magnetic field region as a mixture of the two opposite circular polarizations. But this is possible only if the two components of the initial circular polarization, polarized parallel and perpendicularly to the magnetic field, propagate with different velocities in the magnetic field region.

Therefore, the magnetic field region will behave for a light wave as an anisotropic dielectric.

2. - Calculation of the Polarization Tensor $K_{\mu\nu}(x, x')$.

We have first attempted the calculation using the « bound interaction picture » in which the « bounded field » is the constant magnetic field. No difficulty arises in connection with the vacuum definition, since the negative and positive energy levels of the corresponding Dirac equation have a spacing of $2m^2$. An entirely different situation would have arisen if we had started with a pure electric field ⁽²⁾. In such a case the negative energy levels of the Dirac equation go continuously into the positive ones ⁽³⁾.

We have chosen this particular gauge associated with the magnetic field h_{12}

$$a_1(x) = -\frac{1}{2}h_{12}x_2; \quad a_2(x) = \frac{1}{2}h_{12}x_1; \quad a_3 = a_0 = 0.$$

The vacuum current is correspondingly:

$$\frac{ie}{2} \lim_{x' \rightarrow x} \gamma_\mu \{ \gamma_s [\partial_s' - ie a_s(x')] - m \} \Delta^{(1)}(x', x) = 0.$$

By adding a small arbitrarily varying field $A_\mu(x)$ the vacuum current becomes

$$\delta j_\mu(x) = \frac{i}{2} \int K_{\mu\nu}(x, x') A_\nu(x') d^4x',$$

with

$$K_{\mu\nu}(x, x') = \langle [j_\mu(x), j_\nu(x')] \rangle_0 \varepsilon(x, x') = \\ = -\frac{ie}{2} \text{tr} \{ \gamma_\mu [\gamma_r (\partial_r - ie a_r(x)) - m] \bar{\Delta}(x, x') \gamma_\nu [\gamma_s' (\partial_s' - ie a_s(x')) - m] \Delta^{(1)}(x', x) + \mu \rightarrow \nu \},$$

⁽²⁾ W. H. FURRY: *Phys. Rev.*, **81**, 115 (1951).

⁽³⁾ M. DEMEUR: *Ac. Roy. Belg. Cl. des Sci.*, **28**, fasc. 5 (1952).

and ⁽³⁾

$$(1) \quad \bar{\Delta}(x, x') = \frac{1}{(4\pi)^2} \exp \left[-\frac{ie}{2} h_{12}(x_2 x'_1 - x_1 x'_2) \right] \cdot \int \exp \left[\frac{i}{2} \left(-\beta \lambda + \frac{m^2 + i\gamma_1 \gamma_2 e h_{12}}{\beta} \right) + i \frac{\xi_1^2 + \xi_2^2}{4} e h_{12} \left(\frac{2\beta}{e h_{12}} - \operatorname{ctn} \frac{e h_{12}}{2\beta} \right) \right] \frac{d\beta}{\frac{2\beta}{e h_{12}} \sin \frac{e h_{12}}{2\beta}} =$$

$$= \exp \left[-\frac{ie}{2} h_{12}(x_2 x'_1 - x_1 x'_2) \right] [\bar{\Delta}_d(x, x') - \gamma_1 \gamma_2 \bar{\Delta}_{n.d.}(x, x')],$$

$$(2) \quad \Delta^{(1)}(x, x') = \frac{i}{8\pi^2} \exp \left[-\frac{ie}{2} h_{12}(x_2 x'_1 - x_1 x'_2) \right] \cdot \int \varepsilon(\beta) \exp \left[\frac{i}{2} \left(-\beta \lambda + \frac{m^2 + i\gamma_1 \gamma_2 e h_{12}}{\beta} \right) + i \frac{\xi_1^2 + \xi_2^2}{4} e h_{12} \left(\frac{2\beta}{e h_{12}} - \operatorname{ctn} \frac{e h_{12}}{2\beta} \right) \right] \frac{d\beta}{\frac{2\beta}{e h_{12}} \sin \frac{e h_{12}}{2\beta}} =$$

$$= \exp \left[-\frac{ie}{2} h_{12}(x_2 x'_1 - x_1 x'_2) \right] [\Delta_d^{(1)}(x, x') - \gamma_1 \gamma_2 \Delta_{n.d.}^{(1)}(x, x')],$$

with

$$\xi_\mu = x'_\mu - x_\mu; \quad \lambda = \xi_\mu \xi^\mu.$$

For the following discussion it is convenient to introduce two other functions $\bar{R}(x, x')$, $R^{(1)}(x, x')$ defined by:

$$\bar{R}(x, x') = -\frac{1}{(4\pi)^2} \int \exp \left[\frac{i}{2} \left(-\beta \lambda + \frac{m^2}{\beta} \right) + i \frac{\xi_1^2 + \xi_2^2}{4} e h_{12} \left(\frac{2\beta}{e h_{12}} - \operatorname{ctn} \frac{e h_{12}}{2\beta} \right) \right] \frac{d\beta}{\frac{2\beta}{e h_{12}} \cos \frac{e h_{12}}{2\beta}};$$

$$R^{(1)}(x, x') = \frac{i}{8\pi^2} \int \varepsilon(\beta) \exp \left[\frac{i}{2} \left(-\beta \lambda + \frac{m^2}{\beta} \right) + i \frac{\xi_1^2 + \xi_2^2}{4} e h_{12} \left(\frac{2\beta}{e h_{12}} - \operatorname{ctn} \frac{e h_{12}}{2\beta} \right) \right] \frac{d\beta}{\frac{2\beta}{e h_{12}} \cos \frac{e h_{12}}{2\beta}}.$$

The properties of the γ_i -matrices assure that $K_{\mu\nu}(x, x')$ is an even function of h_{12} , as required by the Furry theorem.

We shall investigate now into the properties of the vacuum current with respect to the two independent gauge transformations of the potential $a_i(x)$, $A_i(x)$. The invariance of the vacuum current respect to the $a_i(x)$ gauge trans-

formation is easily established, because this transformation affects essentially only the phase factor appearing into (1), (2) and leaving the expressions of the form $\bar{\Delta}(x, x')\Delta^{(1)}(x', x)$ invariant. The invariance requirement of the vacuum current with respect to $A_i(x)$ transformations (and consequently the charge conservation) is fulfilled if

$$\partial_\nu K_{\mu\nu}(x, x') = 0.$$

Instead, it is

$$\begin{aligned} \partial_\nu K_{\mu\nu} \propto & -\partial^{(4)}(x-x')[\partial_\mu \Delta_{d.}^{(1)} + \delta_{\mu,12} \partial_\mu R^{(1)}] + i e h_{12} [\bar{\Delta}_{n.d.} \partial_\mu \Delta_{d.}^{(1)} + \\ & + \Delta_{n.d.}^{(1)} \partial_\mu \bar{\Delta}_{d.} + \delta_{\mu,34} (\Delta_{d.}^{(1)} \partial_\mu \bar{\Delta}_{n.d.} + \bar{\Delta}_{d.} \partial_\mu \Delta_{n.d.}^{(1)}) + \delta_{\mu,12} (\Delta_{n.d.}^{(1)} \partial_\mu \bar{R} + \bar{\Delta}_{n.d.} \partial_\mu R^{(1)})], \end{aligned}$$

with

$$\delta_{\mu,lm} = \delta_{\mu l} + \delta_{\mu m},$$

which is different from zero, and by letting $eh_{12} \rightarrow 0$, the r.h.s. reduces to the well known indeterminate expression

$$-\delta^{(4)}(x-x') \partial_\mu \Delta^{(1)}(\lambda).$$

In order to test how the invariant regularization procedure⁽⁴⁾ works in this case, we have simplified the very involved expression of $K_{\mu\nu}(x, x')$ retaining only the lowest order contribution from the magnetic field. Introducing the electromagnetic tensor associated with the magnetic field, the approximate $K_{\mu\nu}(p)$ tensor can be written covariantly in such a way that it is possible to separate gauge invariant expressions from non gauge invariant expressions, such that the latter acquire the typical form:

$$\int_{-1}^{+1} dy \int_{-\infty}^{+\infty} \varepsilon(z) \frac{z^n}{z} \exp \left[i \frac{z}{4} (1-y^2) p^2 \right] \left[R(z) \frac{1-y^2}{4} p^2 + \frac{i}{z} R(z) - i R'(z) \right] dz,$$

where $R(z) = \exp[im^2 z]$ and $n = 2, 3$.

Introducing a convergence factor $\exp[-z|\varepsilon]$ and performing an integration by parts⁽⁵⁾ one obtains the result:

$$\int_{-1}^{+1} dy \int_{-\infty}^{+\infty} \varepsilon(z) n \frac{z^{n-1}}{z} R(z) i \exp \left[i \frac{z}{4} (1-y^2) p^2 \right] dz,$$

⁽⁴⁾ W. PAULI and F. VILLARS: *Rev. Mod. Phys.*, **21**, 434 (1949).

⁽⁵⁾ See reference ⁽⁴⁾, p. 440-441.

and extending this procedure to the whole $K_{\mu\nu}(p)$ expression one obtains finite and gauge invariant result in the second order of the magnetic field. No necessity arises of using the regularization condition

$$R(0) = R'(0) = 0.$$

This was predictable from the observation that the singular $\Delta^{(1)}(x, x')$ and $\bar{\Delta}(x, x')$ functions, developed in power series of h_{12} , can be written down as the sum of the corresponding singular functions without magnetic field $\Delta^{(1)}(\lambda)$ and $\bar{\Delta}(\lambda)$, plus derivatives of the latters with respect to m^2 ; and these derivatives are less singular on the light-cone than the corresponding functions.

This procedure has been proved to be fruitful in the lowest order term in the magnetic field; perhaps it is suitable for handling higher order terms; but we do not know if the development of $K_{\mu\nu}(x, x')$ in power series of eh_{12} is meaningful, because we do not know if $K_{\mu\nu}(x, x')$ is analytic at the point $eh_{12} = 0$. We have not gone further because a more direct approach was used as described in the following.

3. — Gauge Invariant Approach.

The vacuum polarization current is given by:

$$\delta j_\mu(x') = ie \lim_{x'' \rightarrow x'} \text{tr} \gamma_\mu G(x', x''),$$

where $G(x', x'')$ is the Green function of the operator

$$\gamma_\mu [-i\hat{\partial}'_\mu - eA_\mu(x')] + m.$$

According to J. SCHWINGER ⁽¹⁾, $\delta j_\mu(x')$ is equivalently expressed by

$$\delta j_\mu(x') = - \frac{e}{2} \lim_{x'' \rightarrow x'} \int_0^\infty \exp[-im^2s] \text{tr} \langle x'(s) | H_\mu(s) + H_\mu(0) + i\sigma_{\mu\nu} [H_\nu(s) - H_\nu(0)] | x''(0) \rangle ds,$$

where the transformation function $\langle x'(s) | x''(0) \rangle$ obeys the differential equation:

$$i\partial_s \langle x'(s) | x''(0) \rangle = \langle x'(s) | H | x''(0) \rangle,$$

and the operators x_μ and $H_\mu = p_\mu - eA_\mu$ obeys the coupled differential equa-

tions:

$$(3) \quad \frac{dx_\mu}{ds} = 2\Pi_\mu;$$

$$(4) \quad \frac{d\Pi_\mu}{ds} = 2eF_{\mu\nu}\Pi_\nu - ie \frac{\partial F_{\mu\nu}}{\partial x_\nu} + \frac{1}{2}e\sigma_{\lambda\nu} \frac{\partial F_{\lambda\nu}}{\partial x_\mu},$$

with the commutation relations

$$[x_\mu, \Pi_\nu] = i\delta_{\mu\nu}; \quad [\Pi_\mu, \Pi_\nu] = ieF_{\mu\nu}.$$

$F_{\mu\nu}$ is the electromagnetic tensor associated with the potential vector $A_\mu(x)$ and $H = \Pi_\mu^2 - \frac{1}{2}e\sigma_{\lambda\nu}F_{\lambda\nu}$.

We will solve the differential equations (3) (4), by decomposing $F_{\mu\nu}(x)$ into the sum of a constant electromagnetic tensor $h_{\mu\nu}$ (associated with the magnetic field parallel to the x_3 -axis) and the tensor $f_{\mu\nu}(x)$ associated with the small arbitrarily varying field; then introducing first order approximation for the $f_{\mu\nu}(x)$ field we will obtain the exact solution for the $h_{\mu\nu}$ tensor. Similarly the transformation function $x'(s)$ $x''(0)$ will be exact in the $h_{\mu\nu}$ field as long as the varying field $f_{\mu\nu}(x)$ is considered only in first order.

The integration of the coupled equations (4) gives

$$(5) \quad \begin{aligned} \Pi_\mu(s) = & \Pi_\mu(0) \cos(2eh_{\mu\nu}s) + \Pi_\nu(0) \sin(2eh_{\mu\nu}s) + \\ & + \int_0^s \Phi_\nu(s') \sin[2eh_{\mu\nu}(s-s')] ds' + \int_0^s \Phi_\mu(s') \cos[2eh_{\mu\nu}(s-s')] ds'. \end{aligned}$$

(no summation; μ and ν take only the values 1, 2)

$$(6) \quad \Pi_r(s) = \Pi_r(0) + \int_0^s \Phi_r(s') ds'; \quad r = 3, 4,$$

where

$$\Phi_k(s') = 2ef_{k\lambda}(x^*)\Pi_\lambda^* - ie \frac{\partial f_{k\lambda}(x^*)}{\partial x_\lambda^*} + \frac{1}{2}e\sigma_{\lambda\nu} \frac{\partial f_{\lambda\nu}(x^*)}{\partial x_k^*}.$$

$\Phi_k(s')$ is the right hand side of (4) in which the operators x_μ and Π_μ have been approximated with the corresponding starred quantities, which are the solutions of (3) (4) with vanishing $f_{\mu\nu}(x)$. That is

$$x^*(s') = x(0) + I(s')\Pi(0)$$

$$\Pi^*(s') = R(s')\Pi(0),$$

with

$$R(s') = \begin{vmatrix} \cos(2eh_{12}s') & \sin(2eh_{12}s') & 0 & 0 \\ -\sin(2eh_{12}s') & \cos(2eh_{12}s') & 0 & 0 \\ 0 & 0 & 1 & 0 \\ 0 & 0 & 0 & 1 \end{vmatrix},$$

$$I(s') = \begin{vmatrix} \frac{\sin(2eh_{12}s')}{eh_{12}} & \frac{1 - \cos(2eh_{12}s')}{eh_{12}} & 0 & 0 \\ \frac{\cos(2eh_{12}s') - 1}{eh_{12}} & \frac{\sin(2eh_{12}s')}{eh_{12}} & 0 & 0 \\ 0 & 0 & 2s' & 0 \\ 0 & 0 & 0 & 2s' \end{vmatrix}.$$

The introduction of (5) and (6) into (3) gives:

$$(7) \quad x_\mu(s) - x_\mu(0) = 2\Pi_\mu(0) \frac{\sin(2eh_{\mu\nu}s)}{2eh_{\mu\nu}} + 2\Pi_\nu(0) \frac{1 - \cos(2eh_{\mu\nu}s)}{2eh_{\mu\nu}} + \\ + 2 \int_0^s \frac{\sin^2[eh_{\mu\nu}(s-s')]}{eh_{\mu\nu}} \Phi_\nu(s') ds' + \int_0^s \frac{\sin[2eh_{\mu\nu}(s-s')]}{eh_{\mu\nu}} \Phi_\mu(s') ds',$$

(no summation; μ and ν take only the values 1 and 2)

$$(8) \quad x_r(s) - x_r(0) = 2s\Pi_r(0) + 2s \int_0^s \left(1 - \frac{s'}{s}\right) \Phi_r(s') ds', \quad r = 3, 4.$$

By (5) and (7) one obtains

$$(9) \quad \Pi_\mu(s) - \Pi_\mu(0) = eh_{\mu\nu}[x_\nu(s) - x_\nu(0)] + \int_0^s \Phi_\mu(s') ds',$$

$$(10) \quad \Pi_\mu(s) + \Pi_\mu(0) = \frac{eh_{\mu\nu} \sin(2eh_{\mu\nu}s)}{1 - \cos(2eh_{\mu\nu}s)} [x_\mu(s) - x_\mu(0)] + \\ + \int_0^s \frac{\sin[2eh_{\mu\nu}(s-s')]\{\cos[2eh_{\mu\nu}(s-s')] - \cos(2eh_{\mu\nu}s)\}}{1 - \cos(2eh_{\mu\nu}s)} \Phi_\nu(s') ds' + \\ + \int_0^s \frac{\cos[2eh_{\mu\nu}(s-s')] - \cos(2eh_{\mu\nu}s)}{1 - \cos(2eh_{\mu\nu}s)} \Phi_\mu(s') ds',$$

(no summation; μ and ν take the values 1, 2),

and from (6) and (8) one obtains

$$\begin{aligned} \Pi_r(s) - \Pi_r(0) &= \int_0^s \Phi_r(s') ds', \\ \Pi_r(s) + \Pi_r(0) &= \frac{x_r(s) - x_r(0)}{s} + \int_0^s \left(2 \frac{s'}{s} - 1\right) \Phi_r(s') ds' \quad (r = 3, 4). \end{aligned}$$

Since $\Phi_k(s')$ contains already linearly the $f_{\mu\nu}(x)$ field and

$$\lim_{x'' \rightarrow x'} \langle x'(s) | x(s) - x(0) | x''(0) \rangle$$

vanishes whatever the transformation function, it is sufficient in our approximation to use the transformation function of the constant magnetic field with $f_{\mu\nu}(x) = 0$.

Introducing the Fourier transform of

$$f_{\mu\nu}(x) = \frac{1}{(2\pi)^2} \int f_{\mu\nu}(k) \exp[ik \cdot x] d^4k,$$

we have then to calculate the following matrix elements

$$\begin{aligned} (a) \quad & \lim_{x'' \rightarrow x'} \langle x'(s) | \exp[ik \cdot x^*(s')] | x''(0) \rangle \\ (b) \quad & \lim_{x'' \rightarrow x'} \langle x'(s) | \exp[ik \cdot x^*(s')] \Pi_\mu(s') | x''(0) \rangle \\ (c) \quad & \lim_{x'' \rightarrow x'} \langle x'(s) | \sigma_{lm} | x''(0) \rangle, \end{aligned}$$

which will be examined in the appendix.

The covariant result is

$$\begin{aligned} (11) \quad \delta j_\mu(x') &= \frac{2e^2}{(2\pi)^2(4\pi)^2} \int_0^1 dv \int_0^\infty ds \int d^4k \exp[ik \cdot x'] \exp[R] \cdot \\ & \cdot \left\{ \left[\frac{eh_0 \operatorname{ctnh}(eh_0 s)}{\sinh(eh_0 s)} v \sinh(eh_0 sv) - \frac{1}{s} \right] i f_{\mu i}(k) k_i + \right. \\ & - \left[\frac{1}{e^2 h_0^2 s} - \frac{\operatorname{ctnh}(eh_0 s)}{eh_0} \left(1 - v^2 + v \frac{\sinh(eh_0 sv)}{\sinh(eh_0 s)} \right) \right] i e^2 \tilde{h}_{\mu i} f_{i l}(k) \tilde{h}_{l r} k_r \\ & - \left[\frac{1}{e^2 h_0^2 s} - \frac{v \sinh(eh_0 sv) \operatorname{ctnh}(eh_0 s)}{eh_0 \sinh(eh_0 s)} + \frac{2 \cosh(eh_0 sv)}{eh_0 \sinh^3(eh_0 s)} - \right. \\ & \left. \left. - \frac{2 \cosh(eh_0 s)}{eh_0 \sinh^3(eh_0 s)} \right] i e^2 h_{\mu i} f_{i l}(k) h_{l r} k_r \right\}, \end{aligned}$$

with

$$R = -s \left[m^2 + \frac{1}{4} k^2 (1 - v^2) \right] - \frac{e^2}{2} [k_i h_i h_{iv} k_v] \cdot \left[\frac{1}{2} \frac{s(1 - v^2)}{e^2 h_0^2} + \frac{\cosh(e h_0 s v) - \cosh(e h_0 s)}{e^3 h_0^3 \sinh(e h_0 s)} \right],$$

where $\tilde{h}_{rs} = \frac{1}{2} i \varepsilon_{rs\mu\nu} h_{\mu\nu}$ and $\varepsilon_{rs\mu\nu}$ is $+1$, or -1 if $(rs\mu\nu)$ forms an even or odd permutation of $(1\ 2\ 3\ 4)$ and is zero otherwise; h_0 is the real scalar quantity $\sqrt{h_{\mu\nu} h_{\mu\nu}}/2$. In order to obtain (11) two changes of variables have been made, namely

$$s' - \frac{1}{2}s \rightarrow s \frac{v}{2},$$

and

$$s \rightarrow -is.$$

Charge conservation of (11) is easily verified, as well as the even parity of the integral with respect to the magnetic field, (Furry theorem). The $\delta j_\mu(x')$ current contains three terms, the first of which can contribute only if the $J_\mu^{\text{ext}}(x')$ current associated with the $j_{\mu\nu}(x')$ field is different from zero. The other two terms give contribution if at least one of the quantities

$$\frac{\partial f_{12}(x')}{\partial x'_1}; \quad \frac{\partial f_{12}(x')}{\partial x'_2}; \quad \frac{\partial f_{34}(x')}{\partial x'_3}; \quad \frac{\partial f_{34}(x')}{\partial x'_4},$$

is different from zero. The term depending upon $J_\mu^{\text{ext}}(x')$ is the only one that requires charge renormalization. This is accomplished by decomposing the $J_\mu^{\text{ext}}(x')$ dependent term into

$$(12) \quad \left[\frac{e h_0 \operatorname{ctnh}(e h_0 s)}{\sinh(e h_0 s)} v \sinh(e h_0 s v) - \frac{v^2}{s} \right] + \left[\frac{v^2}{s} - \frac{1}{s} \right],$$

which transfers the singularity of the integral at $r = 0$ into the second term of (12).

Performing an integration by parts over v in the second term of (12) we obtain

$$\begin{aligned} & - \frac{e^2}{(4\pi)^2} \frac{2}{3} \int_0^\infty \frac{1}{2s} \exp[-sm^2] ds J_\mu^{\text{ext}}(x') + \frac{2e^2}{(2\pi)^2 (4\pi)^2} \int_0^1 dv \int_0^\infty ds \int d^4k \exp[ik \cdot x'] \exp[R] \cdot \\ & \cdot \left\{ \frac{e h_0 \operatorname{ctnh}(e h_0 s)}{\sinh(e h_0 s)} v \sinh(e h_0 s v) - \frac{v^2}{s} - \right. \\ & \left. - \left(\frac{v^3}{3} - v \right) \left[\frac{1}{2} k^2 v + \frac{e^2}{2} k_i h_i h_{iv} k_v \frac{v}{e^2 h_0^2} - \frac{e^3 h_0}{2} k_i h_i h_{iv} k_v \frac{\sinh(e h_0 s v)}{e^3 h_0^3 \sinh(e h_0 s)} \right] \right\} J_\mu^{\text{ext}}(k), \end{aligned}$$

and the logarithmic divergent multiple of the external current can be ignored if we perform the usual charge renormalization. This does not depend on the magnetic field strength, which is reasonable, the sources of the constant field being located at the infinity.

The finite covariant result can be expressed by

$$(13) \quad \delta j_{\mu}(x') = M_0 \left[\square', h_0^2 \left(\frac{\partial^2}{\partial x_1'^2} + \frac{\partial^2}{\partial x_2'^2} \right), h_0^2 \right] j_{\mu}^{\text{ext}}(x') + \\ + M_1 \left[\square', h_0^2 \left(\frac{\partial^2}{\partial x_1'^2} + \frac{\partial^2}{\partial x_2'^2} \right), h_0^2 \right] \tilde{h}_{\mu l} \tilde{h}_{lr} \frac{\partial f_{lr}(x')}{\partial x_r'} + M_2 \left[\square', h_0^2 \left(\frac{\partial^2}{\partial x_1'^2} + \frac{\partial^2}{\partial x_2'^2} \right), h_0^2 \right] \tilde{h}_{\mu l} \tilde{h}_{lr} \frac{\partial f_{lr}(x')}{\partial x_r'}.$$

The M_i functions cannot be given in closed form, unless one chooses very special $f_{\mu\nu}(x')$ fields.

In the interesting case in which $f_{\mu\nu}(x')$ is the quantized tensor field associated with the free photon field $A_{\mu}(x')$, the expression (13) simplifies to

$$\delta j_{\mu}^{\text{rad}}(x') = M_1 \left[0, h_0^2 \left(\frac{\partial^2}{\partial x_1'^2} + \frac{\partial^2}{\partial x_2'^2} \right), h_0^2 \right] \tilde{h}_{\mu l} \tilde{h}_{lr} \frac{\partial f_{lr}(x')}{\partial x_r'} + \\ + M_2 \left[0, h_0^2 \left(\frac{\partial^2}{\partial x_1'^2} + \frac{\partial^2}{\partial x_2'^2} \right), h_0^2 \right] \tilde{h}_{\mu l} \tilde{h}_{lr} \frac{\partial f_{lr}(x')}{\partial x_r'}.$$

and this current gives rise to an energy density of the photons in the magnetic field

$$(14) \quad -\frac{1}{2} : A_{\mu}(x') \delta j_{\mu}^{\text{rad}}(x') :$$

which adds to the energy density of the free photon field. In a paper to follow we will examine the physical meaning of the non-linear effects contained in (14). We will also study the analytical properties of the M_i functions in the neighbourhood of $h_0 = 0$, and an approximate expression for (14).

* * *

The author is indebted to Prof. J. SCHWINGER for valuable discussions during his stay at the Les-Houches Summer School.

APPENDIX

The matrix elements *a*), *b*) can be calculated following the procedure of reference (1), Appendix A. We give the results

$$a) \lim_{x'' \rightarrow x'} \langle x'(s) | \exp[ik \cdot x^*(s')] | x''(0) \rangle = \exp[ik \cdot x'] \exp[-\frac{1}{2}N] \lim_{x'' \rightarrow x'} \langle x'(s) | x''(0) \rangle,$$

$$b) \lim_{x'' \rightarrow x'} \langle x'(s) | \exp[ik \cdot x^*(s')] I_{\mu}(s') | x''(0) \rangle = \\ = -\exp[ik \cdot x'] \exp[-\frac{1}{2}N] R_{\mu l}(s') I_{\mu}^{-1}(s) R_{l\nu}(s) [1 - I(s') I^{-1}(s)]_{\tau\nu} k_{\tau} \lim_{x'' \rightarrow x'} \langle x'(s) | x''(0) \rangle,$$

where

$$N = i(k_3^2 + k_4^2) \left(2s' - \frac{2s'^2}{s} \right) + i(k_1^2 + k_2^2) \cdot \\ \cdot \left[\frac{\sin(2eh_{12}s')}{eh_{12}} - \frac{[1 - \cos(2eh_{12}s')] \sin(2eh_{12}s)}{eh_{12}[1 - \cos(2eh_{12}s)]} \right],$$

and $\langle x'(s) | x''(0) \rangle$ is given in reference (1) p. 668.

In order to calculate

$$c) \langle x'(s) | \sigma_{lm} | x''(0) \rangle,$$

we notice that a term of this form arises when we calculate the transformation function in the case of a «large» electromagnetic field h_{12} and a «small» electromagnetic field whose only component is $f_{lm} = 1$. Comparing the corresponding transformation function in first order in f_{lm} with the exact one (reference (1) p. 668) we obtain the results: when $l = 1$ and $m = 2$, or $l = 3$ and $m = 4$, σ_{lm} can be brought at the right or left side of the transformation function, according to the fact that σ_{12} commutes with itself and with σ_{25} .

In all the other cases:

$$\langle x'(s) | \sigma_{lm} | x''(0) \rangle = \langle x'(s) | x''(0) \rangle \exp[-i\sigma_{12}eh_{12}s] \sigma_{lm} \frac{\sin(eh_{12}s)}{eh_{12}s}.$$

RIASSUNTO

Abbiamo calcolato la corrente di polarizzazione del vuoto indotta dalla sovrapposizione di un campo elettromagnetico costante, caratterizzato da $\mathbf{e} \cdot \mathbf{h} = 0$, $h^2 - e^2 > 0$, e un «piccolo» campo comunque variabile, senza usare il procedimento perturbativo per quanto si riferisce al campo elettromagnetico costante. Si è inoltre calcolato il contributo alla densità di energia di un campo di fotoni dovuto all'accoppiamento dei fotoni con il campo elettromagnetico costante.

On the Consequences of the Possible Existence of the Hyperdeuteron (*).

M. FERENTZ and S. RABOY

Argonne National Laboratory - Lemont, Illinois

(ricevuto l'11 Giugno 1956)

Summary. — It is suggested that the observation of a hyperdeuteron is an indirect method for detection of the neutral cascade particle which is predicted by the scheme of Gell-Mann and that of Salam and Polkinghorne. The consequences for these schemes are examined and some possible methods for preferential selection of one of the schemes are suggested.

1. — The Hyperdeuteron.

The recent schemes for classifying the new particles ^(1,2) require that the negatively charged cascade particle, Ξ^- , be a member of a charge doublet. Its partner is a neutral particle which should decay « weakly » ($\sim 10^{-10}$ s) in the following way

$$\Xi^0 \rightarrow \Lambda^0 + \pi^0.$$

Direct observation of this decay is clearly difficult, but we suggest that observation of a positively charged hyperfragment of about the same mass as a deuteron is an indirect method for verification of the existence of the Ξ^0 .

Within the G and SP theories this is the only possibility for a hyperdeu-

(*) Work performed under the auspices of the U. S. Atomic Energy Commission.

(¹) M. GELL-MANN and A. PAIS: *Proceedings of the International Physics Conference* (Glasgow, July 1954). This scheme will hereafter be designated as the G. scheme.

(²) A. SALAM and J. C. POLKINGHORNE: *Nuovo Cimento*, **2**, 685 (1955). This scheme will be designated as the SP scheme.

teron since the alternative possibilities $\Lambda^0 + p$, $\Sigma^0 + p$, and $\Sigma^+ + n$ are excluded ⁽³⁾. Experimental evidence of the binding of the Λ^0 to nucleons in the heavier hyperfragments indicates that a nucleon- Λ^0 system would be unbound. The Σ -nucleon possibilities are excluded since the reactions

$$\Sigma^0 + p \rightarrow p + \Lambda^0$$

$$\Sigma^+ + n \rightarrow p + \Lambda^0$$

would proceed rapidly ($\sim 10^{-23}$ s), whereas the only energetically possible decays for the Ξ^0 -p system are weak interactions. A mode of decay of the metastable Ξ^0 -p system has been given by GATTO ⁽⁴⁾.

$${}^2\text{H}^* \equiv (\Xi^0 + p) \rightarrow p + \Lambda^0 + \pi^0.$$

There exists a picture ⁽⁵⁾ which may contain a decay of a hyperdeuteron. A K^- particle is observed to come to rest and produce a star, from which a singly charged hyperfragment ejects a 26 MeV proton, after coming to rest. This observation is consistent with GATTO's suggested decay mode.

It is in the classification of K-mesons that the G and SP schemes differ. In the G scheme the conservation of strangeness is violated in the production of Ξ particles by K^- absorption. In the SP scheme, on the other hand, the process ⁽⁶⁾

$$\tau^- + p + p \rightarrow \Xi^0 + p \equiv {}^2\text{H}^*$$

is fully allowed. Thus, if the creation of hyperdeuterons by a K^- -meson beam is firmly established in the future, this would be a definite indication of nature's preference for the SP as against the G scheme. It should be noted, however, that the observation of hyperdeuterons in cosmic ray events or as a result of nucleon-nucleon events is consistent with both schemes.

The existence of the hyperdeuteron implies that the Ξ -nucleon binding is stronger than the Λ^0 -nucleon binding. In the SP scheme the interaction of the Ξ with nucleons is via the τ field while the Λ^0 interacts via the θ field. There is no reason to believe that the coupling constants of both fields are equal. In the G scheme the coupling of Ξ particles to nucleons is performed via two K-mesons as against the single K-meson coupling of the Λ -nucleon interaction. For large enough coupling constants the two K-meson coupling

⁽³⁾ J. M. BLATT and S. T. BUTLER: *Nuovo Cimento*, **3**, 409 (1956).

⁽⁴⁾ R. GATTO: *Nuovo Cimento*, **3**, 318 (1956).

⁽⁵⁾ E. P. GEORGE, A. J. HERZ, J. H. NOON and N. SOLNTSEFF: *Nuovo Cimento*, **3**, 94 (1956).

⁽⁶⁾ We shall use the term K-mesons when referring to the G scheme or to the experimentally observed mesons. In the SP scheme the two kinds of K-mesons will be designated as τ -mesons and θ -mesons.

can be stronger than the one K-meson coupling. If this were the case hyperons of still higher strangeness would be bound even more strongly to nucleons.

2. - Particles of Higher Strangeness.

The assumption that « Nature abhors » multiply charged elementary particles may be used to delimit the number of types of elementary particles in the G and SP schemes. SALAM and POLKINGHORNE, in their paper, observe that with this assumption only a hyperon triplet (0, 1) and a K-meson singlet (0, 0) might still exist. The (0, 0) K-meson is almost certainly undetectable (lifetime $\sim 10^{-23}$ s) and a (0, 1) hyperon of mass greater than 2800 would go rapidly to a nucleon and a θ . The same assumption applied to the G scheme allows only a nucleon number one, strangeness -3 , negatively charged singlet, and a nucleon number zero, strangeness 2, positively charged singlet, and their anti-particles.

If the $S = -3$ particle has mass greater than 3550 electron masses it would be unobservable because of the fast decay

$$\Omega^- \rightarrow \Xi^- + \bar{K}^0$$

or

$$\Omega^- \rightarrow \Xi^0 + K^-$$

It is reasonable to suppose that the mass of this particle would be greater than 2850 electron masses (the sum of the rest masses of the π and Ξ) and, therefore, would not overlap the mass of the missing SP particle. The detection of a weakly decaying charged particle between 2850 and 3550 electron masses would indicate a preference for the G scheme.

The Ω^- particle would be made in association with three K-mesons and it is unlikely that this particle can be produced in the Bevatron since the threshold is too high.

The hyperon in the event reported by EISENBERG (?) is in the 2800 to 3550 mass range and its weak decay is consistent with

$$\Omega^- \rightarrow \Lambda^0 + K^-$$

in the G scheme. We would expect the alternative modes

$$\Omega^- \rightarrow \Xi^- + \pi^0$$

or

$$\Omega^- \rightarrow \Xi^0 + \pi^-$$

to be observed since these reactions, in fact, require less energy.

(?) Y. EISENBERG: *Phys. Rev.*, **96**, 541 (1954).

If the $S = 2$ boson had mass greater than 1930 electron masses it would not be observable since it would go strongly into two K-mesons. For a mass less than the 1930 electron masses its creation would be expected in association with the Ξ particle. One cosmic ray event ⁽⁸⁾ shows a Ξ^- created with two neutral K-mesons. This cannot be used to exclude the $S = 2$ boson since at high energies the threshold differences would be counterbalanced by the increased phase space available for three body decay.

3. - Conclusions.

1. Any observation of a hyperdeuteron is consistent with at least one of the two schemes discussed.

2. In both the G and SP schemes a hyperdeuteron is uniquely made up of a Ξ^0 bound to a proton.

3. The SP scheme would allow Ξ^0 creation or hyperdeuteron creation as a result of a K^- absorption, while such an observation is forbidden by the G scheme.

4. With the assumption that only singly charged elementary particles exist, the two schemes lead to different properties for as yet unobserved particles. The existence of a weakly decaying charged particle with mass greater than 2800 but less than 3550 is consistent with G but not SP, whereas an observed particle of mass less than 2800 would favor SP.

5. Both the G and SP schemes will be untenable if future experimental results corroborate both the Eisenberg picture and the formation of the Ξ^0 -p hyperdeuteron by K^- -meson absorption.

* * *

We would like to express our appreciation to M. HAMERMESH, G. R. RINGO, and L. C. TENG for many stimulating discussions.

(⁸) S. D. SORRELS, R. B. LEIGHTON and C. D. ANDERSON: *Phys. Rev.*, **100**, 1457 (1955).

RIASSUNTO (*)

Si suppone che l'osservazione di un iperdeutone sia un metodo indiretto per la rivelazione della particella neutra della cascata predetta dallo schema di Gell-Mann e da quello di Salam e Polkinghorne. Si esaminano le conseguenze di tali ipotesi per i predetti schemi e si suggeriscono alcuni metodi possibili per la scelta preferenziale di uno di tali schemi.

(*) Traduzione a cura della Redazione.

On n-Pentane Bubble Chambers.

P. BASSI, A. LORIA, J. A. MEYER (*), P. MITTNER and I. SCOTONI

Istituto di Fisica dell'Università - Padova

Istituto Nazionale di Fisica Nucleare - Sezione di Padova

(ricevuto il 29 Maggio 1956)

Summary. — Both a clean and a dirty n-pentane bubble chamber have been operated. A description is given together with the results of an investigation into the influence which working conditions have on the sensitive time, and the size and number of the bubbles produced along the tracks. The number of bubbles per cm and their size are practically constant over a wide range of the final pressure; the foam limit does not depend on the final pressure. The sensitive time can be appreciably increased by an increase of the final pressure and there is a temperature range of a few degrees where the number of bubbles per cm is practically constant.

1. — Introduction.

The first bubble chamber was made and operated in 1952 by D. A. GLASER ⁽¹⁾. With this instrument the passage of ionizing particles through a superheated liquid is rendered visible by means of the small bubbles of vapour which appear along the trajectories; the superheating is obtained by a sharp decompression of the liquid.

A spherical vapour bubble will grow spontaneously in a superheated liquid when its radius is greater than a critical value r_k . The energy necessary to form in a reversible and isothermic way a bubble of radius r_k is

$$w_k = \frac{16\pi\sigma^3}{3(p_\theta - p)^2},$$

where σ and p_θ are respectively the surface tension of the liquid and the pres-

(*) On leave of absence from the Faculdade de Filosofia, Ciencias e Letras, São Paulo (Brazil).

⁽¹⁾ D. A. GLASER: *Phys. Rev.*, **87**, 665 (1952); **91**, 762 (1952); *Suppl. Nuovo Cimento*, **11**, 361 (1954).

sure of the saturated vapour at the working temperature θ , while p is the hydrostatic pressure ⁽²⁾.

An ionizing particle may be expected to be able to form bubbles if it transfers energy of the order of w_k to the critical volume of radius r_k : in fact, experience shows that it is best to work with liquids of low surface tension, brought to considerable superheating by means of large pressure variations. Conditions favourable to the formation of bubbles can be maintained only for very short periods of time ⁽³⁾, certainly less than 10^{-4} s, and perhaps by some orders of magnitude: this fact has so far prevented counter control of bubble chambers.

The mechanism of bubble formation is not yet fully understood. GLASER ⁽¹⁾ initially proposed an electrical model based on the repulsion of ions of the same sign; this theory has been developed by L. BERTANZA, G. MARTELLI and A. ZACUTTI ⁽⁴⁾. It seems however that the great majority of the ions recombine in 10^{-8} s ⁽⁵⁾, which raises doubts about this type of model.

The bubbles could also be due to a local heating resulting from a direct transfer of kinetic energy from the ions, or clusters of ions, as produced for example by δ -rays, to the nearby molecules during the recombination: however, the lack of precise information about the processes involved renders the basis for the development of such a theory very insecure.

Liquids successfully used are helium, hydrogen, deuterium, some hydrocarbons, sulphur dioxide, methyl alcohol, xenon, tin tetrachloride; the temperature of operation ranging from about -269°C for He to about 390°C for SnCl_4 .

Bubble chambers are of two types, «clean» and «dirty». Clean chambers have their sensitive volume limited by a single glass surface, free from any irregularity: between the sensitive zone and the movable part there must therefore be a temperature gradient. On the other hand the various types of dirty chamber have metallic parts, gaskets etc. in direct contact with the sensitive liquid. Here a temperature gradient is not essential, but may be used to enable the compression system to work at room temperature.

There are two possible modes for the recycling: rapid recycling with cycles of the order of tenths of a second ⁽⁶⁾ in which the bubbles are recompressed practically where they originate, and slow recycling with cycles of the order of a minute, in which the bubbles rise and then coalesce at the summit of the chamber.

In this article we describe in some detail a clean and a dirty n-pentane bubble chamber. They were expanded for periods of about one s at constant intervals — the value of which is called the recycling time — of about one minute from a fixed initial pressure of 25 atm to a regulable final pressure, equal or greater than atmospheric. A greater initial pressure allows faster recycling because the bubbles disappear more quickly. Our results concern

⁽²⁾ M. VOLMER: *Kinetik der Phasenbildung* (Dresden 1939).

⁽³⁾ D. A. GLASER and D. C. RAHM: *Phys. Rev.*, **97**, 474 (1955).

⁽⁴⁾ L. BERTANZA, G. MARTELLI and A. ZACUTTI: *Nuovo Cimento*, **1**, 324 (1955); **2**, 487 (1955).

⁽⁵⁾ L. B. LOEB: *Kinetic Theory of Gases* (London, 1934).

⁽⁶⁾ J. LEITNER, N. SAMIOS, M. SCHWARTZ and J. STEINBERGER: *Rep. Nevis 10 Columbia Univ. New York*.

the influence of working temperature θ , final pressure p , recycling time T and expansion ratio $\delta = \Delta V/V$, where V is the volume of the pentane, on the sensitive time τ during which the chamber reveals the tracks of the particles which pass through it, on the number n of bubbles produced per cm and on the diameter a reached by the bubbles when they are photographed.

The number n itself is not given: reference is made instead to a similar parameter, the apparent bubble density N , which has been directly measured and faithfully reflects the behaviour of n .

2. - Description of the Apparatus.

2.1. *The clean chamber* (*) (Fig. 1) is a glass bottle 1 of square cross section having dimensions of $50 \times 50 \times 150$ mm³, with two faces optically worked and a domed base. It should be capable of withstanding internal pressures of the order of 30 to 40 atm, but for greater security it has been mounted inside a pressure tank having two glass windows 2 and filled with water at 12 atm, equal to half the maximum pressure which has been applied to the pentane. The pressure on the water is obtained by a piston loaded with a suitable weight.

The lower end of the tank is provided with a connector 3 for coupling directly to the terminal flange of the compression system. The bottle is mounted neck downwards and the rim is held tightly onto a corresponding profile on the inner surface of the connector by a force of about 60 kg. This is effected by a lever which transmits its thrust to the base of the bottle via a small plunger 4 mounted in the roof of the tank. A small teflon washer 5 prevents direct contact between the glass rim and the metal, but the seal is made by means of an O-ring 6. Mounted in this way the bottle is not rigidly held by metallic supports and is therefore free from thermal stresses. The choice of water for the liquid to fill the space between the bottle and the tank presents several advantages over the use of other liquids: for example being insoluble in pentane it would not interfere with the functioning of the chamber if a small quantity happened to penetrate inside. Further its high specific heat makes it particularly suitable for thermal stabilization. For this purpose the water is heated by a nichrome resistance 7 insulated with fiber-glass and situated in a groove, machined in the outer surface of the tank. The change in volume of the water with temperature is transmitted via the movements of its compression piston to a relay system which controls the current in the resistance.

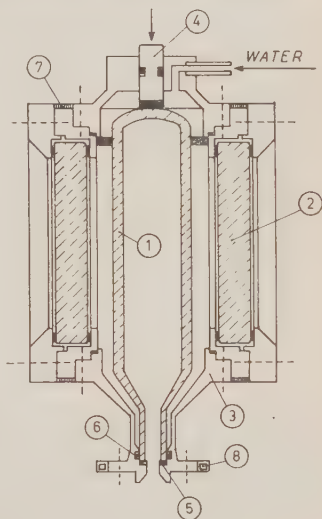


Fig. 1. - The clean chamber in its pressure tank.

(*) P. BASSI, P. MITTNER and I. SCOTONI: *Nuovo Cimento*, 2, 1334 (1955).

The temperature gradient between the sensitive zone and the moving diaphragm is formed in the neck of the bottle by means of the water cooler 8. We measure directly, using a mercury thermometer, the temperature of the metal body of the tank: however it has been noted that this coincides to within 1°C with that of the pentane as deduced from the measured pressure of the saturated vapour.

Operating conditions are reached after a heating time of six hours.

2.2. The dirty chamber (Fig. 2) consists of a brass cylinder 1 which is 70 mm in diameter and 40 mm deep, fitted with two plane glass windows 2; the seals are made with teflon gaskets. The connection to the terminal flange of the compression system is obtained through a tube 3 of 20 mm internal diameter by 170 mm length, machined from the same brass block as the chamber, and along which the temperature gradient is formed.

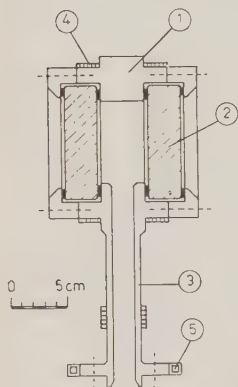


Fig. 2. - The dirty chamber.

There are three heaters: two of them 4, consisting of nichrome wire insulated with fiberglass, are wound directly onto the chamber in grooves, machined in the outer surface of the body. The third is about half way up the vertical connecting tube and, together with a water cooler 5 situated lower down, defines the zone of the temperature gradient. An electric contact thermometer measures the temperature of the main body and maintains it stable to within a few tenths of a degree; a thermocouple located between the thermometer and the lower heater checks the stability of the temperature in the useful zone.

Operating conditions are reached after a heating time of one hour.

2.3. The compression system (Fig. 3) has been used with both chambers since they are interchangeable. It consists, essentially, of a hydraulic lever. The metallic disc 1 of 300 mm diameter is free to move between two volumes, one external (a) and one internal (b). The seal between (a) and (b) is made by means of a rubber membrane, whose periphery is clamped between the metal pieces 2 and 3, while its central part is fixed to the external face of the disc.

Volume (a) is in communication with the atmosphere through holes in the metal piece 2, while, by means of a valve 4 a reduction of pressure may be produced in volume (b): this valve consists of a three-way distributor in which moves a piston operated by a motor. Solid with the disc 1, through a threaded rod 5 screwed into it, is the piston 6 which moves in a cylinder 7 of 50 mm diameter. The front surface of the piston faces volume (c) filled with light mineral oil. When a partial vacuum is produced in (b), a pressure which can reach 35 atm is applied to this liquid.

The relative positions of the disc and the piston can be changed by turning the threaded rod. Thus one can adjust both the stroke and the position of the piston to suit the quantity of liquid in (c) and in the chamber: the stroke may also be adjusted by means of the screwed collar 8.

It is possible to fix the final pressure by means of the synthetic rubber

diaphragm 9, separating volume (c) from volume (d) which is filled with nitrogen. As long as the pressure in (c) is greater than that in (d) the diaphragm rests against the perforated plate 10. The pressure in (c) is transmitted directly to the pentane via the teflon membrane 11 which is free to move between two perforated metal plates. Filling of the chambers is effected through holes in the terminal flange 12 of the compression system.

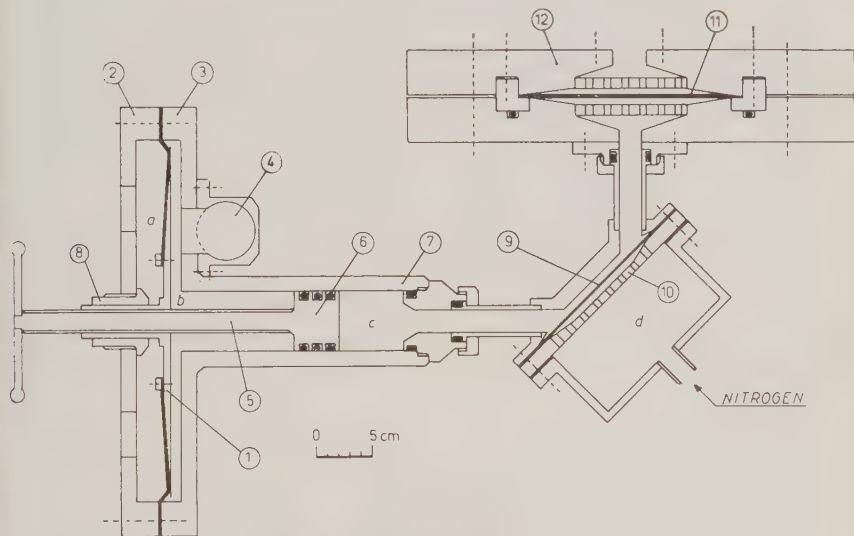


Fig. 3. — The compression system.

A small piston, held in an equilibrium position by a spring, acts on a contact which is closed only during the interval of time in which the pressure in (c) is less than a value determined by the tension of the spring. It is possible to measure the pressure in (c), which is also that in the chamber, by means of a manometer. The recycling is regulated by an arrangement based on time controlled relays.

Photographs are taken with a stereoscopic angle of 35° at a distance of 50 cm from the center of the chamber: the magnification is 0.2. During the decompression the shutters of the cameras remain open and a microsecond flash may be triggered while the contact mentioned is closed.

3. — Results.

3.1. — Since the compression system does not allow the beginning of the cycle, and therefore the beginning of the sensitive time τ to be determined with precision, the sensitivity of the chamber has been explored at random in an interval following the decompression which certainly includes τ . We

have used 1 ms pulses of γ -rays from RaD injected with a repetition time τ' of 40 ms. The delay between the pulse and the flash is $t = 1$ ms.

The mean number of Compton electrons produced by a pulse is about 20 in the clean chamber and 10 in the dirty chamber (Plate I). It may be held that the ratio τ/τ' is equal to the ratio of the number of photographs with pulses to the total number: the pictures were considered as recording a pulse if they showed at least five tracks. The values of τ so obtained lie between 10 and 30 ms.

The counting of the bubbles and the measurement of their diameter a has been carried out by direct observation of the photographs of one camera projected at a suitable magnification onto a screen. Suppose that the magnification is full scale (though this need not be so). To be sure of always having minimum ionization, tracks were selected which had lengths of at least 1 cm, and the counting was confined to portions of 0.5 cm starting from the origin. Twice this number is what we call the bubble density N . It should be noted that

values for N obtained under different conditions may be usefully compared as N differs from the real mean value n of the number of bubbles per cm by a factor which is practically constant for the various cases.

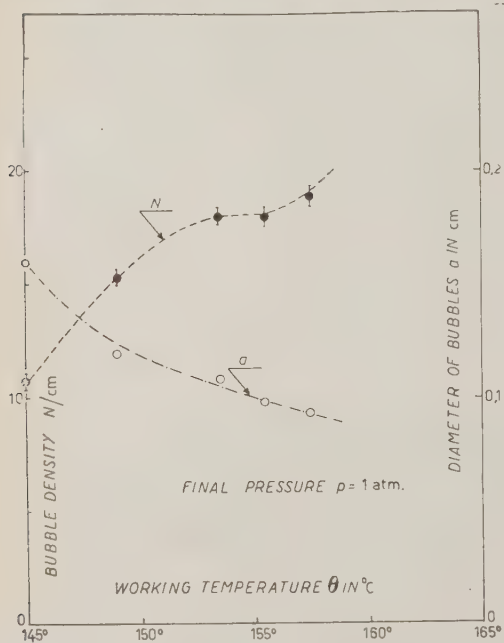


Fig. 4. — The bubble density and the diameter of the bubbles in the clean chamber as a function of the working temperature, for a final pressure of 1 atm.

3.2. — We have found that in our clean chamber the end of τ is determined by boiling from the walls with a frequency which increases with temperature, and actually that by expanding the chamber at 153.5°C without γ -rays, boiling always starts from the walls. This does not invalidate the distinction between clean and dirty chambers, since on comparison considerable differences have been noted particularly in the value of τ : the difference is however not as complete as had been thought.

In Fig. 4 N and a are plotted against temperature θ for final pressure $p = 1$ atm.

The first of these curves shows that there is an interval of θ of a few degrees in which N is practically constant. The second curve shows that a decreases with increasing θ .

In Fig. 5 N and a are given as functions of p for $\theta = 153.5^\circ\text{C}$, the value selected as being in the middle of the range where N is relatively independent of θ . It is to be observed that N is almost constant for the interval of p from



Plate. I. — Compton electrons produced by γ -rays from RaD in the dirty chamber,

1 to 9 atm, i.e. the same value of N extends practically to that value of p beyond which tracks cannot be formed. The interval is quite considerable: at 153.5°C the vapour pressure of pentane is 17 atm. It should be noted that the same number of bubbles per cm are formed although the energy w_k for $p=9$ atm is four times that for 1 atm.

With p increasing above 9 atm, N decreases very rapidly: this explains the occurrence of tracks having abnormally low density if the particles cross the chamber while the pressure is still too high.

PLESSET and ZWICK⁽⁸⁾ have calculated the rate of growth of a spherical homogeneous vapour bubble in a liquid at constant temperature and pressure. Compressibility and viscosity of the liquid are ignored: cooling due to evaporation is instead taken into account. To a first approximation

$$\frac{dr}{dt} = \left(\frac{3}{\pi}\right)^{\frac{1}{2}} (\vartheta - \vartheta') \cdot \left(\frac{K}{\sqrt{D}}\right)_{\vartheta} \left(\frac{1}{c\rho}\right)_{\vartheta'} \cdot \frac{1}{\sqrt{t}},$$

where ϑ is the temperature of the liquid, ϑ' is that at which the pressure of the saturated vapour is equal to the hydrostatic pressure, K is the thermal conductivity, D the diffusivity, c the latent heat of evaporation and ρ the vapour density.

From this expression one sees that:

- 1) for equal working conditions a should be proportional to \sqrt{t} and to K ;
- 2) for constant ϑ' , a should be proportional to $\vartheta - \vartheta'$;
- 3) for constant ϑ , a should decrease with increasing ϑ' .

Previous experimental results^(3,9) agree with conclusion 1). Our measurements seem instead to indicate that a decreases with increasing ϑ for constant ϑ' and practically does not vary with varying ϑ' for constant ϑ . The

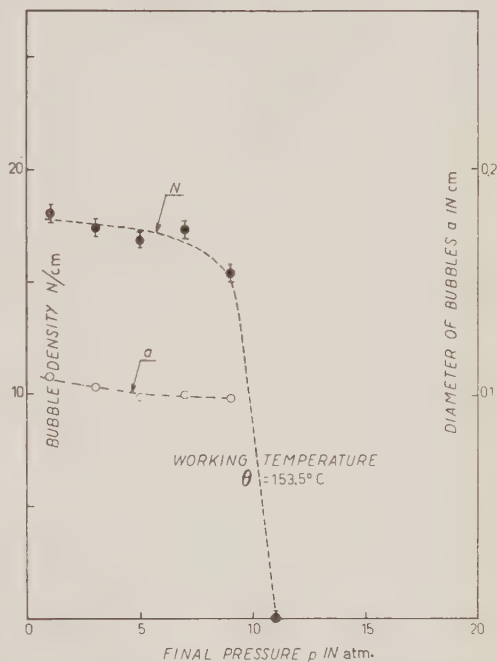


Fig. 5. - The bubble density and the diameter of the bubbles in the clean chamber as a function of the final pressure, for a working temperature of 153.5°C.

⁽⁸⁾ M. S. PLESSET and S. A. ZWICK: *Journ. Appl. Phys.*, **25**, 493 (1954).

⁽⁹⁾ H. C. DITTLER, and T. F. GERECKE: *M. S. Thesis*, Univ. California, Berkeley.

disagreement might be explained by considering that the decrease of pressure is slowed down by the growth of the bubbles.

In Fig. 6 τ is given in terms of ϑ for $p = 1, 7, 9$ and 11 atm: measure-

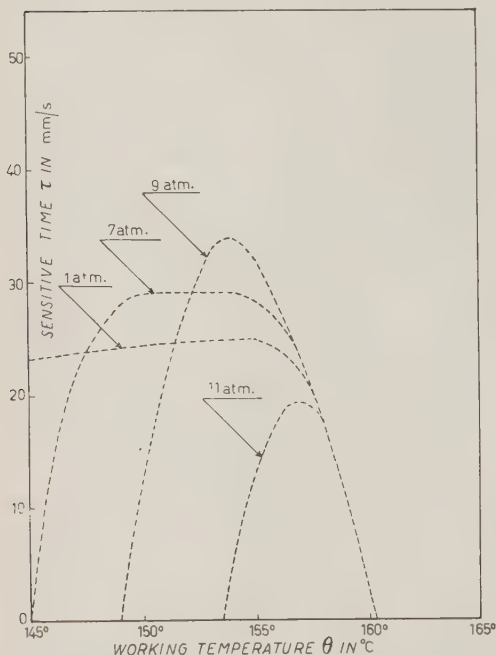


Fig. 6. — The sensitive time of the clean chamber as a function of the working temperature for various final pressures.

ments have been made at intervals of 3 °C and errors in τ are less than 10%. It appears that with a suitable choice of temperature, the sensitive time will increase with an increase of the final pressure of the cycle: for example, passing from 1 to 9 atm at a temperature of 153.5 °C, τ increases from 24 to 34 ms. This may be explained by the observation already made that the superheating of the chamber almost always ends with boiling from the walls. The increase of the final pressure probably lowers the growth of the bubbles with a consequent increase of the sensitive time. From Fig. 6 one sees also that the foam limit, i.e. the temperature above which the liquid cannot be rendered sensitive to radiation, is independent of the final pressure.

3.3. — A dirty chamber can differ to varying degrees from a «clean» chamber in its behaviour. A criterion could be the maximum temperature at

which a surface succeeds in maintaining the superheating for a time equivalent to that of a glass surface free from irregularities. We have found that in pentane, with $p = 1$ atm, instead of a temperature of 150 °C for glass, one obtains ~50 °C for rubber and teflon gaskets and ~100 °C for araldite seals. On the other hand it has been possible to obtain metal surfaces which are as «clean» as glass⁽¹⁰⁾.

In Fig. 7 N and α are given as functions of ϑ for $p = 1$ atm. ϑ has been measured with a mercury thermometer in the metal body of the chamber. This might introduce an error of the order of 1 °C in the temperature of the liquid.

With the dirty chamber there is also an interval of a few degrees over which N is practically constant. The value of 21 for N is slightly higher than the corresponding value of 18 obtained for a clean chamber: perhaps this may

⁽¹⁰⁾ M. ANNIS, P. BASSI, P. MITTNER and I. SCOTONI: *Univ. College Conf. London* (1955).

be explained by the fact that in the clean chamber the bubbles were much larger and overlapping could more easily occur.

In Fig. 8 N and a are given as a function of p for $\theta = 155^\circ\text{C}$: the results are similar to those obtained with the clean chamber.

All the above measurements have been made with a recycling time $T=1$ min and an expansion ratio $\delta=1.107$. Table I shows some data concerning the dependence of τ on p , T and δ , taken at $\theta = 155^\circ\text{C}$.

In addition to the information presented in Table I *a*), we observed that the dependence of τ on p decreases with increasing T and disappears for T greater than 4 min.

This leads one to think that this dependence would be more marked in the case of rapid recycling. We think that in general the dependence of τ on p is due to the influence of the growth of those bubbles which originate at the walls.

The dependence of τ on T indicated by Table I *b*) can be justified by considering that with an increase of T the liquid infiltrates deeper into the interstices of the gaskets, thus lead-

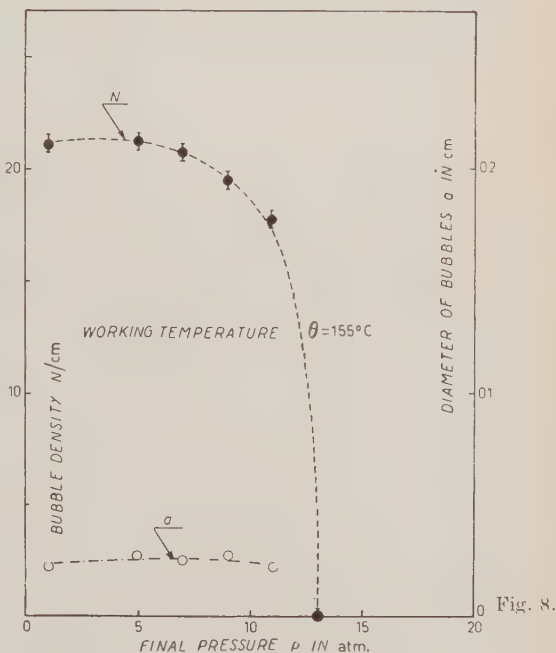
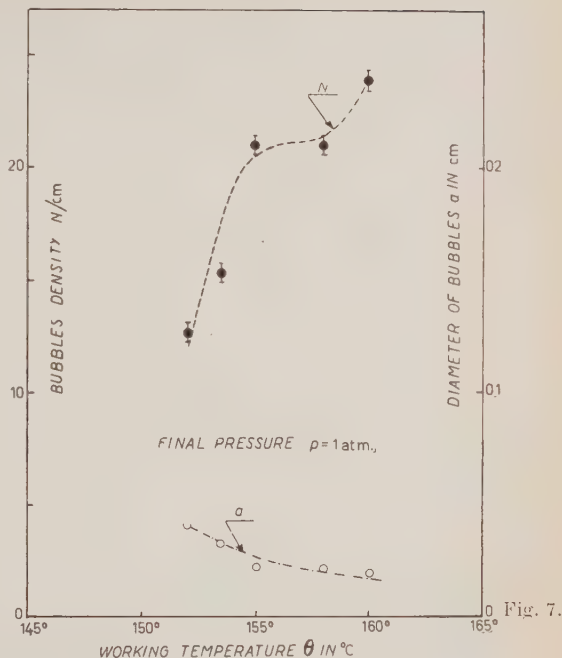


Fig. 7. - The bubble density and the diameter of the bubbles in the dirty chamber as a function of the working temperature, for a final pressure of 1 atm.

Fig. 8. - The bubble density and the diameter of the bubbles in the dirty chamber as a function of the final pressure for a working temperature of 155°C .

TABLE I. — *Dependence of the sensitive time τ of the dirty chamber on final pressure p , recycling time T and expansion ratio δ for a working temperature of 155°C.*

a)	p	1		9	atm	$\delta = 1.107$
	τ	12		17	ms	$T = 1 \text{ min}$
b)	T	1	2	4	min	$\delta = 1.107$
	τ	12	22	29	ms	$p = 1 \text{ atm}$
c)	δ	1.065	1.089	1.107		$T = 2 \text{ min}$
	τ	11	19	22	ms	$p = 1$

ing to an apparently greater degree of cleanliness.

The dependence of τ on δ can be understood if one considers that with increasing δ more time is needed in order to produce the amount of vapour to recompress the liquid. We note also that N and a are necessary largely independent of δ and T .

* * *

We wish to thank Prof. A. ROSTAGNI for the interest he has taken in this work. We are indebted to Dr. M. ANNIS who was associated in the early stages of the experiments. We are grateful to the technicians of this laboratory, and particularly to Mr. B. BALLIN, Mr. E. MACCATO and Mr. G. RIZZATO for their invaluable help. One of us (J.A.M.) wishes to acknowledge a grant from the Conselho Nacional de Pesquisas (Brazil).

RIASSUNTO

Si descrivono due camere a bolle a n-pentano, una pulita ed una sporca. Vengono quindi esposti i risultati di una ricerca sull'influenza che le condizioni di lavoro hanno sul tempo sensibile, sul numero di bolle per cm di traccia e sulla loro grandezza. Il numero di bolle per cm e la loro grandezza sono praticamente costanti in un ampio intervallo della pressione finale; il « foam limit » non dipende dalla pressione finale. Si può allungare il tempo sensibile aumentando la pressione finale e vi è un intervallo di qualche grado nella temperatura in cui il numero di bolle per cm è praticamente costante.

LETTERE ALLA REDAZIONE

(La responsabilità scientifica degli scritti inseriti in questa rubrica è completamente lasciata dalla Direzione del periodico ai singoli autori)

On Certain Hydrodynamical Considerations of an Imperfect Fluid in a General Relativistic Field.

S. BHATTACHARYA

Calcutta

(ricevuto il 7 Aprile 1956)

In this short note let me introduce an outline of hydrodynamical considerations of imperfect fluid. If allowed I may remark that the perfect fluid which pervades the static universe becomes imperfect wherever condensations appear. Professor McVITTE ⁽¹⁾ has shown that universe begins to expand when n condensations appear in different distant regions of the static universe. So it will be of interest to consider the field equations of condensations from this new standpoint and correlate these equations to those of the rest of the universe.

Stress-energy-momentum-tensor ⁽²⁾ of the fluid here is

$$(1) \quad T^{\mu\nu} = -p.g^{\mu\nu} - \frac{2}{3}\mu g^{\mu\nu}\lambda_{0,i}^i + \mu(g^{\mu\alpha}\lambda_{,\alpha}^\nu + g^{\nu\beta}\lambda_{,\beta}^\mu) + (\varrho_{..} + p. + \frac{2}{3}\mu\lambda_{0,i}^i)(dx^\mu/ds)(dx^\nu/ds),$$

where μ = coefficient of viscosity, $\lambda^i = dx^i/ds$ and « s » is proper time. For the meaning of other things TOLMAN's book may be consulted.

From $T_{,v}^{\mu\nu} = 0$ the analogues of classical equations can be written as

$$(2) \quad \left\{ \begin{array}{l} T_{,v}^{1v} = 0 = \partial p. / \partial x + (\varrho_{..} + p. + \frac{2}{3}\mu\lambda_{,1}^1) \frac{\partial u}{\partial t} - \frac{1}{3}\mu \frac{\partial}{\partial x} (u_x + v_y + w_z) - \mu \nabla^2 u, \dots \\ T_{,v}^{4v} = (\varrho_{..} + p. + \frac{2}{3}\mu\lambda_{,i}^i)(u_x + v_y + w_z) + \frac{\partial \varrho_{..}}{\partial t} + \mu \left(\frac{\partial u_i}{\partial x} + \frac{\partial v_i}{\partial y} + \frac{\partial w_i}{\partial z} \right) \end{array} \right.$$

where $dx/ds = u$, $\partial u / \partial x = u_x$; $\partial u_i / \partial x = u_{ix}$ etc. etc., in proper coordinates.

The equation of conservation of mass is

$$(3) \quad (\varrho.\lambda^i)_{,i} = 0,$$

⁽¹⁾ *M.N.R.A.S.*, **91**, 274 (1930-31).

⁽²⁾ *Tolman's Relativity thermodynamics Cosmology*, p. 217, p. 219.

where ϱ_0 = density of proper mass; in proper coordinates (3) becomes

$$(u_x + v_y + w_z) = d \log \varrho / dt.$$

Circulation along a closed curve ⁽³⁾. — Let me define circulation around a closed curve moving with the fluid as

$$\Omega = \int_c \lambda_i dx_i$$

in terms of covariant component of velocity vector.

To calculate the rate of change of circulation w.r.t. proper time around the closed curve c moving with the fluid we take the intrinsic derivative with respect to (w.r.t.) proper time.

Then

$$\begin{aligned} (4) \quad \frac{\delta \Omega}{\delta s} &= \int_c \frac{\delta \lambda_i}{\delta s} dx_i + \int_c \lambda_i d\lambda^i = \\ &= \int_c \left[\frac{d\lambda_i}{ds} - \{ij, l\} \lambda_l \frac{dx^j}{ds} \right] dx_i + 0 = \int_c (\lambda_{i,j} - \lambda_{j,i}) \frac{dx^j}{ds} dx_i. \end{aligned}$$

In proper coordinates of course $\lambda_i = \lambda^i$ because $g_{ij} = g^{ij}$ assume the Galilean values.

Here

$$\begin{aligned} \frac{\delta \lambda_i}{\delta s} &= \frac{d\lambda^i}{ds} - \{ij, l\} \lambda_l \frac{dx^j}{ds} = \frac{d\lambda_i}{ds} - \frac{g^{kl}}{2} \left[\frac{\partial g_{jk}}{\partial x_i} + \frac{\partial g_{ik}}{\partial x_j} - \frac{\partial g_{ij}}{\partial x_k} \right] \lambda_l \frac{dx^j}{ds} = \\ &= \frac{d\lambda_i}{ds} - \frac{g^{kl}}{2} \frac{\partial g_{jk}}{\partial x_i} \lambda_l \frac{dx^j}{ds} \quad (\text{because of summation convention}) = \\ &= \left(\frac{\partial \lambda_i}{\partial x_j} \right) \frac{dx^j}{ds} - \frac{1}{2} \left[\frac{\partial (g_{jk} \lambda^j \lambda^k)}{\partial x_i} - 2g_{jk} \lambda^k \frac{\partial \lambda^j}{\partial x_i} \right] = \left(\frac{\partial \lambda_i}{\partial x_j} \right) \frac{dx^j}{ds} - \left[0 + \lambda^j \frac{\partial \lambda_j}{\partial x_i} \right] = (\lambda_{i,j} - \lambda_{j,i}) dx^j ds, \end{aligned}$$

where $g_{ij} (dx_i/ds) = \lambda_j$ and $\lambda_j \lambda^j = 1$ in generalized co-ordinates and $\lambda_{i,j} - \lambda_{j,i} = 0$ but in proper co-ordinates $\lambda^i \lambda^i = (dx^i/ds)^2 = 1$, or $\lambda^i = \lambda_i = 1$ and $(\lambda_{i,j} - \lambda_{j,i})$ reduce to $(u_{i,j} - u_{j,i}) = 0$.

Comma before an index denotes covariant differentiation w.r.t. that index. In the case of geodesic $(\lambda_{i,j} - \lambda_{j,i})$ vanishes, so circulation along a geodesic is independent of time.

⁽³⁾ *Proc. Camb. Phil. Soc.*, **24**, 478 (1928); also Prof. H. LAMB'S *Hydrodynamics* has been consulted.

On the Positive Excess at Low Energies and at Sea Level.

G. POIANI and G. SALVATORI

Istituto di Fisica dell'Università - Trieste

(ricevuto il 25 Giugno 1956)

The positive excess of the hard component of the cosmic radiation at sea level is fairly well known for energy values ranging from 0.5 to 20 GeV; outside this energy interval the data are rather uncertain because of experimental difficulties or because so far the statistics are poor. At low energies some experimental evidence suggests that the positive excess tends to zero. This circumstance supports the phenomenological theory developed by PUPPI and DALLAPORTA ⁽¹⁾, according to which at sea level the abundance of low energy particles locally generated, sensibly reduces the primary excess. Support to this point of view has been given also by CONVERSI ⁽²⁾ and SHAMOS and MOREWITZ ⁽³⁾.

Using the method suggested by SHAMOS, LEVY and LOWEN ⁽⁴⁾, based on the competition between decay processes and nuclear capture of mesons in samples of different atomic number (carbon and sulphur) we have reconsidered the problem of the positive excess and carried

out measurements at low energies. The experimental set-up is shown in Fig. 1. The trays of counters *A* and *B* constitute the input telescope, the trays

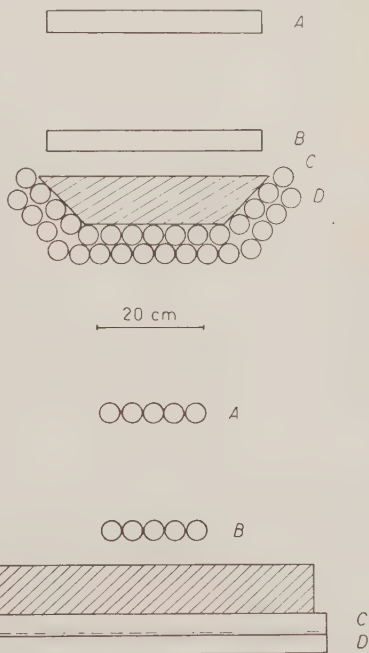


Fig 1. - Experimental arrangement.

⁽¹⁾ *Progress in Cosmic Ray Physics*, ed. J. G. WILSON (1952) p. 317.

⁽²⁾ M. CONVERSI: *Phys. Rev.*, **79**, 749 (1950).

⁽³⁾ H. A. MOREWITZ and M. H. SHAMOS: *Phys. Rev.*, **92**, 134 (1953).

⁽⁴⁾ M. H. SHAMOS, M. G. LEVY and I. S. LOWEN: *Phys. Rev.*, **74**, 1237 (1948).

C and D , placed below the absorbers, reveal through delayed coincidences the electrons from meson decay, which are stopped into the absorber. The electronic circuit is supplied with a delayed coincidence AB, CD_{net} between the trays AB and CD . The width of the pulse from CD is $0.4 \mu\text{s}$; the delay time is fixed within 1.7 and $10 \mu\text{s}$. With the intent to eliminate as much as possible fluctuations in the rise of the pulses, the experimental arrangement has been verified with particular care in order to obtain a ready answer of the electronic circuit to counter pulses. The reaction circuit suggested by PICARD and ROGOZINSKI⁽⁵⁾ has given satisfactory results.

Two series of measurements have been carried out using: (a) concrete absorber of 60 g/cm^2 plus 45 g/cm^2 of lead, and (b) air under a thin layer of about 1 g/cm^2 . The mean momenta concerned with measurements, calculated using Gross curves⁽⁶⁾, taking account of the width of the various overlaying materials, of the angular aperture of the telescope and meson zenithal distribution, were found to be:

$$(a) \ 275^{+300}_{-13} \text{ MeV/c}, \quad (b) \ 87^{+90}_{-4} \text{ MeV/c}.$$

According to these values the number of mesons having momentum included within the maximum value and the mean one is equal to the number of mesons having momentum between the latter and the minimum.

The value of the positive excess has been evaluated using Conversi's relation⁽²⁾:

$$R = \frac{1}{k(N_c/N_s) - 1},$$

where N_c and N_s are the extrapolated values at zero time, corrected for background, of the mesons stopped into the two absorbers (Carbon, 7.7 g/cm^2 , and Sulphur, 7 g/cm^2). The factor k accounts for the relative efficiency of the two absorbers both in stopping the mesons and allowing the decay electrons to go out and become detectable. The value of the k factor is very critical in order to derive from the measurements reliable information on the positive excess since, for instance, a 10% uncertainty on k produces an uncertainty of about 20% on the positive excess, which could mask the decrease of the positive excess at low energies. Since on the other hand the hope to evaluate k with an uncertainty less than about 10% is rather optimistic because its value is influenced by so many physical factors, we have preferred to evaluate k using the Shamos and Morewitz data, obtained with mesons of momentum $300 \pm 70 \text{ MeV/c}$ ($R = 1.06 \pm 0.03$) which is close enough to the momentum determined in the measurement (a). In this way k appears to take the reasonable value 1.075 ± 0.07 . Assuming k constant in the examined energy interval, the positive excess in the series (b) of measurements is:

$$R(87^{+90}_{-4} \text{ MeV/c}) = 1.01 \pm 0.07.$$

This result, although considered in relative sense, confirms that the positive excess tends toward zero at very low energies.

* * *

We are indebted to Prof. P. BASSI for helpful discussions and to Mr. F. DEMANINS for aiding us in the management of the electronic devices.

⁽⁵⁾ E. PICARD and A. ROGOZINSKI: *Jour. Phys. et Rad.*, **14**, 304 (1953).

⁽⁶⁾ D. I. X. MONTGOMERY: *Cosmic Ray Physics* (1949), p. 319.

LIBRI RICEVUTI E RECENSIONI

OSWALD BLACKWOOD, WILLIAM KELLY: *General Physics*, John Wiley & Sons, Inc., New York.

I libri di testo di fisica per gli studenti che frequentano le classi di preparazione ai corsi universitari, sono certamente quelli di più difficile compilazione; la ragione di ciò sta nel fatto che essendo cotesti libri, rivolti a giovani che molto spesso non hanno in modo preciso nè spiccata tendenza per un particolare ordine di studi, nè raggiunta una sufficiente maturità generale, specie nelle matematiche, finiscono molto spesso o col dire troppo poco o col dare alla trattazione una impostazione così esageratamente speculativa che lo studente difficilmente riesce a penetrare nel vivo dei fenomeni fisici e dei metodi che guidano allo studio di essi.

O. BLACKWOOD e W. KELLY, autori del testo *General Physics* di cui recentemente è comparsa la seconda edizione per i tipi di John Wiley, New York, si sforzano, ed in parte riescono, a dare al loro libro una impostazione spiccatamente pratica, nel senso di attingere dalla esperienza quotidiana elementi per introdurre lo studente allo studio della fisica; il testo per ciò è ricco di disegni, grafici e diagrammi che servono bene alla comprensione dei diversi argomenti.

Ai capitoli tradizionali della fisica classica, meccanica, fisica molecolare e calore, vibrazioni e suono, elettricità e magnetismo, ottica, è stato aggiunto un ultimo capitolo sulla «nuova fisica»: in esso vengono dati cenni sulla radioattività e sono introdotte alcune semplici nozioni fondamentali di fisica del nucleo,

con un cenno sui raggi cosmici e sullo sfruttamento della energia nucleare.

Completa la parte espositiva una ricca raccolta di problemi, tratti quasi tutti dalla comune esperienza fisica. Un'appendice fornisce la soluzione dei problemi proposti. Inoltre un largo questionario invita lo studente a formulare le risposte a quesiti che hanno carattere qualitativo ed intuitivo. Ogni capitolo si chiude con un breve sommario.

L'aspetto tecnico della impostazione del libro è forse in alcune parti un po' troppo spinto; così nel capitolo sulla elettronica si corre il rischio che lo studente davanti ad uno schema di un circuito ricevente o trasmettente non comprenda gran che.

L'impiego dello strumento matematico viene fatto con molta moderazione, esso è limitato alle forme più semplici ed è veramente «chiarificatore e generalizzatore dei concetti della fisica intesa come scienza vitale».

Concludendo il libro che presentiamo è un buon testo scolastico da preferire indubbiamente a tanti altri d'intonazione meno tecnica e più diremo «filosofica».

Ottima la stampa e tutta la veste tipografica.

M. SANTANGELO

EVANGELISTA TORRICELLI - *De Infinitis Spiralibus*, a cura di Ettore Carruccio, 1 vol. in-8° di pp. 76. Domus Galilaeana, Pisa, 1955, s. i. p.

L'ordine in cui il prof. CARRUCCIO ha presentato, corredandola di una fedele

traduzione italiana e di utili note, questa famosa memoria del TORRICELLI, è diverso da quello in cui essa è apparsa nel 1919 nell'edizione faentina delle sue *Opere* (vol. I, parte II). È stato tenuto conto infatti delle osservazioni critiche di ETTORE BORTOLOTTI, ed è stato effettuato inoltre un nuovo controllo sulle pagine del manoscritto torricelliano nella raccolta « Discepoli di Galileo » della Biblioteca Nazionale di Firenze.

Della spirale logaritmica, definita dal TORRICELLI nel 1645, viene presentato in questo scritto un metodo di rettificazione, che costituisce il primo esempio storico di rettificazione mediante riga e compasso di un arco di curva. L'introduzione all'attuale edizione fornisce interessanti notizie sul classico problema, che DESCARTES aveva ritenuto insolubile « par les hommes », e sugli ulteriori risultati ottenuti dal TORRICELLI intorno alla spirale che egli chiamava « geometrica », contrapponendola a quella « aritmetica » di ARCHIMEDE.

V. SOMENZI

O. F. MOSSOTTI - *Scritti*. Vol. II, t. II (*Nuova teoria degli Strumenti ottici*), 1 vol. in-8° di pagine 16+306. Domus Galilaeana, Pisa, 1955, L. 4000.

La raccolta degli scritti principali del MOSSOTTI, iniziata nel 1942 da L. GABBA e G. POLVANI, è giunta a completamente con questo secondo tomo del secondo volume, curato da GIOVANNI POLVANI. (Il primo tomo, apparso nel 1951, conteneva *Scritti di Fisica, Meteorologia e vari*, mentre il primo volume era dedicato agli *Scritti di Astronomia, Geodesia e Matematica*).

Il titolo *Nuova teoria degli Strumenti Ottici* copra i quindici capitoli e la *Nota* pubblicati tra il 1858 e il 1861 dal MOSSOTTI negli *Annali di Matematica pura ed applicata*, oltre che nelle suddette ri-

viste, e le *Tavole* del dott. ANGELO FORTI apparse sul *Nuovo Cimento* del 1859. Queste *Tavole* erano state elaborate « per dedurre con semplici interpolazioni i raggi di curvatura di un obbiettivo applanatico composto di tre lenti a contatto » in casi più particolari di quello trattato nel Capitolo III della Parte IV ed ultima della *Nuova Teoria*; il MOSSOTTI stesso fu indotto dalla loro utilità ad integrare tale capitolo con la *Nota* del 1860 ed a considerarle poi come un complemento essenziale della sua opera.

La presente edizione, molto accurata, reca anche le varianti, in genere di importanza trascurabile, fra l'una e l'altra delle diverse pubblicazioni subite dai medesimi scritti.

V. SOMENZI

G. PETIAU - *La théorie des fonctions de Bessel exposée en vue de ses applications à la Physique Mathématique*. Centre National de la Recherche Scientifique, Paris, 1955, p. 477.

Questo volume contiene una ricca e pregevole raccolta di nozioni e di formule sulle funzioni di Bessel e sulle funzioni ad esse collegate. Tale raccolta, che tiene conto anche di recenti risultati, è orientata soprattutto verso le applicazioni fisiche, delle quali sono forniti numerosi ed interessanti esempi.

L'opera è divisa in 24 capitoli, ai quali fanno seguito alcune tabelle numeriche e tavole grafiche. I primi 16 capitoli sono dedicati alla teoria e gli ultimi 8 alle applicazioni.

Poichè è assai difficile riassumere la vastissima materia contenuta nei 16 capitoli di carattere teorico, ci limiteremo a dire che, ad un primo gruppo di 4 capitoli, ove sono definite le funzioni di Bessel di 1^a, 2^a e 3^a specie (funzioni di Hankel) e ne sono studiate le rappresentazioni integrali, fanno seguito altri 4 capitoli

dedicati agli sviluppi asintotici, ai teoremi di addizione e di moltiplicazione, agli zeri delle funzioni di Bessel ed al calcolo di integrali in cui figurano tali funzioni. Seguono 6 capitoli nei quali sono studiati vari tipi di funzioni collegate a quelle di Bessel (funzioni di Lommel, di Anger, di Weber, di Struve, di Kelvin, di Bessel integrali, ecc.), nonché gli sviluppi in serie precedenti secondo tali funzioni (serie di Neumann, di Fourier-Bessel, di Kapteyn, di Schlömilch, ecc.). In due successivi capitoli si parla dei rapporti fra le funzioni di Bessel ed i più comuni sistemi di polinomi ortogonali (di Legendre, di Laguerre, di Tehebytscheff) e dei vari tipi di equazioni differenziali i cui integrali sono esprimibili con funzioni di Bessel.

Seguono, come si è già detto, le applicazioni che danno spesso lo spunto ad interessanti complementi. Sono studiati il problema di Keplero sulle orbite ellittiche (con un cenno sulle funzioni di Bessel di più variabili), il problema di Bernoulli sulle piccole oscillazioni di una catena pesante, il problema dei cammini a caso.

Successivamente si passa a trattare questioni sulla propagazione del calore, sulle vibrazioni delle membrane e delle piastre circolari, sulla diffrazione della luce, sulla propagazione dell'elettricità e delle onde elettromagnetiche.

Infine l'ultimo capitolo è dedicato ad

alcuni problemi di meccanica ondulatoria.

In complesso si tratta di un buon libro che può essere veramente utile ai cultori di matematica sia pura che applicata.

La consultazione è abbastanza facile perchè ogni capitolo è diviso in numerosi paragrafi con titolo; ciò supplisce, almeno in parte, alla mancanza di un indice analitico.

ALDO GHIZZETTI

L. HEFFTER — *Begründung der Funktionentheorie auf alten und neuen Wegen*. Springer-Verlag, Berlin-Göttingen-Heidelberg, 1955, p. 63.

Si tratta di un opuscolo di carattere prevalentemente storico sui concetti e sui teoremi che dominano la teoria delle funzioni analitiche di una variabile complessa.

Dopo un'introduzione di carattere elementare, si espone l'evolversi del concetto di funzione analitica e delle ipotesi poste a base dei fondamentali teoremi di Cauchy e di Morera. Si espongono fra l'altro i contributi di GOURSAT e di LOOMAN-MENCHOFF, quelli dovuti all'Autore e si fanno istruttivi confronti fra le varie possibili trattazioni.

ALDO GHIZZETTI

PROPRIETÀ LETTERARIA RISERVATA
